# Fixed nitrogen loss in two variably anoxic marine environments: the subsurface biosphere of hydrothermal vents (Juan de Fuca Ridge, northeast Pacific) and Saanich Inlet, a British Columbia fjord

by

Annie Bourbonnais
B.Sc., University of Ottawa, 2005
M.Sc., Université du Québec à Montréal, 2007

A Dissertation Submitted in Partial Fulfillment
of the Requirements for the Degree of

DOCTOR OF PHILOSOPHY

in the School of Earth and Ocean Sciences

# Supervisory Committee

Fixed nitrogen loss in two variably marine anoxic environments: the subsurface biosphere of hydrothermal vents (Juan de Fuca Ridge, northeast Pacific) and Saanich Inlet, a British Columbia fjord

by

Annie Bourbonnais
B.Sc., University of Ottawa, 2005
M.Sc., Université du Québec à Montréal, 2007

**Supervisory Committee**

Dr. S. Kim Juniper, (School of Earth and Ocean Sciences)
**Supervisor**

Dr. Moritz F. Lehmann, (School of Earth and Ocean Sciences)
**Departmental Member**

Dr. Roberta C. Hamme, (School of Earth and Ocean Sciences)
**Departmental Member**

Dr. Réal Roy, (Department of Biology)
**Outside Member**

Dr. David A. Butterfield, (National Oceanic and Atmospheric Administration (NOAA) and University of Washington, USA)
**Additional Member**

# Abstract

**Supervisory Committee**

Dr. S. Kim Juniper, (School of Earth and Ocean Sciences)
**Supervisor**

Dr. Moritz F. Lehmann, (School of Earth and Ocean Sciences)
**Departmental Member**

Dr. Roberta C. Hamme, (School of Earth and Ocean Sciences)
**Departmental Member**

Dr. Réal Roy, (Department of Biology)
**Outside Member**

Dr. David A. Butterfield, (NOAA and University of Washington, USA)
**Additional Member**

We investigated oceanic dissolved inorganic nitrogen (N) dynamics, focussing on processes removing bio-available N and ultimately affecting primary productivity, in sulfidic hydrothermal vent fluids discharging from the subsurface on the Juan de Fuca Ridge (northeast Pacific Ocean) and in anoxic bottom waters of Saanich Inlet, a British Columbia fjord, using a combination of geochemical and molecular microbial ecology techniques. During episodes of mixing with oxygenated sea-water, both systems can switch from anoxic to oxic conditions.

Strong inter-site variations in the concentrations and $\delta^{15}N$ of ammonium ($NH_4^+$) in high-T fluids suggested different N sources (deep-sea nitrate ($NO_3^-$) versus organic sediments) for hydrothermally discharged $NH_4^+$. Increase in the isotopic composition of $NO_3^-$ ($\delta^{15}N$ and $\delta^{18}O$), concomitant with decreased [$NO_3^-$], indicated $NO_3^-$ assimilation or denitrification in the subsurface. $NO_3^-$ isotope anomalies, i.e. deviations from the $^{15}N$:$^{18}O$ isotopic enrichment of 1:1 in marine environments, were observed and confirmed the occurrence of $NO_3^-$ regeneration in vent fluids. Denitrification was the dominant N-loss pathway, suggesting that bacterial denitrification out-competes anaerobic $NH_4^+$ oxidation (anammox) in diffuse hydrothermal vent waters. The diversity of denitrifying bacteria encoding the *nirS*-form of nitrite reductase was low in vent fluids. Quantitative polymerase chain reaction (qPCR) analysis revealed that denitrifiers accounted for up to

38% (*nirk*-encoding γ-proteobacteria of the SUP05 cluster) and 8% (*nirS*-encoding bacteria) of the total bacterial abundance. Furthermore, *nirS* gene operational taxonomic units from two vent fields clustered into different groups in the phylogenetic tree, suggesting a link between denitrifying bacterial community membership and small-scale geographic isolation and/or fluid physico-chemical properties. Significant correlations existed between fixed N-loss rates and *in-situ* dissolved inorganic N deficits in the fluids. Based on our rate measurements, and on published data on hydrothermal fluid fluxes and residence times, we estimated that up to ~10 Tg N $yr^{-1}$ could be removed globally in the subsurface biosphere.

In Saanich Inlet, a gradual increase in both the $\delta^{15}N$ and $\delta^{18}O$ of $NO_3^-$ associated with a decrease in $[NO_3^-]$ and an increase in biological excess $N_2$, was observed after bottom water renewal events in fall 2008, following $NO_3^-$ consumption by denitrifiers in an expanding suboxic zone. N-to-O negative $NO_3^-$ isotope anomalies were observed in surface and bottom waters, confirming the occurrence of $NO_3^-$ regeneration and/or external $NO_3^-$ input. Closed and open-system-model derived $NO_3^-$ isotope effects in anoxic bottom waters were lower (as low as ~11‰) than the ~25‰ for water column denitrification reported in other studies, suggesting that ~50% of the denitrification could occur, with a highly suppressed isotope effect, in the sediments of the Inlet.

# Table of Contents

# List of Tables

# List of Figures

# Acknowledgments

I would first like to thank my supervisor Kim Juniper, for being supportive and believing in my capability to achieve my goals. I strongly admire Kim for his outstanding interpersonal abilities. He always seems to resolve difficult situations with his calm and rational manner. Our discussions allowed me to put my project into a global perspective and more importantly, to ask the right scientific questions.

I would equally like to thank Moritz Lehmann, my co-supervisor, for his invaluable intellectual input regarding my geochemical work. Moritz was a model mentor through the project and also helped me to establish indispensable scientific connections. During my Ph.D., and as my former M.Sc. advisor in Montreal, he significantly helped me to become a better scientist. I hope we can continue to collaborate in the future.

I would also like to thank all other members of my Ph.D. committee, all my scientific collaborators, and all members of the Juniper lab at UVic and Lehmann lab in Basel for their practical help and intellectual input on my work. A special thanks to David Butterfield, for inviting me on three scientific cruises to the Juan de Fuca Ridge and considerably help with the logistic of sample collection; Allan Devol, for his fruitful discussions and help with the denitrification rate measurements; Steven Hallam, Marcel Kuypers, Réal Roy, Roberta Hamme and Steven Emerson for welcoming me in their laboratories, and Julie Huber and Rika Anderson, for sharing precious DNA samples. I owe a special thanks to the Couchsurfing community, which allowed me to perform countless laboratory analyses in Vancouver, Bremen, and Seattle. Thanks also to all my cruise buddies, especially Rika Anderson, Helene Ver Eecke, and John Jamieson. Being at sea (and under the sea) have never been so fun!

I would like to thank all the family and friends who supported me and believed in me. First, thank to my mother, Louise and my sister Julie, for understanding why I would move so far to work for so long on my Ph.D. Thanks to my uncles Claude and Jean-Louis for being the closest thing to a father I've ever had. Thanks to Katleen Robert, and Amalis Riera for being exceptional friends and to Maeva Gauthier for organizing the best floathouse parties, and numerous Explorers Club student chapter meetings in Victoria. These represent some of my most memorable Ph.D. moments. I would also like to thank all my other friends that actively supported me during the last five years: to name a few: Abigail Barker, Pavel Kratina and his wife Lucie Jerabkova, Scott Pavey, Steeve Deschênes, Arielle Kobryn, Christina Shallenberg, Amélie Doré, Melissa Lebel, Steven McGehee, Miranda Brintnell and Marcos Lagunas.

A special thank to my friend (and now partner) Ray Holberger. I am forever grateful that you infiltrated my mostly French speaking group. Thank you for travelling around the world with me and always bringing me on "crazy adventures". I feel really lucky to have you!

# Chapter 1
# Introduction

## 1.1. Rationale and preview

Nitrogen (N) is essential for all organisms and often limits marine photosynthetic and chemosynthetic primary productivity in the ocean. The capacity of the ocean to take up and sequester carbon dioxide, a greenhouse gas, through the biological pump is regulated by the availability of fixed N in surface waters. Consequently, several scenarios invoking the indirect role of N to explain changes in past atmospheric $CO_2$ concentrations and climate have been suggested (McElroy, 1983; Falkowski, 1997; Broecker and Henderson, 1998; Altabet *et al.*, 1995, 2002; Ganeshram *et al.*, 1995; 2000; Thunell and Kepple, 2004).

As further explained below (section 1.2.1), N is assimilated by primary producers at the base of the food chain and utilized for proteins synthesis. The oxidized forms of N ($NO_3^-$, $NO_2^-$) can also be used as electron acceptors during respiration under anaerobic or low oxygen conditions concurrently with the oxidation of organic matter by chemoorganoheterotrophic organisms or other inorganic reduced chemicals (e.g. $H_2S$, $NH_4^+$), by chemolithoautotrophic organisms. In the denitrification zones, nitrate is mostly transformed into gaseous $N_2$, but denitrification reactions can also lead to the accumulation of $N_2O$, a potent greenhouse gas, potentially affecting climate.

Even today, no consensus exists on the question of the global N budget being in or out of balance in the ocean, i.e. if the ocean is actually losing or gaining fixed N (Codispoti *et al.*, 2001; Gruber and Sarmiento, 2002; Gruber, 2004; Codispoti, 2007). According to

most recent estimations, $N_2$ fixation would add 100-200 Tg N/year in the ocean (Capone *et al.*, 1997; Falkowski, 1997; Gruber and Sarmiento, 1997; 2002; Karl *et al.*, 2002) and denitrification would remove up to ~450 Tg N/year (Codispoti *et al.*, 2001; Codispoti, 2007), Table 1.1. In contrast, Gruber (2004), and more recently DeVries *et al*. (2012), suggest that the ocean N cycle is in balance. Recently, a significant expansion of oxygen minimum zones (OMZ) in the ocean has been observed (e.g. Stramma *et al*., 2008), potentially increasing global denitrification (e.g. Bianchi *et al*., 2012). Clearly, there is a need to re-evaluate the current estimates of global oceanic $N_2$ fixation and denitrification.

**Table 1.1.** Major sources and sinks in the present oceanic fixed N budgets (in Tg N/year). Modified from Codispoti, 2007.

| Reference | Gruber and Sarmiento, 2002 | Gruber, 2004 | Codispoti *et al.*, 2001 | Codispoti, 2007 |
|---|---|---|---|---|
| **Sources** | | | | |
| $N_2$ fixation | 132 ± 41 | 135 ± 51 | 132 | >>>135 |
| Riverine inputs | 76 ± 14 | 80 ± 14 | 76 | 80 |
| Atmospheric inputs | 30 ± 5 | 50 | 86 | 30 |
| **Sinks** | | | | |
| Benthic denitrification | 95 ± 20 | 180 ± 50 | 300 | >300 |
| Water column denitrification | 80 ± 20 | 50 ± 20 | 150 | >>150 |
| Burial in sediments | 25 ± 10 | 25 ± 10 | 25 | 25 |
| $N_2O$ atmospheric loss | 4 ± 2 | 4 ± 2 | 6 | 4 |
| Organic N export from the ocean | --- | 1 | 1 | --- |
| **Total** | **34 ± 53** | **5 ± 78** | **-188** | **>-234** |

The overall goal of my doctoral research was to assess bio-available (or fixed) N dynamics, particularly N-elimination pathways, in two intermittently anoxic ecosystems 1) hydrothermal vents of the Juan de Fuca Ridge in the northeast Pacific Ocean and 2)

Saanich Inlet, a seasonally anoxic British Columbia fjord, using a combination of isotopic (natural $^{15}N$ tracer experiments) and molecular biology techniques. Both the hydrothermal vents of the Juan de Fuca Ridge and Saanich inlet show temporal and/or spatial gradients in redox conditions. During episodes of advective mixing or diffusive exchange with oxygenated sea-water, both systems can switch from completely anoxic to oxic conditions on short spatial and temporal scales.

In the following sections, I provide more background information on N cycle transformations in the ocean, the use of stable (natural abundance) and labeled isotopes and molecular microbial ecology techniques in the study of bacterially mediated N-cycling and the current state of knowledge regarding N-cycling dynamics in hydrothermal vent systems and Saanich Inlet. I then present the prime objectives and outline of my PhD dissertation.

## 1.2. Background information

### 1.2.1. The marine N cycle

The main external sources of fixed N to the ocean are $N_2$ fixation as well as riverine and atmospheric N inputs. The most important sink of oceanic N is denitrification in the broad sense (including canonical denitrification in both the water column and sediments as well as anammox). The internal cycle of assimilation-remineralization does not affect the overall oceanic N budget. A simplified marine N-cycle is shown in Figure 1.1, and major sources and sinks in Table 1.1.

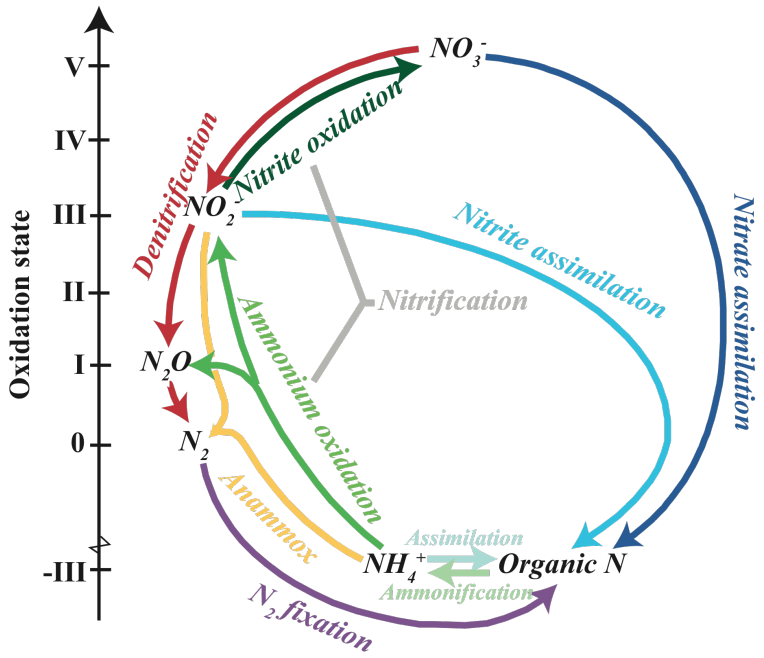


**Figure 1.1.** Simplified oceanic N cycle. Redrawn from Gruber, 2008.

$N_2$ fixation mediated by $N_2$ fixers is the major source of N in the ocean and mainly occurs in the euphotic zone of N-limited, well-lit tropical and subtropical ocean with an abundant aeolian supply of iron (Fe) (Niemi, 1979; Berman-Frank *et al.*, 2001). Fixed N is ultimately transformed to nitrate after the remineralization of organic material and nitrification. $N_2$ fixation, mostly by the filamentous cyanobacteria *Trichodesmium*, has been well documented in the tropical and subtropical North Atlantic and Pacific Oceans (Liu *et al.*, 1996; Capone *et al.*, 1997; 2005; Carpenter *et al.*, 1997; 1999; Karl *et al.*, 2002).

$N_2$ fixation is countered by denitrification and anaerobic ammonium oxidation (anammox) that represent the major sinks of N in the ocean. Heterotrophic denitrification is the dissimilative utilization of nitrate as an electron acceptor during respiration by

facultative anaerobic prokaryotes (for example *Pseudomonas* and *Clostridium*), generally with some combination of the following intermediate products:

$$NO_3^- \rightarrow NO_2^- \rightarrow NO \rightarrow N_2O \rightarrow N_2 \text{ gas} \quad (1.1)$$

Chemolithoautotrophic organisms can also perform denitrification coupled to the oxidation of inorganic reducing substances (e.g. $H_2S$) as a source of energy. Denitrification only occurs in sediments and in the water column of localized regions with high surface primary productivity and low oxygen source waters (i.e. OMZ), with $[O_2]$ <~5 μmol/L, such as the Arabian Sea (Naqvi *et al.*, 1990; 2006; Howell *et al.*, 1997), the Eastern Tropical North Pacific (Deutsh *et al*. 2001; Sigman *et al*., 2005), the Eastern Tropical South Pacific (Dugdale *et al*., 1977; Codispoti *et al.*, 1986; Robinson *et al.*, 2007), the Benguela upwelling system (Tyrrell and Lucas, 2002) as well as productive coastal areas and semi-enclosed Basins, such as Saanich Inlet (Devol, 1991; Middelburg *et al.*, 1996; Brandes and Devol, 2002).

Denitrification was once considered the only important process removing bio-available N in natural environments. Since the early 2000s, anammox, converting nitrite and ammonium into $N_2$ gas and water, has been reported as an important and overlooked N sink in OMZs (Dalsgaard *et al.*, 2003; Kuypers *et al.*, 2003; 2005; Hamersley *et al.*, 2007; Jaeschke *et al.*, 2007; Lam *et al.*, 2009), sediments (Thamdrup and Dalsgaard, 2002; Engstrom *et al.*, 2005; Penton *et al.*, 2006; Amano *et al.*, 2007), estuaries (Trimmer *et al.*, 2003; Tal *et al.*, 2005), and hydrothermal vents (Byrne *et al.*, 2009). The simplified equation for anammox is:

$$NH_4^+ + NO_2^- \rightarrow N_2 + H_2O \quad (1.2)$$

Anammox bacteria are autotrophic and require the co-occurrence of ammonium and nitrite, often found at or near redox interfaces within sediments and in the water column. Here, ammonium originates from the anaerobic degradation of organic material and dissimilatory nitrate/nitrite reduction (i.e. DNRA). Nitrite derives from nitrate reduction by denitrifying bacteria, or from nearby aerobic nitrification of ammonium (Kuenen, 2008). Strous *et al.* (1997) demonstrated that anammox occurred in the absence of oxygen and was even inhibited by oxygen concentrations above 1 μmol $L^{-1}$.

The internal cycle of oceanic N comprises nitrate assimilation by primary producers (plants and heterotrophic bacteria) and the subsequent transformation of organic material back to ammonium and nitrate, by respectively, ammonification and nitrification. During nitrate assimilation in surface waters, nitrate is intracellularly reduced to nitrite and then ammonia, which is required for amino acid synthesis. Photosynthesis supported by nitrate supplied from the depth and assimilated by organisms in surface waters is referred to as new production (Dugdale and Goering, 1967). Particulate organic N (PON) from dead organisms and dissolved organic N (DON) excreted by living mass are converted back to ammonium during the process of ammonification. This ammonium can be either re-assimilated by primary producers (referred to as regenerated production) or nitrified. Nitrification, mediated by nitrifying bacteria, transforms ammonium to nitrite and nitrate. While it was once believed that nitrification only occurred below the surface mixed layer because of inhibition by light, many studies have documented the presence of nitrification at the base of the euphotic zone (Ward *et al.*, 1989; Dore et Karl, 1996; Bianchi *et al.*, 1997; Ward, 2005a).

### 1.2.2. The use of stable isotopes in the study of marine N cycle

#### 1.2.2.1. Isotope fractionation and Rayleigh distillation

Isotopes are atoms of the same element but with a different number of neutrons. The two stable isotopes of N ($^{14}N$ and $^{15}N$) have proved useful in studying the oceanic N cycle. The nitrate molecule can also contain either $^{16}O$ or $^{18}O$, creating isotopologues for nitrate. Isotope fractionation occurs because of the difference in the reaction rates for the different isotopologues. Physicochemical fractionation is caused by the difference in bond energy between isotopes of different nuclear mass. More specifically, the bond strength is greater for the heavier isotope; it thus takes more energy to break the bond for a heavier isotope than for a lighter isotope. Therefore, during biological and chemical reactions, the molecules containing the lighter isotopes react more quickly than the molecules that have the heavier isotopes; as a result the residual substrate becomes enriched in heavier isotopes (e.g., $^{15}N$ and $^{18}O$) while the products are enriched in the lighter isotopes (e.g., $^{14}N$ and $^{16}O$).

The isotopic composition of nitrate ($\delta^{15}N$ and $\delta^{18}O$) is expressed in parts per thousand or permil (‰) units, R being the ratio of $^{15}N/^{14}N$ or $^{18}O/^{16}O$ of the sample and an international standard (air for N and Vienna Standard Mean Ocean Water (V-SMOW) for O).

$$\delta^{15}N \text{ or } \delta^{18}O = ((R_{sample}/R_{reference})-1) \times 1000 \quad (1.3)$$

The isotope enrichment factor ($\varepsilon$ in ‰, where $\varepsilon = \delta^{15}N_{substrate} - \delta^{15}N_{product}$) during biological reactions can be estimated by an approximation of the Rayleigh equation,

which is only appropriate when the reaction is occurring in a closed system (Mariotti *et al.*, 1981):

$$\delta^{15}N_{reactant} = \delta^{15}N_{initial} - \varepsilon(\ln f) \quad (1.4)$$

where $f$ is the fraction of reactant remaining and $\delta^{15}N_{initial}$ is the $\delta^{15}N$ of the initial reactant ($NO_3^-$, $NO_2^-$ or $NH_4^+$ in the case of dissolved inorganic nitrogen (DIN)) N pool.

The equation for an open system, steady-state model, where $NO_3^-$, $NO_2^-$ or $NH_4^+$ is continuously consumed and re-supplied from an infinite reservoir at initial isotopic composition (Altabet, 2001) is:

$$\delta^{15}N_{final} = \delta^{15}N_{initial}\,(f = 1) + \varepsilon \times [1 - f] \quad (1.5)$$

The same equation applies for $\delta^{18}O$ of nitrite and nitrate.

#### 1.2.2.2. Assessing internal N-cycle processes and the input and loss of N in the ocean using N (and O of nitrate) isotopes

Measurement of the fractionation of N (and O of nitrate) isotopes is a useful tool for assessing the transformations characterizing the internal N cycle (i.e. assimilation, ammonification and nitrification) and the input and loss of N through $N_2$ fixation and denitrification occurring in the water column of the ocean, partially overcoming weaknesses inherent in the Redfield stoichiometry approach (i.e. nitrate deficits) (Lehmann *et al.*, 2003; 2005; Sigman *et al.*, 2005; Bourbonnais *et al.*, 2009).

The internal N-cycle does not cause a change in whole oceanic $\delta^{15}N$. This is explained by the complete consumption of nitrate in surface waters of most of the ocean. Consequently, in the absence of other N sources (i.e. $N_2$ fixation, atmospheric

depositions), the complete remineralization of the exported organic material would produce nitrate bearing the same $\delta^{15}N$ as the nitrate originally supplied from below the thermocline and assimilated by the organisms. However, in the surface waters of high latitude HNLC (high nutrient low chlorophyll) regions where iron availability limits primary productivity (Martin *et al.*, 1994; Coale *et al.*, 1996; Boyd *et al.*, 2000; Watson *et al.*, 2000), it has been shown that incomplete nitrate assimilation, with an isotopic effect of ~5‰ (Sigman *et al.*, 1999; Altabet, 2001), increase the $\delta^{15}N$ and $\delta^{18}O$ of the residual nitrate. However, the internal N-cycle processes do not affect the $\delta^{15}N$ of the global ocean because the low $\delta^{15}N$ of the organic material produced under incomplete nitrate assimilation is ultimately remineralized and N-isotopes are subsequently redistributed between different water masses.

Net changes in global oceanic $\delta^{15}N$ are determined by the balance of N sources and sinks (i.e. $N_2$ fixation and denitrification). $N_2$ fixation, the major source of N in the ocean, adds new N with a $\delta^{15}N$ of ~-2-0‰. Very little fractionation is associated with this process as the $\delta^{15}N$ of dissolved $N_2$ is 0.6‰ (relative to atmospheric $N_2$) (Carpenter *et al.*, 1997; 1999; Montoya *et al.*, 2002). This low $\delta^{15}N$ incorporated by $N_2$ fixers is subsequently transferred to the nitrate pool after the complete ammonification and nitrification of the sinking organic material (Liu *et al.*, 1996; Karl *et al.*, 2002; Knapp *et al.*, 2005, 2008; Sigman *et al.*, 2005; Bourbonnais *et al.*, 2009).

Water-column denitrification in localized oceanic areas (mainly the ETSP, the ETNP, the Arabian Sea and the Benguela Upwelling system) increases the $NO_3^-$ $\delta^{15}N$ as a consequence of kinetic N-isotope fractionation (Cline and Kaplan, 1975; Brandes *et al.*, 1998a; Voss *et al.*, 2001; Lehmann *et al.*, 2003; Sigman *et al.*, 2005). The isotope effect

(ε) associated with denitrification is high, with most recent estimates from both laboratory experiments and natural environments clustering around 20-30‰ (Brandes *et al.*, 1998a; Altabet *et al.*, 1999; Voss *et al.*, 2001; Granger *et al.*, 2008). Although sedimentary denitrification is an important sink for oceanic N, no significant isotope effect has been associated with this process (typically <3‰), probably because of the complete consumption of nitrate diffusing into the sediments or the addition of low $\delta^{15}N$ from nitrification that would counterbalance any isotope effect associated with denitrification (Brandes and Devol, 1997, 2002; Sebilo *et al.*, 2003; Lehmann *et al.*, 2004; Alkhatib *et al*., 2011). The large isotope effect associated with water-column denitrification relative to $N_2$ fixation, sets the deep ocean (>2 km) mean nitrate $\delta^{15}N$ to ~5‰ (Liu and Kaplan, 1989; Sigman and Casciotti, 2001); it would otherwise remain at ~0‰.

While N isotopes alone can provide qualitative and semi-quantitative information on single N-cycle transformations, their use is often limited in marine regions where several N-transformations have overprinting effects on both the nitrate concentration and N isotope signatures, for example $N_2$ fixation and denitrification. On the other hand, the measurement of coupled nitrate N and O isotope ratios has the potential to disentangle nitrate consumption and production processes in environments where they occur simultaneously. During nitrate consuming processes in the ocean (i.e. assimilatory and dissimilatory nitrate reduction), nitrate $\delta^{15}N$ and $\delta^{18}O$ has been shown to increase in parallel, with a constant ratio of N versus O isotope enrichment of ~1 for both processes (Casciotti *et al*., 2002; Sigman *et al.*, 2003; Granger *et al.*, 2004; 2008). In contrast to nitrate reduction (dissimilative or assimilative) nitrate $\delta^{15}N$ and $\delta^{18}O$ is affected in

fundamentally different ways during nitrate production (Sigman *et al.* 2005). The $\delta^{15}N$ of nitrified nitrate is dependent on the $\delta^{15}N$ of the precursor molecule (ammonium or nitrite). With respect to the oxygen atom, nitrification represents an absolute source, and most of the O atoms derive from the ambient water so that new nitrate has a $\delta^{18}O$ of 0 to 2‰ (Andersson *et al.*, 1982; Casciotti, 2002; Sigman *et al*., 2009). As a consequence, gross nitrate generation (be it from the remineralisation/nitrification of organic matter from $N_2$ fixing or nitrate assimilating phytoplankton) results in a decoupling of N versus O isotope gradients, and should be indicated by anomalous nitrate dual isotope signatures (e.g. Sigman *et al*. 2005; Bourbonnais *et al*., 2009).

#### 1.2.2.3. Use of $^{15}N$ stable-isotope pairing techniques to determine N-elimination rates

N-elimination (i.e. denitrification, anammox and DNRA coupled to anammox) often (particularly in the open water column) occurs at rates too low to be traced and quantified by concentration changes alone. Stable-isotope pairing techniques are thus commonly used to derive rates for these processes. Here, isotopically labeled substrates (i.e. $^{15}N$ nitrate, nitrite or ammonium) were added to water or sediment samples in *ex-situ* incubations, and the production of $^{29}N_2$ and $^{30}N_2$ was determined using a Isotopic Ratio Mass-Spectrometer (IRMS). $^{15}N$-labeled incubation techniques have been successfully applied to measure rates of different N-elimination pathways in the Eastern Tropical South Pacific (Thamdrup *et al.*, 2006; Hamersley *et al.*, 2007; Lam *et al.*, 2009), the Arabian Sea (Devol *et al.* 2006; Nicholls *et al.*, 2007; Ward *et al.*, 2009) and the Benguela upwelling system (Kuypers *et al.*, 2005).

### 1.2.3. Microbial molecular ecology techniques and the oceanic N cycle

It is difficult, if not impossible, to use laboratory culture techniques to characterize microbial communities in environmental samples since only 0.1-1% of the viable cells are cultivable in many habitats (Handelsman, 2004). A revolution in microbial ecology occurred with recent advances in molecular biological methods that permit culture-independent phylogenetic analysis of natural microbial communities. This has led to the discovery of many uncultivated microbes.

In the following paragraphs, I will explain how we can use 16S ribosomal RNA and functional gene sequences to infer bacterial biodiversity and abundance of anammox and denitrifying bacteria.

#### 1.2.3.1. Diversity of bacterial communities from 16S ribosomal RNA

The small 16S ribosomal subunit gene is central in contemporary molecular microbial ecology because it is present in all prokaryotes and shows functional constancy as it encodes a universal process in every organism (i.e. the manufacture of proteins). Furthermore, the gene is sufficiently long (1540 nucleotides) to provide information about evolutionary history, and horizontal transfer of rRNA genes is limited. The 16S rRNA gene is composed of several sequence domains that have evolved at different rates. Some domains have been conserved across all organisms whereas other regions in the sequence are specific at phylum to subspecies levels. It is thus possible to find nucleotide sequences in the 16S rRNA gene that are conserved across all organisms, to amplify these sequences using polymerase chain reaction (PCR), to perform alignment of

homologous positions with sequences of unknown and uncultivated organisms and to identify near-universally conserved and taxon-specific sequences.

Although 16S rRNA gene sequences allow us to infer microbial diversity and evolutionary relationships, this approach does not provide direct information on microbial physiology and function in the environment. Inferences are possible if a 16S rRNA sequence can be placed in a phylogenetic tree and the metabolisms of some of its closest relatives derived from cultured organisms are known. In such cases, we can suggest that the unknown organism shares some common metabolic characteristics with its closest relatives. Some prokaryotes mediating N cycle processes, for example γ-proteobacteria of the SUP05 cluster, and anammox bacteria can be identified with high confidence based on 16S rRNA gene sequences only. SUP05 bacteria couple the oxidation of reduced sulfur species with nitrate reduction (they only possess the *nirK* form of nitrite reductase, see section 1.2.3.2) and have been identified as major constituents of hydrothermal vent plumes and other sulfide-rich oxygen-deficient marine waters (Sunamura *et al*., 2004; Stevens and Ulloa, 2008; Lavik *et al*., 2009; Walsh *et al*., 2009; German *et al*., 2010; Zaikova *et al*., 2010).

#### 1.2.3.2. Diversity of the denitrifying bacterial communities from functional genes

In general, the processes that are less essential for the cell, for example denitrification, involve only a few genes. Therefore, mutation and gene transfer are more likely to lead to a variation in gene sequences and content, and the relationship between 16S rRNA phylogeny and metabolic function is weakened. Indeed, the ability to conduct

denitrification is found in many organisms that are, in fact, not closely related on the basis of their 16S rRNA sequences (Ward, 2005b). Furthermore, many 16S rRNA sequences of new organisms are not very similar to any cultivated strains so that physiological inferences are not possible.

Functional genes encode the essential enzymes necessary for biogeochemical transformations in the environment. As the main focus of my PhD was the assessment of N elimination in different oceanic environments, only the functional genes involved in the processes of denitrification (Figure 1.2) will be discussed below. For more information about the functional genes involved in other N cycle processes (i.e. nitrification and $N_2$ fixation), see Ward (2005b).

The reduction of nitrate to nitrite during denitrification is catalyzed by either the membrane-bound nitrate reductase (*nar*) encoded by the *narG* gene, or by the periplasmic nitrate reductase (*nap*) encoded by the *napA* gene (Bru *et al.*, 2007). Denitrifying bacteria contains either *narG*, *napA* or both genes (Carter *et al.*, 1995; Roussel-Delif *et al.*, 2005). Most organisms are only capable of performing nitrate reduction, that is, they cannot achieve complete denitrification (Zumft, 1997).

Nitrite reductase is one of the most important enzymes in denitrification because it is responsible for the transformation of dissolved solute (nitrite) to the gaseous pool (NO), thus removing bio-available N and potentially causing N limitation. There are two kinds of nitrite reductase enzymes with different mechanisms of reduction: *nirS* genes encode a cytochrome *cd1* nitrite reductase that contains only Fe in the active site and *nirK* genes encode an enzyme with Copper. Coyne *et al.* (1989) showed that *nirS* genes are more widely distributed and that *nirK* genes were present in only 30% of all known denitrifier

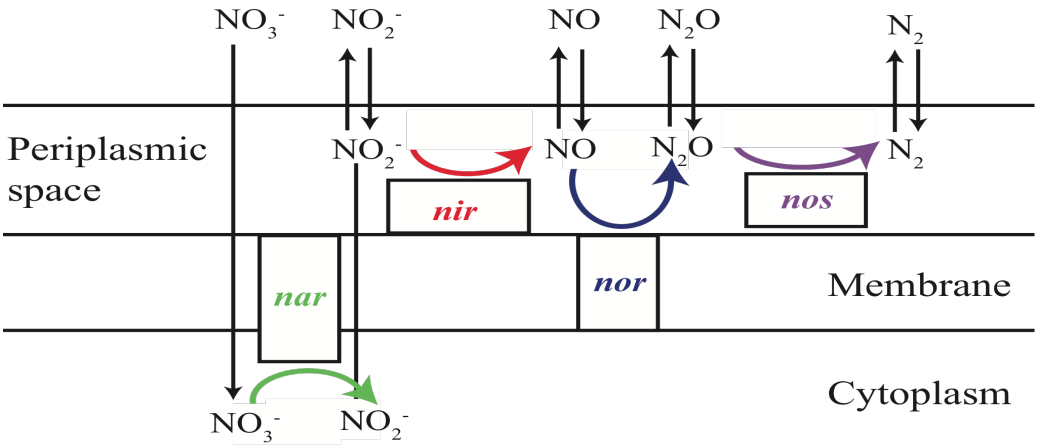


**Figure 1.2.** Enzymes involved in denitrification and their location relative to the cell's cytoplasmic membrane. *nar*: nitrate reductase; *nir*: nitrite reductase; *nor*: nitric oxide reductase; *nos*: nitrous oxide reductase (reproduced from Wallenstein *et al.*, 2006).

species. The final step of denitrification, i.e. the conversion of $N_2O$ to $N_2$, is catalyzed by nitrous oxide reductase, encoded by the periplasmic *nosZ* gene (Scala and Kerkhof, 1998; Stres *et al.*, 2004; Throbäck *et al.*, 2004; Chon *et al.*, 2009).

In the first part of this study, only the functional gene involved in the conversion of $NO_2^-$ to NO (more specifically *nirS*, due to the difficulty to amplify *nirK* in marine samples) will be considered for phylogenetic analysis.

#### 1.2.3.3. Abundance of denitrifiers and anammox bacteria from qPCR

During end-point PCR, a target gene is amplified over a number of cycle to be detectable and vizualized via agarose gel electrophoresis. However, there are biases introduced by this method because all genes within a mixed community are not amplified at equal efficiencies by the primers. The quantity of specific products also depends on PCR conditions or cycle numbers.

Quantitative real-time PCR (qPCR) is a technique used to amplify and simultaneously quantify specific DNA fragments but provides no information on community composition. Gene quantification is achieved during the initial cycles of PCR. At this point in the PCR, the amplification of target DNA is exponential and there are no introduced PCR biases. Fluorescence-based labeling techniques (i.e. *Taq* nuclease assay and SYBR green) are used to detect product yields, i.e. for every cycle, a fluorescent dye accumulates in direct proportion to the yield of amplified PCR product and the increase in fluorescence is recorded. Quantification under specific PCR conditions is achieved by determining the threshold cycle (Ct) at which the increase in fluorescence is above detection limits for a range of known standards and samples. Standard curves (Ct values of standards versus the log of their initial concentration) are prepared for each analysis. The proportion of specific phylotypes is generally expressed relative to the total microbial community determined using the 16S rRNA gene.

### 1.2.4. N cycle dynamics in hydrothermal vent systems and Saanich Inlet

#### 1.2.4.1. Hydrothermal vents

Hydrothermal vents, which have been proposed to be modern analogue to the Archaean anoxic primitive ocean where life originated, are earth surface fissures where geothermally heated and anoxic fluids are discharged and turbulently re-mixed with oxic sea water. The importance of low-temperature vents as a habitat for microbes (Juniper *et al*., 1995; Karl *et al*., 1995; Huber *et al*., 2002; 2003; Mehta *et al.*, 2003; 2005) and

macro-fauna (Tunnicliffe *et al.*, 1985; Hessler and Kaharl, 1985; Tunnicliffe, 1991) is well documented. These extreme environments are oases of life, harbouring a rich faunal community that depends mostly on the reducing power of chemicals dissolved in the hydrothermal fluids, particularly hydrogen sulfide. These reducing substances allow chemolithoautotrophic bacteria to convert carbon dioxide and nutrients into organic matter through chemosynthesis. Thus, chemolithoautotrophic bacteria represent the primary producers in this aphotic setting, which sustain the whole HV food chain. They are either free-living or closely associated with vent fauna through symbiotic relationships. In addition to seafloor biological communities that inhabit the vent discharge zone, microorganisms are known to live within the subsurface conduit system that leads to vent openings.

Little is known about metabolic processes and bacterially-mediated N-cycle dynamics in hydrothermal vents fluids and plumes. Denitrification, i.e. the utilization of nitrate for respiration during chemosynthetic $CO_2$ fixation, has previously been reported in these systems. Butterfield *et al.* (2004) observed nitrate depletion and the presence of both nitrite and nitrous oxide in discharging diffuse fluids at Axial Volcano on the Juan de Fuca Ridge, indicative of active denitrification in the subsurface environment. Bacterial symbionts living within the vestimentiferan *Riftia pachyptila* at the Genesis vent site on the East Pacific Rise and sulfur oxidizing bacteria of the genus *Beggiatoa* from the Guaymas Basin hydrothermal vents have been demonstrated to use nitrate in addition to oxygen as an electron acceptor for the oxidation of hydrogen sulfide (Hentschel and Felbeck, 1993; McHatton *et al*., 1996). More recently, Wang *et al.* (2009) and Xie *et al.* (2010), detected an almost complete spectrum of the functional genes required for

denitrification, i.e. *nar* (nitrate reductase), *nir* (nitrite reductase), *norB* (nitric oxide reductase) and *nosZ* (nitrous oxide reductase), in DNA extracted from hydrothermal vent chimneys of the Juan de Fuca Ridge using functional gene arrays (GeoChip) and metagenomic. Byrne *et al.* (2009) documented, for the first time, the diversity and activity of anaerobic ammonium-oxidizing bacteria mediating anammox in hydrothermal vents of the Mid-Atlantic Ridge. Anammox rates of 60 nmol N $l^{-1}$ $day^{-1}$ or less were derived using $^{15}N$ labeled incubations of hydrothermal chimney and animal samples crushed in sterile seawater under controlled laboratory conditions.

The isotopic composition of DIN in discharging hydrothermal vent fluids, which can potentially provide valuable information about N sources, sinks and transformations in the subsurface, has never been studied before. Hydrothermal vent ecosystems are likely to display unique N-isotope signatures. Rates of prime N-elimination processes (i.e. denitrification and anammox) and dissimilative nitrate reduction to ammonium (DNRA) and the bacterial communities that mediate major N elimination reactions have also never directly been characterized and/or quantified in diffuse vent fluids. Combined studies of N-cycle processes and the associated microbial community in HV systems is critical to better understanding 1) N (and ultimately carbon) transformations occurring in the subsurface biosphere, 2) fundamental patterns of N-isotope dynamics in extreme environments, 3) the effects of environmental factors on the activity and abundances of denitrifying and anammox bacteria, and 4) the role of HV systems in the global oceanic N cycle.

#### 1.2.4.2. Saanich Inlet

Saanich Inlet, a seasonally anoxic fjord, can be used as a natural laboratory to study N-elimination processes in intermittently oxygen deficient zones. The fjord generally shows inverse estuarine circulation (i.e. dense water flows out above the sill and less dense water circulates inward at the surface), is 24 km long, 7.2 to 0.5 km wide and has a maximum depth of ~230 m (Herlinveaux, 1962). The presence of a shallow sill (~70 m) prevents deep water circulation, and thus the re-supply of oxygen to the deep inlet throughout most of the year. Vertical mixing is generally low in the inlet because of weak tides and low winds and thus a mechanism is required to explain the observed high primary productivity during the spring and summer seasons. Gargett *et al.* (2003) proposed that strong spring tidal mixing outside the inlet could reverse the inverse estuarine flow and causes horizontal advective nutrient re-supply in surface waters, promoting phytoplankton blooms. Due to the high primary productivity in surface waters, and the aerobic respiration of the sinking organic matter, the bottom waters regularly become suboxic/anoxic and active denitrification sets in when $O_2$ concentration levels drop below 5μmol $L^{-1}$. Episodic renewal events, generally occurring during the fall, partially flush the anoxic nitrate-depleted bottom waters with oxygenated, nitrate-rich waters from outside the basin (Anderson and Devol, 1973, Gargett *et al.*, 2003).

Saanich Inlet is an ideal site to study denitrification and its sensitivity to changing environmental conditions (e.g., redox). Although Saanich Inlet, because of its size, is insignificant in the marine N cycle, it can be used as an analogue to study coastal eutrophication and understand global patterns of N dynamics in major OMZs of the ocean. Previous studies reported geochemical and microbiological evidence for the

occurrence of denitrification in Saanich Inlet (Cohen, 1978; Tortell *et al*., 2005; Walsh *et al*., 2009; Manning *et al*., 2010; Zaikova *et al*., 2010). However, the relative importance of different N consuming or producing processes in the water-column and the partitioning of water-column and sedimentary denitrification in anoxic bottom waters remained to be investigated.

## 1.3. Objectives and dissertation organisation

This dissertation is organized into six main chapters. The first (present) chapter provides a general introduction and background information to the dissertation, the three subsequent chapters present the first part of the dissertation: i.e. N sinks and transformations and the associated microbial community in the subsurface biosphere of hydrothermal vents of the Juan de Fuca Ridge, the last chapter presents the second part of the dissertation, i.e. a time-series study of dissolved inorganic N isotope dynamics in Saanich Inlet, and finally, a conclusion and future work outlook chapter is presented. The objectives for the 2nd to 5th chapters, representing the core of the dissertation, and written in the form of manuscripts either accepted, submitted, or in preparation to be submitted to scientific peer-reviewed journals, are presented below. I designed all experiments, collected all samples, generally performed all laboratory analyses and wrote the manuscripts documented in this dissertation, with the help of my supervisors and co-authors.

### 1.3.1. Part 1: N sinks, transformations and the associated microbial community in the subsurface biosphere of hydrothermal vents of the Juan de Fuca Ridge

Several hydrothermal vent sites at Axial Volcano (AV), Endeavour Segment (ES) and Cobb Segment (CS) on the Juan de Fuca Ridge in the northeast Pacific Oceans were sampled during 6 major cruises between 2004 and 2009. Clean hydrothermal vent fluid samples were collected and analyzed for nutrient as well as for other chemicals ($Mg^{2+}$, $H_2S$, $N_2O$ etc…) concentrations, DIN isotopic composition and rates of major N-elimination processes (denitrification and anammox) and DNRA. The biodiversity of 16S rRNA and *nirS* genes and abundance of denitrifiers (*nirS* genes and bacteria belonging to the SUP05 cluster) and anammox bacteria were also assessed using molecular biology methods.

The main general objectives of this part of the project were to use stable isotope and molecular biology methods to 1) elucidate DIN isotope dynamics to constrain N transformations and elimination; 2) determine rates and fluxes of N-loss processes and estimate the role of HV systems in the global N budget; 3) describe the biodiversity and abundance of the microbial communities responsible for N elimination and 4) investigate links between denitrifying bacteria diversity and abundance and environmental factors in HV fluids.

In the second chapter, published in *Geochemistry, Geophysics, Geosystems* in February 2012, we discuss, for the first time, the physical and biological processes affecting the concentration and isotope composition of DIN (nitrate $\delta^{15}N$ and $\delta^{18}O$ and ammonium $\delta^{15}N$) in both high and low-T fluids at hydrothermal vents of the Juan de Fuca Ridge. We present evidence for DIN isotope fractionation attributable to N consumption (either

assimilation or denitrification occurring in microbial mats/biofilms) in the subsurface biosphere of hydrothermal vents. We report on previously unseen nitrate N-to-O isotope anomalies, i.e. the deviation from the 1:1 relationship expected for nitrate assimilation and denitrification in marine environments, in the HV fluids, and use a simple isotope box-model to evaluate the possible nitrate regeneration processes responsible for the observed nitrate isotope anomalies.

In the third chapter, published in *Biogeosciences*, we examine the relative importance of potential rates of denitrification, anammox and DNRA in relation to specific microbial agents in diffuse hydrothermal vent fluids of the Juan de Fuca ridge using a combination of $^{15}N$ paired isotope labeling, 16S rRNA gene clone library sequencing and qPCR methods. We assess the diversity and abundance of potential sulfur-oxidizing denitrifiers and examined chemical and physical constraints on the activity and abundance of microbial communities that mediate biological N-loss in the subsurface of hydrothermal vents. This information is used to evaluate the role of the subsurface hydrothermal biosphere in the global oceanic N budget.

In the fourth chapter, submitted to *Geobiology*, we investigated the biodiversity and abundance of 16S rRNA and nitrite reductase (*nirS*) genes in the subsurface biosphere of hydrothermal vents of the Juan de Fuca Ridge, and consider possible links to environmental variables such as diffuse fluid temperature and chemistry (i.e., pH and $H_2S$, $NO_3^-$ and $NH_4^+$ concentrations). We examine *nirS* gene biodiversity in two fluid samples from two different vent fields: AV and ES, as well as *nirS* gene abundance in vent fluids from three different vent fields, i.e. AV, ES and CS. We used 16S rRNA gene pyrotag sequences from the hypervariable V1-V3 region to complement our *nirS* gene

data and describe overall bacterial and putative denitrifying communities in vent fluids, and to investigate similarities between vent fields. Finally, we use our results to assess the effect of environmental controls on *nirS* gene diversity and abundance.

### 1.3.2. Part 2: Time-series study of dissolved inorganic N isotope dynamics in Saanich Inlet, a British Columbia Fjord

In the fifth chapter of the dissertation, in preparation to be submitted to *Marine Chemistry*, we use a ~1 year time-series of nutrient concentrations and dissolved inorganic N isotopes ($\delta^{15}$N-$NH_4^+$ and $\delta^{15}$N and $\delta^{18}$O of $NO_3^-$) collected from April 2008 to April 2009 at a station close to the mouth of the Inlet to constraint N transformations and elimination. Major renewal events from September to October 2008 provided an unique opportunity to follow the development of anoxia and N-loss in bottom waters from a known starting point. We calculate nitrate isotope anomalies and discussed nitrate production processes that are affecting the nitrate isotopic signatures in both surface and bottom waters. We then estimate the isotope effect related to N-loss in bottom waters using Rayleigh closed and open system models as well as the proportion of sedimentary versus water-column denitrification following the bottom-waters renewal events.

During this project, a collaboration with Dr. Roberta Hamme and Cara Manning allowed to concomitantly collect samples for $N_2$/Ar measurements and calculate temporal biological $N_2$ production and denitrification rates. The resulting paper, which I co-authored, has been published in *Marine Chemisry* in 2010 (e.g. see Manning *et al*., 2010). My contribution was to organize all the Saanich Inlet cruises, help collect and analyze samples, and comment on the manuscript.

# Chapter 2
# Subseafloor nitrogen transformations in diffuse hydrothermal vent fluids of the Juan de Fuca Ridge evidenced by the isotopic composition of nitrate and ammonium[1]

## 2.1. Abstract

Little is known about dissolved inorganic nitrogen (DIN) transformations in hydrothermal vent (HV) fluids. Here, we present the first isotopic measurements of nitrate ($\delta^{15}N$ and $\delta^{18}O$) and ammonium ($\delta^{15}N$) from three HV fields on the Juan de Fuca ridge (NE-Pacific). The dominant process that drives DIN concentration variations in low-T diffuse fluids is water mass mixing below the seafloor, with no effect on the DIN isotope ratios. Strong inter-site variations in the concentration and $\delta^{15}N$ of $NH_4^+$ in high-T fluids suggest different subsurface nitrogen (N) sources (deep-sea nitrate versus organic sediments) for hydrothermally discharged ammonium. Low $NH_4^+$ community N isotope effects (<3‰) for net $NH_4^+$ consumption suggest an important contribution from gross ammonium regeneration in low-T fluids. Elevation of HV nitrate $^{15}N/^{14}N$ and $^{18}O/^{16}O$ over deep-sea mean isotope values at some sites, concomitant with decreased nitrate concentrations, indicate assimilatory or dissimilatory nitrate consumption by bacteria in the subsurface, with relatively low community N isotope effects ($^{15}\varepsilon_k$ < 3‰). The low N isotope effects suggest that nitrate assimilation or denitrification occur in bacterial mats,

[1] A version of this chapter has been published. Bourbonnais, A., M. F. Lehmann, D. A. Butterfield, and S. K. Juniper (2012), Subseafloor nitrogen transformations in diffuse hydrothermal vent fluids of the Juan de Fuca Ridge evidenced by the isotopic composition of nitrate and ammonium, *Geochemistry, Geophysics, Geosystems, 13*, Q02T01, doi:10.1029/2011GC003863.

*Please note that an error occurred during the copyediting of this paper: "Endeavor" Segment should be "Endeavour" Segment since this is a proper name. This change has been applied in the version of the manuscript presented in this dissertation.

and/or *in situ* production of low $\delta^{15}N$ nitrate. A significantly stronger relative increase for nitrate $\delta^{18}O$ than for $\delta^{15}N$ was observed at many sites, resulting in marked deviations from the 1:1 relationship for nitrate $\delta^{15}N$ versus $\delta^{18}O$ that is expected for nitrate reduction in marine settings. Simple box-model calculation show that the observed un-coupling of N and O nitrate isotope ratios is consistent with nitrate regeneration by either nitrite reoxidation and/or partial nitrification of hydrothermal ammonium (possibly originating from $N_2$ fixation). Our isotope data confirm the role of subsurface microbial communities in modulating hydrothermal fluxes to the deep ocean.

## 2.2. Introduction

The importance of low-temperature hydrothermal vents (HV) as a habitat for microbes (Jannasch and Mottl, 1985; Juniper *et al*., 1995; Huber *et al*., 2002, 2003; Butterfield *et al*., 2004; Mehta *et al*., 2003, 2005; Mehta and Baross, 2006) and macro-fauna (Tunnicliffe *et al*., 1985; Tunnicliffe, 1991) is well documented. These oases of life harbor high-biomass faunal communities that are sustained by chemoautotrophic bacteria (free-living or in symbiosis) at the base of the food chain, which gain metabolic energy from the oxidation of reducing substances in hydrothermal fluids, particularly hydrogen sulfide.

Nitrogen (N) is an essential nutrient for all vent organisms, as a building block of proteins, but also as a possible energy source. Generally high levels of $NH_4^+$ in high-T fluids (up to ~350°C) and $NO_3^-$ in low-T diffuse fluids (<~50°C) are discharged from HV, serving as potentially important substrate and N source for the chemolithotrophic

bacteria (Butterfield *et al*., 1997; Lam *et al*., 2004). Additional bioavailable N to fulfill the high N requirements of dense bacterial populations in HV systems may be procured through the fixation of molecular N even at temperatures close to the limits of life (Mehta *et al*., 2003, 2005; Mehta and Baross, 2006). On the other hand, denitrification, i.e., the nitrate reduction by chemosynthetic $CO_2$ fixing bacteria (or other suboxic modes of $N_2$ production) may remove $NO_x$ from low-temperature diffuse fluids (Butterfield *et al*., 2004). For example, it has been shown that sulfur-oxidizing bacteria can use nitrate as an electron acceptor for the oxidation of hydrogen sulfide in HV systems (e.g., Hentschel and Felbeck, 1993; McHatton *et al*., 1996). Moreover, Byrne *et al*. (2009) provided phylogenetic and biomarker evidence for the anaerobic oxidation of ammonium (anammox) to $N_2$ gas in deep-sea hydrothermal vents at the Mid-Atlantic Ridge. Anammox can account for a substantial loss of fixed N in various marine environments (e.g., Thamdrup and Dalsgaard, 2002; Dalsgaard *et al*., 2003; Kuypers *et al*., 2003, 2005; Hamersley *et al*., 2007).

The stable N isotope composition of vent organisms has previously been measured to study feeding ecology and trophic structure in HV systems. In earlier work, very low $\delta^{15}N$ (for definition see section 2.3.3) values (~−10 to +4‰) of HV organisms, for example, have been attributed to strong N isotope fractionation during chemosynthetic assimilation of ammonium or the local supply of $^{15}N$-depleted ammonium (Rau, 1981; Paull *et al*., 1985; Van Dover and Fry, 1994; Kennicutt and Burke, 1992; Van Dover, 2002).

As a result of specific isotope effects associated with N cycle transformation, N (and nitrate O) isotope ratios represent a useful tool to assess N fluxes within the ocean. $N_2$ fixation, the major input of bioavailable N to the ocean, adds new N with a $\delta^{15}N$ of ~−2–

0‰ (Carpenter *et al*., 1997, 1999; Montoya *et al*., 2002). The low-$\delta^{15}N$ organic N is subsequently remineralized to dissolved inorganic N (DIN) through coupled ammonification and nitrification, thus leaving clear N-isotopic signatures in the DIN pool (Sigman *et al*., 2005; Knapp *et al*., 2008; Bourbonnais *et al*., 2009). Water column denitrification in suboxic zones displays a strong kinetic N-isotope effect ($\varepsilon$) on the $NO_3^-$ $\delta^{15}N$ (Cline and Kaplan, 1975; Brandes *et al*., 1998a; Voss *et al*., 2001; Lehmann *et al*., 2003; Sigman *et al*., 2003, 2005), with values for $\varepsilon$ in the range of 15–30‰. Nitrate assimilation by algae or bacteria usually fractionates the N isotopes to a lesser extent, with most N-isotope effects reported for natural marine systems clustering around 5‰ (e.g., Altabet, 2001). While N isotopes alone can provide qualitative information on N-cycle transformations, their use is often limited because they do not allow for the quantitative separation of nitrate production and consumption. For example, the N isotope signals of $N_2$ fixation and denitrification can negatively interfere with each other. The coupled measurement of the nitrate N and O isotopic composition has the potential to disentangle nitrate consumption and production processes in environments where they occur simultaneously (or where water masses with the respective N isotope signatures are mixed together). The separation of nitrate consumption from production is possible because, in contrast to denitrification and nitrate assimilation, with a constant ratio of N versus O isotope enrichment of 1:1 in marine settings (Granger *et al*., 2004, 2008; Lehmann *et al*., 2005; Sigman *et al*., 2005), nitrate production affects the $\delta^{15}N$ and $\delta^{18}O$ of new nitrate in fundamentally different ways (Lehmann *et al*., 2003; 2004; Sigman *et al*., 2005; Wankel *et al*., 2007; Bourbonnais *et al*., 2009). The $\delta^{15}N$ of new nitrate is determined by the $\delta^{15}N$ of the organic matter being remineralized (Sigman and Casciotti,

2001). According to current understanding, oxygen isotopes in nitrified nitrate or from nitrite re-oxidation are mostly derived from oxygen in ambient water ($\delta^{18}O \sim 0‰$) and to a minor extent from dissolved oxygen ($\delta^{18}O$ between 23.5‰ and 40‰ in the ocean interior; Bender, 1990; Levine *et al*., 2009) (Andersson and Hooper, 1983; Kumar *et al*., 1983; DiSpirito and Hooper, 1986; Casciotti, 2002; Sigman *et al*., 2009). Hence, the $\delta^{18}O$ of newly generated nitrate is generally insensitive to the origin of the N being nitrified, be it from $N_2$ fixing organisms or from other bacterial/algal biomass. While observational data generally suggest that newly regenerated marine nitrate has a $\delta^{18}O$ close to that of seawater (i.e., ~1.4‰ (Sigman *et al*., 2009)), Buchwald and Casciotti (2010) and Casciotti *et al*. (2010) recently reported that oxygen atom incorporation during ammonium and nitrite oxidation occurs with significant isotope effects.

As outlined above, work over the last two decades has provided (mostly qualitative) evidence for multiple N-cycle reactions in HV systems. Nevertheless, the fate of ammonium that is hydrothermally injected into the water column, and water column nitrate that is mixed into anaerobic hydrothermal vent fluids, is still uncertain. N isotope data for DIN in the high-T fluids barely exist, and the effects N-transformations in the diffuse fluids and HV plumes can have on the subsurface DIN $\delta^{15}N$, prior to incorporation into the food chain, are unknown. HV ecosystems are likely to display unique DIN isotope signatures that may elucidate principal patterns of N (and O) isotope dynamics. In turn, the isotopic ratios of ammonium and nitrate should inform about the activity of ammonium-oxidizing and denitrifying organisms in this ecosystem. Also, in order to successfully use stable N isotopes for determining trophic structures in an

ecosystem, it is crucial to know the base-line $\delta^{15}N$, i.e., the $\delta^{15}N$ of the inorganic substrate that becomes metabolized by the chemosynthetic bacteria at the base of the food chain.

The main goal of this paper is to discuss, for the first time, the physical and biological processes that affect the concentrations and isotope composition of DIN (nitrate $\delta^{15}N$ and $\delta^{18}O$ and ammonium $\delta^{15}N$) in both high and low-T fluids at the Endeavour and Cobb Segments, and Axial Volcano on the Juan de Fuca Ridge (NE-Pacific). We see evidence for DIN isotope fractionation due to N consumption by assimilative N-uptake and denitrification in microbial mats/biofilms within the hydrothermal conduits. We also report on previously unseen nitrate N-to-O isotope anomalies in the HV fluids, and we present our results in light of a simple isotope box-model, which allows us to interpret the nitrate isotope anomalies as evidence for nitrate regeneration through a combination of nitrification and nitrite reoxidation processes.

## 2.3. Material and Methods

### 2.3.1. Site Description and Sample Collection

Hydrothermal vent fluids were sampled at different sites on Axial Volcano, and the Cobb and Endeavour Segments during five summer/autumn cruises between 2004 and 2009 onboard the R/V *Thomas G. Thompson* and R/V *Atlantis*, as part of the New Millennium Observatory (NEMO) and Endeavour-Axial Geochemistry and Ecology Research (EAGER) Projects (Figure 2.1a). The Endeavour and Cobb Segments are located at ~48°N, 129°W and ~46.7°N, 129.4°W, respectively (Figure 2.1a). Four

different vent fields were visited at Endeavour Segment: Sasquatch, High Rise, Main Endeavour Field (MEF) and Mothra (Figure 2.1b). The vents are located at a depth of ~2200–2100 m. Even though Endeavour Segment is sediment-free, it is believed that high concentrations of methane and ammonium observed in hydrothermal fluids originate from the decomposition of organic matter buried at an early stage of the ridge segment's evolution (Lilley *et al*., 1993). Cobb Segment was visited only in 2007 during an exploration dive. The temperature of high-T vent fluids at Cobb Segment is generally lower than at Endeavour, and venting is less vigorous. Axial Volcano (~46°N, 130°W) rises 1100 m above the surrounding ocean floor and has a 3-sided caldera. Active vent sites are located along the caldera boundary fault and along the intersection of the north and south rift zone with the caldera boundary fault at depths of 1500 to 1540 m below sea level (Embley *et al*., 1990; Butterfield *et al*., 2004). The latest eruptions occurred in the Southeast portion of the caldera in 1998 and more recently in 2011 (Figure 2.1c).

Low- and high-T fluids were collected using titanium syringe major samplers (760 ml), collapsible plastic bags with valves (up to 800 ml), and PVC piston samplers with Teflon spring seals on the Hydrothermal Fluid and Particle Sampler (HFPS), using the remotely operated vehicles (ROV) ROPOS and JASON, and the deep submergence vehicle (DSV) ALVIN. *In situ* temperature with HFPS was recorded at 1 Hz during sampling. The values reported here represent the average temperature during sample collection. In general, several sub-samples were collected at each site during each dive, and only the average values for the measured parameters are reported. Samples for nutrient concentration and isotopic measurements were transferred with a syringe into acid-washed and DI-rinsed 60-ml HDPE brown bottles. All fluid samples were purged with

$N_2$ gas for at least 10 min to remove $H_2S$, which interferes with the colorimetric nutrient analysis. Water samples were kept frozen at −20°C until analysis. Additional sample aliquots were collected in 15 ml acid-washed and DI-rinsed HDPE bottles for onshore major element (i.e., $Mg^{2+}$ in this study) analysis at the Pacific Marine Environmental Laboratory and the University of Washington.

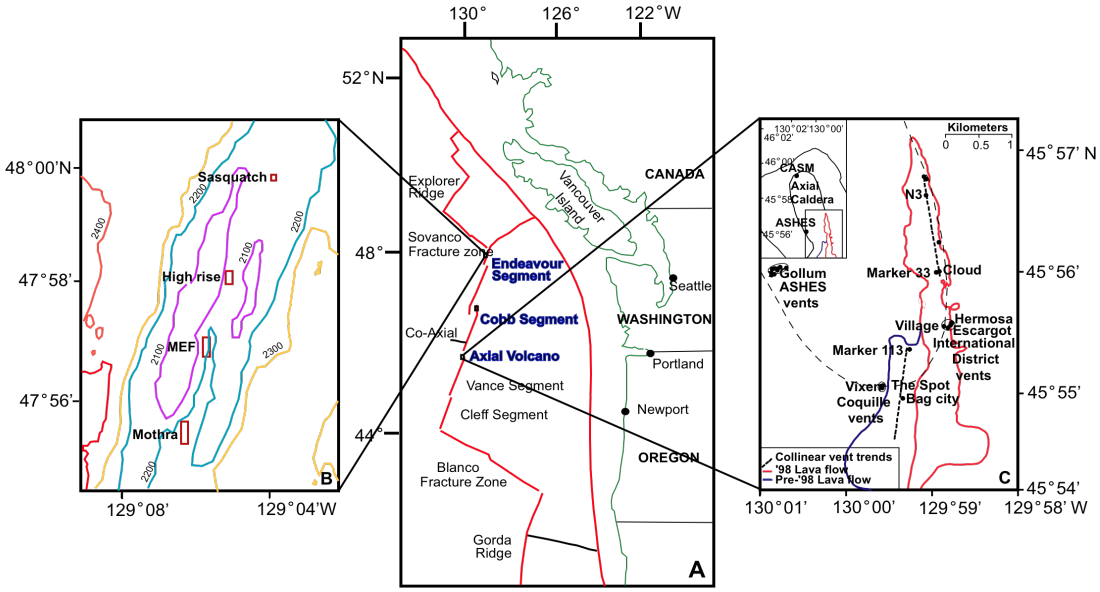


**Figure 2.1.** (**a**) Map of Axial Volcano and the Endeavour and Cobb Segments on the Juan de Fuca Ridge. (**b**) Endeavour Segment and the four major hydrothermal vent fields sampled (Sasquatch, High Rise, Main Endeavour Field and Mothra); (**c**) the summit caldera of Axial Volcano on the Juan de Fuca Ridge with enlarged view or the Southeast portion of the caldera, where an eruption occurred in 1998. The curved dashed line represents the caldera boundary fault where active vent sites are located (modified from Plate 1 in the study by Butterfield *et al*. (2004)). Black dots represent sampled vents. Only vents discussed in the text or in figures are labeled.

### 2.3.2. Nutrient Concentrations

Nitrate, nitrite, ammonium, and phosphate concentrations were analyzed onboard or

onshore using standard colorimetric techniques. In addition, for many samples, $NO_x$ was measured by reduction to nitric oxide (NO) in a heated solution of acidic vanadium (III) and subsequent detection of the NO (Braman and Hendrix, 1989), with a precision for replicate analyses of ±0.2 $\mu$mol/L. The agreement between methods was excellent, and average concentrations are reported, where applicable. $Mg^{2+}$ concentration measurements were performed by ion-chromatography (IC) and by successive titration with EDTA and EGTA for [$Mg^{2+}$] greater than ~48 mmol/kg.

### 2.3.3. Nitrate N and O isotope ratios

Nitrate N and O isotope ratios (denoted as $\delta^{15}N$ and $\delta^{18}O$, with $\delta = (R_{sample}/R_{standard}) - 1] \times 1000$, where R represents the ratio of $^{15}N$ to $^{14}N$ or $^{18}O$ to $^{16}O$, respectively) for samples collected between 2006 and 2009 were measured using the "denitrifier method" (Sigman *et al*., 2001; Casciotti *et al*., 2002). Samples collected in 2004, which were only analyzed two years after sample collection, are not considered, as we found clear evidence for biasing storage effects. The denitrifier method is based on the quantitative conversion of sample nitrate to $N_2O$ by cultured denitrifying bacteria that lack the active $N_2O$-reductase enzyme. $N_2O$ gas was automatically extracted, purified and analyzed online using Tracegas-Isoprime or GasBench II preparation systems coupled to a continuous flow isotope ratio mass spectrometer (IRMS) (Micromass Isoprime Multiflow for samples from 2006 to 2007 and Thermo Finnigan DELTA$^{plus}$ XP for samples from 2008 to 2009). The general target sample size was 20 nmol N for samples with a [$NO_3^-$] > 5 $\mu$mol/L, and 10 nmol N for samples with a [$NO_3^-$] < 5 $\mu$mol/L. *Pseudomonas chlororaphis* (ATCC

#43928) and *P. chlororaphis* (ATCC #13985) (formerly *Pseudomonas aureofaciens*) were used to measure $\delta^{15}N$ and $\delta^{18}O$, respectively. N and O isotope ratios are reported in ‰ relative to atmospheric $N_2$ for N and V-SMOW for O isotopes, respectively. Isotope values were calibrated using an international $KNO_3^-$ reference material (IAEA-N3) with an assigned $\delta^{15}N$ value of +4.7‰ (air) and a reported value of 25.6‰ for $\delta^{18}O$ (V-SMOW) (Böhlke *et al*., 2003). Replicate reproducibility (i.e., the standard deviation of replicate measurements) for the method was generally better than ±0.2‰ for $\delta^{15}N$ and ±0.4‰ for $\delta^{18}O$. For all samples collected before 2008, O isotope data were corrected for O isotope exchange with water during the reduction of nitrate to nitrous oxide, following the scheme described by Casciotti *et al*. (2002), using standards prepared from DI water with a $\delta^{18}O$ of ~865‰-V-SMOW. O-isotope exchange was always less than 5%. Blank contribution was generally below 0.5 nmol (i.e., 3–5% of the target sample size). Correction for O isotope scale contraction caused by O isotope exchange with water is more accurate when multiple nitrate isotope reference materials are used, i.e., IAEA-N3 and USGS-34 (Casciotti *et al*., 2007). This standard bracketing correction has been applied to all 2008 and 2009 samples. Sigman *et al*. (2009) recently reported a systematic difference between the two correction schemes, where the older correction protocol resulted in a slight overestimation of the $\delta^{18}O$ of deep-sea nitrate. Our measurements comply with this observation, and we corrected pre-2008 data accordingly.

The presence of nitrite in mixed samples is known to interfere with the isotopic analysis of nitrate when using the denitrifier method (Granger *et al*., 2006; Casciotti and McIlvin, 2007; Casciotti *et al*., 2007; Granger and Sigman, 2009), because both nitrite and nitrate are converted to $N_2O$. For mixed samples calibrated against nitrate isotope

standards, the presence of nitrite leads to artificially low $\delta^{18}O$ values because of the differential O isotope effects during nitrate versus nitrite reduction to $N_2O$. According to Casciotti *et al*. (2007), the presence of 2% or more of nitrite in a sample can significantly modify the original $\delta^{18}O$. Nitrite concentrations were always lower than ~2 $\mu$mol/L in our diffuse fluid samples (see below) and never higher than 10% of the sum of nitrate and nitrite. In 2008/2009 samples, where the $NO_2^-$ concentrations exceeded 1%, the isotopic composition of nitrate was measured only after nitrite removal with sulfamic acid, following the procedure by Granger and Sigman (2009). For the few samples that contained significant $NO_2^-$ concentration (>2% of the total $NO_x$) and that were analyzed prior to 2008 (and originally calibrated against nitrate isotope standards), we approximated the $\delta^{18}O_{NO3+NO2}$ using the correction factors for $NO_2^-$ on the nitrate calibration scale based on the analysis of pure nitrite standards (Casciotti and McIlvin, 2007; Casciotti *et al*., 2007).

#### 2.3.4. Ammonium N isotope ratios

The $\delta^{15}N$ of ammonium was measured using a combination of the passive ammonia diffusion method (Sigman *et al*., 1997) with persulfate oxidation (Knapp *et al*., 2005) and the denitrifier method (Sigman *et al*., 2001) (also see Houlton *et al*., 2007). Two to fifty ml of hydrothermal vent fluid (60–700 nmol sample ammonium) were pipetted into 30–60 ml glass media bottles. High-concentration samples were diluted with DI to yield at least 10 ml sample solution. A $NH_3$(g) trap consisting of a 5 $mm^2$, pre-combusted (500°C for 4 h) and acidified (~5–10 $\mu$L of 4 N $H_2SO_4$) GF/D glass fiber filter sandwiched

between two sealed Teflon membranes (Millipore, LCWP01300) (Sigman *et al*., 1997), was added to the media bottles. Prior to closing the bottles with a Teflon septum and an aluminum seal, pH was raised significantly above 9.2 by adding MgO (60 mg per ~10 ml sample). Samples were agitated on an orbital shaker at room temperature for 7 days to warrant complete ammonium conversion to $NH_3$(g) under basic conditions, and $NH_3$ trapping in the diffusion packages. The $NH_3$ traps were then removed from the sample bottles, dipped into a 10% HCl solution, and, without any drying step, placed in 10-ml autoclave glass tubes with 6.5 mL of DI water. The test tubes were shaken vigorously in order to open the $NH_3$ traps and release the acidified disks, and the Teflon membranes were removed using clean dull-tipped forceps; these steps have proven to be important for 100% N recovery (without losing some $(NH_4)_2SO_4$ precipitate on the inner surface of the Teflon membranes). One mL of persulfate oxidizing reagent (POR), freshly made daily by dissolving 6 g of certified ACS-grade NaOH and 6 g of certified ACS-grade potassium persulfate (re-crystallized three times in 100 ml of DI water) (Knapp *et al*., 2005; Bourbonnais *et al*., 2009), was then added, and the closed tubes were autoclaved for at least one hour to allow complete ammonium oxidation to nitrate by the POR. After pH adjustment with ACS-grade HCl (pH ~ 3–4), the N isotopic composition of the ammonium-derived nitrate was determined using the denitrifier method as described above. $\delta^{15}N$ values were calibrated with $NH_4^+$ standards of known isotopic composition (IAEA N1, $\delta^{15}N$ of $NH_4^+$ = 0.4‰ and IAEA N2, $\delta^{15}N$ of $NH_4^+$ = 20.3‰), which were processed the same way as the samples, taking the procedural blank into consideration (generally less than 10%). For each standard/sample batch, DI additions and total N

amount were adapted to the N content and volume of the samples. Multiple N isotope analyses of $NH_4^+$ standards showed that the passive ammonia diffusion/oxidation/ denitrifier method produces accurate and reproducible (< ±0.6‰) results. Although we did not observe a marked N isotope fractionation during incomplete N recovery, only the samples with a ~80–100% yield were considered. Most 2008 and 2009 samples with $[NH_4^+]$ higher than ~100 μM were also analyzed using passive ammonia diffusion followed by direct combustion of the $NH_4^+$-loaded filters (sample requirement ~5000 nmol N) in a Thermo Finnigan FlashEA 1112 series Elemental Analyzer coupled to an IRMS (Thermo Finnigan Delta Advantage). Results from both $NH_4^+$ N-isotope techniques agreed well.

## 2.4. Results and discussion

### 2.4.1 Origin and fate of hydrothermally discharged ammonium

During high-T hydrothermal circulation, $Mg^{2+}$ is almost completely removed from the aqueous solution through various water-rock reactions (Edmond *et al*., 1979; Seyfried, 1987). At lower temperatures, mixing of hydrothermal fluids with $Mg^{2+}$-rich and cold seawater elevates the $[Mg^{2+}]$ again. Hence, a linear (inverse) relationship between the temperature of the HV fluid and its $Mg^{2+}$-content exists ($r^2 = 0.90$, Figure 2.2). $[Mg^{2+}]$ can thus be used as an indicator of mixing between zero-$Mg^{2+}$ pure high-T hydrothermal fluids and $Mg^{2+}$-rich (52.9 mmol/kg) low-T crustal seawater.

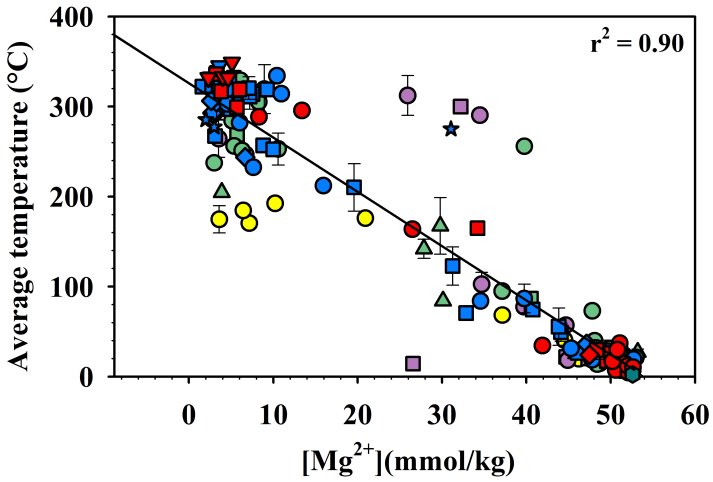


**Figure 2.2.** Magnesium concentrations versus average fluid temperatures at Endeavour Segment (star = Sasquatch, down triangle = High Rise, square = Main Endeavour Field, diamond = Mothra), Cobb Segment (triangle) and Axial Volcano (circle). Magnesium is almost completely removed from the hydrothermal vent fluids at higher temperatures and only slowly removed at lower temperatures. The colors represent the sampling years (yellow = 2004, purple = 2006, green = 2007, blue = 2008 and red = 2009). Standard deviation for sub-samples (n= 2 to 5) collected during the same dive and location is indicated.

Ammonium is the dominant DIN species under the highly reducing conditions encountered in high-T fluids (~200°C to 350°C, or <10 mmol/kg $Mg^{2+}$), with average concentrations decreasing from North to South along the Juan de Fuca Ridge: 1078 ± 4.7 µmol/L (n = 2) at Sasquatch, 863 ± 129 µmol/L (n = 11) at High Rise, 410 ± 53 µmol/L (n = 23) at MEF, and 396 ± 20 µmol/L (n = 5) at Mothra at the Endeavour Segment, 44 µmol/L (n = 1) at Cobb Segment, and 14 ± 3 µmol/L (n = 22) at Axial Volcano (Figures 2.3b–2.3d). $NH_4^+$ concentrations behave mostly conservatively with respect to $Mg^{2+}$, indicating the dilution of high-$NH_4^+$ hydrothermal fluids with zero-$NH_4^+$, oxygenated deep-seawater.

The $\delta^{15}N$ of ammonium in high-T fluids of the Endeavour Segment did not differ among years, but differs significantly among sites, with average values (all years combined) of 4.3 ± 0.7‰ (n = 3) at Sasquatch, 4.2 ± 0.5‰ (n = 11) at High Rise, 3.6 ± 0.4‰ (n = 19) at MEF and 3.1 ± 0.3‰ (n = 5) at Mothra (Figure 2.4a) (Kruskal-Wallis, p-value = 0.009). Since we were primarily interested in variations among vent fields, we grouped the values at the four Endeavour Segment sites for the subsequent discussion. It should be noted that the low average ammonium $\delta^{15}N$ in high-T vent fluids of the Endeavour Segment (3.7 ± 0.6‰ (n = 37)) does not closely match the only existing report on the N isotopic composition of $NH_4^+$ in hydrothermal fluids by Lilley *et al*. (1993), who measured a $\delta^{15}N$ value of 12.4‰, but is consistent with a $\delta^{15}N$ of 2.1‰ for an extinct sulfide chimney from Dante (at MEF) collected during the 2009 cruise (unpublished data).

The average Endeavour Segment ammonium $\delta^{15}N$ was significantly different from the $\delta^{15}N$ of nitrate in Deep-Pacific seawater at ~2100 m depth (5.6 ± 0.2‰ (n = 5), p-value = 0.0003). The average $\delta^{15}N$ of ammonium in high-T fluids of the Cobb Segment was 4.1 ± 0.1‰ (n = 3), i.e., not significantly different from the $\delta^{15}N$ of ammonium at Endeavour Segment (Figure 2.4a). In contrast, the average $\delta^{15}N$ of ammonium in high-T fluids at Axial Volcano was 6.7 ± 1.0‰ (n = 16) (Figure 2.4c), significantly greater than the $\delta^{15}N$ observed at the Endeavour (p-value = $8 \times 10^{-9}$) and Cobb (p-value = 0.007) segments, but not significantly different from the $\delta^{15}N$ of deep-seawater nitrate in the ambient water column at ~1200-1500 m depth (6.4 ± 0.2‰, n = 4) (Figure 2.4c).

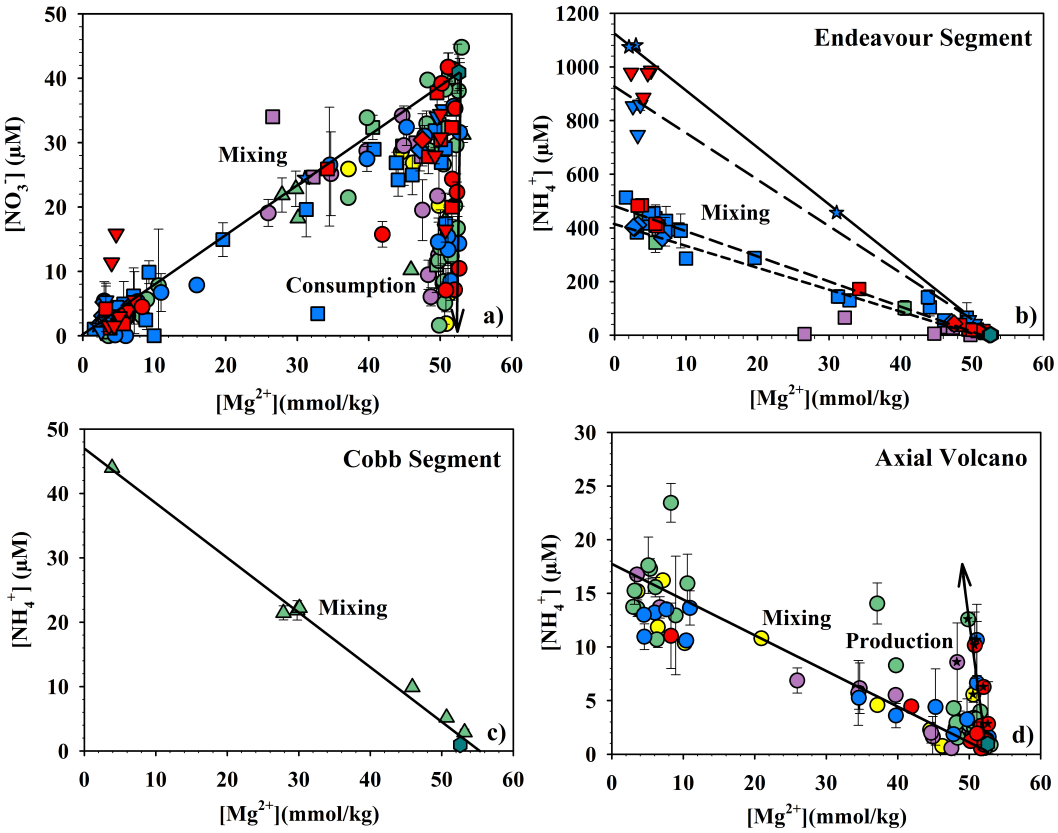


**Figure 2.3. a**) Nitrate (all sites) and ammonium concentrations at **b**) Endeavour Segment, **c**) Cobb Segment and **d**) Axial Volcano versus [$Mg^{2+}$] (note the different scales of the Y axis). In low-T vents, nitrate concentrations that fall below the mixing line between zero-nitrate, ammonium-rich, pure hot hydrothermal vents and nitrate-rich crustal seawater are indicative of microbial nitrate consumption. Ammonium concentration above ~0 µmol/L in low-T waters at Axial Volcano, occurring mainly at the site Marker 113 and its surrounding areas (black stars), is a sign of microbial ammonium production. Symbol and color scheme as in Figure 2.2 legend. The seawater end-member is represented by a turquoise hexagon. Regression lines in **b**): Sasquatch = solid line, High Rise = long dash, Main Endeavour Field = medium dash and Mothra = short dash). Standard deviations for sub-samples (n= 2 to 5) are indicated by the error bars.

Assuming no secondary alterations due to microbial or thermic processes, the $\delta^{15}N$ of ammonium in high-T fluids should reflect that of the original N source. During high-T subsurface hydrothermal circulation, under reducing conditions, nitrate from the deep sea

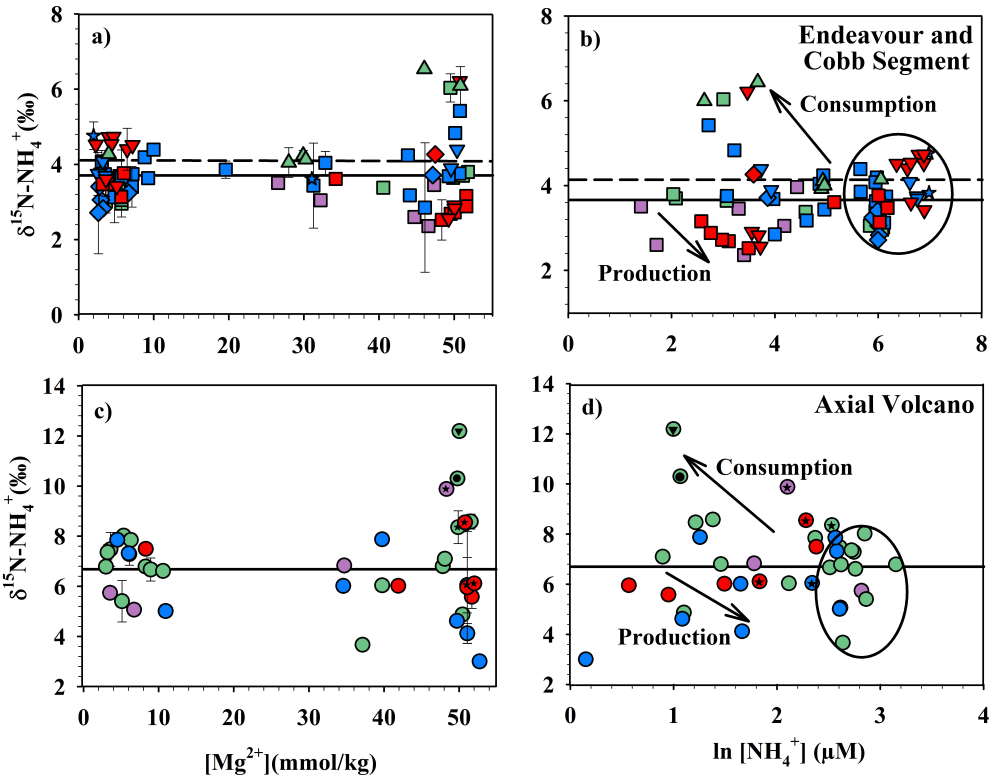


**Figure 2.4.** $\delta^{15}N$–$NH_4^+$ versus [$Mg^{2+}$] and ln [$NH_4^+$] at Endeavour and Cobb Segments (**a, b**), and Axial Volcano (**c, d**). The average $\delta^{15}N$-$NH_4^+$ in high temperature fluids is indicated by the horizontal lines (dashed line for Cobb Segment). Symbol and color scheme as in Figure 2.2 legend. In **b** and **d**, high-T end-members are encircled. The highest $^{15}N$ isotope enrichment was observed at Axial Volcano: Marker 113 (black stars), The Spot (circle), and CASM (down-triangle).

can be abiotically converted to ammonium by transition metal oxides and sulfides as it infiltrates the subsurface through cracks and fissures (e.g., Brandes *et al*., 2008). By mass balance, if fixed N is neither consumed nor produced during high-T reactions, discharging hydrothermal waters should contain $NH_4^+$ at concentrations (and N isotopic composition) that are equivalent to the nitrate of inflowing crustal waters with a deep-sea origin (i.e., ~40 $\mu$mol/L), at least at the un-sedimented (i.e., no apparent organic N source) hydrothermal systems of the Juan de Fuca Ridge. In this context, the elevated ammonium concentrations observed at the un-sedimented Endeavour Segment appear

anomalous (Fig. 2.3b). These have been argued to originate from the decomposition of subsurface organic material in sediments buried at an earlier stage of the ridge formation. Pleistocene turbidite flows from deposits located about ~40 km north of the Juan de Fuca Ridge might be the source of these sediments (Lilley *et al*., 1993). If OM from these deposits was indeed the source for the ammonium at Endeavour, their $^{15}N$ content must have been low compared to the mean $\delta^{15}N\text{-}NO_3^-$ of deep-seawater.

Ammonium can, in theory, also be produced by abiotic reduction of $N_2$ by Fe-minerals in the subsurface high-T hydrothermal fluids, producing newly fixed $NH_4^+$ with a low $\delta^{15}N$ (Brandes *et al*., 1998b; Schoonen and Xu, 2001; Dörr *et al*., 2003). It is widely accepted that the $\delta^{15}N$ of newly fixed N is close to the $\delta^{15}N$ of the dissolved $N_2$, which can either originate from a magmatic source (with a $\delta^{15}N$ value of $-5 \pm 2$‰ (Javoy and Pineau, 1991; Marty and Humbert, 1997)) or from circulating deep-seawater (with a $\delta^{15}N$ value of ~0‰). As pointed out by Lilley *et al*. (1993), it is unlikely that abiotic $N_2$ fixation would occur to such extent only at the Endeavour and Cobb Segments. Moreover, it can be predicted that the average $\delta^{15}N$ of hydrothermal ammonium would be even lower than 3.7‰, at least if high-temperature $N_2$ fixation was the main ammonium source.

At Axial Volcano, the similarity of the $\delta^{15}N$ of ammonium in high-T fluids and deep-seawater nitrate (6.7‰ and 6.4‰, respectively) suggests that seawater nitrate that penetrates from the water column into the anaerobic subsurface through cracks and fissures represents the substrate for complete abiotic reduction to ammonium. However, the ammonium-N concentration in high-T fluids of Axial Volcano was lower than the nitrate-N concentration in the Deep-Pacific by ~26 $\mu$mol/L. This difference, indicating

the net loss of fixed N in the high-T fluids, is likely caused by high-T ammonium ion substitution in secondary minerals during fluid interactions with basaltic rocks. For instance, Hall (1989) and Busigny *et al*. (2005) observed that N (mainly occurring as ammonium ions substituting for $K^+$ and $Na^+/Ca^{2+}$ in minerals) indeed gets enriched in rocks during basalts alteration. Details of the actual N removal mechanism aside, the accordance of the $\delta^{15}N$ of inflowing nitrate and of high-T end-member ammonium implies that the N scavenging in hot hydrothermal fluids must occur without significant N isotope fractionation. In the same line, Holloway *et al*. (2011) found that the $\delta^{15}N$ of ammonium in hydrothermal waters of the Yellowstone National Park with a pH < 5 (the pH range for the high-T fluids in this study was ~3.5 to 5) remained more or less unaffected by water rock interactions.

### 2.4.2. Biological uptake and isotopic fractionation of ammonium N in low-T fluids

Ammonium in low-T fluids (<~50°C) of the subsurface biosphere of hydrothermal vents can be produced either by organic matter remineralization (of both sedimentary and *in situ* produced organic N, e.g., by biotic $N_2$ fixation; Mehta *et al*., 2003, 2005; Mehta and Baross, 2006), and/or dissimilative nitrate reduction to ammonium (DNRA), which has been demonstrated to occur at temperatures up to 70°C (Vetriani *et al*., 2004; Voordeckers *et al*., 2005; Perez-Rodriguez *et al*., 2010). On the other hand, ammonium can be consumed by biological processes in low-T fluids, displaying distinct N-isotope effects, such as ammonium assimilation, aerobic microbial ammonium oxidation (Lam *et al*., 2004; 2008), or anammox (Byrne *et al*., 2009).

In most cases where ammonium concentration gradients appeared to behave conservatively with respect to $Mg^{2+}$, the $\delta^{15}N$ was invariant, confirming simple mixing of high-$NH_4^+$ hydrothermal waters with zero-$NH_4^+$ seawater in low-T hydrothermal fluids (Figures 2.3b–2.3d and 2.4). However, at some sites of the Endeavour Segment and Axial Volcano, net ammonium production or consumption are evidenced by concentrations above or below those expected from conservative mixing in the low-T hydrothermal fluids (Figures 2.3b and 2.3d). Net ammonium production, either via partial DNRA, organic matter remineralization or the $N_2$ fixation/remineralization cycle, corresponded with a decrease of $\delta^{15}N$-$NH_4^+$ with increasing [$NH_4^+$] in low-T fluids (i.e., Hulk at MEF and Hermosa, Vixen, Village and Escargo at AV; Figures 2.4b and 2.4d).

Anomalously high ammonium concentrations were observed at Marker 113 diffuse vent fluids during all sampling campaigns (Figure 2.3d). Yet the $\delta^{15}N$-$NH_4^+$ was either similar to the high-T end-member value or even greater (up to ~10‰, Figures 2.4c and 2.4d), which appears inconsistent with ammonium production by $N_2$ fixation or N isotope fractionation during partial DNRA (both processes would act to produce low $\delta^{15}N$-$NH_4^+$). Remineralization of high $\delta^{15}N$ organic material to ammonium can also not account for the elevated $\delta^{15}N$-$NH_4^+$ values. Reported values of $\delta^{15}N$ of hydrothermal vent fauna are generally low (~−10 to +4‰ (Rau, 1981, and reference therein)), as was the $\delta^{15}N$ of particulate material collected at Axial Volcano sites (4.6 ± 0.2‰ at Marker 33 and Gollum, 2009 cruise, unpublished data; 4.3 ± 1.2‰; Levesque *et al*., 2005). Therefore, we conclude that the elevated ammonium $\delta^{15}N$ values reflect N-isotope fractionation during partial ammonium consumption by bacterial assimilation or nitrification occurring in tandem with ammonium production by processes mentioned earlier. That is, while net

ammonium production is evidenced by non-conservative behavior of the ammonium concentration, the $\delta^{15}N$ indicates that ammonium consumption occurs concurrently. The ammonium $^{15}N$ enrichment was also observed at other sites, where $NH_4^+$ was clearly consumed relative to conservative mixing (up to ~5.5‰ at CASM, Axial Volcano; Figs 2.4c and 2.4d).

The net ammonium consumption N isotope effect can be estimated from the correlation between the natural logarithm of the ammonium concentration and the $\delta^{15}N$ of the residual ammonium (closed-system Rayleigh Model; Mariotti *et al*., 1981). However, open-system aspects and spatial/temporal variability in both the ammonium concentration and $\delta^{15}N$ are likely to prevent any clear Rayleigh-type ammonium N isotope dynamics (Figures 2.3 and 2.4), and, even more importantly, *in situ* regeneration of $NH_4^+$ and the N isotope effects associated with this regeneration will bias estimates for $\varepsilon_{uptake}$ for natural assemblages of bacteria in the diffuse HV fluids. Furthermore, the N isotope effects during ammonium oxidation ($\varepsilon$ = +14 to +38‰; Delwiche and Steyn, 1970; Mariotti *et al*., 1981; Yoshida, 1988; Casciotti *et al*., 2003) and ammonium assimilation ($\varepsilon$ = +14 to +27‰; Hoch *et al*., 1992; Waser *et al*., 1998) by microorganisms and algae in aquatic systems are highly variable and likely influenced by environmental conditions (e.g., substrate concentration and uptake rate), making it difficult to tell the two processes apart based solely on the degree of N-isotope enrichment. A plot of $\delta^{15}N\text{-}NH_4^+$ versus the ln $[NH_4^+]$ (Figures 2.4b and 2.4d) does not indicate obvious Rayleigh-type N-isotope dynamics. A significant relationship between $\delta^{15}N\text{-}NH_4^+$ and ln $[NH_4^+]$ was only observed at Cobb Segment in 2007 ($\varepsilon$ = 1.2‰, $r^2$ = 0.7) and Axial Volcano in 2006 ($\varepsilon$ = 2.6‰, $r^2$ = 0.3), although sample sizes for these data sets were limited. The computed ammonium N

isotope effects can be taken as community N-isotope effects for net ammonium removal, and were much lower than both the N isotope effect expected for aerobic (and anaerobic) ammonium oxidation, as well as for ammonium assimilation at elevated $NH_4^+$ concentrations (Hoch *et al*., 1992). Clearly, production of low-$\delta^{15}N$ $NH_4^+$ occurs through gross ammonium regeneration.

While the $\delta^{15}N$-$NH_4^+$ data alone do not allow us to constrain the actual ammonium removal pathway (uptake versus nitrification) the nitrate N and O isotopes in combination with elevated $\delta^{15}N$-$NH_4^+$ at Marker 113 suggest that partial nitrification of ammonium to nitrate must occur to some extent. The nitrate N and O anomalies that appear to be indicative of nitrate regeneration are discussed in detail below (see section 2.4.4).

### 2.4.3. Nitrate consumption and associated N and O isotope effects in hydrothermal vent fluids

Nitrate $\delta^{15}N$ and $\delta^{18}O$ values close to the N and O isotopic composition of ambient seawater nitrate (~6‰ and 2‰, respectively) (Figures 2.5a–2.5d) suggest that nitrate in both high and low-T (<~50°C) HV fluids mainly originates from mixing with nitrate-replete crustal seawater (~40 $\mu$mol/L in the deep northeast Pacific Ocean). At several low-T fluids sites, however, elevated nitrate $\delta^{15}N$ and $\delta^{18}O$ (i.e., high $Mg^{2+}$) (Figure 2.5), concomitant with decreased [$NO_3^-$] (Figure 2.3a), were observed. This clearly indicates a

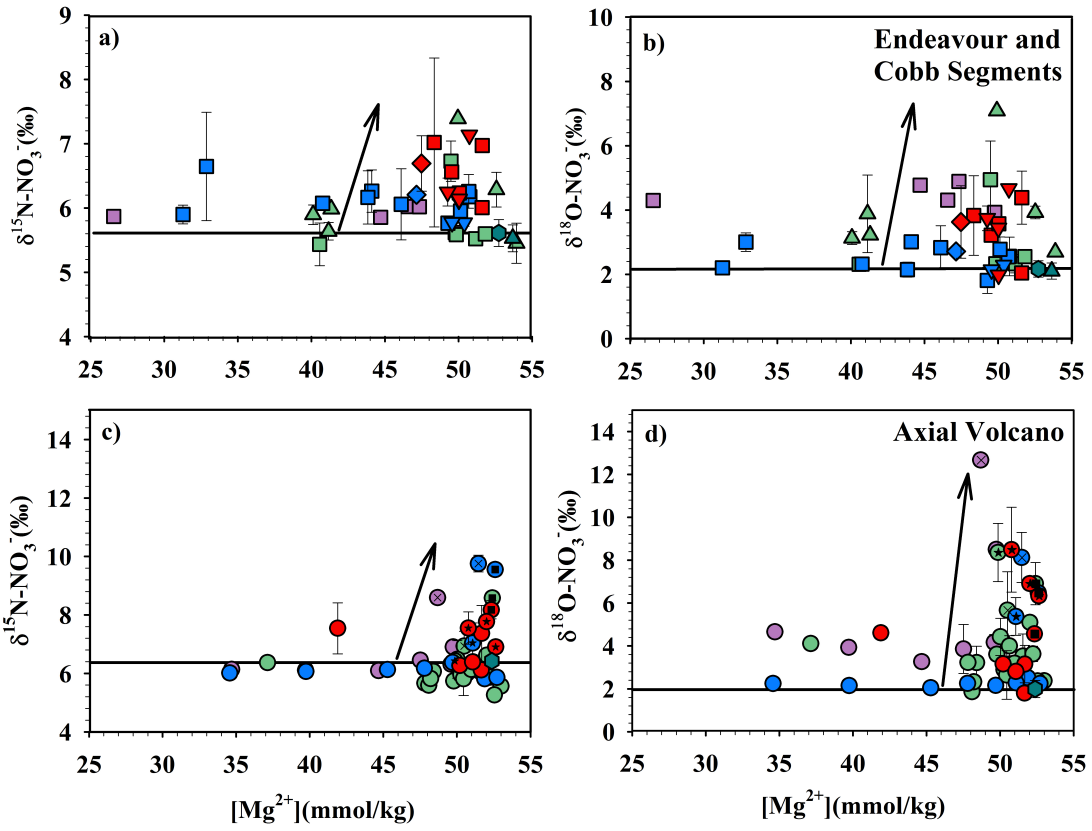


**Figure 2.5.** Nitrate $\delta^{15}N$ and $\delta^{18}O$ versus $[Mg^{2+}]$ at Endeavour and Cobb Segments (**a, b**) and Axial Volcano (**c, d**). Same symbol and color scheme as in Figure 2.2. The seawater (SW) $\delta^{15}N$ end-member is indicated by the solid black lines. Error bars represent the standard deviation for sub-samples (n= 2 to 5) collected at the same time and location. Sites where the highest heavy-isotope enrichments were observed at Axial Volcano are indicated by crosses (Bag City), black stars (Marker 113) and black squares (Cloud). Black arrows indicate isotopic fractionation during nitrate consumption in diffuse fluids (see Figure 2.3a).

N and O isotope fractionating nitrate-consuming process in the low-T subsurface biosphere prior to venting. The $^{15}N$ and $^{18}O$ enrichment in the HV fluid nitrate was greatest at Axial Volcano (up to ~3‰ for $\delta^{15}N$ and ~11‰ for $\delta^{18}O$, Figures 2.5c and 2.5d) compared to the Endeavour and Cobb Segments (between ~1.4‰ and ~2‰ for $\delta^{15}N$ and ~3‰ and ~5‰ for $\delta^{18}O$, respectively, Figures 2.5a and 2.5b). Moreover, we

consistently observed higher relative isotope enrichments for $^{18}O$ versus $^{15}N$ (Figure 2.5). Nitrate $\delta^{15}N$ and $\delta^{18}O$ values in diffuse vent fluids sampled at the same locations fluctuated between years, with no clear temporal trend. In general, the $^{15}N$ and $^{18}O$ isotope enrichment was greater in 2006 and 2009, and lowest in 2008. In the subsequent discussion, we treat each data set separately.

Both assimilative (nitrate uptake by vent organisms) and dissimilative (denitrification) nitrate reduction are likely candidate processes to remove nitrate from HV, as both are known to fractionate nitrate isotopes in other environments (e.g., Brandes *et al*., 1998a; Voss *et al*., 2001; Lehmann *et al*., 2003; Sigman *et al*., 2003). Biogeochemical evidence for respiratory denitrification by autotrophic bacteria has been reported previously for HV systems. For example, it has been shown that bacterial symbionts within the vestimentiferan *Riftia pachyptila* at the Genesis vent site (East Pacific Rise) can facultatively use nitrate as an electron acceptor for the oxidation of hydrogen sulfide, with either nitrite or $N_2$ gas being the metabolic N product (Hentschel and Felbeck, 1993). Similarly, sulfur oxidizing bacteria (e.g., *Beggiatoa* sp.), found at Guaymas Basin hydrothermal vents, can accumulate nitrate at concentrations that are at least 3,000-fold higher than ambient concentrations in their vacuoles, which they subsequently also use for the oxidation of hydrogen sulfide (McHatton *et al*., 1996). In diffuse fluids at Axial Volcano Butterfield *et al*. (2004) observed comparatively high concentrations of nitrite and nitrous oxide (20 to 600 nmol/L), typical intermediates and by-products of denitrification in intermittently anoxic aquatic environments. While these previous studies have highlighted that active denitrification by microbes is likely to occur in hydrothermal fluids, nitrate assimilation for bacterial growth is another important process

to be considered. The observed heavy-isotope enrichments were mostly restricted to the lower-T fluids (<50°C), where microbial cell densities are by far the highest (i.e., up to ~10 times more than in seawater; Butterfield *et al*., 2004). While ammonium is generally the form of fixed N that is preferred during N assimilation, by both photosynthetic organisms and bacteria (Dortch, 1990; Dugdale *et al*., 2007), Lee and Childress (1994) showed that S-oxidizing bacteria that live in symbiosis with the HV tubeworm *Riftia pachyptila* exclusively assimilate nitrate, even under ammonium–replete conditions.

The degree of community N and O isotope fractionation can potentially help us elucidate the pathway of nitrate removal in the HV diffuse fluids. Denitrification in the environment generally occurs with a significant nitrate isotope effect (ε) for both N and O isotopes of ~20 to 30‰ (Cline and Kaplan, 1975, and references therein). In contrast, nitrate assimilation seems to be associated with a significantly lower N-isotope effect of ~5‰ in laboratory cultures and the natural environment (Altabet, 2001; Granger *et al*., 2004). Here we attempt to estimate, for the first time, the community N and O isotope effects for nitrate removal in HV fluids, with the goal of assessing nitrate removal pathways. Analogous to the approach used to estimate the ammonium consumption N isotope effect above, the nitrate removal N and O isotope effects can be approximated using a closed system (Rayleigh) model, where a closed nitrate pool is consumed with a constant isotope effect as described by the equation (Mariotti *et al*., 1981):

$$\delta^{15}NO_3^-{}_{measured} = \delta^{15}NO_3^-{}_{initial} - \varepsilon \{\ln([NO_3^-]_{measured}/[NO_3^-]_{initial})\} \quad (2.1)$$

where the initial nitrate concentration is calculated from the $[Mg^{2+}]$ content of the fluid, and assuming a strict linear mixing relationship between pure hydrothermal vent fluids

and seawater (Figure 2.3a). As explained above, HV systems do not really behave as closed systems, so that the Rayleigh approach is likely to underestimate the community N isotope fractionation (Lehmann *et al*., 2003; 2007; 2009). Alternatively, in an open steady state model, we assume that new seawater with a fixed $\delta^{15}N$ for nitrate is constantly being mixed into the hydrothermal conduits, balancing the loss of nitrate by denitrification and/or N uptake so as to yield a steady state. The associated community N isotope effect is then calculated using the following equation [Altabet, 2001; Sigman *et al*., 2003]:

$$\delta^{15}NO_3^-{}_{measured} = \delta^{15}NO_3^-{}_{initial} + \varepsilon\,(f) \text{ where } f = [NO_3^-]_{consumed}/[NO_3^-]_{initial} \quad (2.2)$$

(Fig. 2.6). The results from both approaches are shown in Table 2.1. The highest isotope effects were obtained using the open system model at Axial Volcano in 2006 (1.9‰ for $^{15}\varepsilon_k$ and 8.6‰ for $^{18}\varepsilon_k$). The lowest isotope effects were observed using a closed-system model at the Endeavour Segment in 2008 (0.4‰ for both $^{15}\varepsilon_k$ and $^{18}\varepsilon_k$). Overall, the differences between the respective models were not very large. Strictly speaking, both models (closed-system and steady state) may not be representative of the real situation, as during hydrothermal circulation mixing is not necessarily continuous but rather episodic. However, modeling efforts by Sigman *et al*. [2003] demonstrated that for different mixing regimes between open steady state and closed systems (i.e., if there is sporadic mixing), the calculated isotope effect should fall between the two extremes.

The herein derived nitrate isotope effects are significantly lower than the ~20–30‰ isotope effect expected for canonical denitrification, and generally closer to the N and O isotope effect of 5‰ expected for nitrate assimilation only. Assuming that denitrification occurs with a N and O isotope fractionation at levels similar to those reported for ocean oxygen minimum zones, the nitrate isotope data suggest that denitrification can account

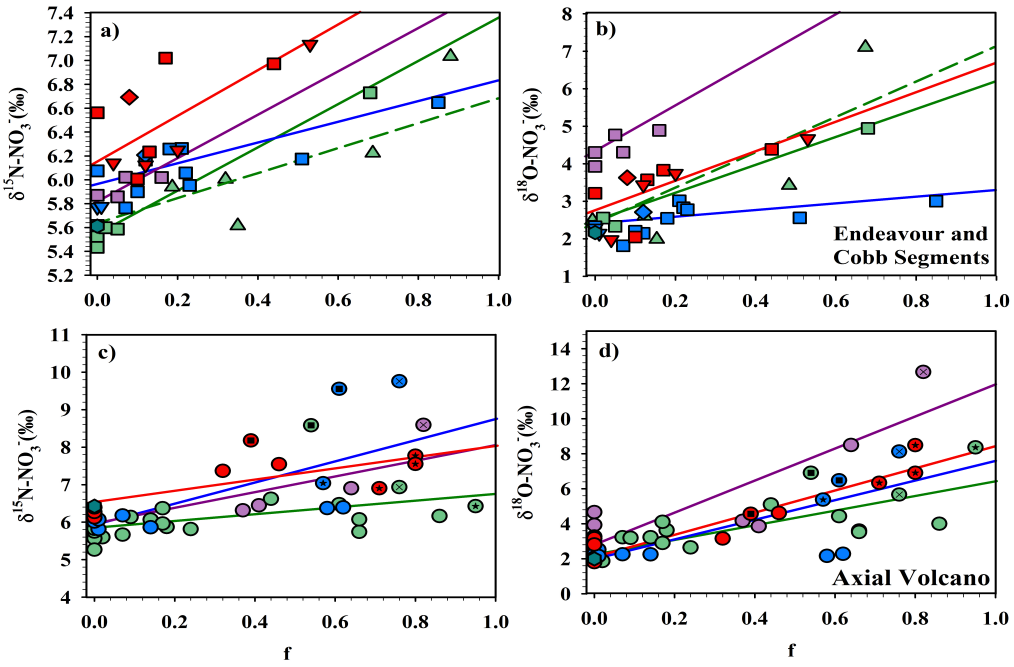


**Figure 2.6.** $\delta^{15}N$ and $\delta^{18}O$ versus *f* (open system "steady-state" model), where *f* is the fraction of nitrate consumed ($[NO_3^-]_{initial}$-$[NO_3^-]_{measured}$); $[NO_3^-]_{initial}$ is considered to be equal to $[Mg^{2+}]_{measured}/[Mg^{2+}]_{sw} \times [NO_3^-]_{sw}$, which is the $[NO_3^-]$ for the corresponding $[Mg^{2+}]$ on the mixing line, i.e. ~40μM, in HV fluids near the seawater end-member (Figure 2.3a**)**, at Endeavour and Cobb Segments (**a, b**) and Axial Volcano (**c, d**). The isotope effects are estimated based on the slopes of the linear regression lines (dashed line for Cobb Segment). Symbol and color scheme as in Figure 2.2. Linear regressions for each year are shown. The colors of the lines correspond to the colors of the symbols (i.e., sampling years). See Table 2.1 for N isotope effect estimations and the $r^2$ of the linear regressions.

only for a minor fraction of the total nitrate removal in the hydrothermal fluids. It is also possible, however, that the N and O isotope fractionation of HV denitrification is suppressed by diffusion limitation (Lehmann *et al*., 2007). Cell growth in the sub-seafloor primarily occurs on fixed surfaces (e.g., microbial mats; Moyer *et al*., 1995). Analogous to the N-isotope-effect suppression due to substrate limitation reported for denitrification in benthic marine environments (Brandes and Devol, 1997; Lehmann *et al*., 2004; 2007), the diffusive nitrate supply to the actual sites of denitrification in such

mats may be limiting so that nitrate is completely consumed. As a consequence, the nitrate N and O isotope effects would be significantly reduced, possibly with an apparent isotope effect of less than 2‰ (Brandes and Devol, 2002). Finally, analogous to our above considerations regarding net N isotope effects of ammonium consumption, $NO_3^-$ depletion is likely to be the net result of co-occurring nitrate consumption and production. Hence, here-reported N and O isotope effects represent community isotope effects that may partly be biased by the regeneration of nitrate and the isotope effects associated with the regeneration processes (e.g., Lehmann *et al*., 2004). At least for the nitrate N isotope ratios, the low apparent isotope effects may demonstrate the occurrence of gross nitrate production, by either nitrification or $N_2$ fixation (and the subsequent remineralization/ nitrification of newly fixed organic N to nitrate). Both processes would increase nitrate concentrations while decreasing nitrate $\delta^{15}N$ values, and thus erase, or at least mask, any N isotope signals resulting from denitrification or nitrate assimilation. Figure 2.6 and Table 2.1 show that the community nitrate isotope effects are larger for $^{18}O$ than for $^{15}N$, especially at Axial Volcano. A ratio of $^{18}O$ versus $^{15}N$ isotope enrichment >1 (between ~1 to 4 (Figures 2.7a and 2.7c)) is atypical for stand-alone denitrification and/or nitrate assimilation in marine environments (Granger *et al*., 2004, 2008). Given previous work (Lehmann *et al*., 2004; Sigman *et al*., 2005; Knapp *et al*., 2008; Bourbonnais *et al*., 2009), such a decoupling of the $^{15}N$ versus $^{18}O$ nitrate isotope enrichment is expected if quantitative N regeneration occurs simultaneously to net N consumption in the vent fluids. In the next section, we will discuss the observed $\delta^{15}N$-$\delta^{18}O$ relationship in the context of possible N regeneration pathways within the HV fluids that can lead to the observed nitrate N-to-O isotope anomalies.

### 2.4.4. Nitrate N-to-O isotope anomalies - Possible causes and constraints on N regeneration

Analogous to the approach proposed by Sigman *et al*. (2005), we quantify the deviation of nitrate isotope values from a 1:1 N versus O isotope fractionation relationship expected for pure denitrification/assimilation, using Δ(15,18):

$$\Delta(15,18) = (\delta^{15}N - \delta^{15}N_m) - [(^{18}\varepsilon/^{15}\varepsilon) \times (\delta^{18}O - \delta^{18}O_m)] \quad (2.3)$$

where $\delta^{15}N_m$ = ~6‰ and $\delta^{18}O_m$ = ~2‰ are the mean $\delta^{15}N$ and $\delta^{18}O$ of deep-seawater, respectively, and $^{18}\varepsilon/^{15}\varepsilon$ is the ratio of N versus O isotope enrichment during denitrification, i.e., 1. An equal enrichment for N and O isotopes (Δ(15;18) = 0‰) can be assumed as a baseline characteristic for pure denitrification (Sigman *et al*., 2005; Granger *et al*., 2008) and $NO_3^-$ assimilation (Granger *et al*., 2004; Lehmann *et al*., 2005). From Figures 2.7b and 2.7d, it can be derived that the Δ(15,18) is negative in $Mg^{2+}$-rich, low-T hydrothermal fluids, where denitrification (and possibly nitrate assimilation) results in the net consumption of nitrate. The Δ(15,18) was significantly higher (up to ~−8.5‰) at Axial Volcano compared to the Endeavour and Cobb Segments (up to ~3‰). The nitrate isotope anomalies also varied between years, (with generally higher anomalies in 2006, 2007, and 2009) although no general temporal pattern could be discerned.

We argue that the Δ(15,18) anomaly observed at some sites is due to the gross production of nitrate coupled to microbial nitrate consumption (assimilation and/or denitrification). However, we currently have few quantitative constraints on the different N fluxes involved or the physical and chemical characteristic of the subsurface biosphere

**Table 2.1.** Estimated nitrate N and O isotope effects according to 1) a "Rayleigh" closed system and 2) an open "steady-state" system model at Endeavour Segment, Cobb Segment and Axial Volcano on the Juan de Fuca Ridge from 2006 to 2009. $r^2$ values for each linear regression are shown in parentheses. Refer to Figure 2.6 for plots and linear regressions of $\delta^{15}N$ and $\delta^{18}O$ of nitrate versus *f*, the fraction of nitrate consumed (open "steady-state" model). p-values ≤ 0.05 (significant relationship) for the linear regressions are indicated by the asterisk next to the $r^2$.

| **Year** | **2009** | | **2008** | | **2007** | | **2006** | | **Average** | |
|---|---|---|---|---|---|---|---|---|---|---|
| **N and O of nitrate isotope effects (‰)** | $^{15}\varepsilon_k$ | $^{18}\varepsilon_k$ | $^{15}\varepsilon_k$ | $^{18}\varepsilon_k$ | $^{15}\varepsilon_k$ | $^{18}\varepsilon_k$ | $^{15}\varepsilon_k$ | $^{18}\varepsilon_k$ | $^{15}\varepsilon_k$ | $^{18}\varepsilon_k$ |
| **Endeavour Segment** | | | | | | | | | | |
| Closed system | 1.3 (0.49*) | 2.6 (0.57*) | 0.41 (0.57*) | 0.41 (0.31*) | 1.0 (0.97*) | 2.3 (0.99*) | 1.7 (0.71*) | 4.3 (0.59*) | **1.1 ±0.6** | **2.4 ±1.6** |
| Open system | 2.0 (0.56*) | 3.9 (0.64*) | 0.90 (0.64*) | 0.96 (0.41*) | 1.7 (0.94*) | 3.7 (0.98*) | 1.8 (0.71*) | 4.7 (0.59*) | **1.6 ±0.5** | **3.3 ±1.6** |
| **Cobb Segment** | | | | | | | | | | |
| Closed system | na | na | na | na | 1.4 (0.85*) | 3.5 (0.88*) | na | na | **1.4** | **3.5** |
| Open system | na | na | na | na | 2.1 (0.76*) | 5.3 (0.80*) | na | na | **2.1** | **5.3** |
| **Axial Volcano** | | | | | | | | | | |
| Closed system | 0.69 (0.41*) | 3.2 (0.93*) | 1.9 (0.57*) | 3.0 (0.58*) | 0.28 (0.11) | 1.6 (0.63*) | 1.2 (0.84*) | 5.1 (0.89*) | **1.0 ±0.7** | **3.2 ±1.4** |
| Open system | 1.5 (0.55*) | 5.9 (0.89*) | 2.9 (0.48*) | 4.6 (0.51*) | 0.90 (0.20*) | 3.8 (0.60*) | 1.9 (0.63*) | 8.6 (0.75*) | **1.8 ±0.9** | **5.7 ±2.1** |

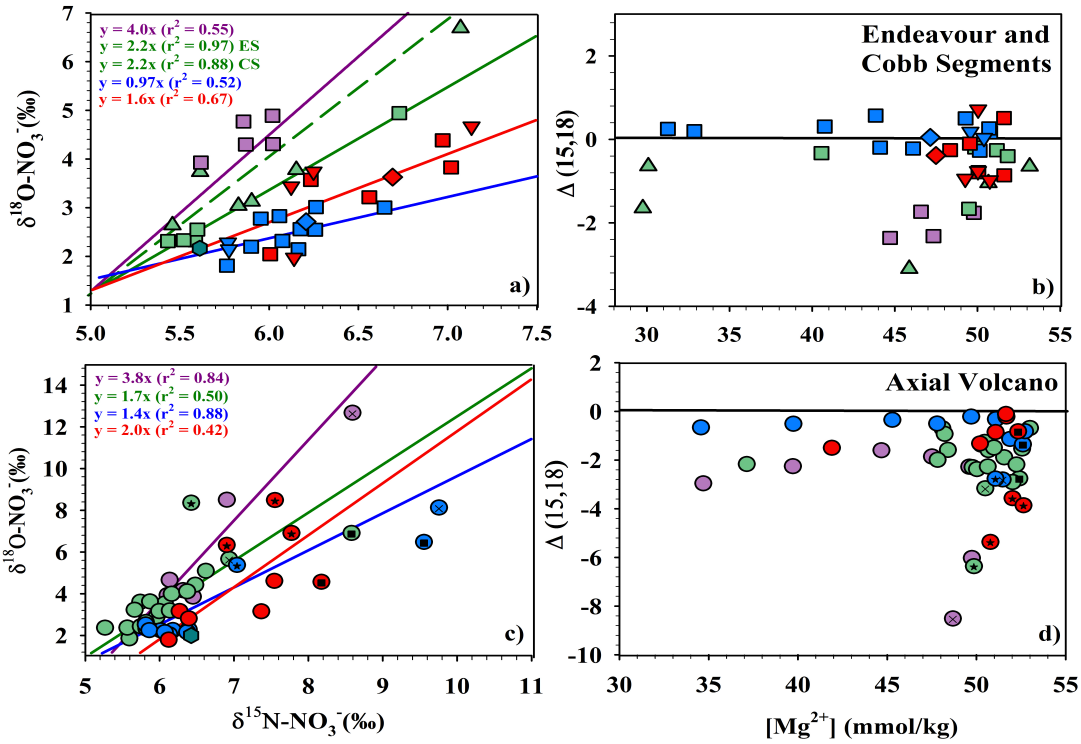


**Figure 2.7.** $\delta^{18}O\text{-}NO_3^-$ versus $\delta^{15}N\text{-}NO_3^-$ and Δ (15,18) versus $Mg^{2+}$ concentration at Endeavour and Cobb Segments (**a, b**), and Axial Volcano (**c, d**). Symbol and color scheme as in Figure 2.2 legend. The ratios of nitrate $^{18}O$ versus $^{15}N$ enrichment are estimated from slopes of the linear regressions (dashed-line for Cobb Segment in **a**).

(e.g., average fluid residence time, volume of hydrothermal conduits, and timing of mixing), so it is impossible to derive rates of processes from our isotope data. Therefore, we will only qualitatively discuss possible causes for the observed nitrate N and O isotope anomalies below. The exact causes for generally larger nitrate isotope anomalies at Axial Volcano compared to the Endeavour and Cobb Segments are unclear, as are the causes of any inter-annual variations. However, supplementary data on bacterial cell densities suggest a link between bacterial growth/activity and the observed expression of the N-to-O isotope anomalies. In fact, we observed a significant relationship ($r^2 = 0.61$, p-value = 0.0001) between bacterial cell counts in diffuse fluids (data from J. A. Baross and

J. F. Holden laboratories) and the N-to-O nitrate anomalies for the years where cell counts were available (2008 and 2009) at Axial Volcano (Figure 2.8). Yet, at Endeavour Segment, where maximum $NH_4^+$ concentrations were observed in the subsurface fluids, the nitrate N- versus O isotope anomaly was rather moderate and there was no correlation with bacterial cell density. Therefore causal links between bacterial biomass, "anomalous" nitrate isotope behavior and, possibly, nitrate regeneration through either ammonium or nitrite oxidation remain uncertain.

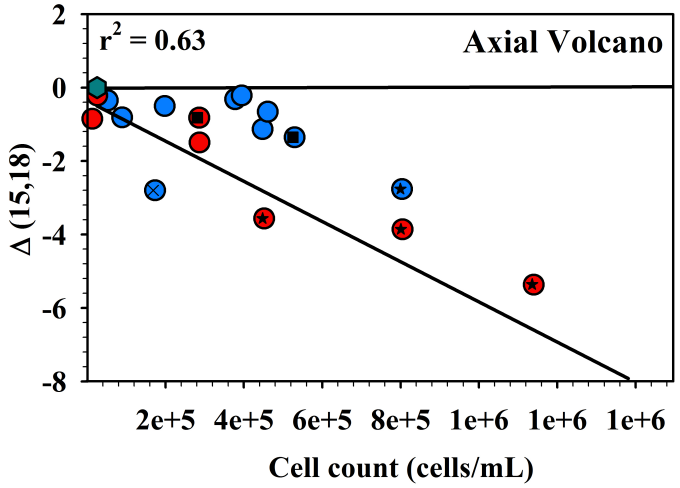


**Figure 2.8.** Δ(15,18) versus bacterial cell count at Axial Volcano (symbol and color scheme as in other figures).

### 2.4.4.1. Partial nitrification and $N_2$ fixation

Ammonium oxidation in deep-sea hydrothermal vent plumes of the Main Endeavour Field, Juan de Fuca Ridge, has been reported by Lam *et al*. (2004; 2008). Byrne *et al*. (2009) also documented the diversity and activity of anammox bacteria in hydrothermal vent chimney samples on the Mid-Atlantic Ridge. Here, the partial re-oxidation of

ammonium at the seawater end of the redox gradient in low-T, aerobic vent fluids would leave the residual $NH_4^+$ enriched in $^{15}N$, while the nitrate produced would be depleted in $^{15}N$ (Delwiche and Steyn, 1970, and references therein). While the $\delta^{15}N$ of newly nitrified nitrate is directly dependent on the $\delta^{15}N$ of the ammonium pool (with an offset that corresponds to the nitrification N-isotope effect), nitrification represents an absolute source with regard to the O isotopes.

The general understanding at the moment is that two-thirds of the O atoms in new nitrate are being derived from ambient water, and that, because of important isotope effects during oxygen atom incorporation during ammonium and nitrite oxidation, the $\delta^{18}O$ of nitrified nitrate should be 0.7–8.3‰ lower than the $\delta^{18}O$ of the seawater (which was measured to be ~0‰ in our 2004 hydrothermal fluid samples, unpublished results) (Buchwald and Casciotti, 2010; Casciotti *et al*., 2010). On the other hand, $^{16}O$ is preferentially extracted during nitrate reduction, causing the $\delta^{18}O$ of the eliminated $NO_3^-$ to be even lower than the $\delta^{18}O$ of the nitrified nitrate. Hence, while nitrification tends to counteract the denitrification/assimilation–driven enrichment of both the $\delta^{18}O$ and $\delta^{15}N$, this balancing effect is generally more pronounced for N than for O so that it can produce nitrate N-vs-O anomalies (more precisely, $\Delta(15,18)$ minima) (Sigman *et al*., 2005). The $\Delta(15,18)$ effect is most marked if ammonium oxidation is not complete, either in an ammonium-replete setting, or when ammonium uptake and nitrification occur simultaneously (i.e., ammonium branching, with the N isotope effect associated with ammonium assimilation being lower than the N isotope effect associated with nitrification) (e.g., Wankel *et al*., 2007).

The N isotope balance predicts that in the HV fluids where partial nitrification generates low-$\delta^{15}N$ nitrate, it simultaneously leaves $^{15}N$-enriched ammonium substrate behind (according to the nitrification N isotope effects of 14–38‰; Delwiche and Steyn, 1970, and references therein). The observed increase of the $\delta^{15}N\text{-}NH_4^+$ in the low-T fluids at some sites of the Endeavour and Cobb Segments, as well as Axial Volcano (Figure 2.4), hence, confirms that oxidation of ammonium is occurring to some extent. We would expect the nitrification-driven $\Delta(15,18)$ minimum to be most pronounced at Endeavour Segment and, to a lesser extent, Cobb Segment, where the measured ammonium concentrations in diffuse HV fluids (up to ~65 μmol/L and ~10 μmol/L, respectively) were often higher than the nitrate concentrations. Furthermore, the average $\delta^{15}N$ of the hydrothermally discharged ammonium was also significantly lower at these sites compared to Axial Volcano, further enhancing the expression of the nitrate isotope anomaly. As discussed above, there were indeed systematic inter-site variations with regard to the $\Delta(15,18)$. However, curiously, the lowest $\Delta(15,18)$ was observed at Axial Volcano, where the influence of incomplete ammonium oxidation is likely to be less important and where, as a consequence, the $\Delta(15,18)$ should be less pronounced ($[NH_4^+]$ in diffuse fluids was close to 0 μmol/L at most sites).

$N_2$ fixation in hydrothermal vents has been previously documented by Mehta *et al*. (2003; 2005) and Mehta and Baross (2006) who found expressed nitrogenase genes (*nif*H) in anaerobic hydrothermal fluids at Axial Volcano and who were able to isolate a methanogenic archeaeon that can fix $N_2$ at a temperature up to 92°C. $N_2$ fixers are assumed to thrive in environments where fixed N forms that are energetically more favorable are scarce. Moreover, an anaerobic environment may be conducive to $N_2$

fixation, as nitrogenase, the enzyme involved in $N_2$-fixation, is inhibited by oxygen (e.g., Berman-Frank *et al*., 2005). $N_2$ fixation may occur in microsites, e.g., microbial mats and particulate material, where $O_2$ and DIN concentrations may be low, providing an important source of bioavailable N for hydrothermal vent organisms in low-T fluids (e.g., Proctor, 1997; Zehr *et al*., 2003). $N_2$ fixation produces organic material with a $\delta^{15}N$ of ~−2 to 0‰ (Carpenter *et al*., 1997, and references therein). Upon ammonification of the $N_2$-fixation-derived biomass and subsequent (incomplete) nitrification after mixing of the anaerobic vent fluids with oxic seawater, low-$\delta^{15}N$ N can be transferred to the $NO_3^-$ pool. Given the nitrate O isotope systematics described above, the $\delta^{18}O$, however, is rather insensitive toward this $N_2$ fixation as the incorporation of O atoms into the newly produced nitrate molecule does not discriminate between possible origins of the precursor N compounds. The above-described nitrification/denitrification mechanism to produce the $\delta^{15}N$-$\delta^{18}O$ decoupling would, hence, be enhanced if newly produced nitrate is derived from the remineralization and nitrification of chemosynthetically fixed $N_2$. And even in the case of complete nitrification of the ammonium, a negative $\Delta(15,18)$ can be expected (Bourbonnais *et al*., 2009).

#### 2.4.4.2. Nitrate/nitrite redox cycle

Nitrate is not only regenerated by the oxidation of ammonium, it can also originate from the re-oxidation of nitrite. Under suboxic conditions in hydrothermal vent fluids, nitrate is reduced to nitrite. Along redox gradients or upon mixing of anaerobic and oxic waters, a large fraction of product nitrite may be re-oxidized to nitrate. We are only

beginning to understand nitrite N and O isotope systematics in nature (Casciotti and McIlvin, 2007; Buchwald and Casciotti, 2010; Casciotti *et al*., 2010). For example, factors that control observed offsets between the $\delta^{15}N$ of nitrate and nitrite in the Eastern Tropical North Pacific OMZ (up to 30‰) are uncertain. However, previous work suggests that nitrite re-oxidation is an even more efficient mechanism for lowering the nitrate $\Delta(15,18)$ (Sigman *et al*., 2005; Casciotti and McIlvin, 2007), as it adds high $\delta^{18}O$ to the nitrate pool. That is, by mass balance, nitrate reduction from a particular nitrate pool and subsequent (complete) nitrite re-oxidation should produce nitrate with a similar $\delta^{15}N$ to that initially consumed. The $\delta^{18}O$ of the re-oxidized nitrite, on the other hand, will likely be higher than the $\delta^{18}O$ of the nitrate consumed, due to the "branching fractionation" (preferential extraction of $^{16}O$) during nitrate reduction (i.e., produced nitrite is enriched in $^{18}O$) and the incorporation of an O-atom with a relatively higher $\delta^{18}O$ (compared to the $\delta^{18}O$ of the O-atom lost during nitrate reduction) during re-oxidation of nitrite to nitrate. If portions of the nitrite are further reduced to gaseous forms of N, both the nitrite $\delta^{15}N$ and the $\delta^{18}O$ are increased in parallel. Therefore, while this redox cycle leaves the $\delta^{15}N$ of nitrate essentially unchanged, it would act to increase the $\delta^{18}O$. If anything, we would expect nitrite oxidation to be the driver of N-to-O nitrate isotope anomalies particularly in higher-T diffuse fluids, where nitrate reduction to nitrite (favored by the more reducing conditions) and subsequent nitrite re-oxidation after mixing with oxygenated deep seawater, is most likely to occur. However, as mentioned earlier, the highest nitrate isotope anomalies were not observed in the highest T (generally < ~50°C) diffuse fluids. In summary, several processes (partial nitrification, $N_2$ fixation, and nitrite oxidation) can theoretically produce similar negative nitrate

Δ(15,18) signatures (Sigman *et al*., 2005; Casciotti and McIlvin, 2007), just as observed at the Juan de Fuca Ridge vent sites. In the next section, we will present results from a simple isotope box model, which we used to assess the relative fluxes of the candidate processes that could explain the N-to-O nitrate isotope anomalies in diffuse vent fluids.

### 2.4.4.3. Estimates on the relative importance of the possible nitrate regenerating processes

We attempt here to assess the role of ammonium oxidation, $N_2$ fixation or nitrite re-oxidation in the hydrothermal conduits of the Juan de Fuca Ridge, applying a simplified steady state one-box model (analogous to the one we used in previous work (Bourbonnais *et al*., 2009)) in order to calculate Δ(15,18) as a function of relative changes in potential N-regenerating and consuming processes (Figure 2.9). In this model, we included nitrate inputs through partial nitrification of hydrothermal ammonium, $N_2$ fixation and seawater mixing, and nitrate removal through bacterial uptake and/or denitrification. Finally the model includes the internal nitrite/nitrate cycle, where a portion of the nitrite from nitrate reduction is re-oxidized to nitrate. The $\delta^{15}N$ of ammonium-derived nitrate is calculated according to Mariotti *et al*. (1981):

$$\delta^{15}N_{product} = \delta^{15}N\text{-}NH_4^+{}_{initial} + \varepsilon_{nit}\{\ln(f)\} \times \{f/(1-f)\} \quad (2.4)$$

where $f$ is the fraction of reactant remaining, $\delta^{15}N\text{-}NH_4^+{}_{initial}$ is the $\delta^{15}N$ of the initial reactant pool, and $\varepsilon_{nit}$ is the kinetic isotope effect of ammonium oxidation to nitrate. We used an average N isotope effect of 26‰ during ammonium oxidation (Delwiche and Steyn, 1970, and references therein). $N_2$ fixation (i.e., the remineralization of newly fixed

OM) adds nitrate with $\delta^{15}N$ of −1‰ (with insignificant isotopic fractionation) (Carpenter *et al*., 1997, and references therein). We assumed that part of the assimilated nitrate would be returned following organic matter ammonification and nitrification (recycled production term in Table 2.2). Therefore, net nitrate uptake is the gross nitrate uptake minus the recycled production. Independent of the original N source (hydrothermal ammonium versus OM from $N_2$ fixation or bacterial uptake), a $\delta^{18}O$ of −3.8‰ is assumed for nitrified nitrate (mean value taken from Buchwald and Casciotti, 2010). With regard to the internal nitrite/nitrate cycling, complete nitrite oxidation returns nitrate with a $\delta^{15}N$ equal to the original nitrate, and a $\delta^{18}O$ of nitrate of 0‰, as also assumed in the study by Sigman *et al*. (2005). Subsurface mixing with seawater adds nitrate with a $\delta^{15}N$ of ~6.0‰ and a $\delta^{18}O$ of ~2.0‰. Nitrate removal occurs either by assimilation or by denitrification. We used average isotope effects of 5‰ for nitrate assimilation (Altabet, 2001), 25‰ for denitrification (Cline and Kaplan, 1975, and references therein) and 1.5‰ (Brandes and Devol, 2002) for nitrate consumption occurring in bacterial mats. Figure 2.10 shows the model results for both Axial Volcano and Endeavour Segment. We simulated seven representative scenarios, in which we varied the relative importance of single N fluxes in order to gain information on their respective potentials for generating the observed Δ(15,18) minima in the diffuse vent fluids (see Table 2.2 and Figure 2.10 for more details on the parameters used for the different scenarios). In the first 3 scenarios, nitrate is produced only by the oxidation of hydrothermal ammonium and we varied the relative rates and extent of hydrothermal $NH_4^+$ oxidation relative to net nitrate uptake. In scenarios 4, 5, and 6, the oxidation of hydrothermal ammonium was suppressed and we varied the relative rate of nitrate production from $N_2$ fixation or nitrite re-oxidation

relative to net nitrate uptake. Finally, in scenario 7, partial ammonium oxidation and nitrite re- oxidation were combined. Across all considered scenarios, we also varied the ratio of denitrification and N uptake, and differentiated between denitrification in the open HV conduits versus that by microbial mats and biofilms on conduit walls (see Table 2.2 and Appendix B.1 for more detail). For all scenarios, decreasing the mixing with deep-seawater (while concomitantly increasing the input of nitrate from one of the three processes mentioned above), caused a decrease in the Δ(15,18).

Our model simulation suggests that all 3 processes are capable of generating nitrate N and O isotope anomalies of a magnitude similar to that actually observed at the Endeavour Segment (minimum Δ(15,18) of −2.4‰). In our simplistic model, nitrite re-oxidation and partial ammonium oxidation can generate very low Δ(15,18) values (<−4.0‰), especially for a lower fraction of ammonium consumed, when N isotope fractionation is fully expressed, whereas $N_2$ fixation has less potential to generate negative Δ(15,18) anomalies. Even at high rates of $N_2$ fixation with no preformed $NO_3^-$, the Δ(15,18) does not exceed ~−3‰. Therefore, at least at Axial Volcano, it seems very unlikely that the entire nitrate isotope anomaly can be attributed to the remineralization of fixed N. Figure 2.10c (Scenario 7) shows that only a combination of processes (for a given ratio of 0.5 for nitrite re-oxidation/net nitrate uptake and for a 75% fractional ammonium consumption) can generate a Δ(15,18) of <−8‰, as at Axial Volcano (−8.3‰). While it seems clear that nitrate production is important in the investigated diffuse hydrothermal fluids, too many unknowns preclude a more quantitative assessment of actual N regeneration pathways. The observed nitrate N and O isotope data are consistent with all of the above candidate processes, but without independent data on

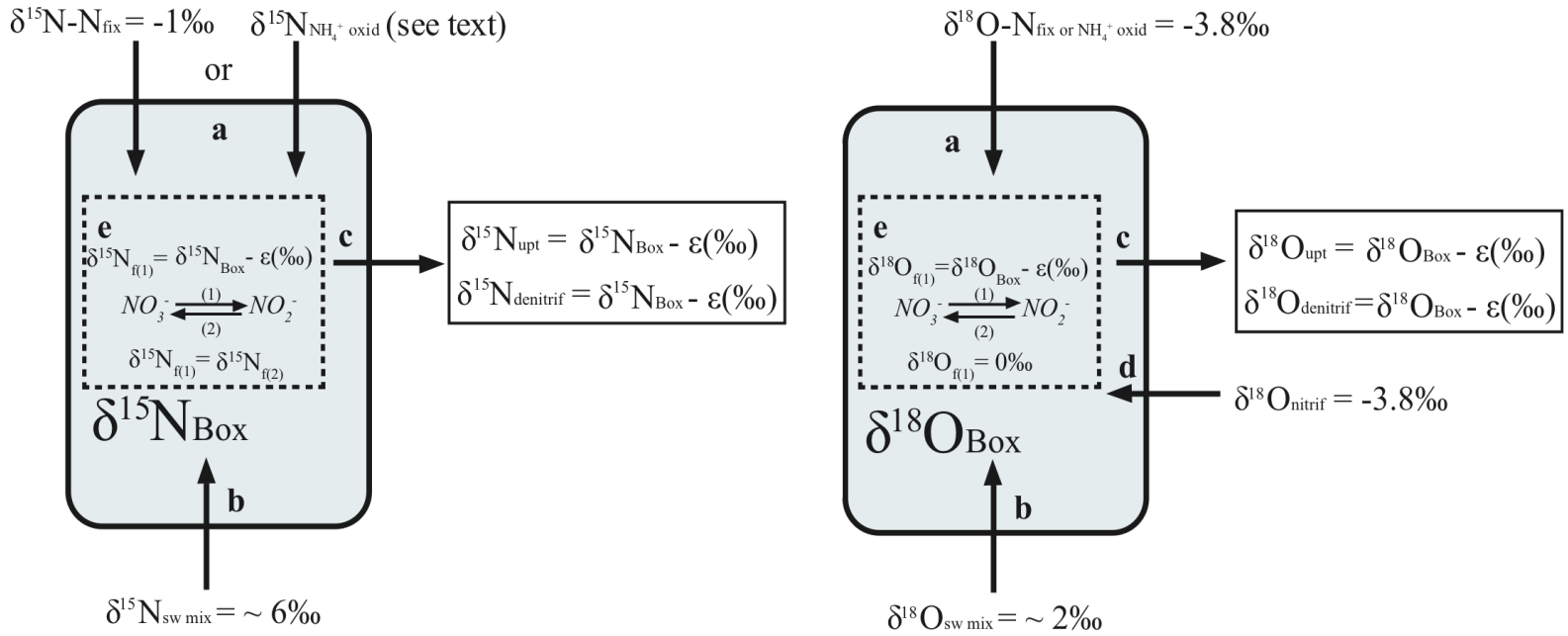


**Figure 2.9.** Simplified steady-state model used in section 2.4.4.3 (adapted from Sigman *et al*., 2005 and Bourbonnais *et al.*, 2009): **a** represents the addition of nitrate from $N_2$ fixation (with a $\delta^{15}N$ of -1‰) or from hydrothermal-ammonium oxidation with a $\delta^{15}N$ that corresponds to the integrated product of partial ammonium oxidation (Mariotti *et al.* 1981), and a $\delta^{18}O$ of -3.8‰ (average value taken from Casciotti *et al.* 2010); **b** is the input of nitrate from mixing with deep-sea water with a $\delta^{15}N$ of ~6‰ and a $\delta^{18}O$ of ~2‰; **c** is the gross nitrate removal by nitrate assimilation and/or denitrification; **d** is the remineralization of newly biosynthesized organic N to ammonium, coupled to nitrification, returning nitrate with a $\delta^{18}O$ of -3.8‰ (and not changing the nitrate $\delta^{15}N$); **e** represents the internal cycle of $NO_3^-$ reduction and $NO_2^-$ re-oxidation (see text and Appendix B.1. for detail).

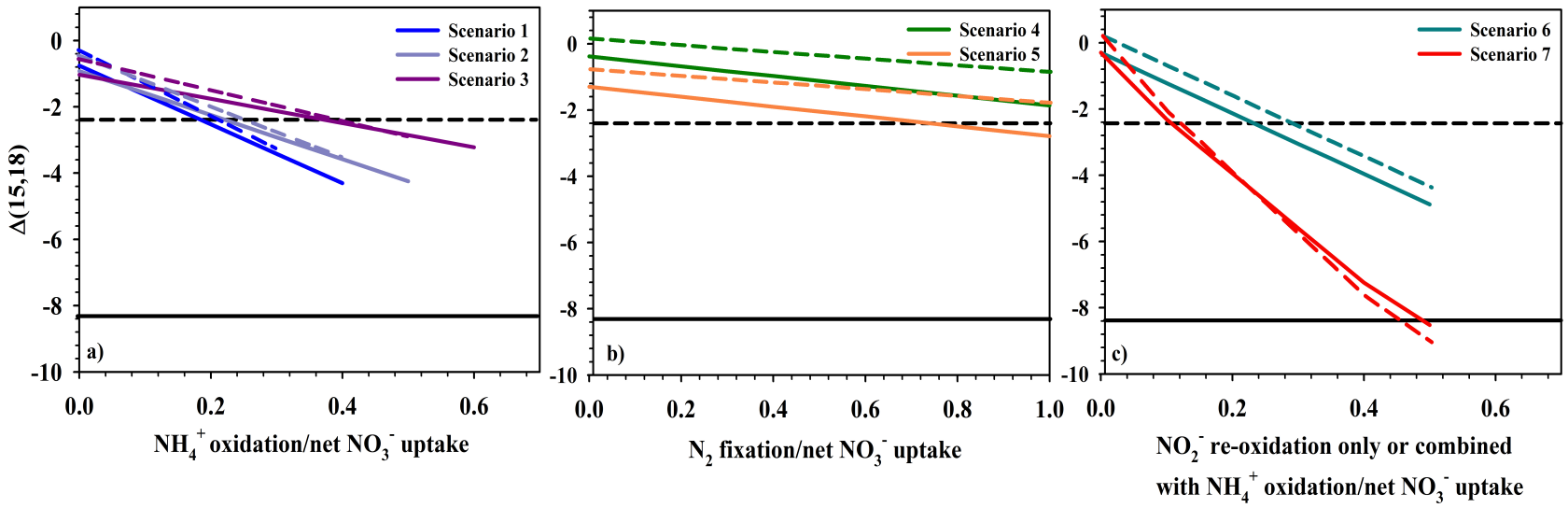


**Figure 2.10.** Model results for Δ(15,18) for simulation scenarios presented in Table 2.2 for Axial Volcano (plain lines) and the Endeavour Segment (dashed lines): (**a**) partial ammonium oxidation, (**b**) $N_2$ fixation, and (**c**) nitrite re-oxidation (rates always relative to net nitrate uptake). Maximum Δ(15,18) observed at Axial Volcano (~8.3‰) and Endeavour Segment (~2.4‰) are indicated by horizontal black lines.

**Table 2.2.** Model simulation scenarios described in the discussion (section 2.4.4.3). Corresponding values for Δ(15,18) for the various simulations are provided in Figure 2.10.

| **Scenarios** | 1 | 2 | 3 | 4 | 5 | 6 | 7 |
|---|---|---|---|---|---|---|---|
| **Process considered** | Fractional crustal $NH_4^+$ oxidation (Fig. 2.10, a) | | | $N_2$ fixation (Fig. 2.10, b) | | $NO_2^-$ re-oxidation (Fig. 2.10, c) | $NO_2^-$ re-oxidation and fractional $NH_4^+$ oxidation (Fig. 2.10, c) |
| fraction $NH_4^+$ consumed (%) | 25 | 50 | 75 | na | na | na | 75 |
| denitrification/gross nitrate uptake | 0.25 | 0.5 | 0.25 | 0.5 | 0.25 | 0.4 | 0.4 |
| % denitrification in microsites | 0 | 50 | 25 | 25 | 50 | 0 | 0 |
| recycled production/$NO_3^-$ assimilation | 0.5 | 0.75 | 0.5 | 0.75 | 0.5 | 0.2-0.5 | 0.2-0.5 |

actual rates, the Δ(15,18) data do not allow us to reliably predict the relative importance of nitrite re-oxidation and nitrification of hydrothermal ammonium versus nitrification of $N_2$-fixation derived ammonium, particularly at those sites where nitrification is incomplete (Wankel *et al*., 2007).

## 2.5. Summary and concluding remarks

First-time measurements of nitrate $\delta^{15}N$ and $\delta^{18}O$ and ammonium $\delta^{15}N$ from vent fields of the Juan de Fuca Ridge (northeast Pacific) reveal significant inter-field variations in the isotopic composition of DIN in HV diffuse waters. Highest $\delta^{15}N$ of $NH_4^+$ were observed at Axial Volcano in high-T fluids (6.7‰), indicating that deep-sea water nitrate (6.4‰) represents the original source of N for ammonium in the hot subsurface. The

$NH_4^+$ concentration in high-T fluids at Axial Volcano was lower than the $NO_3^-$ in the seawater source, suggesting N enrichment in the rocks during basalt alteration (associated with no apparent isotope effect). The $\delta^{15}N$ of ammonium in high-T fluids was significantly lower at both the Endeavour (3.7‰) and Cobb Segments (4.1‰), implying a low-$\delta^{15}N$ sedimentary source at those sites. DIN concentration changes are mostly driven by advective mixing, but at some sites we have clear DIN isotopic evidence for biological N transformations in habitable lower temperature diffuse HV fluids. As for the actual N consuming and regenerating processes, our isotope data are ambivalent. Lowered $NH_4^+$ community N isotope effects (<3‰) for net $NH_4^+$ consumption suggest an important contribution from gross ammonium regeneration. The generally reduced apparent nitrate N isotope fractionation suggests that fixed N uptake by bacteria is the most important N consuming process. Nitrification and denitrification are also likely to occur in microbial mats/biofilms, within the low-temperature HV conduits, where substrate diffusion limitation can lead to the underexpression of biological N isotope fractionation processes. We observed clear, and, at this magnitude, previously unseen nitrate N-to-O isotope anomalies in the HV fluids, varying strongly from site to site and from year to year, indicating spatial and temporal variations in relative rates of the nitrate regeneration versus consuming processes. We interpreted negative $\Delta(15,18)$ signatures as evidence for nitrate regeneration either by nitrite reoxidation, partial nitrification of hydrothermal ammonium and/or $N_2$ fixation and the remineralization/nitrification of the newly fixed N. Using a simple isotopic box model, we demonstrated that all three processes can produce negative $\Delta(15,18)$ at levels that were observed at the Endeavour Segment, but only a combination of processes (e.g., nitrite re-oxidation and partial $NH_4^+$ oxidation in

Figure 2.10c, scenario 7) can generate Δ(15,18) values <−8‰, as observed at Axial Volcano. While we cannot provide conclusive evidence with regard to the actual nitrate regenerating pathways at work, it is striking that the largest observed Δ(15,18) correspond to highest bacterial cell densities at Axial Volcano, implying an important role of microorganisms in shaping DIN concentration and DIN isotope gradients in the subsurface and in diffuse HV fluids at this vent field. Here-presented DIN isotope data thus provide qualitative evidence that net loss of N from hydrothermal fluids can be attributed to microbial processes in diffuse fluids, highlighting the role of subsurface microbial communities in modulating hydrothermal geochemical fluxes to the deep ocean. Yet, limited knowledge of the physical characteristic of the subsurface biosphere of hydrothermal systems prevents more quantitative estimates on overall N elimination rates in HV. The strong variability of these systems over short time scales further complicates any modeling efforts. Time series sampling at shorter intervals could perhaps improve our knowledge of the processes that fractionate N isotopes in low-T vent fluids. Future studies of the microbial community mediating N-cycle processes, integrated with N isotope data, are required to gain an in-depth understanding of microbial pathways that turn over or produce fixed N in hydrothermal diffuse fluids. In the same vein, denitrification, anammox and DNRA rate measurements in discharging vent fluids are ongoing (A. Bourbonnais *et al*., manuscript in preparation, 2012), and should yield a more complete picture of N-elimination processes in the subsurface biosphere of hydrothermal systems.

# Chapter 3
# Activity and abundance of denitrifying bacteria in the subsurface biosphere of diffuse hydrothermal vents of the Juan de Fuca Ridge[2]

## 3.1. Abstract

Little is known about fixed nitrogen (N) transformation and elimination at diffuse hydrothermal vents where anoxic fluids are mixed with oxygenated crustal seawater prior to discharge. Oceanic N sinks that remove bio-available N ultimately affect chemosynthetic primary productivity in these ecosystems. Using $^{15}N$ paired isotope techniques, we determined potential rates of fixed N loss pathways (denitrification, anammox) and dissimilatory nitrate reduction to ammonium (DNRA) in sulfidic hydrothermal vent fluids discharging from the subsurface at several sites at Axial Volcano and the Endeavour Segment on the Juan de Fuca Ridge. We also measured physico-chemical parameters (i.e. temperature, pH, nutrients, $H_2S$ and $N_2O$ concentrations) as well as the biodiversity and abundance of chemolithoautotrophic nitrate-reducing, sulfur-oxidizing γ-proteobacteria (SUP05 cluster) using sequence analysis of amplified small subunit ribosomal RNA (16S rRNA) genes in combination with taxon-specific quantitative polymerase chain reaction (qPCR) assays. Denitrification was the dominant N loss pathway in the subsurface biosphere of the Juan de Fuca Ridge, with rates of up to ~1000 nmol N $L^{-1}$ $day^{-1}$. In comparison, anammox rates were always

[2] A version of this chapter is published in the journal *Biogeosciences*: Bourbonnais, A., Juniper, S. Kim, Butterfield, D. A., Devol, A. H., Kuypers, M. M. M., Lavik, G., Hallam, S. J., Wenk, C. B., Chang, B. X., Murdock, S. A., and Lehmann, M. F. (2012). Activity and abundance of denitrifying bacteria in the subsurface biosphere of diffuse hydrothermal vents of the Juan de Fuca Ridge, *Biogeosciences,* 9, 4661–4678.

<5 nmol N $L^{-1}$ $day^{-1}$ and below the detection limit at most of the sites. DNRA rates were up to ~150 nmol N $L^{-1}$ $day^{-1}$. These results suggest that bacterial denitrification out-competes anammox in sulfidic hydrothermal vent waters. Taxon-specific qPCR revealed that γ-proteobacteria of the SUP05 cluster sometimes dominated the microbial community (SUP05/total bacteria up to 38%). Significant correlations were found between fixed N loss (i.e., denitrification, anammox) rates and *in-situ* nitrate and dissolved inorganic nitrogen (DIN) deficits in the fluids, indicating that DIN availability may ultimately regulate N loss in the subsurface. Based on our rate measurements, and on published data on hydrothermal fluid fluxes and residence times, we estimated that up to ~10 Tg N $year^{-1}$ could globally be removed in the subsurface biosphere of hydrothermal vents systems, thus representing a small fraction of the total marine N loss (275->400 Tg N $year^{-1}$).

## 3.2. Introduction

Nitrogen is an essential macronutrient for all organisms, and oceanic N sinks that remove biologically available N via denitrification and anaerobic ammonium ($NH_4^+$) oxidation (anammox) ultimately limit marine primary productivity. Denitrification, the stepwise reduction of nitrate ($NO_3^-$) to $N_2$ gas, is mediated by both heterotrophic and autotrophic bacteria, and occurs in the anoxic and suboxic oceanic water-column (Codispoti *et al.*, 2001; Lavik *et al.*, 2009; Ward *et al.*, 2009; Grote *et al.*, 2012) and sediments (e.g. Christensen *et al.*, 1987). For the past decade, anammox, i.e the conversion of $NH_4^+$ and nitrite ($NO_2^-$) to $N_2$ gas by autotrophic anaerobic bacteria, has

also been reported to account for a significant part of the N loss in oceanic anoxic zones (Dalsgaard *et al.*, 2003; Kuypers *et al.*, 2003; 2005; Lam *et al.*, 2009; Jensen *et al.*, 2011). While studies of N cycling in marine ecosystems have concentrated on oxygen-deficient waters in coastal and open ocean oxygen minimum zones and sediments (see references above), little is known about metabolic processes and bacterially-mediated N-cycle dynamics that occur in the extensive subsurface biosphere of hydrothermal vent systems.

Hydrothermal fluids are formed when seawater circulates through the upper oceanic crust at mid-ocean ridges where it is heated and chemically altered in the subsurface, and rises back to the seafloor. The fluids are either discharged directly through high-temperature vents (up to ~400ºC) or through diffuse, low temperature (low-T) vents (typically <50ºC) following subsurface mixing with crustal seawater. Ecosystems at seafloor vents are sustained by biomass production through chemolithoautotrophic bacteria and archaea that gain their metabolic energy primarily from the oxidation of reduced sulfur species and molecular hydrogen ($H_2$) present in vent fluids (e.g. Jannasch and Mottl, 1985).

Observations of abundant and diverse microbial populations at low-T vents (e.g. Huber *et al.*, 2002; 2007; Alain *et al.*, 2004), as well as $NO_3^-$ removal in the sub-seafloor mixing zone (Butterfield et al, 2004), and stable isotope measurements of dissolved N species in hydrothermal fluids of the Juan de Fuca Ridge (Bourbonnais *et al.*, 2012a) provide insight into microbial N processes in the subsurface biosphere. There are also more conclusive evidences for both denitrification and anammox activity in hydrothermal vent systems. For example, Wang *et al.* (2009) detected an almost complete spectrum of the functional genes required for denitrification, i.e. *nar* ($NO_3^-$ reductase), *nir* ($NO_2^-$

reductase), *norB* (nitric oxide (NO) reductase) and *nosZ* (nitrous oxide ($N_2O$) reductase), in DNA extracted from hydrothermal vent chimneys of the Juan de Fuca Ridge using functional gene arrays (GeoChip). Byrne *et al.* (2009) documented, for the first time, the presence and activity of anammox bacteria in hydrothermal vents of the Mid-Atlantic Ridge. Their reported anammox rates, measured from an aqueous mixture of chimney samples, were low (up to 60 nmol N $L^{-1}$ $day^{-1}$). Major metabolic pathways for fixed N loss have never directly been quantified in discharging hydrothermal fluids, and environmental controls on the activity and abundance of microbial populations that are responsible for fixed N loss processes as these fluids rise through the subsurface remain to be determined.

Information on the specific microbial agents mediating N loss in the subsurface biosphere of hydrothermal vent systems is still emerging. Culture-independent molecular surveys of microbial diversity in these systems have identified 16S rRNA gene sequences affiliated with known autotrophic denitrifiers (e.g. López-García *et al.*, 2002; Hodges and Olson, 2009). ε-proteobacteria are generally the dominant group of chemolithoautotrophs in hydrothermal vent fluids (López-García *et al.*, 2003; Alain *et al.*, 2004; Nakagawa *et al.*, 2005a; Huber *et al.*, 2007; 2010). Cultivation studies have confirmed that many of these ε-proteobacteria retain the capacity to oxidize reduced sulfur species and $H_2$, while reducing $NO_3^-$ or other electron acceptors (e.g. $O_2$, $S^0$ and $S_2O_3^-$) (Nakagawa *et al.*, 2005a; Takai *et al.*, 2006).

At least one denitrifying γ-proteobacterial group is also known from hydrothermal environments. 16S rRNA gene sequences affiliated with SUP05 γ-proteobacteria, related to the gill symbionts of deep-sea clams and mussels, have been identified as major

constituents of redox-active hydrothermal vent plumes (Sunamura *et al.*, 2004; German *et al.*, 2010). SUP05 was first described in the Suiyo Seamount hydrothermal plume by Sunamura *et al.* (2004) and later associated with oxygen-deficient marine waters in the eastern tropical South Pacific (Stevens and Ulloa, 2008), the Namibian upwelling system (Lavik *et al.*, 2009) and the northeastern subarctic Pacific (Walsh et al, 2009; Zaikova *et al.*, 2010). Ecophysiological studies, metagenome assembly and gene expression profiling indicate that SUP05 couples the oxidation of reduced sulfur species with $NO_3^-$ reduction (Lavik *et al.*, 2009; Walsh *et al.*, 2009, Stewart *et al.*, 2012). Based on these observations, SUP05 populations would be expected to inhabit subsurface conduits and mixing zones that supply diffuse hydrothermal vents. In these branched interstitial spaces, sulfide concentrations are high and there is episodic re-supply of $NO_3^-$ from entrained crustal seawater.

In the present study, we examined the relative importance of rates of denitrification, anammox and dissimilative $NO_3^-$ reduction to $NH_4^+$ (DNRA) in relation to specific microbial agents in diffuse hydrothermal vent fluids of the Juan de Fuca Ridge, using a combination of $^{15}N$ paired isotope labelling, 16S rRNA gene clone library sequencing and quantitative polymerase chain reaction (qPCR) methods. We then used these results to assess the diversity and abundance of potential sulfur-oxidizing denitrifiers and evaluated chemical and physical constraints on the activity and abundance of the microbial communities that mediate biological N loss in the subsurface of hydrothermal vents. Finally, we extended our interpretation to consider the role of the subsurface hydrothermal biosphere in modulating geochemical N fluxes in the deep ocean.

## 3.3. Material and Methods

### 3.3.1. Site description and sample collection

Discharging fluids were sampled at different diffuse vent sites on Axial Volcano and the Endeavour Segment, both located on the Juan de Fuca Ridge, in the northeast Pacific Ocean (Fig. 3.1). Sampling took place during 4 summer/autumn cruises in August 2007, June and August-September 2008 and June 2009 using submersibles supported by the CCGS *John P. Tully* and the R/V *Atlantis* during the New Millennium Observatory (NeMO) and Endeavour-Axial Geochemistry and Ecology Research (EAGER) Projects.

The latitude/longitude coordinates of sampled vents are given in Table 3.1. At Endeavour Segment, diffuse vents were sampled in the Main Endeavour (ME), High Rise (HR) and Mothra (M) vent fields at depths of 2100-2300m. Sediments that are now buried by ridge basalts are thought to be the origin of anomalously high methane ($CH_4$) and $NH_4^+$ concentrations observed in vent fluids at this site (Lilley *et al.*, 1993). Axial Volcano is the volcanically most active site on the Juan de Fuca Ridge, and rises 700 m above the ridge crest. It has a rectangular shaped caldera (3 × 8 km) that lies between two rift zones, with vents located near the caldera fault and along the rift zones, at depths of 1500 to 1550m. The diffuse vents were sampled in the ASHES, CASM and South Rift Zone vent fields. A January-February 1998 seafloor volcanic eruption covered most of the South Rift Zone vent field with volcanic material and resulted in the formation of new vents (Embley *et al.*, 1999). A more recent eruption was detected in July 2011 (Chadwick *et al.*, 2012).


**Figure 3.1**. Map of the hydrothermal vent fields, i.e. Axial Volcano and Endeavour Segment on the Juan de Fuca Ridge (northeast Pacific Ocean), indicated by red stars. See Table 3.1 for precise location of the sampled vent sites.

Hydrothermal fluids were sampled using two different devices. During the June 2008 cruise, low and high temperature fluids were collected using a suction sampler, that pumped water into 2 L acrylic jars mounted on the remotely operated vehicle (ROV) ROPOS. The jars were flushed several times prior to sample collection. During all other cruises, samples were collected using the Hydrothermal Fluid and Particle Sampler (HFPS) mounted on the ROV JASON or the deep submergence vehicle (DSV) ALVIN. HFPS samples were collected either in collapsible Tedlar® bags with valves (of up to ~600 mL volume each), or in PVC piston samplers with Teflon spring seals. The average

inlet temperature during sample collection was calculated from *in-situ* temperature recorded at 1 Hz.

During the June 2008 cruise, samples for denitrification rate measurements were transferred without contact with the atmosphere to 500 mL amber bottles, capped with silicone stoppers containing two lengths of 1/16 inch nylon tubing with valves, and connected to the suction jar by 1/8- and 5/16-inch Tygon tubes, as described in Devol *et al.* (2006). During the August-September 2008 cruise, $^{15}N$-labeling experiments for rate determinations were directly conducted in the Tedlar® collapsible bags. Samples were stored for typically less than 1 hour in a cool room after each dive until further processing. Subsamples were taken from the collapsible bags using a syringe, and transferred into acid-washed and DI-rinsed 60-mL HDPE brown bottles for nutrient concentration determination. All nutrient sub-samples were purged with $N_2$ gas for at least 10 minutes in order to remove hydrogen sulfide ($H_2S$), which potentially interferes with colorimetric nutrient analyses. The purged nutrient samples were kept frozen at -20$^{o}$C until analysis.

### 3.3.2. Physico-chemical properties

Chemical analyses of fluid samples were conducted on board within less than ~8 hours after sampling. pH was analyzed potentiometrically with a standard deviation of 0.01 pH unit. Magnesium ($Mg^{2+}$) concentrations were analyzed as in Butterfield *et al.* (2004). Hydrogen sulfide and $NH_4^+$ concentrations were analyzed using standard colorimetric methods (methylene blue (Cline, 1969) and indophenol blue (Solorzano, 1969) methods,

respectively), with standard precisions of 4% and 7%, respectively. $NO_x$ ($NO_3^-$ and $NO_2^-$) was measured by chemiluminescence, i.e. reduction to NO in a heated solution of acidic vanadium (III) and subsequent detection of NO (Braman and Hendrix, 1989), with an analytical precision for replicate analyses of ± 0.2 μmol $L^{-1}$. Nitrate, $NO_2^-$, and phosphate ($PO_4^{3-}$) were also analyzed on shore using a colorimetric Astoria II nutrient autoanalyzer following methods described in Barwell-Clarke and Whitney (1996). Dissolved $NO_x$ concentrations measured colorimetrically and by chemiluminesce were generally in good agreement. Nitrous oxide concentrations were measured onboard immediately after sample collection. Replicates of 25 mL fluid samples and blanks (DI water only) were anaerobically transferred into 60 mL syringes prefilled with 12 mL of ultra-pure He, shaken for 10 minutes to ensure complete equilibration, and the gas phase was injected into 12 mL evacuated exetainers and analyzed on a Varian CP-3800 gas chromatograph equiped with an electron capture detector (ECD). Calibration curves were constructed from five serial two-fold dilutions of a concentrated $N_2O$ standard (~1250 nmol $N_2O$ $L^{-1}$) from a reference ultra-pure $N_2O$ gas tank. Dissolved [$N_2O$] was calculated using the Weiss and Price (1980) parametric equation for the solubility of $N_2O$ in seawater, accounting for any blank contribution. One to five sub-samples were collected at each sampling site (for all physico-chemical parameters except $N_2O$) during each dive and, where applicable, only the average and standard deviation for all sub-samples at a given site is reported.

### 3.3.3. Denitrification, anammox and DNRA rates

During the two 2008 cruises, isotopically-labeled incubations were conducted at the measured *in-situ* sample temperatures in 500 mL amber glass bottles or Tedlar® bags. We followed the Devol *et al.* (2006) protocol, with some modifications. The bottles (i.e. one bottle for each time point) for the June 2008 samples were pre-incubated for 12 hours before the start of the incubations to remove any oxygen from seawater entrained during sampling by the suction pump. All other samples (August-September 2008) were not pre-incubated. Anoxia in the samples was verified by an Oxoid anaerobic resazurin indicator (BR0055). Added $^{15}N\text{-}NO_3^-$ (~10 μmol $L^{-1}$) never represented more than 46% of the ambient $NO_3^-$ concentration (Table 3.1). At 3 different time points (between 0 and ~48 hours) ~125 mL of sample was transferred, without contact with the atmosphere, into 160-180 mL evacuated glass bottles (i.e. two bottles (June 2008) or one bottle (August-September 2008) for each time point), poisoned with 100 μl of saturated mercuric chloride ($HgCl_2$) and equiped with gas tight 9 mm bore Louwers-Hapert single or double O-ring valves (Emerson *et al.,* 1999). $CO_2$ was placed in the neck immediately after sample collection and the neck was sealed with a vinyl cap to avoid air contamination. In the shore-based laboratory, less than ~5 months after sampling, the flasks were weighed and the dissolved gases in the water samples were equilibrated with the headspace in a constant temperature water bath, overnight. The liquid was then removed using a vacuum pump, leaving most (>95%) of the gas behind. The remaining gas was transferred to a stainless steel tube immersed in liquid He. Water and $CO_2$ were cryogenically trapped during the gas extraction process and oxygen was removed using a hot copper furnace, to avoid isobaric interference during the analysis of $^{30}N_2$. A known amount of $^{36}Ar$ was also

added during this step to determine the absolute concentrations of Ar in the samples. Gas samples were then analyzed for mass ratios 28:40, 29:28; 30:28 and 36:40, relative to in-house standards with known gas ratios, on a Finnigan Delta XL mass spectrometer at the University of Washington. Average precision based on duplicate measurements was 0.6% for the $N_2$/Ar ratio, 0.01‰ for $\delta^{29}N_2$ and 2‰ for $\delta^{30}N_2$ (where $\delta^{30}N_2 = [(R^{30}_{sample}/R^{30}_{standard}) -1]\times1000$ and $\delta^{29}N_2 = [(R^{29}_{sample}/R^{29}_{standard}) -1]\times1000$; R represents the molar ratio of mass 29 (or mass 30) to mass 28 $N_2$ in a sample or in the standard (air), respectively). Denitrification rates were calculated according to Devol *et al.* (2006) and Ward *et al.* (2009), assuming that the time zero points represent background $N_2$ concentrations.

Denitrification, anammox and DNRA rates were also measured in duplicate during the 2009 cruise following a slightly different protocol. ~20 μmol $L^{-1}$ $^{15}N$-labeled $NO_3^-$, $NO_2^-$ or $NH_4^+$ were added to the hydrothermal vent fluids as soon as possible after sample collection. Sample vials were then purged with helium (He), and sample aliquots were anaerobically transferred to 12 mL exetainers and incubated at the measured *in-situ* temperature without headspace (see Kuypers *et al.*, 2005) for up to ~53 hours. About 10 μmol $L^{-1}$ natural-abundance $NH_4^+$ was also added in the $^{15}N$-$NO_2^-$ experiments. At specific time points, 1 mL of water was removed and replaced with He, and a saturated $HgCl_2$ solution was added to stop biological activity. The production of $^{29}N_2$ and $^{30}N_2$ for all labeled experiments was determined in the headspace through isotope ratio mass spectrometry (IRMS) measurements (VG Optima Micromass), using air as a standard, approximately one month after sample collection. Denitrification and anammox rates were calculated according to Nielsen (1992) and Thamdrup *et al.* (2006), considering

only the linear portions of the curves. The errors on the slopes of the regression lines were calculated (see Fig. 3.2 and 3.3).

For DNRA rate measurements, 6 mL exetainers were filled with fluid samples (from the 12 mL exetainers above, after incubating with $^{15}N\text{-}NO_3^-$ or $NO_2^-$ and measuring the $^{29}N_2$ and $^{30}N_2$ in the headspace for denitrification rates). About 5 μmol $L^{-1}$ $^{14}NH_4^+$ was added, to increase the background $NH_4^+$ concentration, and the headspace was flushed with 5 mL He gas using a Hamilton gas-tight syringe to remove labeled $^{15}N_2$ product from the previous experiment. 1 mL of water was removed and replaced with He, following which 200 μL of a freshly made sodium hypobromite solution was added to the exetainer to convert $NH_4^+$ to $N_2$. The solution was mixed using a vortex mixer for at least 30 seconds. In addition, three replicates of a mixture made from 10 μmol $L^{-1}$ of $Na^{15}NO_3$ and 10 μmol $L^{-1}$ $^{14}(NH_4)_2SO_4$ were used as abiotic controls and were treated as samples. The exetainers were inverted to prevent any gas loss and samples were incubated overnight at room temperature. The production of $^{29}N_2$ and $^{30}N_2$ for all labeled experiments was then determined in the headspace through IRMS measurements as described above, and DNRA rates were calculated (from the production of $^{29}N_2$ only). The calculated conversion factor, i.e. the fraction of $NH_4^+$ converted to $N_2$ from the abiotic controls, was close to 90% and data were corrected accordingly.

### 3.3.4. Environmental DNA extraction and diversity profiling

#### 3.3.4.1. DNA extraction

Environmental DNA (eDNA) was extracted from 0.2 μm Sterivex filters (Millipore) following the protocol described in Huber *et al.* (2002) with some modifications. 20 μl of proteinase K (10mg/mL) was added with the sodium dodecyl sulfate (SDS; 20%) before incubation at 65°C for 2 hours, instead of at the beginning of the extraction together with extraction buffer. 200 μl lysozyme (50 mg/mL) was also added at this step. Finally, the eDNA was resuspended in 95 μL of TE buffer (10 mM Tris, 1 mM EDTA, pH 8.0) and was stored at -80°C.

#### 3.3.4.2. PCR, cloning and sequencing

Following dilutions of the original eDNA obtained from Cloud (AV, 2007), Bag City (AV, 2008), Hulk (2008b), Godzilla (ES) and Phang (ES) vents, near complete 16S rRNA genes were amplified using primers targeting the bacterial domain: B8F (5'-AGAGTTTGATCCTGGCTGAG-3') and B1492R (5'-GGTTACCTTGTTACGACTT-3') under the following PCR conditions: 2 min at 94°C, followed by 30 cycles of 94°C for 30 s, 55°C for 45 s, 72°C for 2 min, and a final extension of 10 min at 72°C. Each 20 μl reaction contained 1μl of template DNA, 1μl of a 5μmol $L^{-1}$ forward and reverse primer, respectively, 2μl of 8μmol $L^{-1}$ deoxynucleotide solution, 1.25μl of a 50 μmol $L^{-1}$ $MgCl_2$ solution, 2.75μl of a 1× Invitrogen PCR Buffer, and 1 U (unit) of Taq DNA polymerase (Bio-Rad). The PCR amplification products were visualized by UV excitation following electrophoresis on ~1% (wt/vol) agarose gels stained with SYBR safe (Invitrogen), reconditioned to eliminate heteroduplexes (Thompson *et al.* 2002) and purified using the QIAquick PCR Purification Kit according to the manufacturer's

instructions. DNA was ligated into a pCR® 2.1 TOPO® vector (Invitrogen) and transformed into chemically competent TOP10F' One Shot® *E. coli* cells following the manufacturer's instructions. Transformants (white colonies) were randomly picked, grown in LB + Ampicillin, and cloned inserts were amplified with the vector primers M13F (5'-GTAAAACGACGGCCAG-3') and M13R (5'-CAGGAAACAGCTATGAC-3') in a 50 μL reaction mixture described in Forget *et al.* (2010). Inserts (218 in total, ~30 to 60 at each site) were sequenced at the High-Throughput Genomics Unit (University of Washington) or at the University of Victoria using the PCR primers B8F, B1492R, B515F (5'-GTGCCAGCMGCCGCGGTAA-3') and B907R (5'-CCGTCAATTCMTTTRAGTTT-3').

#### 3.3.4.3. Phylogenetic analysis

All sequences were edited manually using Sequencher v.4.7 (Gene Codes Corporation). The open source Bellerophon application (http://comp-bio.anu.edu.au/bellerophon/bellerophon.pl) (Huber *et al.*, 2004) and PinTail (Ashelford *et al.*, 2006) were used to detect chimeric sequences. Chimeras were excluded from further analysis. Nucleotide sequences (213 in total) were aligned using the ClustalW Application (Thompson *et al.*, 1994) in BioEdit (version 7.0.5.3) and manually checked. Closest relatives were identified for each sequenced clone using BLAST (Altschul *et al.*, 1990). Sequences were classified for phylogenetic analysis using the Ribosomal Database Project (RDP) Classifier tool (Wang *et al.*, 2007). Maximum likelihood trees were

inferred by PhyML (version 3.0 for Windows) (Guindon *et al.*, 2010) using the HKY85 model of nucleotide evolution with 100 bootstrap replicates.

#### 3.3.4.4. Richness and diversity analysis

Rarefaction curves were calculated using MOTHUR version 1.22.2 (Shloss et al, 2009). Sequences with <97% similarity were treated as distinct operational taxonomical units (OTU). OTU richness was calculated using the Chao-1 estimator (Chao, 1984). Diversity in the small subunit (SSU) rRNA clone libraries was determined using the Shannon index (H) (Krebs, 1999). The coverage for each clone library was calculated as in Ravenschlag *et al.* (1999) according to the formula:

$$C = [1 - (n_1/N) \times 100] \quad (3.1)$$

where $n_1$ is the number of different OTUs within the library and $N$ is the total number of clones sequenced. See Table 3.2 for 16S rRNA gene clone libraries information and OTUs richness (Chao-1) and diversity (Shannon) estimates.

#### 3.3.4.5. Sequences accession numbers

Sequences were deposited to GenBank under the accession numbers JQ712372-JQ712487.

### 3.3.5. Total bacterial cells and abundance of SUP05 and anammox bacteria

Total cell abundances in diffuse hydrothermal fluids collected in 2008 and 2009 were determined by epifluorescence microscopy following DAPI staining in the laboratories of J. Holden (University of Massachusetts) and J. Baross (University of Washington). Total bacterial and SUP05 group specific SSU rRNA gene copy numbers were determined by qPCR using an Opticon® 2 DNA Engine Real-Time PCR detection system (Bio-Rad) according to Zaikova *et al.* (2010). The following primer pairs were used for the quantification of Bacteria: 27F, (5′-AGAGTTTGATCCTGGCTCAG); DW519R (5′-GNTTTACCGCGGCKGCTG) and SUP05: Ba519F (5'-CAGCMGCCGCGGTAANWC-3') and 1048R, 5'-CCATCTCTGGAAAGTTCCGTCT-3').

We used the same standard as Zaikova *et al.* (2010) to quantify total and SUP05 bacteria with initial concentrations of $2.8 \times 10^{10}$ copies/μL and $8.5 \times 10^{8}$ copies/μL, respectively, as determined from PicoGreen assays using the Quant-iT PicoGreen® dsDNA kit (Invitrogen). For all qPCR assays, calibration curves were constructed with six 10-fold dilutions of the standards. The limit of detection, set above the Ct (cycle threshold) values of the no-template controls, was generally less than ~50 copies $mL^{-1}$ for total and SUP05 bacteria qPCR assays for all triplicate samples. The amplification efficiency for each run was estimated by the slope of the standard curve according to the equation: $E= (10^{-1/slope})$ and was in all cases above 95%.

We also assessed anammox bacterial abundances using a qPCR approach following the method described in Humbert *et al.* (2012). Standard curves were prepared by serial dilution of a plasmid preparation of an anammox clone from Lake Lugano, Switzerland

(Wenk *et al.*, 2012). All samples and standards were run in triplicates on a Rotor-gene™ 3000 Real-Time PCR detection system (Corbett Research). No anammox bacteria were detected in any of the samples from this study, while anammox-bacteria amended control samples yielded positive results (data not shown).

## 3.4. Results

### 3.4.1. Physico-chemical properties

Temperature, pH, and $Mg^{2+}$, $N_2O$, $H_2S$, $PO_4^{3-}$, $NO_3^-$, and $NH_4^+$ concentrations are summarized in Table 3.1 for all low-T vent fluids sampled at Axial Volcano and Endeavour Segment. Diffuse fluid temperatures ranged from 7 °C (Cloud, AV) to 37 °C (Hermosa, AV) and pH varied between ~5.5 and 7.0. Magnesium concentrations ranged between 42 and 53 mmol/kg, and were generally close to the [$Mg^{2+}$] for background seawater (53 mmol/kg). Magnesium is almost completely removed from aqueous solution during high-T hydrothermal circulation through various water-rock reactions, and resupplied during mixing with crustal seawater at lower temperatures (Edmond *et al.*, 1979). As a result, a clear linear relationship exists between temperature and [$Mg^{2+}$] (Butterfield *et al.*, 2004; Bourbonnais *et al.*, 2012a), and [$Mg^{2+}$] can thus be used as a proxy for the degree of mixing in the hydrothermal vent fluids. Nitrous oxide concentrations ranged between ~0 (not detectable after blank correction) and 347 nmol $L^{-1}$, similar to previous observations at Axial Volcano (Butterfield *et al.*, 2004). Hydrogen sulfide concentrations were generally high (up to 1300 µmol $L^{-1}$ at Marker

113, AV). Phosphate concentrations varied from 1.5 to 4 μmol $L^{-1}$ (compared to ~3 μmol $L^{-1}$ in background seawater). Nitrate concentrations ranged from 1.6 μmol $L^{-1}$ (Marker 113, AV, 2007) to 41.7 μmol $L^{-1}$ (Hermosa, AV) and were generally lower than background deep-sea water (~40-42 μmol $L^{-1}$). Nitrite concentrations were low, accounting for generally less than 2% (data not shown in Table 3.1) of total $NO_x$.

Ammonium concentrations were generally low (<4 μmol $L^{-1}$ at most sites) at Axial Volcano, compared to Endeavour Segment where $[NH_4^+]$ was between 15 μmol $L^{-1}$ and 56 μmol $L^{-1}$. Lower $NH_4^+$ concentrations (1 to 4 μmol $L^{-1}$) were observed in the ROPOS suction samples from the June 2008 cruise, and are likely the result of dilution by entrainement of surrounding seawater during sampling with this less efficient device (versus the dedicated vent fluid sampler) rather than reflecting actual *in-situ* concentrations. In an attempt to estimate the net consumption or production of fixed N (i.e., $NO_3^-$ and $NH_4^+$) in diffuse HV fluids, we calculated $NO_3^-$, $NH_4^+$ and DIN deficits, according to the following equations that take water mixing into account:

$$NO_3^-{}_{deficit} = [([Mg^{2+}]_{meas}/[Mg^{2+}]_{sw}) \times [NO_3^-]_{sw}] - [NO_3^-]_{meas} \quad (3.2)$$

$$NH_4^+{}_{deficit} = [(1-[Mg^{2+}]_{meas}/[Mg^{2+}]_{sw}) \times [NH_4^+]_{high\text{-}T}] - [NH_4^+]_{meas} \quad (3.3)$$

$$DIN_{deficit} = NO_3^-{}_{deficit} + NH_4^+{}_{deficit} \quad (3.4)$$

where $[NO_3^-]_{meas}$, $[NH_4^+]_{meas}$, and $[Mg^{2+}]_{meas}$ are $NO_3^-$, $NH_4^+$ and $Mg^{2+}$ concentrations measured in diffuse fluids, respectively, $[NO_3^-]_{sw}$ and $[Mg^{2+}]_{sw}$ are $NO_3^-$ and $Mg^{2+}$ concentrations in background seawater collected near AV and ES, and $[NH_4^+]_{high\text{-}T}$ is the $NH_4^+$ concentration in the high-T end-member. $[NO_3^-]_{sw}$ is constant at ~40 μmol $L^{-1}$ and the average $NH_4^+$ concentrations in high-T vent fluids varies between vent fields: 14 μmol $L^{-1}$ (AV), 396 μmol $L^{-1}$ (ES, M), 410 μmol $L^{-1}$ (ES, ME), 863 μmol $L^{-1}$ (ES, HR)

(data from Bourbonnais *et al.*, 2012a). Nitrate, $NH_4^+$ and DIN deficits ranged from 38 μmol $L^{-1}$ (Marker 113, AV, 2007) to −2 μmol $L^{-1}$ (Hermosa, AV), from 16 μmol $L^{-1}$ (Fairy Castle, ES) to −12 μmol $L^{-1}$ (Marker 113, AV, 2007) and 30 μmol $L^{-1}$ (Bag City, AV) to −3 μmol $L^{-1}$ (Hermosa, AV), respectively (Table 3.1) (with negative values indicating a surplus).

### 3.4.2. Potential rates of denitrification, anammox and DNRA

Production of $^{29}N_2$ and $^{30}N_2$ during *ex-situ* incubations generally showed linear behavior during the incubation period (Fig. 3.2). Nitrate concentration changes in the incubations (not shown) were generally qualitatively consistent with observed $N_2$ production trends. Even at sites where we measured the lowest denitrification rate of 0.5 nmol $L^{-1}$ $day^{-1}$ (Easter Island, ES, 2008b), the associated $\delta^{29}N_2$ and $\delta^{30}N_2$ increases (1.3‰ and 9.0‰, respectively) were well within the average precision of the measurements (see section 3.3.3), so that we can state that the rate detection limit is < 0.5 nmol $L^{-1}$ $day^{-1}$. Parallel incubations of 2009 samples with addition of either $^{15}N$-labeled $NO_3^-$ or $NO_2^-$ generally yielded similar denitrification and DNRA rates, usually with less than 30% variation between the two series of incubations. Average rates for both series of incubations (2009 samples) are indicated in Fig. 3.3 when production of $^{29}N_2$ and $^{30}N_2$ was linear.

**Table 3.1.** Physico-chemical and microbiological properties of the sampled vent fluids at Axial Volcano (AV) and the Endeavour Segment (ES) on the Juan de Fuca Ridge. Values shown are means ± one standard deviation for all samples collected from a given vent on each cruise. 2008a and 2008b refers to samples collected during the June and August-September 2008 cruises, respectively. n is the number of sub-samples and na means not analyzed.

| Field | Vent | Year | Lati-tude | Longi-tude | Depth (m) | n | Temp. (°C) | pH | $[Mg^{2+}]$ (mmol $kg^{-1}$) | $[N_2O]$ (nmol $L^{-1}$) | $[H_2S]$ (µmol $L^{-1}$) |
|---|---|---|---|---|---|---|---|---|---|---|---|
| AV | Bag City | 2007 | 45.92 | 129.99 | 1533 | 3 | 13.7 ± 0.9 | 6.5 ± 0.1 | 50.5 ± 1.3 | na | 39.3 ± 19.3 |
| AV | Cloud Pit | 2007 | 45.93 | 129.98 | 1521 | 3 | 6.5 ± 0.2 | 6.9 ± 0.1 | 52.4 ± 0.1 | na | 76.5 ± 130.3 |
| AV | Gollum | 2007 | 45.93 | 130.01 | 1544 | 2 | 22.0 ± 0.5 | 5.4 | 50.5 ± 0.1 | na | 154.3 ± 24.5 |
| AV | Marker 113 | 2007 | 45.92 | 129.99 | 1523 | 3 | 31.2 ± 0.4 | 5.7 ± 0.2 | 49.9 ± 0.9 | na | 1324.6 ± 71.1 |
| AV | Bag City | 2008b | 45.92 | 129.99 | 1532 | 3 | 11.2 ± 0.0 | 6.5 ± 0.2 | 51.5 ± 0.1 | na | 55.3 ± 48.4 |
| AV | Cloud Pit | 2008b | 45.93 | 129.98 | 1522 | 4 | 6.8 ± 0.0 | 6.9 ± 0.0 | 52.6 ± 0.0 | na | 1.9 ± 0.3 |
| AV | Marker 33 | 2008b | 45.93 | 130.98 | 1520 | 4 | 18.5 ± 2.1 | 5.8 ± 0.1 | 47.8 ± 0.7 | na | 434.0 ± 43.9 |
| AV | Marker 113 | 2008b | 45.92 | 129.99 | 1521 | 3 | 23.5 ± 3.5 | 6.0 ± 0.1 | 51.1 ± 0.6 | na | 947.0 ± 176.3 |
| AV | Gollum | 2009 | 45.93 | 130.01 | 1542 | 5 | 14.2 ± 1.2 | 5.7 ± 0.0 | 51.7 ± 0.2 | 256.8 ± 9.4 | 89.6 ± 11.6 |
| AV | Hermosa | 2009 | 45.93 | 129.98 | 1519 | 3 | 37.0 ± 4.1 | 5.6 ± 0.3 | 51.1 ± 0.9 | 78.0 ± 4.3 | 253.2 ± 160.3 |
| AV | Marker 33 | 2009 | 45.93 | 129.98 | 1520 | 4 | 34.4 ± 0.9 | 5.5 ± 0.0 | 41.9 | 214.4 ± 0.4 | 711.7 ± 19.0 |
| AV | Marker 113 | 2009 | 45.92 | 129.99 | 1521 | 4 | 29.9 ± 5.0 | 6.1 ± 0.1 | 50.8 ± 0.4 | 11.3 ± 9.4 | 1020.0 ± 194.2 |
| AV | Bkgd | 2009 | 45.90 | 130.00 | >1200 | 6 | 3.0 ± 0.5 | 7.1 ± 0.4 | 52.4 ± 0.3 | na | 0.4 |
| ES | Clam bed | 2008a | 47.96 | 129.09 | 2188 | 1 | 21.2 ± 4 | na | na | na | na |
| ES-ME | Easter Island | 2008a | 47.95 | 129.10 | 2199 | 2 | 20 | na | na | na | na |
| ES-ME | Hulk | 2008a | 47.95 | 129.10 | 2201 | 2 | 25 | na | na | na | na |
| ES-M | Cauldron | 2008b | 47.93 | 129.11 | 2249 | 3 | 36.3 ± 4.7 | 6.4 ± 0.1 | 47.1 ± 0.5 | na | 219.6 ± 61.0 |
| ES-ME | Easter Island | 2008b | 47.95 | 129.10 | 2197 | 4 | 16.6 ± 3.6 | 6.7 ± 0 | 50.8 ± 0.1 | na | 11.9 ± 3.7 |
| ES-HR | Godzilla | 2008b | 47.97 | 129.09 | 2135 | 3 | 21.7 ± 8.6 | 6.2 ± 0.3 | 49.6 ± 1.7 | na | 169.6 ± 126.5 |
| ES-ME | Hulk | 2008b | 47.95 | 129.10 | 2197 | 3 | 16.4 ± 1.7 | 6.5 ± 0.1 | 50.7 ± 0.6 | na | 92.4 ± 8.2 |
| ES-HR | Fairy Castle | 2009 | 47.97 | 129.09 | 2157 | 2 | 23.4 ± 1.8 | 6.2 | 49.3 ± 0.2 | 346.5 ± 4.3 | 245.0 ± 35.4 |
| ES-ME | Hulk | 2009 | 47.95 | 129.10 | 2198 | 4 | 29.5 ± 10.6 | 6.3 ± 0.3 | 48.3 ± 1.9 | BDL | 212.5 ± 132.7 |
| ES-M | Phang | 2009 | 47.92 | 129.11 | 2277 | 5 | 24.1 ± 1.7 | 6.5 ± 0.3 | 47.5 ± 2.0 | 107.0 ± 14.6 | 255.6 ± 133.6 |
| ES | Bkgd | 2009 | 48.00 | 129.10 | >2000 | 8 | 2.2 ± 0.3 | 7.3 ± 0.2 | 52.7 ± 0.4 | na | 1.0 |

**Table 3.1.** (continued) Physico-chemical properties of the sampled vent fluids at Axial Volcano and the Endeavour Segment on the Juan de Fuca Ridge.

| Field | Vent | Year | $[PO_4^{3-}]$ ($\mu mol\ L^{-1}$) | $[NO_3^- + NO_2^-]$ ($\mu mol\ L^{-1}$) | $[NO_3^-]$ deficit ($\mu mol\ L^{-1}$) | $[NH_4^+]$ ($\mu mol\ L^{-1}$) | $[NH_4^+]$ deficit ($\mu mol\ L^{-1}$) | DIN deficit ($\mu mol\ L^{-1}$) | Cell count $mL^{-1}$ |
|---|---|---|---|---|---|---|---|---|---|
| AV | Bag City | 2007 | 3.5 ± 0.5 | 8.6 ± 2.7 | 31.4 ± 4.7 | 1.9 ± 0.7 | -1.4 ± 3.0 | 30.0 ± 4.8 | na |
| AV | Cloud Pit | 2007 | 3.1 ± 0.2 | 18.1 ± 1.8 | 23.4 ± 4.2 | 1.4 ± 0.3 | -1.4 ± 3.0 | 22.0 ± 4.2 | na |
| AV | Gollum | 2007 | 4.2 ± 0.2 | 26.7 ± 0.4 | 13.3 ± 3.7 | 3.1 ± 0.9 | -2.6 ± 3.0 | 10.7 ± 3.8 | na |
| AV | Marker 113 | 2007 | 3.5 ± 0.0 | 1.6 ± 0.5 | 37.9 ± 3.7 | 12.6 ± 0.4 | -11.9 ± 2.9 | 26.0 ± 3.8 | na |
| AV | Bag City | 2008b | 2.6 ± 0.1 | 9.1 ± 3.0 | 30.6 ± 4.8 | 1.8 ± 0.1 | -0.4 ± 3.0 | 30.1 ± 4.8 | $(1.7 \pm 0.6) \times 10^5$ |
| AV | Cloud Pit | 2008b | 3.2 ± 1.7 | 16.0 ± 0.4 | 24.5 ± 3.9 | 1.4 ± 0.2 | -0.3 ± 3.0 | 24.2 ± 3.9 | $(5.3 \pm 0.4) \times 10^5$ |
| AV | Marker 33 | 2008b | 3.9 ± 0.9 | 31.2 ± 1.6 | 5.6 ± 3.9 | 1.9 ± 0.6 | 0.4 ± 2.8 | 6.0 ± 3.9 | $(2.0 \pm 0.5) \times 10^5$ |
| AV | Marker 113 | 2008b | 3.5 ± 0.4 | 15.8 ± 4.6 | 23.6 ± 5.9 | 10.7 ± 3.3 | -9.2 ± 4.4 | 14.4 ± 6.8 | $(8.0 \pm 0.3) \times 10^5$ |
| AV | Gollum | 2009 | na | 14.1 ± 5.2 | 15.5 ± 5.2 | 2.6 ± 0.7 | -1.3 ± 3.0 | 14.1 ± 5.2 | $(2.6 \pm 1.0) \times 10^4$ |
| AV | Hermosa | 2009 | na | 41.7 ± 2.2 | -2.4 ± 4.4 | 1.9 ± 1.1 | 4.4 ± 3.1 | -2.9 ± 4.5 | $(1.3 \pm 0.5) \times 10^4$ |
| AV | Marker 33 | 2009 | na | 15.7 ± 2.0 | 16.5 ± 3.6 | 4.4 ± 0.2 | -3.6 ± 2.4 | 15.8 ± 3.7 | $(2.8 \pm 0.5) \times 10^5$ |
| AV | Marker 113 | 2009 | na | 7.1 ± 3.4 | 32.0 ± 5.0 | 10.2 ± 3.1 | -8.6 ± 4.2 | 23.4 ± 5.9 | $(1.1 \pm 0.2) \times 10^6$ |
| AV | Bkgd | 2009 | 2.7 | 41.5 ± 3.8 | 0 | 0.4 ± 0.3 | -0.4 ± 0.3 | -0.4 ± 5.4 | na |
| ES | Clam bed | 2008a | na | 39.9 | na | 0.9 | na | na | $(9.2 \pm 0.3) \times 10^5$ |
| ES-ME | Easter Island | 2008a | na | 37.9 | na | 4.3 | na | na | $(2.3 \pm 0.1) \times 10^5$ |
| ES-ME | Hulk | 2008a | na | 36.3 | na | 3.3 | na | na | $(2.3 \pm 0.1) \times 10^5$ |
| ES-M | Cauldron | 2008b | 3.2 ± 0.8 | 29.2 ± 3.3 | 7.2 ± 4.8 | 47.6 ± 3.2 | -5.6 ± 5.2 | 1.6 ± 6.1 | $(4.7 \pm 1.0) \times 10^5$ |
| ES-ME | Easter Island | 2008b | 2.5 ± 0.6 | 17.8 ± 4.7 | 21.4 ± 5.1 | 15.2 ± 1.2 | 0.1 ± 2.6 | 21.5 ± 5.6 | $(1.3 \pm 0.3) \times 10^5$ |
| ES-HR | Godzilla | 2008b | 1.5 ± 0.2 | 34.1 ± 3.1 | 4.1 ± 5.0 | 56.3 ± 34.1 | -4.5 ± 44.3 | -0.4 ± 35.3 | $(2.6 \pm 0.6) \times 10^5$ |
| ES-ME | Hulk | 2008b | 2.4 ± 0.1 | 29.6 ± 1.3 | 9.5 ± 3.9 | 21.7 ± 2.5 | -5.8 ± 5.5 | 3.7 ± 5.1 | $(2.8 \pm 0.5) \times 10^5$ |
| ES-HR | Fairy Castle | 2009 | na | 28.0 ± 1.3 | 10.0 ± 2.3 | 41.4 ± 3.8 | 15.5 ± 6.8 | 25.5 ± 9.6 | $(6.1 \pm 2.2) \times 10^4$ |
| ES-ME | Hulk | 2009 | na | 27.8 ± 2.6 | 9.4 ± 3.6 | 38.0 ± 20.5 | -3.8 ± 25.6 | 5.6 ± 21.4 | $(1.0 \pm 0.4) \times 10^5$ |
| ES-M | Phang | 2009 | na | 30.4 ± 4.1 | 6.2 ± 4.7 | 42.7 ± 20.8 | -3.3 ± 25.6 | 2.9 ± 21.5 | $(4.4 \pm 1.5) \times 10^4$ |
| ES | Bkgd | 2009 | 3.1 | 40.6 ± 2.0 | 0 | 1.4 ± 2.2 | -1.4 ± 2.2 | -1.4 ± 3.7 | $(2.5 \pm 0.9) \times 10^4$ |

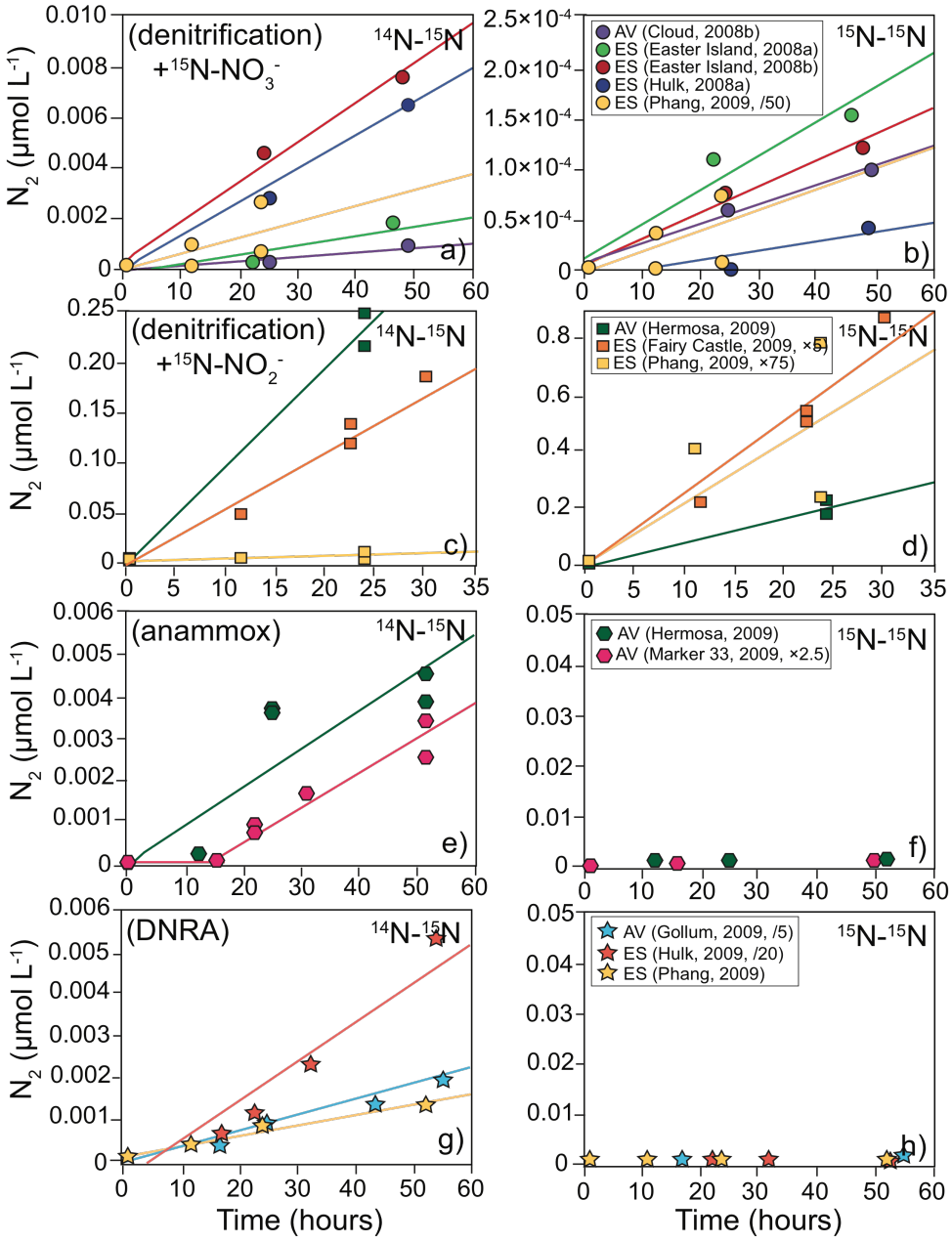


**Figure 3.2.** Production of $^{14,15}N_2$ and $^{15,15}N_2$ over time for selected $^{15}N$-labeled incubations: addition of $^{15}NO_3^-$ (**a, b**), $^{15}NO_2^-$ (c, d), $^{15}NH_4^+$ (**e, f**) and $^{15}NO_3^-$ followed by the addition of hypobromite (see text for more detail) (**g, h**) to measure potential denitrification (**a, b, c, d**), anammox (**e, f**), and DNRA (**g, h**) rates in diffuse hydrothermal vent fluids. All $N_2$ values were normalized to 0 µmol $L^{-1}$ at time t=0. Values for duplicate measurements are shown for all 2009 incubations. Values at some sites were multiplied or divided (numbers next to vent names and sampling years in legends) to fit on the same scales.

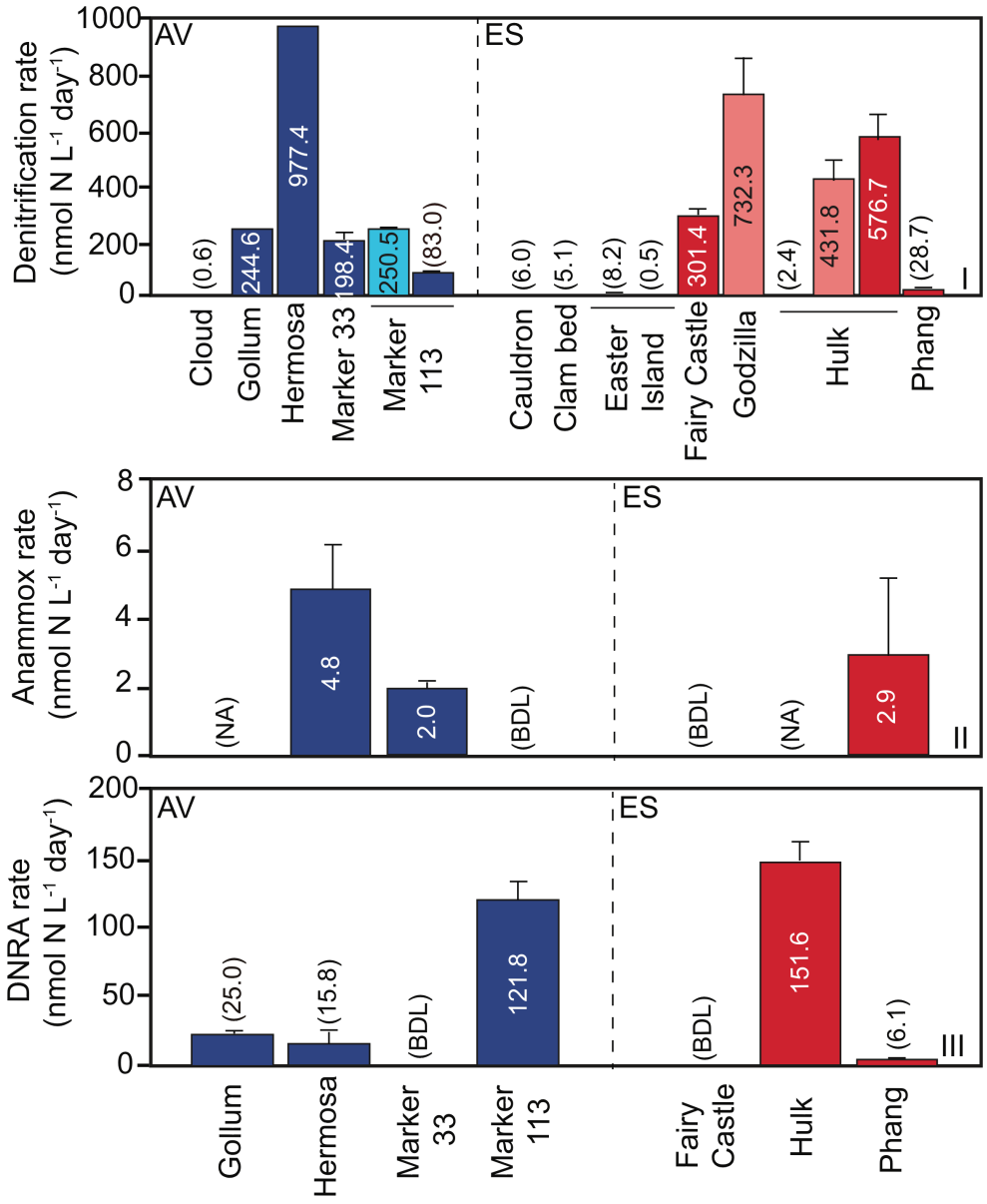


**Figure 3.3.** Denitrification (I), anammox (II) and DNRA (III) rates in nmol N $L^{-1}$ $day^{-1}$ at Endeavour Segment (ES) and Axial Volcano (AV) on the Juan de Fuca Ridge. The average denitrification and DNRA rates obtained from both $^{15}NO_3^-$ and $^{15}NO_2^-$ -labeled incubations during the 2009 cruise are shown when linear relationships were obtained (i.e. at Marker 113 (AV), Marker 33 (AV), Fairy Castle (ES), Phang (ES) and Hulk (ES)). Note the different scales for the y-axis. Numbers inside bars or in brackets are actual values. Color of the bar represents the sampled vent field (i.e. AV= blue and ES= red) and color intensity (i.e. no color, medium and dark) represents sites sampled during the June 2008 (always low rates, i.e Clam bed (ES), Easter Island (ES) and Hulk (ES) (first bars)), August-September 2008 and June 2009 cruises, respectively. Vertical lines represent the error propagation of the standard errors of the slopes of the linear relationships represented in Fig. 3.2 (i.e. $^{14,15}N_2$ and/or $^{15,15}N_2$ versus time).

Denitrification rates in diffuse vent fluids varied strongly between sites, ranging from 0.5 nmol N $L^{-1}$ $day^{-1}$ (Easter Island, ES, 2008b) to 977 nmol N $L^{-1}$ $day^{-1}$ (Hermosa, AV) (Fig. 3.3). Some temporal variability was observed at sites sampled multiple times. For example, measured denitrification rates ranged from 2 nmol N $L^{-1}$ $day^{-1}$ (2008a) to 577 nmol N $L^{-1}$ $day^{-1}$ (2009) at Hulk (ES) and from 83 nmol N $L^{-1}$ $day^{-1}$ (2008b) to 251 nmol N $L^{-1}$ $day^{-1}$ (2009) at Marker 113 (AV). Denitrification rates were always relatively low at Easter Island, ES (i.e. 8 nmol N $L^{-1}$ $day^{-1}$ (2008a) and 0.5 nmol N $L^{-1}$ $day^{-1}$ (2008b)). No significant differences were found between denitrification rates at Axial Volcano and Endeavour Segment for all samples collected during the 2008 and 2009 cruises or during individual cruises (Mann-Whitney test for non-parametric data, 95% confidence limit).

Anammox rates in vent fluids were below 5 nmol N $L^{-1}$ $day^{-1}$ at Hermosa (AV), Marker 113 (AV) and Phang (ES) and below the detection limit (BDL) for the two other measured sites (Marker 113, AV and Fairy Castle, ES). DNRA rates ranged from BDL at Marker 33 (AV) and Fairy Castle (ES) to 152 nmol N $L^{-1}$ $day^{-1}$ (Hulk, ES) (Fig. 3.3). There was no significant difference in DNRA rates between Axial Volcano and Endeavour Segment (Mann-Whitney test, 95% confidence limit).

### 3.4.3. Composition of 16S rRNA gene clone libraries and abundance of SUP05 bacteria

Bacterial diversity in diffuse vent fluids was generally high (Shannon index ≥2.9) except at Hulk, ES (Shannon index of 1.7) (Table 3.2). 16S rRNA gene clone libraries derived from Cloud (AV), Bag City (AV), Godzilla (ES) and Phang (ES) were dominated by ε-proteobacteria (up to ~80% of total clones sequenced at Bag City, AV). The

dominant genera of ε-proteobacteria were, in order of abundance, *Sulfurovum* (up to 56% of total clones at Godzilla, ES), *Sulfurimonas* (up to 19% of total clones at Bag City, AV), *Arcobacter* (up to 23% of total clones at Bag City) and *Nitratifractor* (up to 7% of total clones at Phang, ES) (Fig. 3.4). Fig. C.1 presents a partial 16S rRNA gene ε-proteobacteria tree showing phylogenetic relationships for all 16S rRNA gene sequences in these four major ε-proteobacteria genera.

**Table 3.2.** Bacterial 16S rRNA gene clone libraries information and OTUs richness (Chao-1) and diversity (Shannon) estimates. Sequences with a similarity ≥97% are considered the same OTU. Uncertainties for the Chao-1 estimator (in brackets) and the Shannon index represents 95% confidence intervals.

| Vent field | Site | Year | Volume of fluid filtered (L) | Avera-ge fluid temp. (°C) | # of clones sequ-enced | # of OTU | Cove-rage (%) | Chao-1 estima-tor | Sha-nnon index (H') |
|---|---|---|---|---|---|---|---|---|---|
| AV | Cloud | 2007 | 3.0 | 6.8 | 60 | 39 | 50 | 133 (74-295) | 3.47 ± 0.43 |
| AV | Bag City | 2008 | 1.6 | 11.2 | 43 | 26 | 63 | 43 (31-82) | 3.09 ± 0.25 |
| ES | God-zilla | 2008 | 4.0 | 29 | 28 | 19 | 50 | 67 (37-179) | 2.95 ± 0.29 |
| ES | Hulk | 2008 | 4.0 | 24.8 | 60 | 18 | 77 | 60 (31-161) | 1.72 ± 0.43 |
| ES | Phang | 2009 | 2.7 | 24 | 27 | 19 | 56 | 34 (25-67) | 2.94 ± 0.27 |

In contrast, the 16S rRNA clone library derived from the Hulk (ES) site showed a dominance of γ-proteobacteria, accounting for up to 77% of the sequences (Fig. 3.4). Sequences affiliated with SUP05 were generally the most prevalent γ-proteobacteria, accounting for up to 68% of the total 16S rRNA gene clone library at Hulk, ES (Fig. 3.4). The abundance of SUP05 bacteria (relative to total bacteria) measured by qPCR was up to 38% at this site. At all other sites, the relative abundance of SUP05 bacteria was

generally lower than 4%, except at Cloud (AV, 2007; 26%), Marker 33 (AV, 2008; 7.9%) and Bag City (AV, 2008; 5.4%) (Fig. 3.5, Table C.1). At Cloud (AV), Bag City (AV) and Hulk (ES), γ-proteobacteria of the SUP05 sequences were most similar to hydrothermal vent bacteria from an iron chimney-like structure on Volcano 19 in the South Pacific Ocean (99%) (Forget *et al.*, 2010), and to water column bacteria from Saanich Inlet, a seasonally anoxic fjord (e.g. clone FGYC_49P14 and clone SHBH489), corresponding to phylotype SI-1 identified by Walsh *et al.* (2009). No γ-proteobacteria from the Arctic96BD-19 clade (see Bano and Hollibaugh, 2002) were detected in our samples (Fig. 3.6).

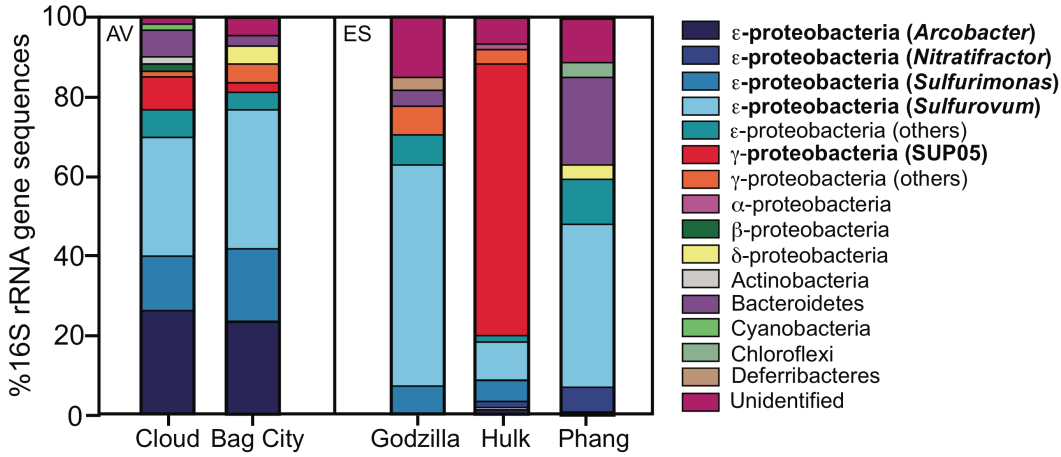


**Figure 3.4.** Composition of the 16S rRNA gene clone libraries recovered from DNA extracted from 5 DNA samples from diffuse vent fluids at Axial Volcano (AV) and the Endeavour Segment (ES) on the Juan de Fuca Ridge: Cloud (AV07-CP), Bag City (AV08-BC), Hulk (ES08-H), Godzilla (ES08-G), and Phang (ES09-P). SUP05 and other potential nitrate reducing bacteria are in bold. Note that only a limited number of clones were sequenced at each site. See Table 3.2 for more information about DNA samples and 16S rRNA gene clone libraries.

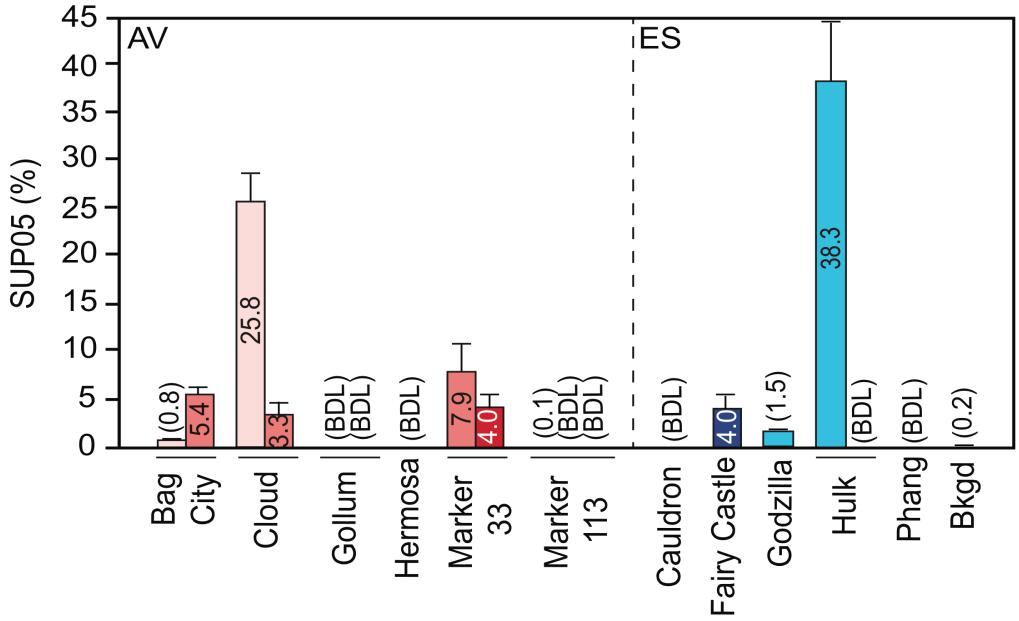


**Figure 3.5.** SUP05 relative abundance (in %, relative to 16S rRNA gene copy number $mL^{-1}$ seawater) at Axial Vocano (AV) and the Endeavour Segment (ES) on the Juan de Fuca Ridge. Same color scheme as in Fig. 3.3 (paler colors represent samples from the 2007 cruise). Actual values are indicated inside the bars or within parentheses. Bkgd is a background sample that was collected near the Endeavour Segment in 2009. See Table 3.1 for chemico-physical properties of sampled sites. Copy numbers per mL seawater of bacterial 16S rRNA genes (for both total and SUP05 bacteria) are available as Supplementary Materials, Table C.1.

### 3.4.4. Relation between denitrifying bacteria activity and abundance, as well as environmental factors

Relationships between potential activities and abundance of denitrifying, anammox and DNRA bacteria (ex-situ rates) as well as environmental physico-chemical factors (e.g. temperature, pH, $PO_4^{3-}$, $H_2S$ and $N_2O$ concentrations) were evaluated using multiple Spearman's rank order correlations for non-parametric data. Since denitrification rates were not significantly different between the two sampled ridge segments (i.e. Axial Volcano and Endeavour Segment), we pooled data from all vent fields and years for our analysis. Significant negative relationships were observed between denitrification rate

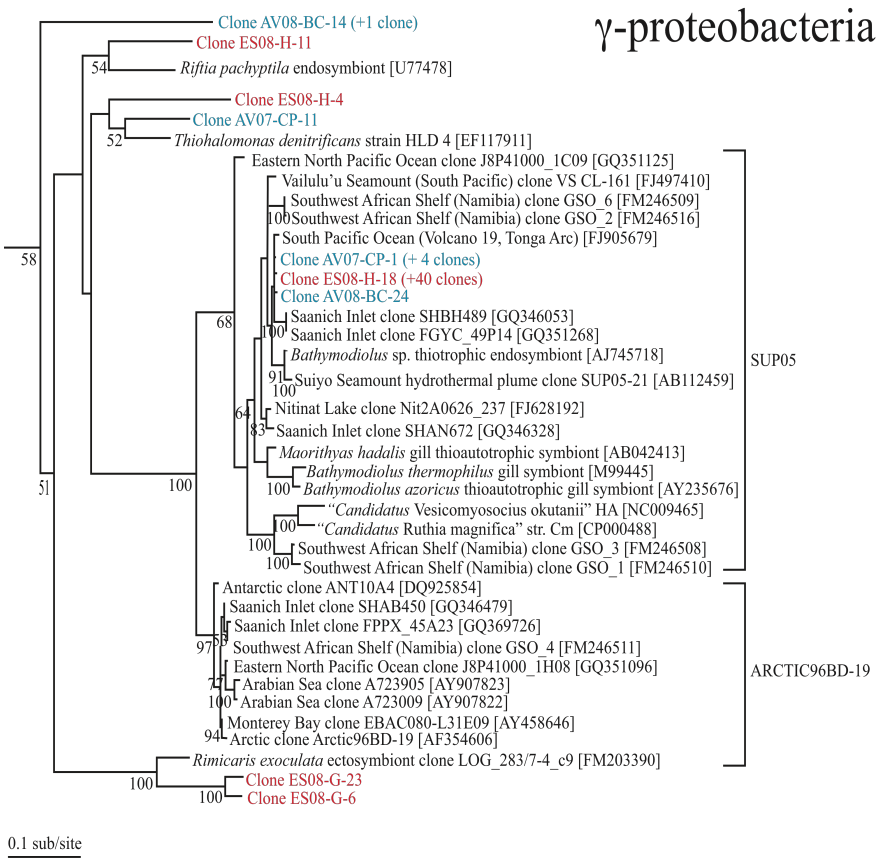


**Figure 3.6.** Partial 16S rRNA gene γ-proteobacteria phylogenetic tree constructed using the maximum likelihood method implemented in PHYML. Clone prefixes were assigned as follows: the first letters indicate the vent fields: AV= Axial Volcano (in blue) and ES= Endeavour Segment (in red), followed by the year (07= 2007 and 08=2008) and the last letters the diffuse vent sampled: CP= Cloud Pit, BC= Bag City, H= Hulk, and G= Godzilla. The last numbers indicate clones #. The number of clones that are ≥97% identical to a given hydrothermal vent clone is indicated in parentheses. GenBank accession numbers are provided (in brackets) for all other clones not sequenced in this study. The percentage of 100 bootstrap resamplings above 50% is indicated. The scale bar indicates the number of amino acid substitutions per site.

and the *in-situ* $NO_3^-$ deficit (Spearman's rho= -0.55, p-value= 0.05, n=13) (Fig. 3.7a), and between the anammox rate and the total DIN deficit (Spearman's rho= -0.95, p-value= 0.01, n=5) (Fig. 3.7b), although sample size was limited for the latter dataset. It should be noted that since we added the same amount of $^{15}N$-labeled $NO_3^-$ in all incubations performed during the same year, the degree of correlation (and significance) observed

between total $NO_3^-$ (including $^{15}N$-labeled $NO_3^-$ added before the incubations) and denitrification rates was similar (Spearman's rho= -0.68, p-value= 0.01, n=13).

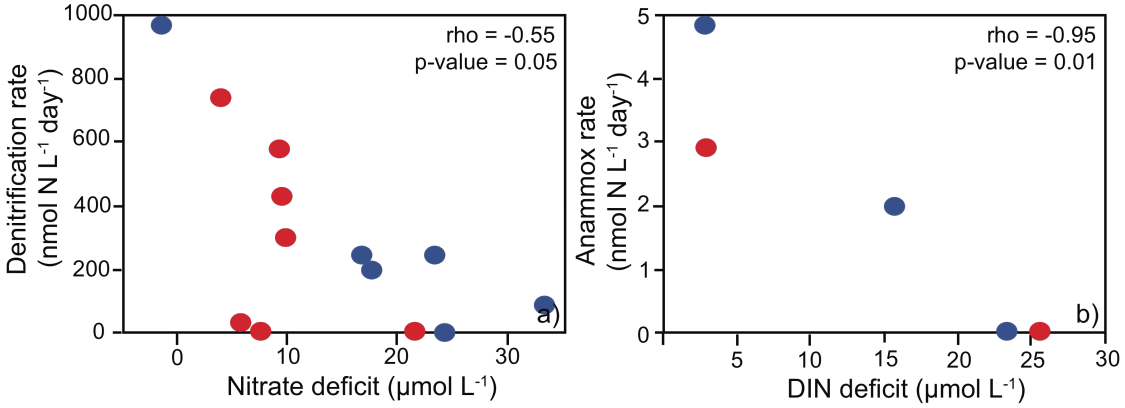


**Figure 3.7.** Relationships between potential denitrification rate and $NO_3^-$ deficit (**a**), and potential anammox rate and total DIN deficit (**b**) in hydrothermal vent fluids of the Juan de Fuca Ridge. See text for details. Hydrothermal vent fluids sampled from Axial Volcano and the Endeavour Segment are indicated in blue and red, respectively. Spearman's rank correlation coefficient (rho) and p-value are shown. Reported errors for denitrification and anammox rates were derived from standard errors of the regression coefficients.

## 3.5. Discussion

### 3.5.1. Denitrification as dominant N sink in low-T HV fluids

Our results suggest that denitrification is by far the dominant N loss process in the subsurface hydrothermal biosphere of the Juan de Fuca Ridge (Fig. 3.3). Denitrification rates in discharging hydrothermal fluids were up to ~500 times higher than anammox rates and up to 160 times higher than DNRA rates. It is interesting to note that unusually high $NH_4^+$ concentrations (up to ~13 µmol $L^{-1}$), possibly produced during DNRA, were

observed at Marker 113 (AV) in 2007, 2008 and 2009. The rates presented here are potential *ex-situ* rates (measured at *in-situ* temperatures), without accounting for possible pressure effects. Devol *et al.* (2006) reported no significant differences in denitrification rates measured *in-situ* and *ex-situ* for samples from the Arabian Sea oxygen deficient zone, at a depth range of 150 to 300m. While barophilic bacteria from great depths in the ocean are known to have pressure-dependent metabolic and growth rates (reviewed by Yayanos, 1995), there is currently no evidence to suggest that bacteria from the depths encountered here (1500 to 2200 m) should have different metabolisms at sea surface pressures. Nonetheless, future studies should investigate the potential effects of pressure on microbial metabolism at these depths.

At some sites, $N_2$ production by denitrification was significantly higher than what is generally observed for other open ocean and coastal oxygen-deficient zones. For example, denitrification rates ranged from 9.1 (open ocean) to 33.2 (coastal) nmol N $L^{-1}$ $day^{-1}$ in the Arabian Sea (Devol *et al.*, 2006). Our higher rates were similar to rates reported by Lavik *et al.* (2009) for chemolithoautotrophic denitrification coupled to sulfide oxidation in the Namibian shelf waters (i.e. ~600 nmol N $L^{-1}$ $day^{-1}$) and by Manning *et al.* (2010) in Saanich Inlet, a highly productive British Columbia (Canada) fjord (up to ~200 nmol N $L^{-1}$ $day^{-1}$). From a hydrochemical point of view, cold seeps are environments that are very similar to hydrothermal vents, albeit with lower discharge rates, since they contain high concentrations of reducing substances such as $H_2S$ and $CH_4$. Bowles and Joye (2011) recently reported heterotrophic denitrification rates of up to 32 μmol N $L^{-1}$ $day^{-1}$, in surficial cold seep sediments with *Beggiatoa* sp. mats in the Gulf of Mexico, suggesting that N loss via denitrifying bacteria (whether autotrophic or

heterotrophic) could be an important process in both of these deep-sea reducing environments.

Although complete denitrification is almost certainly dominant, we note that estimates of total $NO_3^-$ conversion to gaseous products reported here may be conservative underestimates as we only measured $N_2$ and not $N_2O$ production. Measured [$N_2O$] in sampled fluids was as high as 347 nmol $L^{-1}$ (Fairy Castle, ES), which is in the same range than [$N_2O$] measured by Butterfield *et al.* (2004) in diffuse fluids from Axial Volcano (20-600 nmol $L^{-1}$). Some denitrifiers, including sulfur-oxidizing bacteria, lack the gene coding for $N_2O$ reductase (*nosZ*), so that the final product of denitrification is $N_2O$. In particular, the *nosZ* gene was not found in the metagenome of the SUP05 bacteria (Walsh *et al.* 2009), suggesting that their energy metabolism can result in net $N_2O$ production. $N_2O$ is also produced during nitrification (Betlach and Tiedje, 1981), which can occur in subsurface hydrotheral conduit systems as a result of the discontinuous mixing of anoxic hydrothermal fluids and oxic seawater. Indeed, Wang *et al.* (2009) reported the presence of bacterial and archaeal *amoA* (ammonia monooxygenase) genes required for nitrification in HV chimneys of the Juan de Fuca Ridge. This additional process confounds any attempt to estimate the relative proportion of $N_2O$ produced during denitrification only. Also, $N_2$ production at the microbial community level should be seen as the definitive end product of N loss, whereas $N_2O$ produced by distinct groups of denitrifiers could be further reduced to $N_2$ by other groups of bacteria.

Potential anammox rates were relatively low (<5 nmol N $L^{-1}$ $day^{-1}$, Hermosa, AV) in HV fluids, compared to denitrification. In fact, we rarely observed any $NH_4^+$ deficits in HV fluids, but rather a surplus of $NH_4^+$ with respect to $NH_4^+$ concentrations expected for

conservative mixing (Table 3.1). This, in fact, supports net $NH_4^+$ production, rather than consumption by anammox. For comparision, Byrne *et al.* (2009) measured potential anammox rates of up to 60 nmol N $L^{-1}$ $day^{-1}$ in an aqueous mixture of HV chimneys from the Mid-Atlantic Ridge. Their rates are higher than ours possibly because of the increased microbial population density of their aqueous mixture compared to diffuse hydrothermal fluids. Our low to undetectable anammox rates agree with our microbiological results (see section 3.3.5).

As observed in previous studies in other sulfidic marine environments (e.g. Lavik et al, 2009), our results indicate that during $N_2$ production, fast growing denitrifying bacteria (doubling time as short as ~1.5 hour for sulfide-oxidizing autotrophic denitrifiers, Sievert *et al.*, 2008) generally out-compete slow-growing anammox bacteria (doubling times of ~2 weeks, Strous *et al.*, 1999) for $NO_x$ in diffuse fluids. Also, it has been suggested that fluctuating oxic-anoxic conditions could favor the more metabolically versatile denitrifying bacteria over anammox bacteria. Indeed, many denitrifiers can survive for extended periods of time in the absence of $NO_x$ (Risgaard-Petersen *et al.*, 2005) and perform aerobic respiration or use other electron acceptors (e.g., Fe), and this may confer them a competitive advantage over anammox bacteria in environments with variable redox conditions.

### 3.5.2. Denitrifier community in the subsurface biosphere

Denitrifying bacteria have been reported to belong to diverse phylogenetic groups (Zumft, 1997). The capacity for autotrophic denitrification has been documented for α−,

β−, γ− and ε-proteobacteria in a wide range of environments (e.g. hydrothermal vents, deep-sea redox transition zones, sediments, soils, and inland soda lakes; review by Shao *et al.* 2010). Denitrification capacity has also been identified in extremophile Archaea (see review by Cabello *et al.*, 2004). Archaea only constituted a small component of the total microbial community associated with the vent fluids sampled in this study (qPCR archaeal abundance up to 6% at Cauldron, ES - data not shown) and in a survey of diffuse hydrothermal fluids from Mariana Arc seamounts (typically less than 3%; Huber *et al.*, 2010). Therefore, archaeal denitrification was not further addressed.

Chemolithoautotrophic ε-proteobacteria have been identified as the dominant species in different hydrothermal habitats such as water column plumes, discharging fluids (i.e. subsurface) and living in symbioses with vent animals, using both culture and molecular approaches (López-García *et al.*, 2003; Alain *et al.*, 2004; Nakagawa *et al.*, 2005a; Huber *et al.*, 2010). Culture experiments by Nakagawa *et al.* (2005a) showed that ε-proteobacteria strains isolated from HV fluids, colonization devices and annelid polychaete tubes at the Iheya North hydrothermal field in the Okinawa Trough were able to couple $H_2$, $S_2O_3^{2-}$ and $S^0$ oxidation with $O_2$ or $NO_3^-$ reduction, illustrating the versatility of bacterial metabolisms in these environments. In addition, the same authors showed that some isolates preferentially used $NO_3^-$ as an electron acceptor during sulfide oxidation, even in the presence of oxygen. These autotrophic denitrifying ε-proteobacteria included members of the genera *Sulfurimonas* (comprising *Sulfurimonas paralvinellae* sp. (Takai et al, 2006)), *Sulfurovum* (comprising *Sulfurovum* sp. NBC37-1 (Inagaki *et al.*, 2004)) and *Nitratifractor* (i.e. *Nitratifractor Salsuginis*; Nakagawa *et al.*, 2005b). Additionally, Sievert *et al.* (2008) and Grote *et al.* (2012) reported that other ε-

proteobacteria of the genus *Sulfurimonas* (*Sulfurimonas denitrificans* str. DMS1251 and *Sulfurimonas gotlandica* str. GD1) isolated from marine environments can perform both chemolithoautotrophic denitrification (coupled to sulfur oxidation) and heterotrophic denitrification. All of the above-mentioned ε-proteobacteria genera, plus the genus *Arcobacter*, were generally present in HV fluids (Fig. 3.4 and C.1) and represented up to 77% (Bag City, AV) of the 16S rRNA gene clone librairies. ε-proteobacteria of the genus *Arcobacter* have also been shown to perform sulfur oxidation with denitrification in pure cultures (e.g. Gevertz *et al.*, 2000) and in the environment (Lavik *et al.*, 2009).

Our qPCR results indicate that γ-proteobacteria, mostly belonging to the SUP05 cluster, were particularly abundant in specific hydrothermal vent fluid samples (Hulk, ES (up to 38%) and Cloud, AV (up to 26%); Fig. 3.5). This finding was qualitatively supported by sequence abundances in 16S rRNA gene clone libraries. SUP05 is a clade of chemolitoautotrophic γ-proteobacteria capable of oxidizing reduced sulfur compounds using $NO_3^-$ as terminal electron acceptor (Lavik *et al.*, 2009; Walsh al., 2009). A BLAST search revealed that SUP05 sequences were generally present in samples from hydrothermal vent systems, but had not been specifically identified as such in previous studies. For example, SUP05 sequences in this study shared a 99%-similarity with a bacterial sequence from an iron oxide chimney-like structure on Volcano 19, in the South Tonga Arc, (accession (acc.) #: FJ905679; Forget *et al.*, 2010) and 98%-similarity relative to sequences from the Suiyo Seamount hydrothermal plume (e.g. acc. #: AB112459, AB112455 and AB112451) (Fig. 3.6). Moreover, bacteria of the SUP05 clade, which seem to only possess the *nirK* form of $NO_2^-$ reductase (Walsh *et al.*, 2009) were generally more abundant than *nirS* genes based on qPCR assays, which represented

up to ~8% of the total bacterial abundance in hydrothermal vent fluids of the Juan de Fuca Ridge (A. Bourbonnais, unpublished data). This suggests that SUP05 bacteria can represent an important fraction of the total denitrifying population in the subsurface biosphere of HV systems. It should be noted that because denitrifiers are highly diverse, it is virtually impossible to confirm the capacity of an organism to perform denitrification based solely on phylogenetic affiliation. Studies of the genes involved in the denitrification process, e.g. $NO_2^-$ reductase (*nirS* and *nirK*), and $N_2O$ reductase (*nosZ*) could represent a more direct approach to describing denitrifying bacterial communities from a functional perspective.

### 3.5.3. Environmental controls on denitrifier (and anammox) activity and abundance

Potential environmental controls on denitrifier activity and abundance in the subsurface biosphere of the Juan de Fuca hydrothermal vents can be evaluated by comparing measured microbiological attributes with physical, chemical and biological fluid properties.

$NO_2^-$ and $NO_3^-$ supply have been shown to stimulate denitrification and influence the distribution of denitrifying genes in marine, estuarine (e.g. Jayakumar *et al.*, 2004; Dong *et al.*, 2009) and terrestrial (e.g. Bradley *et al.*, 1992; Smith *et al.*, 2006; Opdyke *et al.*, 2007; Zhong *et al.*, 2010) environments. The significant negative relationship observed between denitrification rates and *in-situ* $NO_3^-$ deficit (Spearman's rho= -0.55, p-value= 0.05) suggests that $NO_3^-$ supplied by mixing between $NO_3^-$-poor hydrothermal fluids and

$NO_3^-$-rich crustal seawater may ultimately regulate denitrification in the subsurface biosphere of hydrothermal vents.

We also found a significant relationship between anammox rates and the DIN deficit, but this relationship should be interpreted with caution because of the limited number of measurements available for comparison (Fig. 3.7b). Previous studies have found that anammox was stimulated by $NH_4^+$, $NO_2^-$ and/or $NO_3^-$ additions (e.g. Trimmer *et al.*, 2005). No correlation was found between anammox rate and $NH_4^+$ deficit in this study. In fact, net $NH_4^+$ production seemed to be occurring, as indicated by a general $NH_4^+$ surplus at most sites, probably through DNRA or organic matter decomposition. Our results suggest that, if anything, $NO_x$ rather than $NH_4^+$ modulates anammox rates in the vent fluids. Additionally, it should be noted that, in agreement with most recent observations from a mesotrophic Swiss lake (Wenk *et al.*, 2012) we were able to measure low anammox rates, despite the high $H_2S$ concentration of up to 1000 μmol $L^{-1}$ in the fluids, suggesting that anammox growth is not completely inhibited by $H_2S$, as previously suggested by Jensen *et al.* (2008).

Our molecular results suggest that sulfide-oxidizing denitrifiers represent a relatively large fraction of the total bacterial community at some subsurface hydrothermal environments. Sulfur driven autotrophic denitrification has been reported to be a significant process in other hydrothermal systems (López-García *et al.*, 2003 and references therein). The lack of a significant relationship between denitrification rates and observed [$H_2S$] suggests that $H_2S$ concentrations are not limiting denitrification. Furthermore, we cannot exclude that a portion of the total denitrification in hydrothermal

vent fluids is heterotrophic. High heterotrophic denitrification rates have been measured in a similar (cold seep) environment (Bowles and Joye., 2011).

The fact that no correlations were observed between total microbial abundance (measured by DAPI counts and qPCR) and denitrification rates suggests that, overall, denitrifiers represent only a minor fraction of the total microbial community. Indeed, in most samples, the relative abundance of SUP05 bacteria was less than 10% (except for Cloud, AV, 2007 (SUP05= 26%) and Hulk, ES, 2008 (SUP05= 38%) Fig. 3.5). The lack of significant correlations between denitrification rate and SUP05 abundances is also not surprising, because SUP05 bacteria probably only represent a portion of the total denitrifying community. Other potential candidates in our fluids include members of the ε-proteobacteria, as discussed in section 3.5.2. Also, we only analyzed the DNA fraction of the microbial community, not gene expression. However, there are generally delays observed between enzyme synthesis, expression and formation of denitrification products (e.g. see Baumann *et al.*, 1996), such that it is generally difficult to directly relate gene transcriptional activity to denitrification rate measurements.

Other factors, e.g. pH and temperature, have been shown to influence N loss rates (e.g. Bradley *et al.*, 1992; Opdyke *et al.*, 2007; Zhong *et al.*, 2010). In this study, no relationship was found between pH and temperature, and denitrification rates. Interestingly, higher temperatures did not seem to inhibit denitrification, suggesting the potential importance of mesophilic organisms in mediating N-cycle processes in the subsurface biosphere. In fact, the highest denitrification rate (~1000 nmol N $L^{-1}$ $day^{-1}$) was measured at Hermosa (AV), where the highest fluid temperature (37ºC) sampled in this study was observed.

### 3.5.4. Total N loss in the subsurface biosphere of diffuse hydrothermal vents

Total N loss fluxes in hydrothermal vent systems are difficult to accurately quantify given the observed high variability of flow rates (e.g. Sarrazin *et al.* 2009) and our rudimentary knowledge of fluid residence times in the subsurface. Codispoti (2007) first estimated that ~10 Tg N is lost every year during hydrothermal denitrification, assuming a hydrothermal flow associated with ridges and ridge flanks of $2.4 \times 10^{16}$ kg $y^{-1}$ (Schultz and Elderfield, 1997), an initial average $NO_3^-$ concentration of 30 μmol $L^{-1}$, and that denitrification occurs along the entire flow pathway. The latter assumption in particular may not be reasonable, as it includes the high-T portion of the HV systems. Hence this is likely a gross over-estimate of total net N loss in hydrothermal systems. On the other hand, Codispoti (2007) did not consider $N_2$ fixation, which would add new $NO_3^-$ to HV fluids, compensating in part for N loss by denitrification, thus allowing an even larger gross N loss. $N_2$ fixation has indeed been reported to occur in hydrothermal vent fluids of the Juan de Fuca Ridge (e.g. Mehta and Baross, 2006).

Given recent advances in our understanding of the important role of the subsurface biosphere of diffuse hydrothemal vents in modulating geochemical fluxes in the deep ocean (e.g. Wankel *et al.*, 2011; Bourbonnais *et al.*, 2012a), we attempt here to improve upon Codispoti's estimate and at least derive a possible range of values for gross global marine N loss occuring in the subsurface biosphere, based on denitrification rates measured in this study and current knowledge of hydrothermal flow and fluid residence times in the subsurface. We used the following equation to derive gross global N loss (in Tg $year^{-1}$) in the subsurface biosphere of hydrothermal vents:

$$\text{N loss (Tg N year}^{-1}\text{)} = \text{denitrification rate} \times \text{volume flux} \times \text{residence time} \qquad (3.5)$$

We used an average denitrification rate of 240 nmol N $L^{-1}$ $day^{-1}$, representative of all vent fields and years sampled in this study and a hydrothermal fluid volume flux of $6.3 \times 10^{15}$ to $1.6 \times 10^{16}$ $L^{-1}$ $year^{-1}$, considering both axial (10% at 350°C and 90% at 5°C) and off-axial (5-15°C) hydrothermal flows (Elderfield and Schultz, 1996). We based our range of values for residence times on data from Johnson *et al.* (2010) and Foustoukos *et al.* (2009). Johnson *et al.* (2010) calculated a crustal residence time of 2.1 years (assuming 10% porosity) for the across-axis flow in the Endeavour Segment axial valley, Juan de Fuca Ridge, using conductive heat flow measurements. Foustoukos *et al.* (2009) estimated a crustal residence time of only a few tens of hours for the very shallow circulation cells feeding low-T diffuse vents adjacent to the Endeavour high-temperature fields, using $CO_2$/CO equilibrium data. For our calculations, we assumed a range of residence times in the subsurface between 24 hours and 2 years, and assumed that only 5% to 25% of the subsurface hydrothermal system, including the recharge zone, is microbiologically active. Using this approach, we estimated that a range from 0.001 to 9.9 Tg N $year^{-1}$ could be removed globally by denitrification in hydrothermal vent systems.

Coincidently, our upper range of ~10 Tg $year^{-1}$ for N loss in hydrothermal systems is the same as reported by Codispoti (2007), although his study did not measure denitrification rates. Our upper estimate is relatively low, when compared to estimates of the global ocean fixed N sink by benthic and water-column denitrification between ~250 to more than 400 Tg N $year^{-1}$ for the global ocean (Gruber, 2004; Codispoti, 2007). We should note that our upper estimate may still be conservative, as it assumes that all denitrifying organisms are in the flowing water (i.e. not attached to surfaces in the flow

path (e.g. microbial mats)). Our results nonetheless confirm the possible role of the subsurface biosphere in modulating geochemical fluxes in general, and fixed N fluxes, in particular.

### 3.6. Summary and final remarks

In this study we report, for the first time, potential denitrification, anammox and DNRA rates in diffuse hydrothermal vent fluids of the Juan de Fuca ridge. The activity of denitrifying bacteria in this subsurface biosphere and its prevalence over anammox and DNRA were confirmed by $^{15}N$ paired isotope experiments at 13 different sites at Axial Volcano and the Endeavour Segment on the Juan de Fuca Ridge. Potential denitrification rates in subsurface hydrothermal vent fluids varied strongly in space and with time. The high denitrification potential observed at some sites (up to ~1000 nmol N $L^{-1}$ $day^{-1}$, Hermosa, AV) indicates that denitrification is a significant N sink in the subsurface biosphere of hydrothermal systems. Cloning and sequencing of the 16S rRNA genes revealed the dominance of ε– and γ–proteobacteria in hydrothermal vent fluids, with the potential to oxidize sulfide or $H_2$, using $NO_3^-$ as terminal electron acceptor. Our qPCR results indicated that a single cluster of γ-proteobacteria, i.e. the sulfur-oxidizing, $NO_3^-$-reducing SUP05 bacteria, contributed up to 38% of the total bacterial population at some sites (Hulk, ES, 2008), implying a potentially important role for chemolithoautotrophic denitrification in hydrothermal vent fluids. While this study suggests that denitrification, possibly coupled to sulfide oxidation, is an important process in hydrothermal vents of the Juan de Fuca Ridge, more phylogenetic analysis of functional genes related to

denitrification (e.g., *nirS*, *nirK*, *nosZ*) will be essential to better document and understand denitrifying microbial communities in the subsurface biosphere.

Our comprehension of environmental controls on N transformations in hydrothermal fluids is still very limited. In this study, denitrification, DNRA and anammox rates did not appear to be affected by most measured physico-chemical factors. Significant negative relationships were only observed between denitrification, anammox rate and *in-situ* $NO_3^-$ and DIN deficits, respectively. This implies that bioavailable inorganic N availability may ultimately regulate N loss and transformations in the subsurface biosphere of hydrothermal vents of the Juan de Fuca Ridge.

Combining potential rates from this study with published data on hydrothermal vent fluid residence times in the subsurface and annual seawater fluxes through these systems, we estimated that up to ~10 Tg N $year^{-1}$ could be removed by denitrification in the subsurface of the world's hydrothermal systems, suggesting that hydrothermal vent denitrification represents a minor, but significant fraction, of total marine fixed N loss.

# Chapter 4
# Diversity and abundance of Bacteria and *nirS*-encoding denitrifiers associated with the Juan de Fuca Ridge hydrothermal system

## 4.1. Abstract

Denitrification results in the loss of bioavailable nitrogen and ultimately affects chemosynthetic primary production in hydrothermal vent ecosystems. Here we describe diversity and abundance of denitrifying bacteria in the subsurface biosphere of hydrothermal vents on the Juan de Fuca Ridge using a combination of quantitative polymerase chain reaction, small subunit ribosomal RNA (SSU or 16S rRNA) pyrotag and nitrite reductase (*nirS*) clone library sequencing methods. Bacterial communities were diverse but dominated by members of the ε- and γ-proteobacteria. Statistical analyses of 16S rRNA gene pyrotags revealed that bacterial community structure varied significantly between most sampled vent fluids but not significantly between different vent fields. Richness and evenness of *nirS* genes recovered from the Endeavour Segment and Axial Volcano sites were low, with average Shannon diversity indices of 1.2 and 1.4, respectively. Although the majority of *nirS* genes recovered from both sites clustered into different operational taxonomic units, a single shared sequence affiliated with the γ-proteobacteria represented more than half of all sequences recovered when clustered at 97% identity. Total *nirS* gene abundance varied from ~0 to 8% relative to bacterial 16S rRNA gene abundance and no significant relationships between *nirS* gene abundance and measured environmental variables were identified. Overall, our results demonstrate that

the diversity of the *nirS* gene-containing bacterial community is rather low under the extreme conditions encountered in the subsurface biosphere of hydrothermal vents, and suggest that small-scale geographic isolation, and possibly fluid temperature and chemistry, play important roles in shaping bacterial and denitrifier populations inhabiting these systems.

## 4.2. Introduction

Since their discovery in the late 1970's, hydrothermal vents have served as model ecosystems to understand the origin and limits of life in extreme environments and the evolution of symbiotic interactions. Multitrophic interactions and food web structure in hydrothermal vent ecosystems are typically sustained by chemolithoautotrophic bacteria harnessing metabolic energy from the oxidation of molecular hydrogen, elemental sulfur, thiosulfate and hydrogen sulfide (e.g. Jannasch and Mottl, 1985; Schrenk *et al.*, 2010). Nitrogen (N) is an essential macronutrient for all organisms, and its availability has the potential to limit chemosynthetic primary production at seafloor vents and beneath the seafloor in the subsurface hydrothermal biosphere. In these settings, bioavailable N is mainly supplied by nitrate-rich seawater that is entrained and transformed during hydrothermal circulation and by autochthonous $N_2$ fixation (Mehta *et al.*, 2003; 2005; Mehta and Baross, 2006), whereas N loss occurs primarily via denitrification (Bourbonnais *et al.*, 2012a).

The process of denitrification involves stepwise reduction of $NO_3^-$ through a series of intermediates including nitrite ($NO_2^-$), nitric oxide (NO), and nitrous oxide ($N_2O$)

ultimately resulting in dinitrogen production ($N_2$). Nitrite conversion to gaseous nitrogen oxides (NOx) and dinitrogen results in N loss, and in the case of $N_2O$, greenhouse gas production. Nitrite reduction can be catalyzed by two structurally different, but functionally equivalent enzymes, the homotrimeric copper-containing enzyme encoded by *nirK*, and the homodimeric cytochrome *cd1*-nitrite reductase encoded by *nirS*. The nitrite reductase gene has been widely used as a functional marker to investigate the diversity and abundance of denitrifying bacteria in terrestrial (e.g. Henry *et al.*, 2004; Chon *et al.*, 2009), estuarine and marine environments (e.g. Braker *et al.*, 2000, 2001; Nogales *et al.*, 2002; Liu *et al.*, 2003; Jayakumar *et al.*, 2004; 2009; Castro-González *et al.*, 2005; Santoro *et al.*, 2006; Falk *et al.*, 2007; Oakley *et al.*, 2007; Smith *et al.*, 2007). Most studies have used the *nirS* gene because of reported difficulties with existing *nirK* primers, especially for marine environments (e.g. Braker *et al.*, 2000; Jayakumar *et al.*, 2004).

Evidence for denitrification has been reported for both seafloor and sub-seafloor hydrothermal habitats. Previous studies, using GeoChip and metagenomic approaches to investigate the microbial communities inhabiting hydrothermal vent chimneys on the Juan de Fuca Ridge (JFR), detected functional gene repertoires mediating the denitrification process, including nitrate reductase (*nar*), nitrite reductase (*nir*), nitric oxide reductase (*nor*) and nitrous oxide reductase (*nos*) (Wang *et al.,* 2009 and Xie *et al.*, 2010). More recently, we (Bourbonnais *et al.* 2012a; 2012b) reported depleted $NO_3^-$ in combination with the enrichment of the heavy nitrate N and O isotopes in low temperature (low-T) diffuse flow fluids on the JFR, which is consistent with isotope fractionation during active $NO_3^-$ reduction. Potential denitrification rates up to 1000 nmol

N/day were always several fold higher than anammox (<5 nmol N/day) rates, indicating that at least on the JFR, denitrification is the dominant $NO_3^-$ consuming process within the subsurface biosphere with unconstrained feedback on chemosynthetic primary production.

The investigation of the diversity and abundance of denitrifiers in the subsurface biosphere of hydrothermal vents is necessary to better understand nutrient cycling and mass balance in these systems. Previous studies have reported large differences in $NH_4^+$ concentrations in hydrothermal vent sites on the JFR including diffuse flow fluids from Axial Volcano and the Endeavour Segment (Lilley *et al.*, 1993; Bourbonnais *et al.*, 2012a). The higher $NH_4^+$ concentrations commonly found in Endeavour Segment vent fluids have the potential to influence the activity and diversity of denitrifying bacteria. Geographic isolation can also play an important role in shaping bacterial communities (e.g. Braker *et al.*, 2001; Falk *et al.*, 2007), potentially confounding our understanding of variability in physico-chemical factors, when comparing samples from distant vent fields.

Here we investigate the diversity and abundance of small subunit ribosomal RNA (SSU or 16S rRNA) and *nirS* genes in relation to environmental parameters (temperature, pH, $H_2S$, $NO_3^-$ and $NH_4^+$ concentrations) in several hydrothermal vent sites on the JFR including diffuse flow fluids from Axial Volcano and the Endeavour Segment. We expand on sequencing results to include *nirS* abundance measures using quantitative PCR from Axial Volcano, Endeavour Segment and the Cobb Segment and re-sampled the Endeavour Segment site within a 24 hour period to explore temporal variability.

## 4.3. Materials and methods

### 4.3.1. Site description and water sampling

Samples were collected at hydrothermal vents of the Endeavour (~48ºN, 129ºW) and Cobb (~46.7ºN, 129ºW) (~2100-2200 m depth) Segments and Axial Volcano (~46ºN, 130ºW, ~1500 m depth) on the JFR, northeast Pacific Ocean, during two research cruises in August 2007 and June 2009 onboard the R/V Thompson and the R/V Atlantis, respectively, as part of the New Millenium Observatory (NEMO) and Endeavour-Axial Geochemistry and Ecology Research (EAGER) Projects (Fig. 4.1). The caldera of Axial Volcano rises 1100 m above the surrounding ocean floor, and has been the site of seafloor volcanic eruptions in 1998 and 2011 (Chadwick *et al.*, 2012).

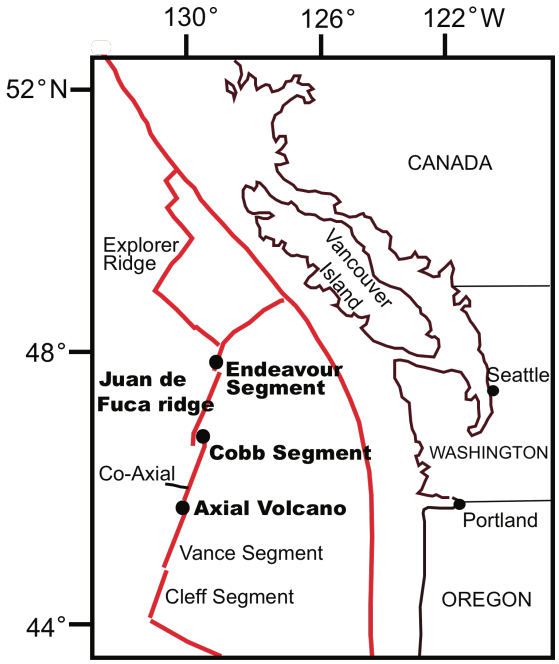


**Figure 4.1.** Map of sampled vent fields: Axial Volcano and the Endeavour and Cobb Segments on the JFR (modified from Figure 4.1 in Bourbonnais *et al.*, 2012b).

The Remotely Operated Vehicle (ROV) JASON and the Deep Submergence Vehicle (DSV) Alvin were used to collect all fluid samples. Fluid samples for chemical analysis were collected using titanium gas-tight samplers, non-gas-tight titanium syringe ("Major") samplers, collapsible Tedlar plastic bags with valves, or PVC piston samplers with Teflon spring seals on the Hydrothermal Fluid and Particle Sampler (HFPS). Vent fluid sub-samples were transferred from the collapsible bags using a syringe into acid-washed and deionized water-rinsed 60-ml HDPE brown bottles for nutrient concentrations. Fluid samples for nutrient analysis were bubbled with $N_2$ gas for at least 10 minutes in order to remove $H_2S$, which interferes with the colorimetric nutrient analysis. Water samples were kept frozen at -20$^{o}$C until analysis.

For DNA samples, ~3L of low-temperature hydrothermal fluid was pumped through the titanium and Teflon fluid manifold of the HFPS and filtered *in-situ* onto Millipore Sterivex-filters for subsequent DNA extraction and microbial analysis. During the 2009 cruise, a barrel sampler mounted on a large elevator was used to collect ~170 L of diffuse fluids at one of the sites (Hulk1), that were then filtered through four Steripaks (~40-50 L each) as further described in Anderson *et al.* (2011). The temperature of this barrel sample was not measured during collection, but the fluid chemistry (dissolved silica and Mg content) clearly indicated that the average temperature was near 125°C. After each dive, the Sterivex and Steripak filters were stored at -80$^{o}$C until analysis.

### 4.3.2. Measurements of physical and chemical properties

Fluid samples were analyzed on board for pH, hydrogen sulfide and ammonium typically within 8 hours of arriving on deck and within 24 hours of seafloor sampling. pH was analyzed immediately upon sample collection using the potentiometric method with a standard deviation of 0.01 pH unit for replicate analyses,. Hydrogen sulfide, dissolved silica and ammonium concentrations were analyzed using colorimetric methods (methylene blue, molybdenum blue and indophenol blue methods, respectively), with standard deviations of 4%, 1% and 7%, respectively. The sum of nitrate plus nitrite was measured by reduction to nitric oxide (NO) in a heated solution of acidic vanadium (III) and subsequent detection of the NO (Braman and Hendrix, 1989), with a precision for replicate analyses of ± 0.2 μmol $L^{-1}$. Nitrate, nitrite, ammonium and phosphate were also analyzed on shore using a colorimetric nutrient analyzer technique, with a precision of ± 0.2 μmol $L^{-1}$. Dissolved NOx (nitrate and nitrite) concentrations measured colorimetrically and by chemiluminescence were generally in good agreement. One to five sub-samples were collected at each site, during each dive, and only the average for all sub-samples is reported.

#### 4.3.3. DNA extraction

DNA was extracted from Sterivex filters following the protocol described in Huber *et al.* (2002) with some modifications, as described in Bourbonnais *et al.* (2012b). The DNA was resuspended in 95μL of tris-EDTA (TE) buffer (10 mM Tris, 1 mM EDTA, pH 8.0) and stored at -80°C. The DNA in the Steripak collected at Hulk in 2009 was extracted at the University of Washington using an adapted protocol similar to the one

described in Huber *et al.* (2002) and Bourbonnais *et al.* (2012b), but using about 10 times more reagent for each Steripak filter. The centrifugation steps at 6000 rpm for 5 min, and collection of the residual supernatant from the filter before and after adding the DNA extraction buffer (DEB) and sodium dodecyl sulfate (SDS) and Proteinase K were omitted when extracting DNA from Steripaks. Filters were incubated at 65˚C for 10 minutes, the liquid was drawn off and added to a collection tube, and mixed with a solution of phenol:chloroform:isoamyl alcohol (25:24:1). The latter was centrifuged at 3000 rpm at room temperature. This step was repeated with the supernatant in a 1:1 mixture of chloroform: isoamyl alcohol. DNA was finally re-suspended in 400 μL of TE buffer.

### 4.3.4. PCR amplification and cloning

#### 4.3.4.1. 16S rRNA gene fragments

16S rRNA gene clone libraries were constructed to complement the *nirS* gene clone libraries from Hulk1 (2009) (Barrel sampler, Endeavour Segment) and Shepherd vent (2007) (CASM field, Axial Volcano), as well as for other samples used to quantify *nirS* abundance, where DNA was available (i.e. collected at the following vent sites: Bag City, T&S and Forum (2007 samples) and Hulk2 and Phang (2009 samples)). DNA samples (except for Hulk1, see below) (4–12ng) were PCR-amplified using Takara Ex Taq premix (Fisher). All PCR reactions were performed in a final volume of 50 μL containing 25μL of Premix Taq, 1 μM of each primer and sterile MiliQ $H_2O$ to up to 50 μL. PCR

amplifications were performed targeting the V1-V3 region of the 16S rRNA gene, using a general reverse primer (R519: 5'-CAGGWATTACCGCGGCKGCTG) combined with B primer (Roche: CCTATCCCCTGTGTGCCTTGGCAGTCT) in combination with unique tagged forward primer (F63-targeted: 5'-XXXXXXXXXXCAGGCCTAACACATGCAAGTC, where X represents different tags (64 in total)) combined with A primer (Roche: CCATCTCATCCCTGCGTGTCTCCGACTCAG). PCR conditions were as follows: after a denaturing step of 30s at 98°C, samples were processed through 30 cycles consisting of 10s at 98°C, 30s at 55°C and 30s at 72°C. The final extension step was done at 72°C for 4m 30s. Following amplification, samples were purified using AMPure Beads (Beckman Coulter Genomics), quantified by Nanodrop and sent to the Plateforme d'Analyses Biomoléculaires (Institut de Biologie Intégrative et des Systèmes, Université Laval) for pyrosequencing using a 454 GS-FLX DNA Sequencer with Titanium Chemistry (Roche) and the procedure described by the manufacturer.

For the Hulk1 sample (collected using the Barrel sampler), ~100 published sequences from Sanger sequencing (Anderson *et al.*, 2012; accession numbers: JQ678511-JQ678591) were used for phylogenetic analysis. Metagenomic and pyrosequencing analysis for this sample will be presented in a different publication. Another water sample collected at the same location during the same dive where the Barrel sampler was deployed (Hulk2) is used here for comparison purposes and to explore temporal variability (the physico-chemical properties and 16S rRNA biodiversity for the two samples were different).

#### 4.3.4.2. *nirS* gene fragments

Fragments of the *nirS* gene were amplified using the primer pairs nirS1F (5'-CCTAYTGGCCGCCRCART-3') -nirS6R (5'-CGTTGAACTTRCCGGT-3') (amplicon size: 890 bp) first described by Braker *et al.* (1998), and used in several subsequent studies (Braker et al, 2000; Priemé *et al.*, 2002; Jayakumar *et al.*, 2004; 2009; Castro-Gonzáles *et al.*, 2005; Falk *et al.*, 2007; Oakley *et al.*, 2007). It should be noted that we attempted to amplify *nirK* genes using the primer pair nirK1F (5'-GGMATGGTKCCSTGGCA-3')-nirK5R (5'-GCCTCGATCAGRTTRTGG-3') (amplicon size: 514 bp) (Braker *et al.*, 1998) for several DNA samples from Axial Volcano and Endeavour Segment. We obtained a band of the right size (~514 bp) when using DNA extracted from hydrothermal fluids at Hulk1 and Zen Garden1 (see Table 4.1), but further sequencing and BLAST searches revealed that these were not similar to any *nirK* sequences in the NCBI Genbank and thus probably resulted from non-specific amplification. Other studies have reported similar difficulties with amplifying *nirK* genes from seawater samples using these primers (e.g. Braker *et al.*, 2000; Jayakumar *et al.*, 2004). Denitrifying bacteria in marine environments may also possess a distinct *nirK* structural type (e.g. see Ellis *et al.*, 2007). We subsequently focused our efforts using the functional gene *nirS* to examine the diversity of denitrifying bacteria.

The *nirS* gene fragments were amplified using a 25μl PCR mixture containing 1μl of template DNA, 0.625 μL each 10 μM forward and reverse primers, 2 μL 10 μM deoxynucleotides, 5 μL of 5X Herculase II buffer with MgCl (Sratagene), and 1 U of Herculase II fusion DNA polymerase (Stratagene) under the following PCR conditions: 3 min at 94°C, followed by 40 cycles of 94°C for 40 s, 56°C for 40 s, 72°C for 1 min and a

final extension of 10 min at 72°C. Amplicons were visualized by UV excitation on a ~1% agarose gel stained with ethidium bromide prepared using 0.5× TAE. DNA fragments from 8 independent PCR reactions were excised from agarose gels with a scalpel and purified using the QIAquick Spin gel purification kit (Quiagen). The DNA present in each tube following purification was eluted with 50 μl water (pH: 7.0-8.5). The contents of the tubes were combined, and concentrated using a SpeedVac until the DNA concentration read on a Nanodrop was ~150 ng $\mu L^{-1}$ for *nirS* (final volume: 4-5 μl). 200-450 ng DNA was ligated into a pCR®II-Blunt-TOPO® vector (Invitrogen) and transformed into One Shot® Electrocomp™ *E. coli* cells following the manufacturer's intructions. The following electroporation conditions were used: Voltage: 2250 V, Capacitance: 25 μF, Resistance: 200 Ω and the length and width of the space filled with cells inside the electroporation cuvette was 2mm. White colonies were randomly picked and transferred onto 96 well culture plates (2 plates for each sample) with LB + 10% Glycerol Medium + Kanamycin. One plate from each cloning was then sent to the Michael Smith Genome Sciences Centre in Vancouver (BC), where the amplified inserts were sequenced bidirectionally with M13F and M13R primers.

### 4.3.5. Richness, diversity and phylogenetic analysis

MOTHUR 1.23.0 (Schloss, 2009) was used to process all 16S rRNA gene pyrosequences (7806, 8955, 3329, 7721, 9033, and 7817 sequences in total for Bag City, Forum, Shepherd, T&S, Hulk2 and Phang (see Table 4.1), respectively). All pyrosequences (on average ~450 bp) were pre-processed (i.e., primers were removed and

sequences containing ambiguous bases, shorter than 350 bp and of low quality (qaverage <25) were removed) and aligned using the SILVA alignment (available on the MOTHUR website: http://www.mothur.org/wiki/Silva_reference_alignment), and pre-clustered to remove sequences due to pyrosequencing errors (Huse *et al.*, 2010). UChime was used to remove potentially chimeric sequences (Edgar *et al.*, 2011). After these steps, 22585 sequences remained, i.e. 4498, 5188, 2275, 4332, 4991, and 4301 sequences, for Bag City, Forum, Shepherd, T&S, Hulk2 and Phang, respectively (Fig. 4.2a)). Pyrosequences were then separated into OTUs using the furthest neighbor clustering method and a taxonomy was assigned to each OTU using the MOTHUR-formatted version of the RDP training set available on the MOTHUR website (http://www.mothur.org/w/images/4/49/RDPTrainingSet.zip).

All *nirS* sequences were edited manually using Sequencher v.4.7 (Gene Codes Corporation). The open source Bellerophon application (http://comp-bio.anu.edu.au/bellerophon/bellerophon.pl) (Huber *et al.*, 2004) and PinTail (Ashelford *et al.*, 2006) were used to detect chimeric sequences. Chimeras were excluded from further analysis. Nucleotide sequences were aligned using the ClustalW Application (Thompson *et al.*, 1994) in BioEdit (version 7.0.5.3) and manually checked. Closest related sequences were identified for each OTU using the BLAST tool available on the National Center for Biotechnology Information (NCBI) website. *nirS* nucleotide sequences were then converted to amino acid sequences.

Rarefaction curves were calculated using MOTHUR, sequences with <97% similarity being treated as distinct operational taxonomic units (OTUs). The coverage for each clone library was calculated as in Ravenschlag *et al.* (1999). $\alpha$-diversity calculators

(community richness (ACE, and Chao1 estimators) and diversity (Shannon (H) and inverse Simpson's indexes) were calculated for each of the SSU rRNA and *nirS* genes clone library. Observed richness corresponded to the number of OTUs detected. OTUs evenness was calculated as in Mulder (2004) (Table 4.2).

β-diversity calculators (two samples) were also determined to compare community richness (shared ACE and Chao1 estimators), membership (i.e., qualitative indices: Jaccard and Sorensen similarity coefficients based on the observed and Chao1 estimated richness) and structure (i.e., quantitative indices: abundance-based Jaccard and Sorensen (Chao, 2005), Smith and theta (Smith *et al.*, 1996) and Yue and Clayton theta (Yue and Clayton, 2005) similarity coefficients) (see Table 4.3 for more detail). An analysis of similarities (ANOSIM) implemented in MOTHUR was used to test for significant differences in 16S rRNA bacterial communities between vent fields (i.e. Axial Volcano and Endeavour Segment). Fast UniFrac (http://bmf2.colorado.edu/fastunifrac/) was used to test for significant differences in 16S rRNA gene and *nirS*-encoding bacterial community membership and structure between sampled vents (using both the P test (Martin *et al.*, 2002) and the UniFrac distance metric (Lozupone and Knight, 2005)).

A nearest-neighbor interchanges maximum likelihood tree (GTR+CAT model) was constructed with FastTree 2 (Price *et al.*, 2010) using all 16S rRNA gene V1-V3 pyrotag sequences for subsequent analysis in Fast UniFrac (Hamady *et al.*, 2009). *nirS gene* maximum likelihood tree was inferred by PhyML (version 3.0 for Window) (Guindon *et al.*, 2010) using a LG model of amino acids substitution with 1000 bootstrap replicates.

### 4.3.6. Nucleotide sequence accession numbers

16S rRNA gene V1-V3 pyrotag sequences were deposited in the National Center for Biotechnology Information Sequence Read Archive (SRA) under the accession number SRA051604. *nirS* sequences were deposited to GenBank under sequence accession numbers JX459951-JX459971.

### 4.3.7. Quantification of Bacteria, Archaea, and *nirS* genes by quantitative PCR

Total bacterial and archaeal gene copy numbers were determined by qPCR and run on an Opticon® 2 DNA Engine Real-Time PCR detection system (Bio-Rad) according to the protocol described in Zaikova *et al.* (2010). The following primers were used: Bacteria: (27F, 5'-AGA GTT TGA TCC TGG CTC AG-3'), Archaea: (20F, 5'-TTC CGG TTG ATC CYG CCR G-3') coupled to a universal reverse primer (DW519R, 5'-GNT TTA CCG CGG CKG CTG-3').

Our qPCR protocol to measure the abundance of the denitrifying gene coding for nitrite reductase (*nirS*) was adapted from Chon *et al.* (2009). The following primer pair, from Braker *et al.* (1998) was used: nirS2F (5'-TAC CAC CCS GAR CCG CGC GT-3') and nirS3R (5'-GCC GCC GTC RTG VAG GAA-3'). Each 20 μL amplification reaction contained 10 μL of SsoFastTM EvaGreen® Supermix, 1 μL each 500 nM forward and reverse primers, 6 μL of DNAse-free water and 2 μL of template DNA. Reactions were run on a Bio-Rad CFX96 system under the following conditions: initial enzyme activation at 98°C for 2 min, followed by 45 cycles of denaturation at 98°C for 1 sec, annealing/elongation at 67°C for 5 sec and a plate read. A melting curve from 67°C to

98°C, held at each 0.5°C increment for 5s was then performed to check the specificity of the reaction. The amplicon length was additionally verified by agarose gel electrophoresis. qPCR data were analyzed with the Bio-Rad CFX Manager Software version 1.6.

For all qPCR essays, calibration curves were constructed using a series of six 10-fold dilutions of the standards. The standards used for the calibration curves for Bacteria and Archaea qPCR analysis were the same as in Zaikova *et al.* (2010). Standard concentrations, determined from PicoGreen essays using the Quant-iT PicoGreen® dsDNA kit (Invitrogen) ranged from $2.8 \times 10^{10}$ copies $\mu L^{-1}$ (Bacteria) to $3.8 \times 10^{7}$ copies $\mu L^{-1}$ (Archaea). The standard used for *nirS* quantification was prepared from the clone ES09-H-70 (which was identical to clone ES09-H-1 represented in Fig. 4.6) in our *nirS* gene clone library from Endeavour Segment. Approximately 1 μL of the glycerol culture stock was inoculated in a culture of 2 mL LB medium and incubated at 37°C for 12-16 hours on a shaker. The cells were harvested by centrifugation in a conventional microcentrifuge at room temperature. A Qiagen® Plasmid Mini Kit was used to extract and purify the plasmid DNA according to the manufacturer's instructions. Residual *E. coli* genomic DNA was removed using a plasmid-safe DNase™ treatment (Epicenter® Biotechnologies) followed by a phenol/chloroform/isoamyl alcohol treatment as described in Zaikova *et al.* (2010). The plasmid DNA was sequenced bidirectionally using M13 primers and proved to be identical to the *nirS* clone ES09-H-70 sequence obtained earlier from the glycerol stock. The final DNA concentration of the plasmid, quantified by a PicoGreen essay, was $8.5 \times 10^{8}$ copies $\mu L^{-1}$.

All samples were analyzed in triplicate and different dilutions were used to test for the presence of any PCR-inhibiting compounds. The detection limit for all qPCR essays, set above the Ct values of the less concentrated standard and the no-template controls (<40 cycles or undetected), was generally less than ~50 copies/ml for total Bacteria and Archaea and ~10 copies/ml for *nirS* genes qPCR essays for all triplicate samples. The $r^2$ values of the calibration curves were generally >0.99. The amplification efficiency for each run was estimated from the slope of the standard curve according to the equation: $E= (10^{-1/slope})$ and was above 95%. Melting-curve analyses were performed to check the specificity of the reactions for all standards and samples and amplification products were selected and visualized on a ~1% agarose gel stained with ethidium bromide prepared using 0.5× TBE.

Mann-Whitney tests for non-parametric data were used to compare *nirS* abundances between sampling years at Axial Volcano and different vent fields for 2009 samples. Spearman's rank correlations were used to relate environmental variables to qPCR *nirS* gene abundances.

## 4.4. Results and discussion

### 4.4.1. Physico-chemical properties

All physico-chemical properties for the studied sites, i.e., depth, pH, temperature, and $H_2S$, $NO_3^-$, and $NH_4^+$ concentrations are presented in Table 4.1. Temperature ranged between 6.2°C (Cloud) and ~125°C (Hulk). pH ranged from 5.4 (Gollum and Diva) to

6.9 (Cloud), and decreased in the lower-T fluids (<50°C) as temperature increased ($r^2$= 0.34, p-value). [$H_2S$] was highest in the high-T fluids. Hot fluids mixing with seawater below the seafloor (and subsequent dilution) causes sulfide concentrations to decrease with decreasing temperature (Jannash and Mottl, 1985). Sulfide oxidation can also occur as a result of this mixing process, and sulfate reduction by free-living bacteria, or bacteria attached to conduit walls may occur at temperatures below 120°C (e.g. McCollom and Shock, 1997; Huber *et al.*, 2002). Nitrate concentrations varied from ~2 (Marker 113) to ~40 μmol/L, compared to ~40 μmol/L in background seawater, indicating nitrate consumption during hydrothermal circulation at the low-T end (Butterfield *et al.*, 2004; Bourbonnais *et al.*, 2012a). Ammonium concentrations were significantly lower at Axial Volcano (from ~1 (Diva) to 13 μmol/L (Marker 113) compared to Endeavour Segment (up to 190 μmol/L at Hulk1). Based on ammonium concentrations and N isotope results, Butterfield *et al.* (2004) and Bourbonnais *et al.* (2012a) attributed [$NH_4^+$] that were slightly higher than expected from seawater-hot fluid mixing to biological production in the sub-seafloor mixing zone (organic matter remineralization and dissimilative nitrate reduction to ammonium (DNRA)). [$NH_4^+$] in lower-T fluids at Endeavour Segment did not significantly deviate from the mixing line between high-T fluids (>350°C) (i.e. [$NH_4^+$] up to ~400 μmol/L at the Main Endeavour Field) and seawater, and thus could be explained in terms of simple mixing of these two end-members (Bourbonnais *et al.*, 2012a). Phosphate was never limiting (data not shown).

**Table 4.1.** Physico-chemical properties of hydrothermal vent fluids at Axial Volcano (AV), Cobb Segment (CS) and Endeavour Segment (ES) on the JFR. Standard deviation for 2 to 5 samples collected during the same dive at the same vent location is indicated. The two vent sites (Shepherd (AV) and Hulk (ES)), where *nirS* genes were cloned and sequenced, are in bold. Data from Bag City, Cloud Pit, Gollum and Marker 113 collected in 2007 and all data from 2009 (except Diva and Hulk1) are from Bourbonnais *et al.* (2012b). Bkgd = Background seawater.

| Field/ sample year | Vent/ | Lati-tude | Longi-tude | Depth (m) | Temp. (°C) | pH | $[H_2S]$ ($\mu$mol $L^{-1}$) | $[NO_3^- + NO_2^-]$ ($\mu$mol $L^{-1}$) | $[NH_4^+]$ ($\mu$mol $L^{-1}$) |
|---|---|---|---|---|---|---|---|---|---|
| AV07 | Bag City | 45.92 | 129.99 | 1533 | 13.7±0.9 | 6.5±0.1 | 39.3±19.3 | 8.6±2.7 | 1.9±0.7 |
| AV07 | Cloud Pit | 45.93 | 129.98 | 1521 | 6.5±0.2 | 6.9±0.1 | 76.5±130.3 | 18.1±1.8 | 1.4±0.3 |
| AV07 | Forum | 45.95 | 129.98 | 1524 | 6.2±0.3 | 6.4±0.2 | 39.6±7.7 | 29.7±4.5 | 0.6±0.1 |
| AV07 | Gollum | 45.93 | 130.01 | 1544 | 22.0±0.5 | 5.4 | 154.3±24.5 | 26.7±0.4 | 3.1±0.9 |
| AV07 | Marker 113 | 45.92 | 129.99 | 1523 | 31.2±0.4 | 5.7±0.2 | 1324.6±71.1 | 1.6±0.5 | 12.6±0.4 |
| **AV07** | **Shepherd** | **45.99** | **130.03** | **1582** | **24.4±3.8** | **6.0±0.1** | **121.4±37.1** | **13.9±5.8** | **2.7±0.5** |
| AV07 | The Spot | 45.92 | 129.99 | 1535 | 30.0±0.1 | 5.8±0.0 | 455.7±72.6 | 11.7±2.6 | 2.9±0.6 |
| AV07 | T&S | 45.99 | 130.03 | 1580 | 73.0 | 5.7 | 389.1 | 30.9 | 4.3 |
| AV07 | Zen Garden1 | 45.94 | 129.98 | 1518 | 23.8±0.5 | 5.9 | 144.3±12.7 | 12.4±2.6 | 4.0±0.1 |
| AV07 | Zen Garden2 | 45.94 | 129.98 | 1518 | 7.3 | 6.6 | 1.4 | 13.2 | 2.1 |
| AV09 | Diva | 45.93 | 129.98 | 1520 | 16.9±1.1 | 5.4±0 | 123.5±4.9 | 39.2 | 1.2 |
| AV09 | Gollum | 45.93 | 130.01 | 1542 | 14.2±1.2 | 5.7±0 | 89.6±11.6 | 24.4±3.6 | 2.6±0.7 |
| AV09 | Hermosa | 45.93 | 129.98 | 1519 | 37.0±4.1 | 5.6±0.3 | 253.2±160.3 | 41.7±2.2 | 1.9±1.1 |
| AV09 | Marker 33 | 45.93 | 129.98 | 1520 | 34.4±0.9 | 5.5±0 | 711.7±19.0 | 15.7±2.0 | 4.4±0.2 |
| AV09 | Marker 113 | 45.92 | 129.99 | 1521 | 29.9±5.0 | 6.1±0.1 | 1020.0±194.2 | 7.1±3.4 | 10.2±3.1 |
| AV | Bkgd | 45.90 | 130.00 | >1200 | 3.0±0.5 | 7.1±0.4 | 0.4±0.3 | 41.5±3.8 | 0.4±0.3 |
| CS07 | Not dead yet | 46.69 | 129.38 | 2402 | 27.2±3.3 | 6.4±0.6 | 0.8±0.1 | 31.3±1.2 | 2.9±0.5 |
| ES09 | Fairy Castle | 47.97 | 129.09 | 2157 | 23.4±1.8 | 6.2 | 245.0±35.4 | 28.0±1.3 | 41.4±3.8 |
| **ES09** | **Hulk1** | **47.95** | **129.10** | **2198** | **13-125**[a] | **5.7** | **645** | **7.2** | **190.0** |
| ES09 | Hulk2 | 47.95 | 129.10 | 2198 | 29.5±10.6 | 6.3±0.3 | 212.5±132.7 | 27.8 | 38.0±20.5 |
| ES09 | Phang | 47.92 | 129.11 | 2277 | 24.1±1.7 | 6.5±0.3 | 255.6±133.6 | 30.4±4.1 | 42.7±20.8 |
| ES | Bkgd | 48.00 | 129.10 | >2000 | 2.2±0.3 | 7.3±0.2 | 1.00±0.4 | 40.6±2.0 | 1.4±2.2 |

**a.** From Anderson *et al*., 2011. Lower limit inferred from temperature probe readings at the same vent site and upper limit calculated from $[Si^{4+}]$.

### 4.4.2. Composition of 16S rRNA genes clone libraries and difference among vent fields

α-diversity (single sample analyses) and β-diversity (multiple sample analyses) calculators are summarized in Tables 4.2 and 4.3, respectively. High coverage (>~91%) was achieved for all samples pyrosequenced in this study. Rarefaction analysis of 16S rRNA gene V1-V3 pyrotag data revealed high bacterial diversity at the 3% difference level (Fig. 4.2). Each sample contained an elevated number of OTUs (from 1070 at Bag City to 190 at Shepherd) and of unique OTUs (abundance =1) (from 22% (Shepherd) to 39% (Bag City) of the total OTUs). Few OTUs were shared between the different vent fluid samples. A maximum of 143 shared OTUs was observed at the sites Forum and T&S, which represented 70% of the sequences between these two samples (Table 4.3). Only one OTU, a α-proteobacteria classified in the *Methylonatrum* genus, representing 0.14% of the total sequences, was shared among all 6 samples. Shannon diversity indices varied from 4.4 at Shepherd to 6.3 at Bag City for V1-V3 pyrotag sequences. The lowest diversity (Shannon index= 3.7) was observed at Hulk1, although the coverage was comparatively low for this sample (66%, Table 4.2), because only a few clones (100 in total) were sequenced using the Sanger method (see Anderson *et al.*, 2012). Similarly high bacterial diversity, with high numbers of rare OTUs, has been previously documented in hydrothermal vent systems using a pyrosequencing approach (e.g. Huber *et al.*, 2007; 2010).

**Table 4.2.** Biodiversity and predicted richness of 16S rRNA and *nirS* gene sequences from hydrothermal vent fluids of the JFR. Sample names were assigned as follow: the first letters indicate the vent fields (AV and ES), followed by the year (07= 2007 and 09=2009) (see Table 4.1) and the first letters of the diffuse vent sampled (BC= Bag City, F= Forum, S= Shepherd, TS= T&S, H= Hulk, and P= Phang).

| Gene | Sample | Coverage (%) | $S_{obs}$[a] | $S_{ACE}$[a] | $S_{Chao1}$[a] | H′[b] | 1/D[c] | E[d] |
|---|---|---|---|---|---|---|---|---|
| **16S rRNA** | AV07BC | 90.8 | 1070 | 1514 | 1468 | 6.28 | 244.6 | 0.90 |
| | AV07F | 96.4 | 527 | 729 | 718 | 4.66 | 34.3 | 0.74 |
| | AV07S | 94.2 | 190 | 213 | 215 | 4.44 | 53.2 | 0.85 |
| | AV07TS | 94.0 | 757 | 1013 | 973 | 5.68 | 110.7 | 0.86 |
| | ES09H1[f] | 66.0 | 53 | 183 | 112 | 3.69 | 39.9 | 0.93 |
| | ES09H2 | 93.8 | 845 | 1155 | 1180 | 5.59 | 79.3 | 0.83 |
| | ES09P[e] | 95.6 | 566 | 739 | 815 | 5.22 | 63.0 | 0.82 |
| ***nirS*** | AV07S | 96.7 | 9 | 11.3 | 9.8 | 1.20 | 2.39 | 0.55 |
| | ES09H1[f] | 92.1 | 12 | 60.3 | 22.5 | 1.42 | 2.64 | 0.57 |

**a.** Number of different OTUs observed ($S_{obs}$) or statistical predictions using the ACE ($S_{ACE}$) or Chao1 ($S_{Chao1}$) richness estimators.
**b.** Shannon index, higher number represents more OTUs diversity.
**c.** Reciprocal of Simpson's index, higher number represents more OTUs diversity.
**d.** Evenness, varying between 0 to 1. Higher number represents a more evenly distributed community.
**e.** Sanger sequencing is also available for that sample in Bourbonnais *et al.* (2012b).
**f.** Collected from Barrel sampler. Sanger sequences are from Anderson *et al.* (2012), accession numbers: JQ678511- JQ678591.

The bacterial communities in the vent fluids were primarily dominated by Proteobacteria, more precisely ε-, and for two samples (Shepherd and Hulk1), γ-proteobacteria. ε-proteobacteria accounted for 3.6% (Shepherd) to 72% (Hulk2) of the total sequences at each site. α-proteobacteria represented ~20% of the total bacterial community at Shepherd and Hulk2, but their abundance was typically lower than 4% at all other sites. β- and δ-proteobacteria generally only constituted a minor fraction of the total bacterial community. β-proteobacteria were most abundant at Hulk1 (8%) and Shepherd (~1.5%). δ-proteobacteria represented up to 17% of the total 16S rRNA gene sequences at Bag City, but their abundance was lower than 5% at all other sampled sites.

Bacteroidetes represented another important phylum at some sites, accounting for up to ~10% of the total bacteria at Shepherd and Hulk1 (Fig. 4.3).

Previous studies using culture-dependent (Nakagawa *et al.*, 2005a) and culture-independent (López-García, 2003; Alain *et al.*, 2004; Nakagawa *et al.*, 2005a; Huber *et al.*, 2007; 2010) approaches have generally revealed ε-proteobacteria to be the dominant class in diverse hydrothermal vent habitats. The main ε-proteobacteria genera detected (5% or more in at least one clone library) were *Sulfurovum* (up to 43% at Phang), *Sulfurimonas* (up to 26% at Forum), *Arcobacter* (up to 16% at Bag City), *Hydrogenimonas* (up to 13% at Phang), *Thioreductor* (up to 10% at Hulk), and *Nitratifractor* (up to 7% at Phang) (Fig. 4.3). Culture experiments have demonstrated that several chemolithoautotrophic species (some being mesophilic or thermophilic) within all the above-mentioned genera isolated from hydrothermal vent environments are capable of nitrate reduction, mainly coupled to sulfur and/or hydrogen oxidation. These genera include *Sulfurovum lithotrophicum* (Inagaki *et al.*, 2004), *Sulfurimonas autotrophica* (Inagaki *et al.*, 2003), *Sulfurimonas paralvinellae* (Takai *et al.*, 2006), *Thioreductor micantisoli* (Nagakawa *et al.*, 2005c) *Nitratiruptor tergarcus* and *Nitratiruptor salsuginis* (Nagakawa *et al.*, 2005b) from hydrothermal sediments, a polychaete nest and vent chimney structures of the Okinawa Trough (Japan), *Arcobacter sulfidicus* (Heylen *et al.*, 2006, Sievert *et al.*, 2007), and *Hydrogenimonas thermophila* from a black smoker in a Central Indian Ridge hydrothermal field (Takai *et al.*, 2004). γ-proteobacteria represented the dominant class at Shepherd and Hulk1, where they represented ~47% and 39% of the total bacterial diversity. However, for all other sampled sites, γ-proteobacteria typically represented less than 15% of the total bacteria (Fig. 4.3). The dominant γ-proteobacteria

genera observed were *Alteromonas* (up to 8% at Hulk1), *Halomonas* (up to 11% at Shepherd), *Neptunomonas* (up to 9% at Forum), *Pseudoalteromonas* (up to 10% at Hulk) and *Pseudomonas* (~5% at Shepherd and 11% at Hulk1). Culture experiments have shown that some species (mostly heterotrophic) from these genera isolated from, or near, hydrothermal vent environments were capable to perform nitrate reduction (and often complete denitrification) for example, *Halomonas neptunia*, *Halomonas suldidaeris*, *Halomonas axialensis*, and *Halomonas hydrothermalis* isolated from North and South Pacific hydrothermal vent fields (Kaye *et al.*, 2004), and *Pseudomonas stutzeri* (strain MT-1) from mud of the Mariana Trench at 11 000 m depth (Tamegai *et al.*, 1997).

Other studies have identified chemolithoautotrophic γ-proteobacteria of the SUP05 cluster, that couple the oxidation of reduced sulfur species with nitrate reduction as important constituents of bacterial diversity in deep-sea hydrothermal vent environments and plumes (e.g. Sunamura *et al.*, 2004; German *et al.*, 2010; Bourbonnais *et al.*, 2012b; Anderson *et al.*, 2012). For example, qPCR assays targeting SUP05-specific 16S SSU showed that bacteria of the SUP05 cluster respectively represented up to 38% and 27% of the total bacterial community in diffuse vent fluids at Hulk (Endeavour Segment) in 2008 and at Cloud Pit (Axial Volcano) in 2007 (Bourbonnais *et al.*, 2012b). However, SUP05 bacteria always represented less than 2% of the total microbial community in all 16S rRNA gene samples sequenced in this study (Table C.2).

Various non-abundance and abundance-based β-diversity calculators suggest differences in both bacterial community membership and structure among individual vent sites (Table 4.3). UniFrac distance metric and a P-test confirmed that all of the 16S rRNA gene bacterial communities in the sampled vent fluids were significantly different (p-

value ≤ 0.001) from each other in terms of membership (non-abundance weighted), except for T&S and Forum, and most sites were different in terms of structure (abundance-weighted), except for the communities found at Forum and T&S, Hulk2 and Phang, and T&S and Hulk2 (95% significance level, see Table C.3). The difference between time series data from two sites collected for different time periods in this study was likely caused by the different sampling methods and differences in average fluid temperature and chemistry rather than temporal variability (Hulk1 (~30°C) was collected for ~24 hrs, whereas Hulk2 (>100°C) was collected in less than 1 hour during the same dive; Table 4.1, Fig. 4.3). Opatkiewicz *et al.* (2009) reported on the temporal stability in community structure at individual hydrothermal vents of the JFR. However, overall, no clear relationship between 16S rRNA gene community membership and structure, and specific environmental factors could be identified.

As discussed in section 4.4.1, physico-chemical properties at the sampled sites at Axial Volcano and the Endeavour Segment vent fields differed significantly, especially in terms of their $NH_4^+$ concentrations (see Table 4.1). More recently, a study by Huber *et al.* (2010) found significant large and local-scale geographic differences in ε-proteobacteria communities in diffuse vent fluids between hydrothermal seamounts and individual vents of the Mariana Arc, suggesting a link between geographic isolation, rather than geochemical factors, and microbial community membership at this location. Therefore, despite the two fields being in the same subseafloor microbial province, i.e. the Juan de Fuca mid-ocean ridge (see Schrenk *et al.*, 2010), it is reasonable to expect differences in bacterial communities between the two vent fields. However, a UPGMA tree describing the dissimilarity between samples (based on the Yue and Clayton theta values (Fig. 4.4)

**Table 4.3.** Similarity coefficients used to compare 16S rRNA gene V1-V3 tag sequences and *nirS* gene bacterial community richness, membership and structure in hydrothermal vent fluids sampled at two different vent fields (Endeavour Segment and Axial Volcano) on the JFR. The percentage of shared sequences is indicated in brackets. Sample names as in Table 4.2.

| | **Richness**[a] | **Membership**[b] | | | | **Structure**[c] | | | |
|---|---|---|---|---|---|---|---|---|---|
| | **$S_{obs,\ chao1\ and\ ACE}$** | **$J_{class}$** | **Sor $_{class}$** | **$J_{est}$** | **Sor $_{est}$** | **$J_{abund}$** | **Sor $_{abund}$** | **the-ayc** | **the-tan** |
| **16S rRNA gene** | | | | | | | | | |
| AV07BC/F | 94 (37%) | 0.94 | 0.88 | 0.93 | 0.88 | 0.86 | 0.76 | 0.95 | 0.87 |
| AV07BC/S | 10 (14%) | 0.99 | 0.98 | 0.99 | 0.98 | 0.98 | 0.97 | 0.98 | 0.98 |
| AV07BC/TS | 74 (37%) | 0.96 | 0.92 | 0.96 | 0.92 | 0.90 | 0.81 | 0.92 | 0.90 |
| AV07BC/ES09H2 | 91 (32%) | 0.95 | 0.90 | 0.95 | 0.90 | 0.87 | 0.77 | 0.98 | 0.89 |
| AV07BC/ES09P | 18 (11%) | 0.99 | 0.98 | 0.99 | 0.98 | 0.99 | 0.98 | 1.00 | 0.99 |
| AV07F/S | 14 (13%) | 0.98 | 0.96 | 0.98 | 0.96 | 0.96 | 0.92 | 0.96 | 0.96 |
| AV07F/TS | 143 (70%) | 0.88 | 0.78 | 0.88 | 0.78 | 0.60 | 0.43 | 0.74 | 0.63 |
| AV07F/ES09H2 | 70 (32%) | 0.95 | 0.90 | 0.94 | 0.89 | 0.87 | 0.77 | 0.99 | 0.89 |
| AV07F/ES09P | 37 (25%) | 0.97 | 0.93 | 0.95 | 0.91 | 0.95 | 0.90 | 0.99 | 0.96 |
| AV07S/TS | 19 (20%) | 0.98 | 0.96 | 0.98 | 0.97 | 0.95 | 0.90 | 0.97 | 0.95 |
| AV07S/ES09H2 | 10 (6.3%) | 0.99 | 0.98 | 0.99 | 0.98 | 0.98 | 0.96 | 1.00 | 0.99 |
| AV07S/ES09P | 11 (8.9%) | 0.99 | 0.97 | 0.99 | 0.97 | 0.97 | 0.94 | 1.00 | 0.97 |
| ES09H2/P | 111 (22%) | 0.91 | 0.84 | 0.90 | 0.82 | 0.72 | 0.56 | 0.88 | 0.78 |
| AV07TS/ES09H2 | 94 (40%) | 0.94 | 0.89 | 0.94 | 0.88 | 0.88 | 0.79 | 0.98 | 0.90 |
| AV07TS/ES09P | 48 (54%) | 0.97 | 0.93 | 0.96 | 0.93 | 0.96 | 0.92 | 0.99 | 0.97 |
| ***nirS*** | | | | | | | | | |
| AV07S-ES09H1 | 1 (59%) | 0.95 | 0.90 | 0.97 | 0.94 | 0.58 | 0.41 | 0.25 | 0.58 |

**a.** Number of shared OTUs observed ($S_{obs}$) and shared richness estimates from the Chao1 ($S_{Chao1}$) and ACE ($S_{ACE}$) estimators for an OTU definition (>97% identical sequences).
**b.** Jaccard (J) and Sorenson (Sor) similarity coefficients based on the observed richness (class) or the Chao1 estimated richness (est). The maximum value of 1 indicates that samples are entirely dissimilar.
**c.** Abundance-based Jaccard ($J_{abund}$) and Sorenson ($Sor_{abund}$) similarity coefficients and Yue and Clayton theta (theayc) and Smith theta (thetan) similarity coefficients. The scale ranges from 1 (entirely dissimilar) to 0 (identical).

and principal coordinates analysis (PCoA) (Fig. C.2)) showed that vent fluids bacterial communities were not clearly clustered according to vent fields. Analysis of similarities (one-way ANOSIM test) using the distance matrix generated with the Yue and Clayton measure, detected no significant groupings between vent fields at a 95% confidence level (r-value=0.57, p-value= 0.07, 1000 permutations), although sample size was low, particularly at Endeavour Segment.

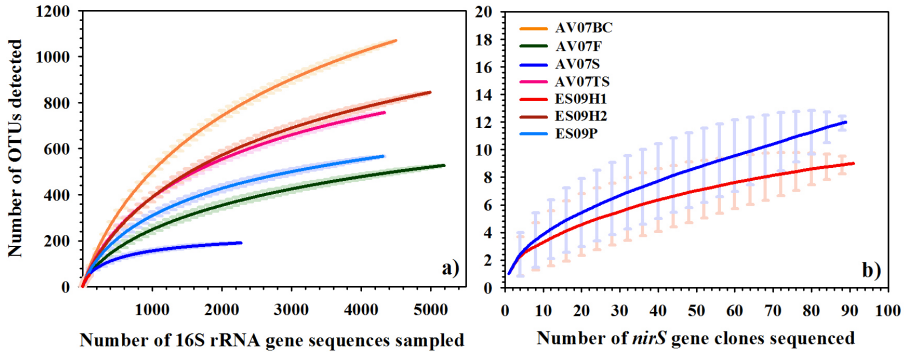


**Figure 4.2.** Rarefaction curves showing **a**) 16S rRNA and **b**) *nirS* genes OTUs richness in DNA extracted from hydrothermal fluids at the Endeavour Segment and Axial Volcano on the JFR. OTUs are defined at the ≥97% sequence identity level. Errors bars representing 95% confidence intervals are indicated. The number of 16S rRNA pyrosequences represents the number of sequences obtained after final processing (i.e. screening, sorting, pre-clustering and chimera removal, see text for more detail). Sample names as in Table 4.2.

### 4.4.3. Composition of *nirS* gene clone libraries and comparison to other marine environments

PCR-products that were ~890 bp long were obtained with *nirS* primers from DNA extracted from one diffuse fluid sample at each vent field, i.e. Shepherd (Axial Volcano) and Hulk1 (Endeavour Segment). We tried to amplify *nirS* in other DNA samples from

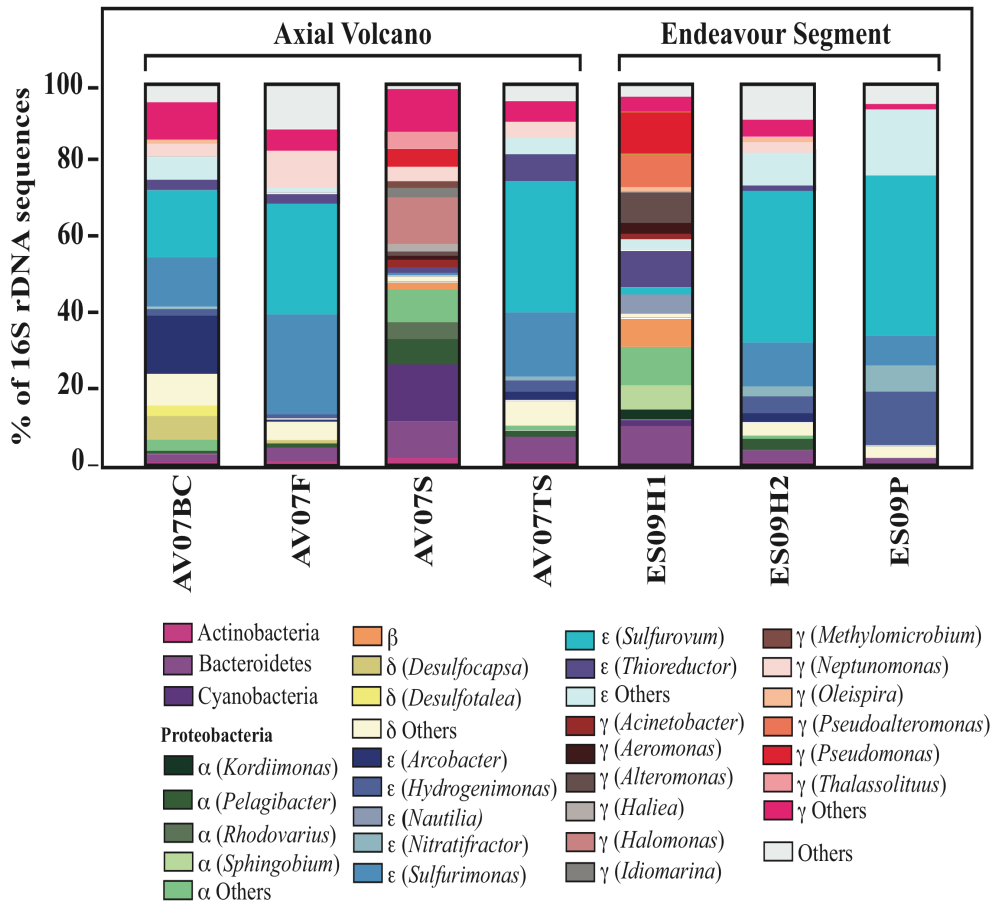


**Figure 4.3.** Relative abundance of all taxon ≥2% (for at least one sample) in hydrothermal vent fluids of the JFR. The genus is indicated in brackets for members of the proteobacteria. All sequences, except ES09H1, are pyrosequences from the hypervariable V1-V3 region of the 16S rRNA gene (see text for more detail). 16S rRNA gene sequences for ES09H1 are from Anderson *et al.* (2012), accession numbers: JQ678511- JQ678591. Sample names as in Table 4.2.

nearby vent sites with no success, probably because of the lower DNA concentrations (and *nirS* absolute abundances) in these samples. As a result, *nirS* absolute gene abundances (in copies $mL^{-1}$ seawater) were highest for the Shepherd and Hulk1 samples (see section 4.4.5, Table 4.4).

Coverage was high for both samples, i.e. 97% at Shepherd and 92% at Hulk1, for a total of 91 and 89 sequences, respectively (Table 4.2, Fig. 4.2b). Diversity was relatively

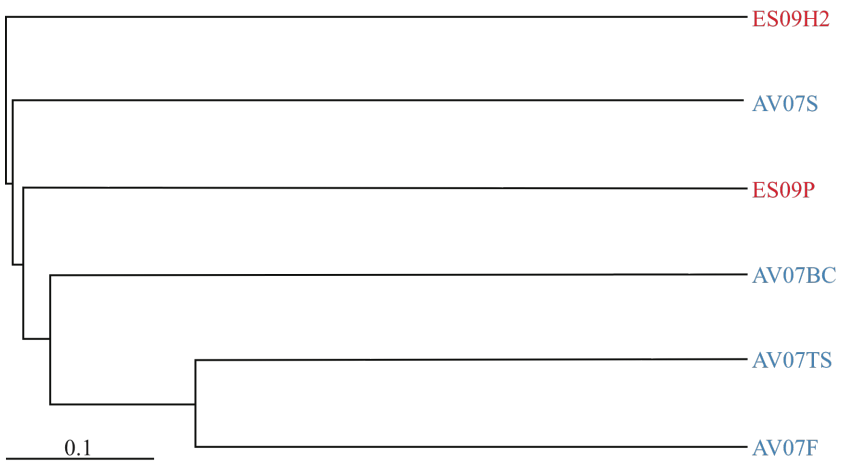


**Figure 4.4.** UPGMA dendrogram comparing the similarity of 16S rRNA gene bacterial communities at six diffuse vent fluids of the JFR based on the Yue and Clayton theta similarity coefficient at the 3% difference level as calculated in MOTHUR. The length of the scale bar represents a distance of 0.1. Sample names as in Table 4.2.

low at both sites, with Shannon indices of 1.2 and 1.4 at Shepherd and Hulk1, respectively. Only 9 and 12 OTUs, for a total of 20 distinct OTUs at the 3% nucleic acid difference level, were observed (Tables 4.2 and 4.3). Similarly low *nirS* gene diversity has been reported for water column samples from the oxygen minimum zones of the Black Sea (Oakley *et al.*, 2007) and Arabian Sea, especially at a more advanced denitrification stage (Jayakumar *et al.*, 2009). The substantial nitrate depletion relative to background seawater observed at both sites (~70% at Shepherd and ~80% at Hulk1, see Table 4.1) could thus indicate progression of denitrification and explain the low *nirS* diversity.

Figures 4.5 and 4.6 show that our *nirS* sequences grouped into 4 main clusters in the phylogenetic tree, and further divided into 7 subclusters, The resulting OTUs displayed, respectively, more than 72% and 70% (Shepherd) and 86% and 77% (Hulk1) similarity at the amino acid level to the closest uncultured and cultured organisms in the NCBI

database, respectively. Both *nirS* clone libraries were dominated by an OTU grouping in cluster IVb, which was 99% similar at the amino acid level to a γ-proteobacteria, *Pseudomonas* sp. BA2.5, isolated from sediments collected in the middle of the macrotidal, hypernutrified and muddy estuary of the River Colne in the United Kingdom (Nogales *et al.*, 2002). This OTU represented 58% and 59% of the total sequences at Shepherd and Hulk1.

For all other OTUs, except at Hulk1, where 26% of the clones (cluster IVb) were most closely related (94% identity) to *Pseudomonas fluorescens* WH6 (isolated from a wheat rhizhosphere in Benton County, Oregon, USA), unshared OTUs were more closely related to uncultured bacteria from environmental samples. Most other OTUs, i.e. 6 at Shepherd (clusters I, IIIb and IVa) and 5 at Hulk1 (clusters IIb and IIIa), were most closely related to *nirS* sequences from uncultured bacteria isolated from sediments of the Chesapeake Bay estuary (72% to 99% identity). These OTUs represented 35% (Shepherd) and 11% (Hulk1) of the total sequences. Other OTUs were most closely related to *nirS* sequences from uncultured organisms from a rice field soil from China (85% identity, 1 OTU, cluster IIIa), the water column of the Central Baltic Sea (92-94% identity, 3 OTUs, cluster IIa), sediments of the Hai River in China (72-76% identity, 2 OTUs, cluster IVa), and deep-sea sediments near an East Pacific Rise hydrothermal field (91% identity, 1 OTU, cluster IIIb).

The majority of *nirS* OTUs were most closely related to cultured γ-proteobacteria, representing 62% of the sequences at Shepherd (72-100% identity, clusters IIIb, IVa, and IVb) and 88% of the sequences (94-100% identity, cluster IVb) at Hulk1. The dominance

of *nirS* denitrifying communities by γ-proteobacteria in these different environments is not surprising. As mentioned in section 4.4.2, γ-proteobacteria represented the dominant class at both sites. Furthermore, a larger portion of both the 16S rRNA gene and *nirS* gene sequences were closely associated with the metabolically versatile genus *Pseudomonas* (cluster IVb) at Hulk1 compared to Shepherd (Figures 4.3, 4.5, 4.6).

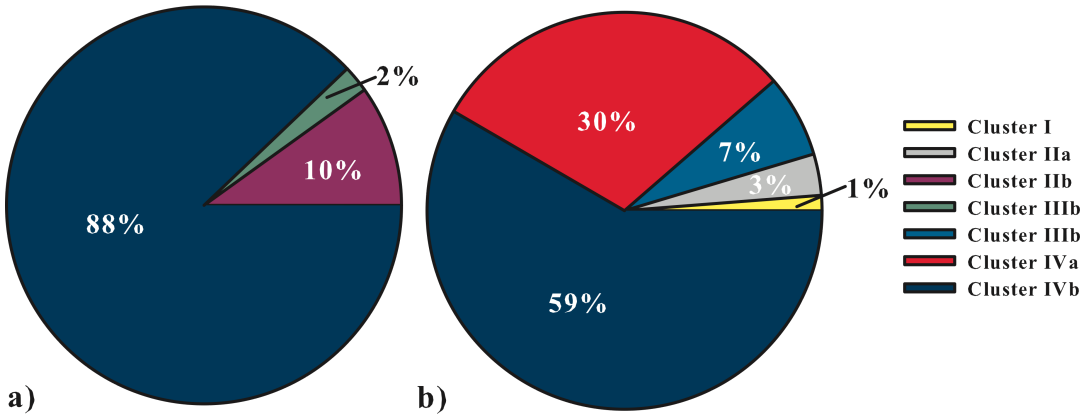


**Figure 4.5.** Relative abundance (in %) of *nirS* genes grouping in different clusters of the phylogenetic tree (Fig. 4.6) in hydrothermal vent fluids of **a**) Endeavour Segment (Hulk1) and **b**) Axial Volcano (Shepherd) (see Table 4.2).

*nirS* OTUs most closely related to cultured β-proteobacteria represented 35% of the sequences at Shepherd (70-77% identity, clusters I, IIIb and IVa) and 2% of the sequences at Hulk1 (86-89% identity, cluster IIIa). The rest of the *nirS* sequences were most closely related to cultured α-proteobacteria, representing 3% of the sequences at Shepherd (71-74% identity, cluster IIa) and 10% of the sequences at Hulk1 (~85% identity, cluster IIb). α- and β-proteobacteria were detected in our 16S rRNA gene sequences at both sites, representing up to 20% and 8% of the total bacterial communities, respectively (section 4.4.2, Fig. 4.3).

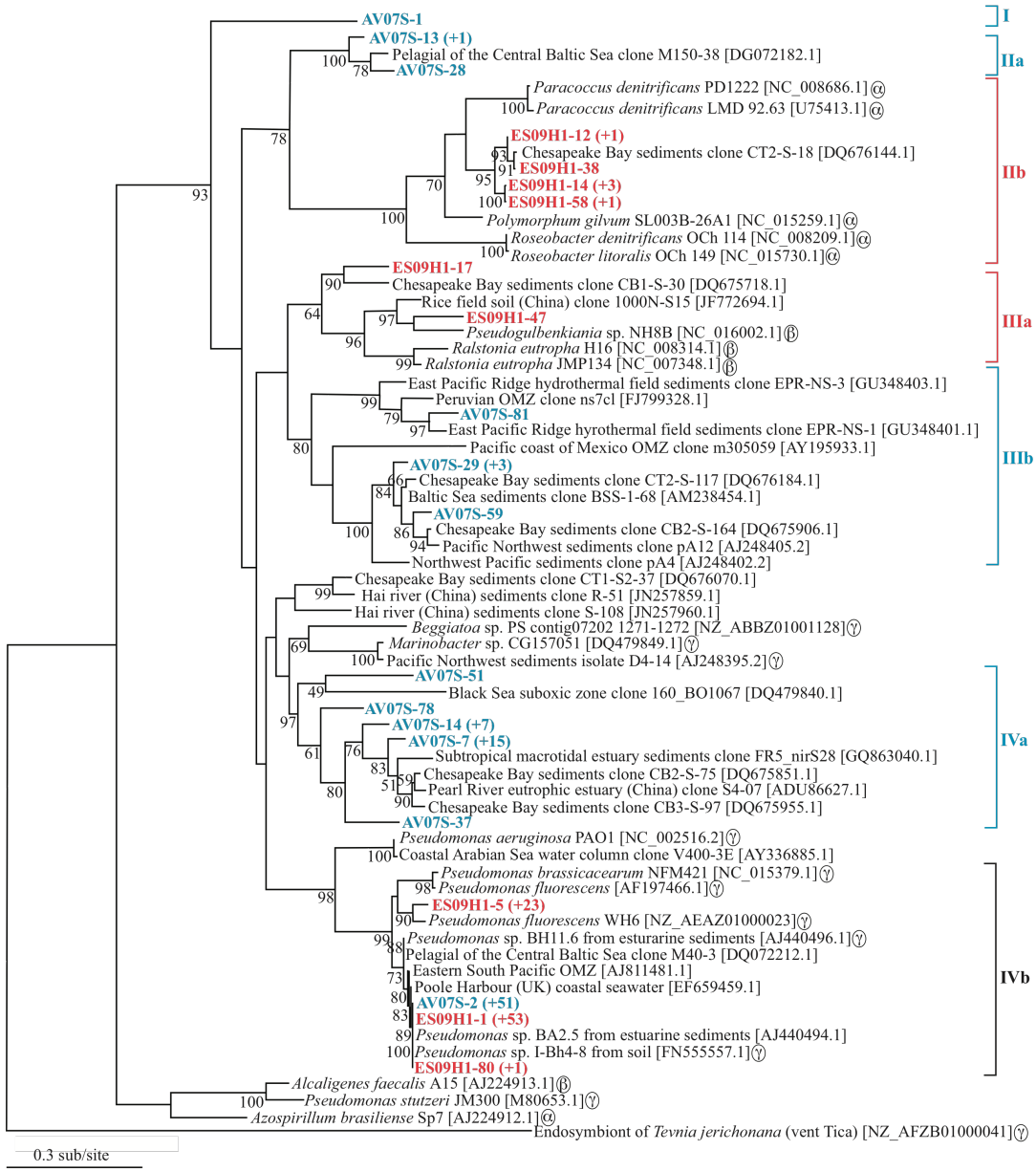


**Figure 4.6.** Phylogenetic tree of *nirS* sequences from hydrothermal vent fluids at Axial Volcano and Endeavour Segment on the JFR. Tree was calculated by the maximum likelihood method based on an alignment of partial sequences of ~230 amino acids. Sample names were assigned as in Table 4.2. The last numbers indicate clones #. The number of clones ≥97% identical (OTU definition) is indicated in parentheses. GenBank accession numbers are provided (in brackets) for other cultured bacteria and environmental clones not sequenced in this study. The percentage of 1000 bootstrap resamplings above 50% is indicated. The scale bar indicates the number of amino acid substitutions per site.

No *nirS* sequences were closely related to any known *nirS*-containing ε-proteobacteria, although this bacterial class represented 3% (Shepherd) and 19% (Hulk1) of the 16S rRNA clone libraries. A BLAST search revealed that no ε-proteobacteria were ever amplified with the nirS1F-nirS6R primer pair developed by Braker *et al.* (1998) and used in the majority of terrestrial and marine *nirS* biodiversity studies published to date (Braker *et al.*, 2000 and references therein). However, genome sequencing of both *Sulfurovum lithotrophicum* (Nakagawa *et al.*, 2007) and *Sulfurimonas autotrophica* (Sievert *et al.*, 2008), showed that these organisms possess the *nirS*-form of nitrite reductase. As mentioned in section 4.4.2, these genera were both present in our 16S rRNA gene clone libraries. Our *nirS* sequences were significantly different from the *nirS* sequences from *Sulfuruvum lithotrophicum* (up to 24% identity at the amino acid level) and *Sulfurimonas autotrophica* (up to 12% identity). Furthermore, a BLAST search showed that the regions where the *nirS* primers used in this study usually anneal were not conserved for these two *nirS* sequences. We can thus conclude that the Braker *et al.* (1998) *nirS* primer pair likely does not detect members of the ε-proteobacteria. Shepherd and Hulk1 were the only two samples dominated by γ-proteobacteria among the 6 samples pyrosequenced, and where abundances of ε-proteobacteria represented a lower portion of the total 16S rRNA sequences (Fig. 4.3). The lack of specificity of these primers for ε-proteobacteria might thus also help to explain why we were not able to successfully amplify *nirS* in the other samples, which were generally dominated by ε-proteobacteria.

Few studies have sequenced *nirS* genes in hydrothermal vent environments. *nirS* sequences in this study shared identity of $\leq 45\%$ with a sequence from a γ-proteobacteria

endosymbiont of the deep-sea tubeworm *Tevnia jerichonana* (vent Tica, 9°N, East Pacific Rise) (acc: NZ_AFZB01000041) (out-group, Fig. 4.6). Furthermore, a metagenomic study by Xie *et al.* (2010) showed that the majority of the genes involved in denitrification in a black smoker chimney in the Mothra hydrothermal vent field at the JFR were most closely related to β and α- proteobacteria, rather than γ-proteobacteria. This contrasts with our results and suggests that distinct *nirS* communities can be found in different hydrothermal vent habitats.

#### 4.4.4. *nirS* genes biodiversity differences between vent fields

*nirS* sequences at Axial Volcano and Endeavour Segment clearly did not cluster together in the phylogenetic tree. Only 1 OTU, most closely related to the γ-proteobacteria *Pseudomonas* sp. BA2.5 isolated from estuarine sediments, was shared (Table 4.3). All unshared OTUs grouped in distinct phylogenetic clusters most closely associated to cultured α- and β-proteobacteria: clusters I, IIa, IIIb, and IVa at Shepherd and clusters IIb and IIIa at Hulk1 (section 4.4.3, Figures 4.5 and 4.6).

Various β-diversity calculators (Table 4.3) suggested a marked difference in community membership (non-abundance weighted), with similarity coefficients always higher than 0.90 (with 1 indicating completely dissimilar communities). The two *nirS* communities were more similar in terms of structure (abundance weighted), mostly because the only shared OTU represented more than 50% of the total *nirS* sequences at both sites. UniFrac distance metric (p-value: 0.02) and P-test (p-value ≤ 1.0e-03) revealed a significant difference in *nirS* community membership at both sites. No significant

difference was detected in *nirS* community structure. However, biasing effects are often observed during DNA amplification by PCR in a multi-template sample (i.e. the most abundant sequences are linearly selectively amplified (Gonzalez *et al.*, 2012), and abundance-weighted analyses must be taken with extreme caution.

In this study, the differences in *nirS* community membership could be caused by physical isolation (e.g. see Braker *et al.*, 2001; Falk *et al.*, 2007). Using Terminal Restriction Fragment Length Polymorphism and correspondence analysis, Braker *et al.* (2001) showed that both 16S rRNA gene and *nirS* sequences in marine sediments from Puget Sound and the Washington margin clustered according to geographic location. In our study, since no clear clustering was observed between vent fields for 16S rRNA gene bacterial communities, there is no reason to attribute differences in *nirS* community membership at Shepherd and Hulk1 to large-scale geographic isolation. Small-scale geographic isolation and the ecological history specific to individual vent sites have been shown to be important factors in shaping microbial community structures in hydrothermal vent ecosystems. Opakiewicz *et al.* (2009) and Huber *et al.* (2010) found that total bacteria and ε-proteobacteria community structures were distinct in diffuse vent fluids at different locations at Axial Volcano and active seamounts of the Mariana Arc. Moreover, the bacterial community structures remained distinct at five diffuse hydrothermal vent sites over six years (1998-2004), despite important changes in fluid chemistry (Opakiewicz *et al.* 2009). Our results confirm those of the earlier studies, as we also generally found distinct bacterial community structures at our JFR vent sites (Tables 4.3 and C.3).

The observed differences in *nirS* community membership could also be caused by differences in fluid physico-chemical factors between individual vents or vent fields. Previous studies have established links between physico-chemical factors and nitrite reductase (*nirS* and *nirK*) biodiversity in marine environments. For example, Jayakumar *et al.* (2004; 2009) found that *nirS* gene diversity was enhanced by higher nitrite concentrations in the denitrifying water column of the Arabian sea, and that *nirS* and *nirK* diversity decreased as denitrification progressed. Changes in *nirS* community compositions were also observed along environmental gradients in oxygen minimum zones of the Eastern South Pacific, Baltic Sea and Black Sea (Castro-Gonzáles *et al.*, 2005; Falk et al, 2007; Oakley *et al.*, 2007). More recently, Jones *et al.* (2010) analyzed all *nir* sequences accessible in public repositories using UniFrac and reported that both *nirS* and *nirK* genes, although responding differently to environmental gradients in different environments, were clustering according to habitat salinity.

The two sites sampled for *nirS* biodiversity (Shepherd, Axial Volcano and Hulk, Endeavour Segment) differed mostly in their [$NH_4^+$], [$H_2S$] and temperatures (Table 4.1). Previous studies have shown that temperature can cause changes in *nirS* and *nirK* community composition in soils (Braker *et al.*, 2010) and affect *nirS* gene expression in *Pseudomonas mandeli* (Saleh-Lakha *et al.*, 2009). Given that vent fluid temperature, chemistry and 16S rRNA gene bacteria communities have been observed to change over short periods of time (e.g. at the Hulk site in this study, see Fig. 4.3), we expect the denitrifying bacterial communities to be similarly highly dynamic. For example, nitrate availability (following ammonium nitrification at the oxic end of the redox gradient) could affect denitrifying bacteria diversity in diffuse vent fluids, similar to what has been

observed in oxygen minimum zones (e.g. Jayakumar *et al.*, 2009). Also, since chemolithotrophic denitrifying bacteria of diverse phylogenetic affiliations have been shown to oxidize sulfur, while using nitrate as an electron acceptor, $H_2S$ availability could also potentially affect *nirS*-encoding denitrifying bacteria diversity (see review by Shao *et al.*, 2011).

In this study, we did not observe clear trends between 16S rRNA gene bacterial community membership/structure and environmental factors, even when normalizing chemistry data to $[Si^{4+}]$ to account for varying degree of subseafloor seawater mixing between vents. This contrasts with observations by Opatkiewicz *et al.* (2009) who found significant correlations between bacteria community composition and temperature (or $[Mg^{2+}]$, which is indicative of the degree of mixing), and ε-proteobacteria community composition and hydrogen, sulfur and iron chemistry at Axial Volcano. However, we cannot exclude that major differences in fluid chemistry at the different vent fields could have a selective effect on denitrifying bacteria. Indeed, homogenization of bacterial communities from stable subseafloor habitats (e.g. biofilms) during sampling could obscure trends linking physico-chemical parameters and microbial community composition, as previously suggested by Opatkiewicz *et al.* (2009). Geochemical factors are thus likely to shape denitrifying communities at the JFR, just as observed in other estuarine and marine studies. Below, we examine the relationship between qPCR *nirS* abundance and fluid physico-chemistry.

#### 4.4.5. qPCR *nirS* gene abundance and effect of environmental factors

Bacterial abundance, measured by qPCR, varied from ~$2\times10^3$ copies $mL^{-1}$ (at the sites Not dead yet and Diva) to $4\times10^6$ copies $mL^{-1}$ (Hulk1). Archaeal abundance ranged from ~0 copies $mL^{-1}$ (Gollum, Not dead yet, Hulk2) to $3\times10^3$ copies $mL^{-1}$ (Marker 113/07). Archaea typically represented less than ~3% of the total microbial population, which is consistent with a study by Huber *et al.* (2010) of hydrothermal vent fluids of the Mariana Arc seamounts. *nirS* gene abundance varied from $4\times10^1$ copies $mL^{-1}$ (Diva) to $4\times10^3$ copies $mL^{-1}$ (Hulk2) and represented less than 8% of the total bacterial population (Table 4.4). No significant differences (at 95% confidence level) in *nirS* abundances were found between sampling years (p-value=0.2 for 2007 versus 2009 samples collected at Axial Volcano) or between vent fields (p-value=0.07 for 2009 samples collected at Axial Volcano versus Endeavour Segment).

Correlations between marine *nirS* gene abundances and environmental factors have been reported in previous studies. For example, Smith *et al.* (2007) and Dong *et al.* (2009) observed a decline in the abundances of three different *nirS* phylotypes in sediments as nitrate concentrations and denitrification rates decreased along the hyper-eutrophic Colne estuary (United Kingdom). However, our study found no significant correlations between *nirS* gene abundance and environmental factors (i.e. temperature, pH, and hydrogen sulfide, nitrate and ammonium concentrations) in diffuse vent fluids at the 16 different investigated sites.

Several factors could explain the lack of correlation. Other than the homogenization of bacterial communities from subseafloor biofilms during diffuse fluid sampling that could obscure evidence of links between geochemistry and denitrifier abundance (as mentioned above), our methods only measured one part (*nirS*-encoding bacteria) of the denitrifying

**Table 4.4.** Copy numbers of total bacterial 16S rRNA genes (based on qPCR assays), and % Archaea and nitrite reductase (*nirS*) genes in hydrothermal vent fluids of the JFR. % Archaea and *nirS* genes are denoted relative to total bacterial abundances. The background seawater sample was collected near Endeavour Segment. Error propagation on standard deviations for triplicate qPCR essays is indicated. Bacteria data from Bag City, Cloud Pit, Gollum and Marker 113 collected in 2007 and all data from 2009 (except Diva and Hulk1) are from Bourbonnais *et al.* (2012b). Sample names as in Table 4.1.

| Field/ sample year | Vent | Tempe-rature (°C) | Volume filtered (L) | Bacteria (copies/mL seawater) | Archaea (%) | *nirS* genes (%) |
|---|---|---|---|---|---|---|
| AV07 | Bag City | 13.2 | 3.15 | $(14.0\pm0.4) \times 10^4$ | 1.3±0.8 | 1.8±0.2 |
| AV07 | Cloud Pit | 6.8 | 3.01 | $(16.0\pm0.6) \times 10^3$ | 1.4±0.8 | 1.7±0.2 |
| AV07 | Forum | 5.7 | 2.05 | $(0.3\pm0.2) \times 10^6$ | 0.04±0.04 | 0.4±0.3 |
| AV07 | Gollum | 21.7 | 2.55 | $(2.2\pm0.2) \times 10^4$ | BDL | 3.2±0.4 |
| AV07 | Marker 113 | 31.3 | 2.62 | $(9.8\pm0.7) \times 10^5$ | 0.34±0.03 | 0.04±0.01 |
| AV07 | Shepherd | 25.0 | 3.05 | $(1.6\pm0.3) \times 10^5$ | 0.47±0.08 | 1.7±0.4 |
| AV07 | The Spot | 30.0 | 3.56 | $(4.6\pm0.3) \times 10^5$ | 0.06±0 | 0.09±0 |
| AV07 | T&S | 75.9 | 2.81 | $(1.3\pm0.3) \times 10^5$ | 0.7±0.2 | 1.2±0.4 |
| AV07 | Zen Garden1 | 23.7 | 3.40 | $(4.0\pm0.2) \times 10^3$ | 0.29±0.02 | 2.7±0.4 |
| AV07 | Zen Garden2 | 7.2 | 2.90 | $(1.2\pm0.1) \times 10^5$ | 0.10±0.01 | 0.39±0.07 |
| AV09 | Diva | 17.7 | 2.51 | $(2.2\pm0.1) \times 10^3$ | 2.0±0.4 | 1.7±0.2 |
| AV09 | Gollum | 12.7 | 3.03 | $(5.2\pm0.0) \times 10^3$ | BDL | 7.8±0.6 |
| AV09 | Hermosa | 40.4 | 2.64 | $(6.6\pm0.3) \times 10^3$ | 2.3±0.3 | 3.3±0.5 |
| AV09 | Marker 33 | 34.5 | 3.00 | $(3.2\pm0.3) \times 10^4$ | 0.13±0.01 | 0.37±0.05 |
| AV | Marker 113 | 30.1 | 3.38 | $(0.9\pm0.2) \times 10^5$ | 0.06±0.01 | 2.5±0.5 |
| CS07 | Not dead yet | 24.3 | 2.55 | $(1.6\pm0.2) \times 10^3$ | BDL | 4.9±0.8 |
| ES09 | Fairy Castle | 28.9 | 2.53 | $(0.4\pm0.1) \times 10^5$ | 0.8±0.2 | 0.17±0.05 |
| ES09 | Hulk1 | 13-130 | 45.0 | $(36.0\pm0.2) \times 10^5$ | 0.01±0 | 0.12±0.01 |
| ES09 | Hulk2 | 22.8 | 3.00 | $(1.0\pm0.4) \times 10^5$ | BDL | 0.4±0.1 |
| ES09 | Phang | 24.0 | 2.71 | $(1.1\pm0.2) \times 10^5$ | 0.5±0.1 | 1.6±0.3 |
| ES | Bkgd | 1.8 | 3.00 | (4.9±0.6) × 105 | 0.11±0.01 | BDL |

community. Indeed, using a GeoChip approach, Wang *et al.* (2009) found that the *nirK* form of nitrite reductase could be more abundant than *nirS* in chimney samples from the Main Endeavour and Mothra hydrothermal vent fields on the JFR. Sample limitation also precluded measurement of expressed *nirS* genes, which can be done by reverse transcription qPCR (e.g. see Smith *et al.*, 2007 and Chon *et al.*, 2009). However, Smith *et*

*al.* (2007) and Dong *et al.* (2009) found no correlation between *nirS* transcripts in sediments and environmental variables for most *nirS* phylotypes quantified in the Colne estuary. Environmental controls on *nirS* gene abundance (expressed or not) in estuarine and marine environments thus remain unclear and should be the focus of future research.

### 4.5. Concluding remarks

This study conducted at hydrothermal vent sites on the Juan de Fuca Ridge provides a first-time description of *nirS* biodiversity and abundance in the subsurface biosphere of mid-ocean ridge hydrothermal systems. Despite the low diversity of *nirS* genes in diffuse fluids at the sampled hydrothermal vent fields (Axial Volcano (Shepherd, ~30°C), and Endeavour Segment (Hulk1, >100°C)), we found significant differences in *nirS* community membership between the two sites. Since 16S rRNA gene bacterial communities in vent fluids sampled at the 6 studied different sites showed no vent field scale patterns, it is difficult to attribute differences in *nirS*-encoding bacterial assemblages to large-scale geographic isolation. Small-scale geographic isolation and the different physico-chemical properties of the diffuse vent fluids at the time of sampling are likely to ultimately modulate (*nirS*) denitrifying bacterial diversity, as has been also observed in other studies in marine environments (e.g. Jayakumar *et al.*, 2004; 2009; Castro-Gonzáles *et al.*, 2005; Falk *et al.*, 2007; Oakley *et al.*, 2007; Opatkiewicz *et al.* 2009; Huber *et al.*, 2010). Factors controlling *nirS* abundances remain unclear, as no significant relationships were found between *nirS* abundance and measured physico-chemical variables.

To better understand environmental controls, and spatial and temporal variations in denitrifying functional gene (*nirS*, *nirK*, *nosZ*) biodiversity and abundance, future studies will need to be broader in scope, comparing samples from many different hydrothermal vent habitats. Analogous to massive pyrosequencing of short sequences of conserved regions of the 16S rRNA genes (e.g. this study, Huber *et al.*, 2007; 2010), functional gene pyrosequencing is a promising tool that could be better exploited in the future to expand the existing functional gene database and describe microbial diversity in hydrothermal vent systems and in other environments.

# Chapter 5
# Nitrate elimination and regeneration as evidenced by dissolved inorganic nitrogen isotopes in Saanich Inlet, a seasonally anoxic fjord

## 5.1. Abstract

In this study, we used natural abundance isotope measurements of dissolved inorganic nitrogen species to evaluate the effect of different oxygenation regimes on nitrogen (N) transformation and elimination in the surface and bottom waters of Saanich Inlet, a seasonally anoxic fjord in British Columbia, Canada. We analyzed dissolved nutrient concentrations and the N (and O) isotope composition of nitrate ($NO_3^-$) and ammonium ($NH_4^+$) at different depths throughout the water column near the mouth of the inlet between November 2007 and April 2009. A gradual increase in both the $NO_3^-$ $\delta^{15}N$ and $\delta^{18}O$, associated with a decrease in $NO_3^-$ concentration and an increase in biological excess $N_2$, was observed after bottom water renewal events in September-October 2008, indicating $NO_3^-$consumption by denitrifying bacteria in an expanding suboxic zone. Closer to the hypoxic/suboxic transition, an increase in the $\delta^{15}N$ of $NH_4^+$ following the renewal event indicated net consumption (e.g. by micro-aerobic, anaerobic $NH_4^+$ oxidation, $NH_4^+$ uptake and/or anammox). Deviations from a 1:1 correlation between the $NO_3^-$ $\delta^{15}N$ and $\delta^{18}O$ ($\Delta$(15,18)), which are characteristic for both assimilatory and dissimilatory $NO_3^-$ uptake in the ocean, were observed in surface waters and close to the hypoxic/suboxic transition. Lowered $\Delta$(15, 18) values can most plausibly be explained by aerobic nitrification of newly remineralized $NH_4^+$ and/or low $\delta^{15}N$-$NO_3^-$ inputs from

atmospheric precipitation in the surface mixed layer and $NO_3^-$ regeneration through $NH_4^+$ oxidation and/or the reoxidation of nitrite ($NO_2^-$) in deeper waters. Closed and open system model-derived N isotope effects for $NO_3^-$ calculated from time-series samples collected near the sediments in anoxic bottom waters were significantly lower (as low as ~11‰) than the biological N isotope effects of ~20-30‰ for water column denitrification reported in other studies. We argue that the reduced N isotope effect is mainly due to the combined effects of water column and sediment denitrification, the latter occurring with a highly suppressed N isotope fractionation at the ecosystem level. We estimated that ~50% of the denitrification occurs within the sediments of the Inlet.

## 5.2. Introduction

Nitrogen is an essential and often limiting macronutrient for primary producers in the surface ocean. As a consequence, it is an important modulator of the marine biological pump and thus of the ocean's capacity to sequester atmospheric $CO_2$ in its interior (e.g. Falkowski, 1997). The availability of fixed (bioavailable) N in marine environments is regulated by the balance between N-sources, mainly from $N_2$ fixation and atmospheric inputs, and N loss by microbial processes. The two main N-elimination processes are denitrification, the sequential reduction of $NO_3^-$ to a gaseous product (nitrous oxide ($N_2O$) or $N_2$), and anaerobic $NH_4^+$ oxidation (anammox), the reduction of $NH_4^+$ and $NO_2^-$ to $N_2$ gas. Both processes require suboxic conditions and occur in the water-column in ocean regions with high surface primary productivity and low oxygen source waters (i.e. Oxygen Minimum Zones (OMZs) (e.g. Deutsch *et al.,* 2001; Kuypers

*et al.,* 2003; 2005; Sigman *et al.,* 2005; Lam *et al.,* 2009), as well as in productive coastal areas and semi-enclosed basins (e.g. Naqvi *et al.,* 2006; Manning *et al.,* 2010). Denitrification and anammox also occur in suboxic shelf and pelagic sediments (e.g. Christensen *et al.,* 1987; Thamdrup and Dalsgaard, 2002; Penton *et al.,* 2006).

Existing estimates on global N fluxes are afflicted with large uncertainty, and it is an ongoing debate whether the marine N budget is in or out of balance (Codispoti *et al.,* 2001; Gruber, 2004; Codispoti, 2007; Bianchi *et al.,* 2012; DeVries *et al.,* 2012). Benthic denitrification is thought to represent the largest fixed N sink in the global ocean (Brandes and Devol 2002; DeVries *et al.,* 2012), yet extrapolation from discrete flux measurements is problematic (e.g. Lehmann *et al.,* 2005) so rates derived from these are expected to have large uncertainties. Nitrate isotopes, which better integrate over space and time, have recently been used to more accurately constrain this term (e.g. Sigman *et al.,* 2003). An ongoing expansion of OMZs in the ocean has been observed over the last decades (e.g. Stramma *et al.,* 2008), with likely impacts on the absolute and relative importance of single N loss processes, both in the water column and within ocean sediments (e.g. Bianchi *et al.,* 2012). Better constraining N-input and loss terms globally, but also regionally in different oceanic environments, represents an important rationale of current research and is of paramount importance for the comprehension of the impact of global N inventory changes on other element cycles and the global climate.

Saanich Inlet, a seasonally anoxic fjord, can be used as a model system to better understand coastal eutrophication and N loss in major marine OMZs that ultimately affect global patterns of primary productivity. The fjord shows inverse estuarine circulation (i.e. dense water flows out above the sill and less dense water circulates inward at the

surface). The presence of a shallow sill at ~70 m depth prevents deep-water circulation, and thus re-supply of oxygen to the deep inlet throughout most of the year (Herlinveaux, 1962). Vertical mixing is generally low in the inlet because of weak tides and low winds. However, strong spring tidal mixing outside the inlet can reverse the surface water flow and cause horizontal advective nutrient re-supply in the photic zone, promoting periodic summer blooms (Gargett *et al.,* 2003). Following primary productivity in surface waters of Saanich Inlet, and the resulting aerobic degradation of the sinking organic matter (OM) by microbial respiration, the bottom waters regularly become suboxic (suboxia, defined here as $[O_2]$ <2-10 μmol/kg, and generally associated with denitrification and Mn reduction; Bianchi *et al.,*2012) and then anoxic ($[O_2]$ = 0 μmol/kg, generally indicative of active Fe and sulfate reduction) (Richards, 1965). Episodic renewal events, occurring during late summer/early fall (i.e. September/October), partially flush the anoxic, $NO_3^-$-depleted bottom waters with oxygenated, $NO_3^-$-rich waters from outside the basin (Anderson and Devol, 1973; Manning *et al.,* 2010). Extensive research has been conducted in Saanich Inlet over the last decades, and previous studies have reported geochemical and microbiological evidence for the occurrence of denitrification (Cohen, 1978; Tortell *et al.,* 2005; Manning *et al.,* 2010; Walsh *et al.,* 2009; Zaikova *et al.,* 2010). However, ambiguities still exist with regards to Saanich Inlet N-cycling processes and rates. The relative importance of different $NO_3^-$ consuming and regeneration processes in the water-column and the partitioning between water-column and sedimentary denitrification in the anoxic bottom waters, for example, remain to be investigated.

Stable isotope measurements represent a useful tool to study N-cycle transformations in marine environments. Both $NO_3^-$ assimilation and denitrification increase the $NO_3^-$

$\delta^{15}N$ (with $\delta=[(R_{sample}/R_{standard})-1] \times 1000$, where R represents the ratio of $^{15}N$ to $^{14}N$) as a consequence of kinetic N-isotope fractionation (Cline and Kaplan, 1975; Brandes *et al.,* 1998a; Altabet, 2001; Voss *et al.,* 2001; Lehmann *et al.,* 2003; Sigman *et al.,* 1999; 2005). A N isotope enrichment factor ($\varepsilon_{ass}$, where $\varepsilon= \delta^{15}N_{substrate} - \delta^{15}N_{product}$) of ~5‰ has been reported for $NO_3^-$ assimilation (Sigman *et al.,* 1999; Altabet, 2001). The isotope enrichment factor ($\varepsilon_{den}$) associated with microbial denitrification is high, with most recent estimates from both laboratory experiments and natural environments clustering around 25‰ (Brandes *et al.,* 1998a; Barford *et al.,* 1999; Voss *et al.,* 2001; Granger *et al.,* 2008). In contrast, the apparent $NO_3^-$ isotope effect of sedimentary denitrification, or more precisely, its expression in the ocean water column ($\varepsilon_{sed\_app}$), is significantly lower (between ~1 and 5‰) mostly because of the complete consumption of the porewater $NO_3^-$ under diffusion-limiting conditions and/or the production of low-$\delta^{15}N$ $NO_3^-$ through nitrification (Brandes and Devol, 1997; Lehmann *et al.,* 2007; Alkhatib *et al.,* 2012). While the exact controls on $\varepsilon_{sed\_app}$ are complex (Lehmann *et al.,* 2007; Alkhatib *et al.,* 2012), the relatively large difference between the N isotope effects of water-column versus sedimentary denitrification makes the use of oceanic $\delta^{15}N$-$NO_3^-$ an effective tool for gaining information on the relative importance of both processes in the global ocean (Brandes and Devol 2002) or in single ocean basins (Sigman *et al.,* 2003; Lehmann 2005).

While N isotopes alone can provide qualitative and semi-quantitative information on single N-cycle transformations, they are less informative in oceanic regions where several N-transformations have overprinting effects on both the $NO_3^-$ concentration and N isotope signatures. However, the measurement of coupled $NO_3^-$ N and O isotope ratios

has the potential to disentangle $NO_3^-$ consumption and production processes in environments where they occur simultaneously (Sigman *et al.,* 2005; Casciotti and McIlvin, 2007; Bourbonnais *et al.,* 2009; 2012a). This is possible because the $\delta^{15}N$ and $\delta^{18}O$ of $NO_3^-$ are affected in fundamentally different ways during $NO_3^-$ consumption and production, as further explained below (section 5.5.3).

Here we present nutrient concentrations and inorganic dissolved nitrogen isotope data for Saanich Inlet collected during a ~1 year time-series sampling program in 2008/9. The main goal of this study was to constrain N transformations throughout the water column. Of particular interest was to determine the N isotope effects of N elimination reactions in the anaerobic bottom waters and sediments of the inlet (denitrification and $NH_4^+$ oxidation to $N_2$), and to use dissolved inorganic nitrogen (DIN) isotope signatures to assess the relative importance of $NO_3^-$ regeneration and denitrification in the water column and within Saanich Inlet sediments. Major renewal events in September-October 2008 provided a unique opportunity to follow the development of suboxia, N loss, and the associated N isotope dynamics in bottom waters, starting from a homogenized and oxygenated water column. While understanding N transformations and N isotope dynamics in the Saanich Inlet is interesting in its own right, this study could help to improve our understanding of N loss dynamics in OMZs and intermittently anoxic marine environments. Saanich Inlet is different in several major ways from OMZs, e.g. the rates of processes are faster, the controls on water renewal are different, and it goes from oxic to suboxic and then anoxic generally every year while OMZs are typically stably suboxic. However, these two environments are affected by the same N loss processes, and more

importantly, the recurring cycle in Saanich Inlet allows us to easily study the evolution of N loss under changing redox conditions.

## 5.3. Material and methods

### 5.3.1. Study site, sampling regime and hydrographic data

All samples were collected at a station near the mouth of Saanich Inlet (48°39' N, 123°30' W, Fig. 5.1), with a maximum depth of 190 m, in November 2007 and between April 2008 and April 2009 during ten half-day cruises onboard the *MSV John Strickland*. We also sampled a station in Haro Strait (48°39' N, 123°30' W, maximum water depth of 347 m) in April 2009. Our main sampling station is close to the sill and thus strongly affected by episodic deep water renewal events, supplying oxygenated waters, which can be considered the "background" water source, prior to inlet-internal N-inventory altering processes. Samples for nutrients analysis were collected with 12-2L Niskin bottles mounted on a CTD rosette in 60 mL acid-washed and rinsed HDPE bottles and stored at -20°C. Ammonium concentration samples were analyzed immediately. Salinity, temperature, and photosynthetically active radiation (PAR) were measured using Seabird Electronics 19 CTD sensors. Oxygen concentrations were measured both using a Seabird Electronics SBE 43 sensor and by Winkler titration, as described in Manning *et al.* (2010).

### 5.3.2. Nutrient concentrations

Nitrate, $NO_2^-$, and phosphate ($PO_4^{3-}$) concentrations were analyzed using an Astoria-Pacific colorimetric nutrient autoanalyzer following methods described in Barwell-Clarke and Whitney (1996), with a precision (i.e. the standard deviation of replicate analyses) of ±0.2 µmol/L. Ammonium concentrations for all months, except April 2008, were measured using the fluorometric method by Holmes *et al.* (1999) with a precision of ±0.04 µmol/L. The indophenol blue method (Solorzano, 1969) was used in April 2008, with a precision of ~0.1 µmol/L.

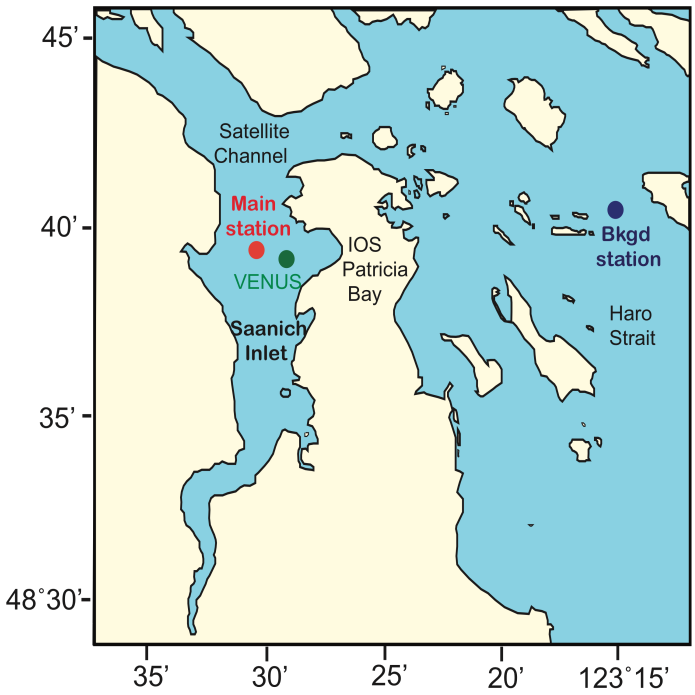


**Figure 5.1.** Map of Saanich Inlet showing the main station sampled at the mouth of the Inlet (maximum depth of ~190 m), the VENUS CTD and the background (Bkgd) station in Haro Strait. The Inlet is 24 km long, 7.2 to 0.5 km wide and has a maximum depth of 215 m (Herlinveaux, 1962).

### 5.3.3 Nitrate N and O isotopic composition

Nitrate $\delta^{15}N$ and $\delta^{18}O$ were measured using the "denitrifier method" (Sigman *et al.,* 2001; Casciotti *et al.,* 2002), which is based on the quantitative conversion of sample $NO_3^-$ to $N_2O$ by cultured denitrifying bacteria that lack the active $N_2O$-reductase enzyme. $N_2O$ gas was automatically extracted, purified and analyzed on-line using Tracegas-Isoprime and GasBench II preparation systems coupled to continuous flow mass spectrometers (Isoprime and Thermo Finnigan DELTA$^{plus}$ XP). The general target sample size was 20 nmol for samples with a $[NO_3^-] > 5$ µmol/L and 10 nmol for samples with a $[NO_3^-]$ of 1-5 µmol/L. *Pseudomonas chlororaphis* (ATCC #43928 and #13985) were used to measure the $\delta^{15}N$ and $\delta^{18}O$. N and O isotope ratios (in ‰) are reported relative to atmospheric $N_2$ for N and V-SMOW for O isotopes, respectively. Isotope values were calibrated using the following international $KNO_3^-$ reference materials: (IAEA-N3) with a reported $\delta^{15}N$ value of +4.7‰ (versus air) and a reported value of 25.6‰ (versus V-SMOW) for $\delta^{18}O$ and USGS-34, with a reported value of -1.8‰ (versus air) for $\delta^{15}N$ and -27.9‰ (versus V-SMOW) for $\delta^{18}O$ (Böhlke *et al.,* 2003). Reproducibility of the method based on replicate samples was generally better than ±0.2‰ for $\delta^{15}N$ and ±0.4‰ for $\delta^{18}O$. The O isotope scale contraction due to O isotope exchange with water (always less than 5%) was corrected for by using USGS-34 and IAEA-N3 standards as described in Casciotti *et al.* (2007). The blank contribution was generally below 0.5 nmol (i.e., 3- 5% of the target sample size).

The presence of $NO_2^-$ interferes with the isotopic analysis of $NO_3^-$ when using the denitrifier method, leading to artificially $\delta^{18}O$-depleted values for mixed samples calibrated against $NO_3^-$ isotope standards only (see Casciotti and McIlvin, 2007, Casciotti

*et al.,* 2007, Granger and Sigman, 2009). We thus removed $NO_2^-$ following the procedure by Granger and Sigman (2009) in all samples containing significant $NO_2^-$ (≥1% of the total $NO_2^- + NO_3^-$ concentration). Briefly, 100 µl of a 1% sulfamic acid solution was added to 5 mL of water sample and isotopic standards in a test tube, allowed to react for 5 minutes, and the pH was immediately adjusted to near neutral using a 1 M NaOH solution. These samples were then analyzed using the denitrifier method.

### 5.3.4 Ammonium N isotopic composition

The $\delta^{15}N$ of $NH_4^+$ was measured using the passive ammonia diffusion method (Sigman *et al.,* 1997) combined with persulfate oxidation and the denitrifier method (Houlton *et al.,* 2007) following the procedure described in Bourbonnais *et al.* (2012a), with a precision generally <0.5‰ for replicate measurements. Briefly, ~60 mL of water sample containing 60-200 nmol $NH_4^+$ standards of known isotopic composition (IAEA N1, $\delta^{15}N$ of $NH_4^+$ = 0.4‰ and IAEA N2, $\delta^{15}N$ of $NH_4^+$ = 20.3‰) or DI water (blanks) were pipetted into 100 mL glass media bottles. The dissolved $NH_4^+$ was trapped onto an acidified glass fiber disc sandwiched between two teflon membranes (i.e. $NH_3$ trap, see Sigman *et al.,* 1997; Bourbonnais *et al.,* 2012a). The $NH_3$ traps were removed from the sample bottles, the filter-trapped $NH_4^+$ (as $(NH_4)_2SO_4$) was transferred to 10 mL tubes, DI water (6.5 mL) and Persulfate Oxidizing Reagent (POR) (1 mL) were added, and the tubes were closed and autoclaved for at least one hour to oxidize the sample $NH_4^+$ to $NO_3^-$. The $NO_3^-$ concentration was analyzed as described above. Sample pH was then adjusted to 3-6 by adding 1N HCl and the samples were analyzed for $^{15}N/^{14}N$ using the

denitrifier method (as described above). Only samples with good $NH_4^+$ recovery (~80-100%) were considered. The procedural N blank coming from the POR reagent and the $NH_3$ diffusion was ~15 nmol (generally less than 20% of the sample). To account for the procedural blank and minor instrumental isotope scale compression, $\delta^{15}N$ values were calibrated using the IAEA N1 and IAEA N2 standards, which were processed the same way as the samples.

## 5.4. Results

### 5.4.1. Hydrographic data and nutrient concentrations

Measured variables changed significantly throughout the year, corresponding to seasonal fluctuations in primary productivity in surface waters and, in turn, organic flux-controlled OM respiration and the gradual development of anoxia in bottom waters. Episodic deep-water intrusion events were observed in spring 2008 (between April and May) and in fall 2008 (between September and October). As discussed in Manning *et al.* (2010), these renewal events were correlated with periods of weak tidal currents, which enabled inflowing waters from the Haro Strait to retain a sufficiently high density to displace the bottom waters. The spring 2008 renewal event was confirmed by a deepening of the hypoxic/suboxic transition, at ~ 10μmol/kg [$O_2$], from ~120 m to ~160 m (Fig. 2). Although the deep-water ventilation reached down to 160 m water depth in this spring event, complete oxygenation of the water column down to the bottom (at ~190m) did not occur (see Manning *et al.*, 2010; Grundle and Juniper, 2011). In contrast,

the fall renewal events (3 in total, see Manning *et al.,* 2010) led to the complete re-oxygenation of the bottom waters, displacing ~50% of the deep-water volume at our sampling site during September and October 2008 (Manning *et al.* (2010) (Fig. 5.2). Also in 2007, by November, the bottom waters were already oxygenated, suggesting fall ventilation (data not shown). After the September-October 2008 renewal events, the bottom waters returned to suboxic conditions by December 2008, and the hypoxic/suboxic transition remained above ~120 m depth until April 2009.

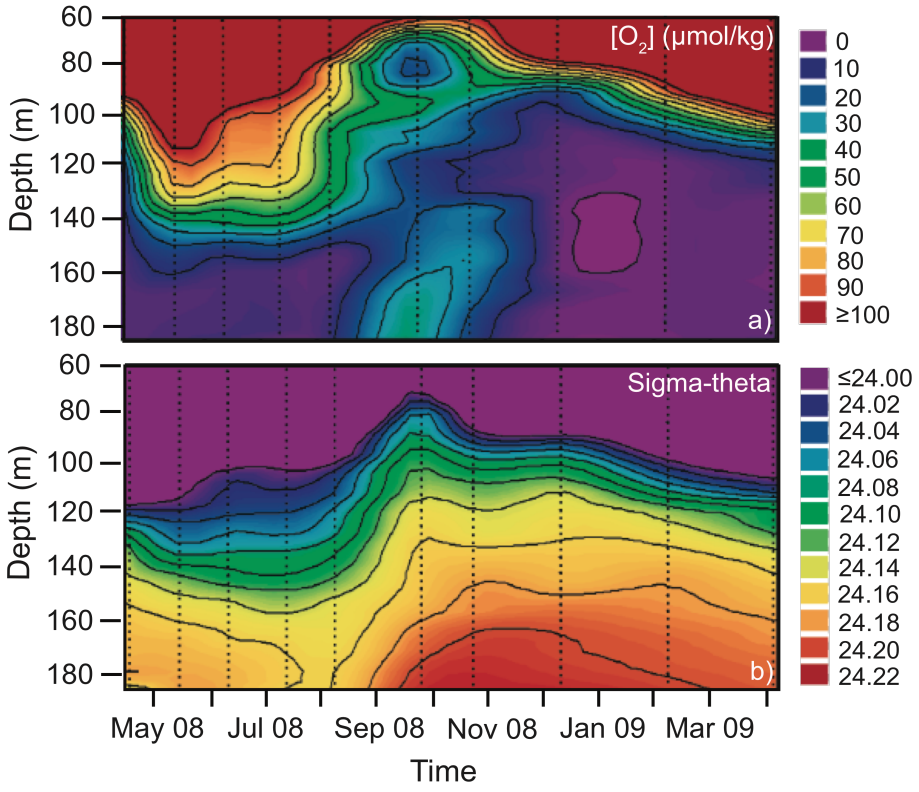


**Figure 5.2.** Seasonal variations in bottom water [$O_2$] (µmol/kg), **a**), and sigma-theta (kg/m$^3$), **b**), at the main sampled station (Fig. 5.1) in Saanich Inlet and after a series of major renewal events in September-October 2008. Dotted lines indicate actual sampling dates. Sill depth is 70 m. Modified from Manning *et al.* (2010). The black contour lines represent the concentrations labeled in the legend.

Nitrate in surface waters was depleted to below the detection limit during spring and summer, because of $NO_3^-$ assimilation by phytoplankton. During late summer, fall and early winter, $NO_3^-$ concentrations were ~14-18 µmol/L in the first 5 m (except in February 2008, when [$NO_3^-$] was ~4 µmol/L), because of reduced primary productivity (Timothy and Soon, 2001). Decreasing concentrations were always observed above the hypoxic/suboxic transition, which varied between ~105 m (December 2008) and 165 m (May 2008) depth, indicating the diffusive flux of $NO_3^-$ towards the suboxic zone and the consumption of $NO_3^-$ by denitrification, except following renewal events where the whole waters column was oxygenated (Fig. 5.3a, b; the two panels presenting data before and after renewal events, respectively). Nitrite, which can be produced both by nitrification in oxic waters and denitrification under anoxic conditions (Ward, 1982; Anderson and Levine, 1986), never accumulated by more than ~0.6 µmol/L, except in April 2008 and 2009, when concentrations up to 1.4 µmol/L were measured between ~115 and 165 m depth, and October 2008, when concentrations of up to 1 µmol/L were measured in surface waters (0-10 m depth). A primary $NO_2^-$ maxima was sometimes observed at ~10 m depth and below and seemed to correspond to times with the highest fluorescence measurements in the photic zone (up to 68 mg Chl a/$m^3$ at 4 m depth), indicating links between high algal cell densities, enhanced organic material (OM) remineralization, and nitrification of newly remineralized $NH_4^+$ in the subsurface. A secondary $NO_2^-$ maxima was observed near the hypoxic/suboxic transition, suggesting enhanced $NO_2^-$ accumulation by (incomplete) denitrification during OM degradation in bottom waters (Fig. 5.3, c, d). Elevated [$NO_2^-$] (0.6 – 1.2 µmol/L) were also observed in Saanich Inlet in October 2008 by Grundle and Juniper (2011) at ~0-30 m depth, corresponding to

enhanced $NH_4^+$ and $NO_2^-$ oxidation rates in and just below the euphotic zone. Ammonium concentrations generally > ~3 μmol/L were measured near or below the pycnocline (~2 to 70 m depth), and below the hypoxic/suboxic transition during the most productive spring and summer months (e.g. see Timothy and Soon, 2001 for primary productivity measurements), indicating accumulation of $NH_4^+$ during aerobic and anaerobic OM remineralization, respectively (Fig. 5.3, e, f). In surface waters, $PO_4^{3-}$ was generally depleted, but not bio-limiting, especially during the productive spring and summer months. [$PO_4^{3-}$] increased to ~2-3 μmol/L at or below the pycnocline and continued to increase to 5-6 μmol/L at or below the hypoxic/suboxic transition (Fig. 5.3, g, h).

### 5.4.2. DIN isotopes

The N isotopic composition of $NH_4^+$ that accumulated below the euphotic zone in the upper water column was highly variable, without consistent trend and with values from ~0‰ (April 2009) to 7‰ (May 2008) (Fig. 5.4). In general, the $\delta^{15}N$ of $NH_4^+$ in the anaerobic water column (where measurable) were significantly higher than that within the pycnocline. Two major trends were observed in the anaerobic deep waters, suggesting N isotope fractionation during $NH_4^+$ consumption: the $\delta^{15}N$ of the $NH_4^+$ tended to increase with time from ~8‰ in April 2008 to ~12‰ in August 2008 at 185 m, and from the near bottom waters toward the suboxic/hypoxic transition, with decreasing $NH_4^+$ concentrations (from ~12‰ to ~16‰ in August 2008). Interestingly, $NH_4^+$ $\delta^{15}N$ values in April 2008 and 2009 were similar (less than 0.4‰ difference), suggesting recurring patterns that underlie a seasonal cycle.

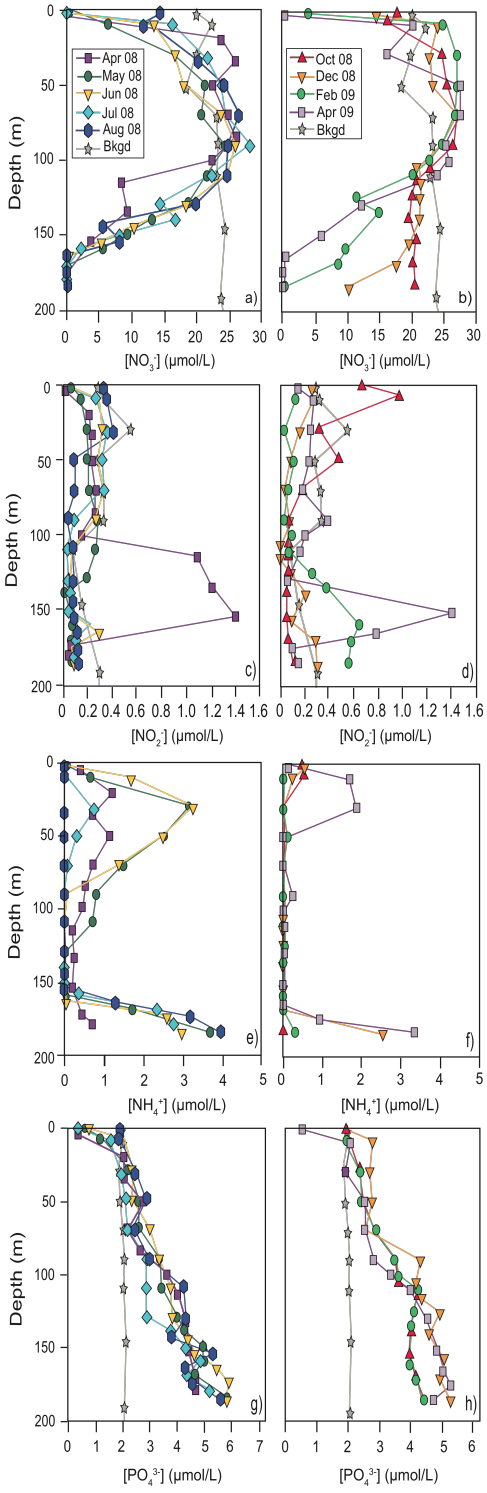


**Figure 5.3.** Depth profiles of $NO_3^-$ (**a, b**), $NO_2^-$ (**c, d**), $NH_4^+$ (**e, f**) and $PO_4^{3-}$ (**g, h**) concentrations at the main sampled station (Fig. 5.1) in Saanich Inlet from April 2008 to August 2008 before (left plots) and after (right plots) a series of major renewal events in September-October 2008.

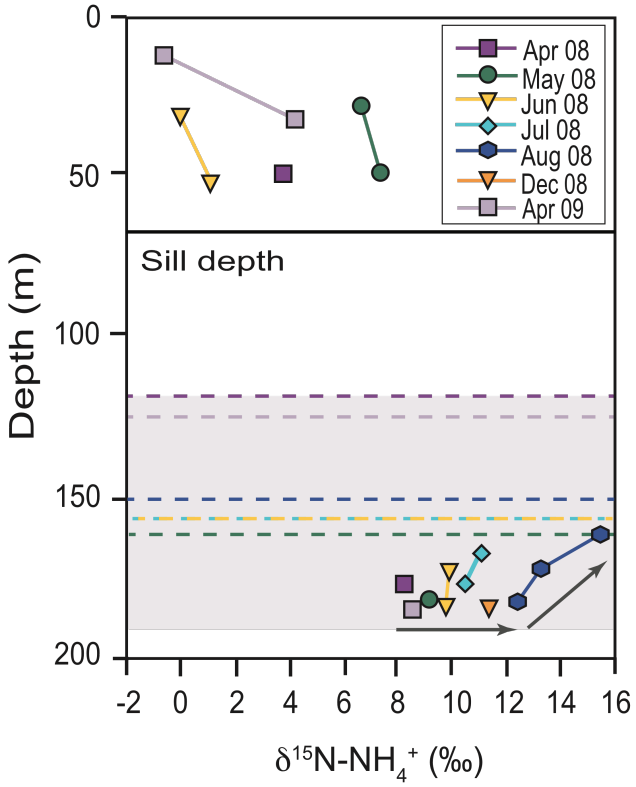


**Figure 5.4.** $\delta^{15}N\text{-}NH_4^+$ versus depth (m) below the euphotic zone (pycnocline) and in anoxic bottom waters. Dashed coloured lines (and grey shaded area) indicate the approximate depth of the hypoxic/suboxic transition ($[O_2] < 10$ μmol/kg) for every month $\delta^{15}N\text{-}NH_4^+$ was measured in bottom waters, whereas the solid black line indicates sill depth (~75 m depth). Black arrows indicate an increase in the $\delta^{15}N\text{-}NH_4^+$ over time and closer to the hypoxic/suboxic transition (the later associated with a decrease in $[NH_4^+]$, see Fig. 5.3) in bottom waters before a series of major renewal events in September-October 2008.

During the productive period, $NO_3^-$ $\delta^{15}N$ and $\delta^{18}O$ slightly increased in the euphotic zone (first 10 m) with decreasing $NO_3^-$ concentrations. Between ~20 m to 100 m water depth, the $NO_3^-$ isotopic composition was essentially invariant (between ~7-8‰ and ~2‰ for $\delta^{15}N$ and $\delta^{18}O$, respectively) and very close to depth-averaged values of 7.3‰ and 1.8‰ observed at the background station in Haro Strait. Additionally, the $\delta^{15}N$ of $NO_3^-$ at these depths were similar to the average $\delta^{15}$ of $N_2$ excess of 7.5‰ measured by Manning *et al.* (2010) in bottom waters (~130-185 m depth) of the Inlet during the spring and

summer of 2008 when $NO_3^-$ was completely consumed, confirming that the $N_2$ produced was similar to the original isotopic composition of the fixed N pool. With time after the renewal events, and towards the hypoxic/suboxic transition, the $NO_3^-$ $\delta^{15}N$ and $\delta^{18}O$ increased with decreasing concentrations. Maximum values of 28‰ and 24‰, respectively, were measured at 150 m in April 2008 (Fig. 5.5).

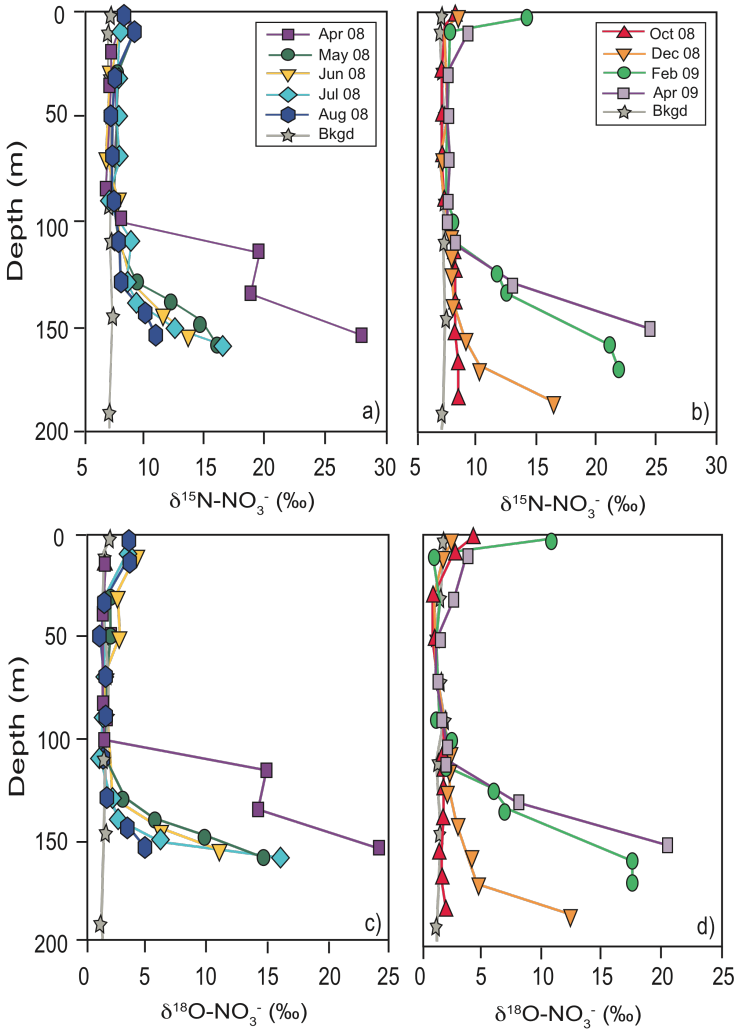


**Figure 5.5.** Depth profiles of $\delta^{15}N$ and $\delta^{18}O$ of $NO_3^-$ (in ‰ relative to atmospheric $N_2$ for N and V-SMOW for O) before (**a, c**) and after (**b, d**) a series of renewal events in September-October 2008.

## 5.5. Discussion

In the subsequent sections, we first compare nutrient-based data on the DIN deficit ($DIN_{def}$) in the bottom waters to $N_2$ excess data by Manning *et al.* (2010). We will discuss possible causes of the observed discrepancy, providing a first insight into suboxic $N_2$ production and N-deficit generation in the Saanich Inlet. We then provide putative evidence for microaerobic or anaerobic $NH_4^+$ oxidation below the hypoxic/suboxic transition and make estimates on the N isotope effect of the $NH_4^+$ consumption. Discussing observed $NO_3^-$ N-vs.-O isotope anomalies, (i.e. the deviation from a $\delta^{15}N$-$\delta^{18}O$ relationship expected for sole assimilation or denitrification in marine environments) we aim to assess the importance of $NO_3^-$ regeneration in the photic zone and in deeper portions of the inlet near the hypoxic/suboxic transition both of which are net $NO_3^-$ consuming zones within the Saanich Inlet water column. Finally, we estimate the community N isotope effect related to N loss in bottom waters using closed and open system models, and we use the observed community isotope fractionation to gain constraints on the partitioning of sedimentary versus water-column denitrification after bottom-water renewal events.

### 5.5.1. Geochemical constraints on the N deficit in Saanich Inlet

Below, we compare the $DIN_{def}$ and $N_2$ excess (from Manning *et al.,* 2010) in the bottom waters of Saanich Inlet. $DIN_{def}$ is calculated from the fixed N concentration normalized to the $PO_4^{3-}$ concentrations (assuming a constant N:P stoichiometry during photosynthesis and OM remineralization) (e.g. Gruber and Sarmiento, 1997; Codispoti *et*

*al.,* 2001; Devol *et al.,* 2006). $N_2$ excess, the concentration of $N_2$ generated locally from denitrification/anammox, is calculated from $N_2$/Ar measurements (Codispoti *et al.,* 2001; Devol *et al.,* 2006; Manning *et al.,* 2010).

We calculated the $DIN_{def}$ according to the following equation:

$$DIN_{def} = DIN_{exp} - DIN_{obs} \quad (5.1)$$

where $DIN_{exp}$ is the [DIN] that is expected in the absence of N loss processes and $DIN_{obs}$ is the [DIN] measured. We approximated $DIN_{exp}$ using measured $PO_4^{3-}$ concentrations and assuming a robust relationship between [DIN] and [$PO_4^{3-}$] in waters that have not undergone fixed N loss by denitrification or anammox, i.e. samples from the surface (0-20 m) in Saanich Inlet and from the background station in Haro Strait:

$$DIN_{exp} = 14.4(PO_4^{3-}{}_{obs} - 0.53) \quad (5.2)$$

as shown in Fig. 5.6. The factor 14.4 represents the average N/P ratio during OM uptake and remineralization in Saanich Inlet, which is similar to the ratio of 14.9 derived by Devol *et al.* (2006) in the Arabian Sea. This ratio is lower than the standard Redfield ratio of 16. Source waters from the North Pacific Ocean (Haro Strait) flowing into the Inlet have already been affected by N loss processes occurring in the water-column or sediments outside the Inlet, which perturbs the absolute N:P ratio of any specific water sample. By comparing water samples within the surface layer, away from active denitrification, the 14.4 (eq. 2) slope should represent only nutrient uptake and remineralization within the inlet.

The $N_2$ excess is calculated based on the deviation between the measured and equilibrium $N_2$/Ar ratios. By normalizing to the noble gas Ar, whose concentration is affected by physical processes but not biological processes, we remove some of the

effects of physical processes that would cause both $N_2$ and Ar to deviate from equilibrium concentrations. Additionally, since $N_2$ and Ar have somewhat different physical properties, we corrected for non-local effects on $N_2$/Ar ratios by measuring the average $N_2$/Ar ratios at Haro Strait, outside the inlet (Manning *et al.,* 2010). We calculated the $N_2$ excess as:

$$[N_2]_{excess} = ((\Delta N_2/Ar)_{meas} - (\Delta N_2/Ar)_{bkg}) \times [N_2]_{eq} \quad (5.3)$$

$$\Delta N_2/Ar = [(N_2/Ar)_{meas} / (N_2/Ar)_{eq}] - 1 \quad (5.4)$$

In the first equation, $(\Delta N_2/Ar)_{meas}$ and $(\Delta N_2/Ar)_{bkg}$ are the measured Saanich Inlet and background values and $[N_2]_{eq}$ is the equilibrium concentration of $N_2$. In the second equation, $(N_2/Ar)_{meas}$ is the sample $N_2$/Ar ratio and $(N_2/Ar)_{eq}$ is the equilibrium ratio for the potential temperature and salinity of the sample depth (Hamme and Emerson, 2004). In anoxic zones well below the photic layer, $N_2$ excess can solely be attributed to N loss by denitrification and/or anammox.

We compared the DIN deficit calculated from nutrient data to the $N_2$ excess calculated from $N_2$/Ar data (Fig. 5.6). In contrast to previous research reporting $N_2$ excess that was about equal (Chang *et al.,* 2010) or twice (Devol *et al.,* 2006) the $DIN_{def}$, $DIN_{def}$ was up to 1.8 times the $N_2$ excess in this study (Fig. 5.7). This discrepancy is best explained by the release of iron and manganese oxyhydroxide-bound $PO_4^{3-}$ during the reduction and dissolution of the adsorbents under anoxic conditions. Such redox-sensitive desorption reactions have been found to affect phosphorus dynamics in other marine environments, e.g. the Santa Barbara Basin and the Baltic Sea (Shiller *et al.,* 1985; Reed *et al.,* 2011). Preferential remineralization of organic phosphorus (relative to nitrogen) has also been observed in suboxic sediments (Ingall and Jahnke, 1994). The observed increase in $PO_4^{3-}$

concentrations above (>75 m depth, from mixing with deeper waters) and below the hypoxic/suboxic transition, provide further indication for excess $PO_4^{3-}$ release in the anaerobic waters and within sediments (Fig. 5.3, g, h).

To account for the effect of preferential $PO_4^{3-}$ remineralization and desorption of $PO_4^{3-}$ from iron or manganese oxides, we used the fixed N deficit based on $N_2$ excess only (Fig. 5.7, c, d) in the following discussion.

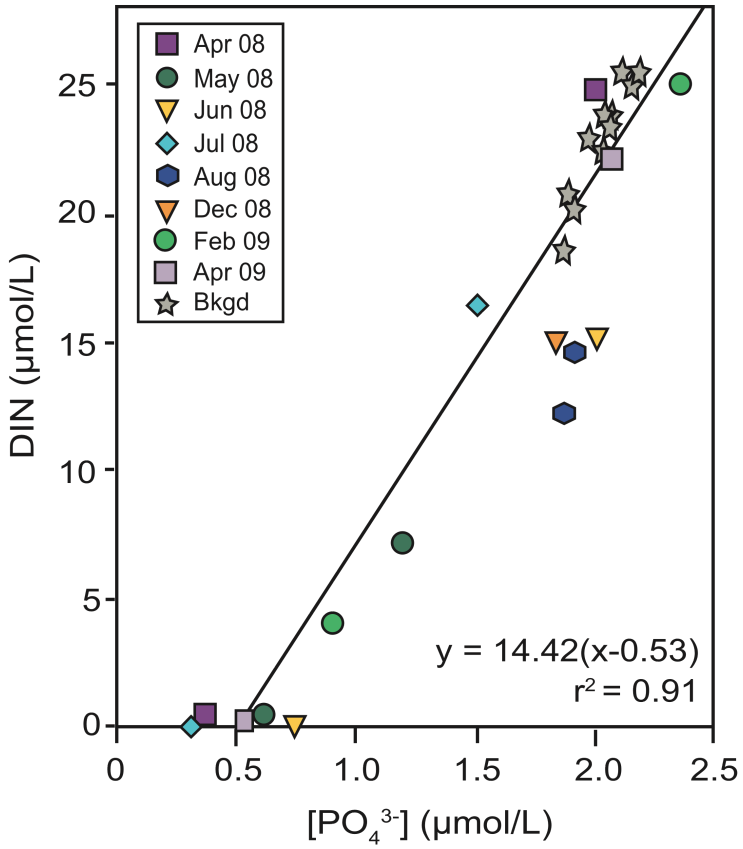


**Figure 5.6.** Relation between [DIN] and $[PO_4^{3-}]$ for surface waters unaffected by anoxic processes at the sampled station in Saanich Inlet (≤20 m depth) and outside the Inlet at the background station in Haro Strait.

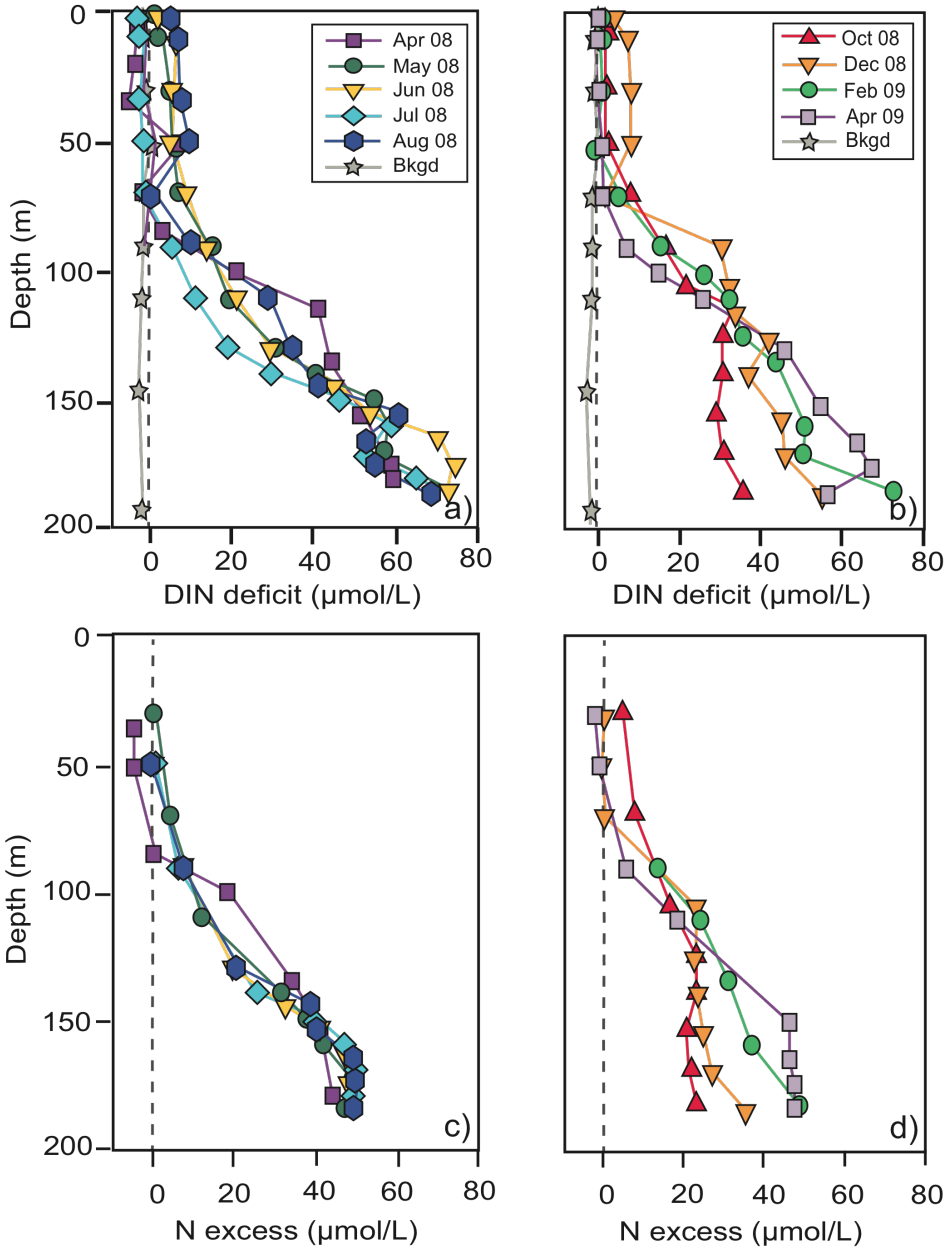


**Figure 5.7.** $DIN_{def}$ (**a, b**) calculated from nutrient concentrations (see text for more detail) and biological N excess (for direct comparison with $DIN_{def}$) (**c, d**) from $N_2$/Ar measurements, adapted from Manning *et al.* (2010) at the sampled station in Saanich Inlet before (**a, c**) and after (**b, d**) a series of major renewal events in September-October 2008. N excess at the background station has been subtracted from the N excess at the main sampled station to obtain the biological N excess produced within the Inlet. Surface (0-25 m depth) N excess data (not shown) could not be constrained because of local physically-induced differential heating effects on Ar and $N_2$ (see Manning *et al.,* 2010). DIN and N excesses of 0 are indicated by vertical dashed grey lines.

### 5.5.2. The N isotopic signature of ammonium in the Saanich Inlet water column

The increase in $\delta^{15}N\text{-}NH_4^+$ with depth (Fig. 5.4) in surface waters is consistent with previous studies in marine environments. Zooplankton excrete $^{15}N$-depleted $NH_4^+$ in the shallow waters, leading to a 3 to 4‰ enrichment in $^{15}N$ for a heterotrophic organism relative to its food source (e.g. Minagawa and Wada, 1984; Checkley and Miller, 1989). Upon death of the organisms, the $^{15}N$-enriched sinking OM is remineralized deeper in the water column, leading to the observed N isotope partitioning in the $NH_4^+$ pool. The temporal changes in $\delta^{15}N$ of $NH_4^+$ over time may reflect, to some extent, variations in the degree of $NO_3^-$ utilization in the euphotic zone and changes in community composition, with the OM N isotopic signal being ultimately transferred to the $NH_4^+$ pool by OM remineralization. Indeed, Nakatsuka *et al.* (1992) reported changes in the $\delta^{15}N$ of particulate OM during the progression of a nutrient-controlled phytoplankton bloom in Saanich Inlet, with high $NO_3^-$ concentrations and low $\delta^{15}N$ at the beginning of the bloom and low $NO_3^-$ and high $\delta^{15}N$ following near complete $NO_3^-$ depletion. No such clear temporal trend was observed in this study, because blooms in Saanich Inlet follow a fortnightly cycle based on tidal cycles and monthly sampling cannot capture these variations (Gargett *et al.,* 2003). Furthermore, fluctuations in the relative partitioning between $NH_4^+$ assimilation and nitrification (and the N isotope branching associated with the two processes, e.g. see Wankel *et al.,* 2007), is likely to overprint any trend that may be associated with $\delta^{15}N$ changes in the N source at a given depth.

Ammonium concentrations in the bottom waters increased with depth (Fig. 5.3, g, h), while $\delta^{15}N\text{-}NH_4^+$ increased over time and from the bottom toward the hypoxic/suboxic transition (i.e. in August 2008). Velinsky *et al.* (1991) also observed a decrease in $NH_4^+$

concentrations associated with $\delta^{15}N\text{-}NH_4^+$ enrichments toward the $O_2/H_2S$ transition in Saanich Inlet in August 1989 (from 10‰ at 175 m depth to up to 16‰ at 140 m depth, which was also the maximum value measured in this study in August 2008).

Two main processes can produce $NH_4^+$: OM remineralization and dissimilative nitrate reduction to ammonium (DNRA). Anoxic OM remineralization coupled to heterotrophic denitrification (or anaerobic degradation processes by organotrophic bacteria using other electron acceptors in the absence of $NO_3^-$: e.g. $MnO_2$) can produce $NH_4^+$ from the organic N. $NH_4^+$ can also be produced by DNRA, since extensive bacterial mats of *Beggiatoa* spp., a chemoautotrophic bacteria known to couple DNRA with sulfur oxidation, have been observed on sediments at the bottom of Saanich Inlet (Juniper and Brinkhurst, 1986). While Velinsky *et al.* (1991) speculated that the $\delta^{15}N\text{-}NH_4^+$ in bottom waters may be influenced by the decomposition of suspended particulate nitrogen (PN), mostly because $\delta^{15}N$-PN showed similar values and also decreased with depth, the observed decreasing $NH_4^+$ concentrations from the bottom toward the hypoxic/suboxic interface as well as relatively low to no $NH_4^+$ accumulation in bottom waters during some months (e.g. February 2009), clearly indicated $NH_4^+$ consumption.

Several $NH_4^+$ consuming processes, discussed below, have been proposed to occur in OMZs sediments or the water-column: 1. $NH_4^+$ oxidation to $NO_2^-$/ $NO_3^-$ by microaerobic $NH_4^+$ oxidizing bacteria or anaerobic $NH_4^+$ oxidizing bacteria (coupled to manganese oxide reduction), 2. $NH_4^+$ uptake by bacteria, and 3. anaerobic $NH_4^+$ oxidation to dinitrogen gas coupled to $NO_2^-$ reduction (anammox) or manganese oxide reduction. The latter process (i.e. $NH_4^+$ oxidation to $N_2$ gas coupled to manganese oxide reduction) has never been documented in marine environments; Kuypers *et al.,* 2006).

$NH_4^+$ consumption by microaerobic $NH_4^+$ oxidation to $NO_3^-$ (i.e. nitrification) is a plausible process to explain the highest values of $\delta^{15}N\text{-}NH_4^+$ occurring just below the hypoxic/suboxic transition, given that the <1μM $NH_4^+$ depth generally follows the hypoxic/suboxic interface (at least before the bottom-water renewal event in September/October 2008) and that the $NH_4^+$ depletion and $\delta^{15}N$ systematically increased toward this interface. Recent studies have measured significant $NH_4^+$ oxidation rates under low to undetectable oxygen concentrations, suggesting that at least some aerobic nitrifying bacteria are tolerant to microaerobic/suboxic oxygen concentrations (Lam *et al.,* 2007; Füssel *et al.,* 2012). In this study, the limit of detection for our dissolved [$O_2$] CTD sensor was ~5 μmol/kg, such that the anoxic transition could not clearly be discerned. Velinski *et al.* (1991) also suggested that nitrification, enhanced by periodic flushing and shorter residence times of the anoxic bottom waters in Saanich Inlet, might explain the high $\delta^{15}N\text{-}NH_4^+$ observed in August 1989 because of the high isotope effect associated with this process (+14 ‰ to +38‰; Mariotti *et al.,* 1981; Yoshida, 1988; Casciotti *et al.,* 2003). Microbially-mediated anaerobic $NO_3^-$ or $NO_2^-$ production during $NH_4^+$ or $NO_2^-$ oxidation coupled to manganese reduction is also a plausible process that has been documented in marine sediments (Hulth *et al.,* 1999; Javanaud *et al.,* 2011). However, $NO_3^-$ regeneration associated with microaerobic or anaerobic nitrification should cause a deviation from the expected 1:1 trend between $\delta^{15}N$ and $\delta^{18}O$ observed in marine environments, as further explained in section 5.5.3.1.2. While atypical dual $NO_3^-$ isotope signatures were generally observed below the hypoxic/suboxic transition, no such anomalies were present in the bottom waters in August 2008, where the highest $\delta^{15}N\text{-}NH_4^+$ values were measured below the hypoxic/suboxic transition.

Alternative processes, i.e. $NH_4^+$ uptake and anammox, could explain the increase in $\delta^{15}N\text{-}NH_4^+$ without potentially causing such $NO_3^-$ isotope anomalies. Biosynthetic $NH_4^+$ uptake has been proposed as the dominant $NH_4^+$ consuming process below the $O_2/H_2S$ interface in the Black Sea and Framvaren Fjord, Norway, based on $NH_4^+$ isotopic fractionation, and most likely also occurs in Saanich Inlet (Velinsky *et al.,* 1991). Additionally, while it is difficult to discriminate for this process purely from our $[NH_4^+]$ and $\delta^{15}N\text{-}NH_4^+$ profiles, anammox cannot be excluded as recent rate measurements indicated that this process is seasonally significant in Saanich Inlet (Alyse Hawley, personal communication). Anammox is inhibited by $O_2$ (e.g. see Kalvelage *et al.,* 2011), but could occur just below the hypoxic/suboxic transition, where a $NO_2^-$ peak is generally observed. Further geochemical (rates measurements) and microbiological evidence is needed to better discriminate between the different processes that ultimately lead to the observed decline in $NH_4^+$ and increase in $\delta^{15}N\text{-}NH_4^+$ between the bottom of the SI and hypoxic/suboxic transition.

### 5.5.3. Processes affecting nitrate N and O isotopic composition

The dual (N and O) isotopic composition of $NO_3^-$ has been used to disentangle N consumption and production processes in diverse marine environments, such as $NO_3^-$ assimilation or denitrification and $N_2$ fixation (Sigman *et al.,* 2005; Knapp *et al.,* 2008; Bourbonnais *et al.,* 2009; 2012a). During $NO_3^-$ consumption in the ocean (i.e. assimilatory or dissimilatory $NO_3^-$ reduction), the $NO_3^-$ $\delta^{15}N$ and $\delta^{18}O$ have been shown to increase in parallel, with a constant ratio of ~1:1 for both processes (Casciotti *et al.,*

2002; Sigman *et al.,* 2003; Granger *et al.,* 2004; 2008). In contrast to $NO_3^-$ reduction, $NO_3^-$ production affects the $NO_3^-$ $\delta^{15}N$ and $\delta^{18}O$ in fundamentally different ways (Sigman *et al.,* 2005). The $\delta^{15}N$ of nitrified $NO_3^-$ is dependent on the $\delta^{15}N$ of the precursor molecule ($NH_4^+$ or $NO_2^-$), whereas most of the O atoms derive from the ambient water (with a $\delta^{18}O$ of ~0‰) (Casciotti, 2002; Sigman *et al.,* 2009). The $\delta^{18}O$ of newly produced $NO_3^-$ was recently estimated to be less than the mean $\delta^{18}O$-of deep-sea waters $NO_3^-$ of ~1.4‰ (Sigman *et al.,* 2009) as a result of significant O isotopic fractionation associated with O incorporation during $NH_4^+$ and $NO_2^-$ oxidation (Casciotti *et al.,* 2010; Buchwald and Casciotti., 2010). As a consequence, gross $NO_3^-$ generation (from the remineralization/nitrification of OM from $N_2$ fixing or $NO_3^-$ assimilating phytoplankton) results in a decoupling of N versus O isotope gradients, and should be indicated by anomalous dual $NO_3^-$ isotope signatures (Sigman *et al.,* 2005; Casciotti and McIIvin, 2007; Knapp *et al.,* 2008; Bourbonnais *et al.,* 2009; 2012a).

We calculated $NO_3^-$ isotope anomalies , i.e. the deviation from a 1:1 relationship expected during nitrate assimilation or denitrification, using the following equation from Sigman *et al.* (2005):

$$\Delta(15,18) = (\delta^{15}N-\delta^{15}N_m) - [(^{18}\varepsilon/^{15}\varepsilon)\ (\delta^{18}O -\delta^{18}O_m)] \quad (5.5)$$

where $\delta^{15}N_m$ =7.3‰ and $\delta^{18}O_m$ =1.8‰ are the mean $\delta^{15}N$ and $\delta^{18}O$ values of the source waters observed at the background station in Haro Strait, and $^{18}\varepsilon/^{15}\varepsilon$ is the ratio of N versus O isotope enrichment of 1:1 observed during pure $NO_3^-$ assimilation (Granger *et al.,* 2004; Lehmann *et al.,* 2005) and denitrification (Granger *et al.,* 2008).

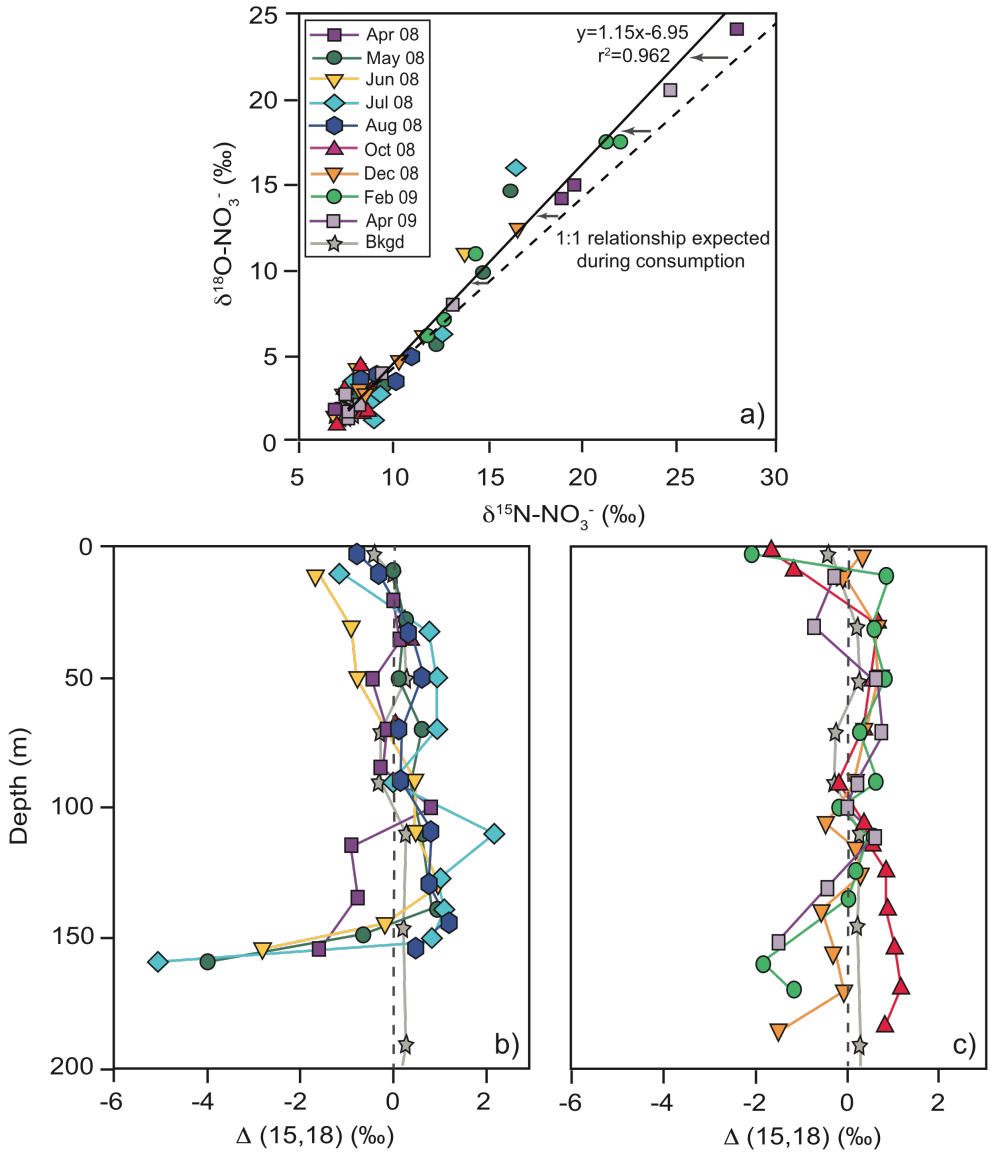


**Figure 5.8.** Relationship between $\delta^{15}N$ (versus air) and $\delta^{18}O$ (versus V-SMOW) of $NO_3^-$ (**a**) and depth profiles of Δ(15,18) measuring the deviation from the 1:1 relationship between $\delta^{18}O$ and $\delta^{15}N$ observed during assimilatory or dissimilatory $NO_3^-$ reduction in marine environments before (**b**) and after (**c**) a series of major renewal events in September-October 2008. Equation from the linear regression is indicated in a). The expected 1:1 relationship during $NO_3^-$ assimilation or denitrification is indicated by the dotted dark grey lines. Arrows in a) indicate slight deviations from a pure 1:1 relationship.

We observed modest negative $NO_3^-$ isotope anomalies, i.e., a higher increases in $\delta^{18}O$ relative to $\delta^{15}N$, (0 to -2‰) in surface waters. Even lower Δ(15,18) values (up to -5‰)

were observed in bottom waters of the Inlet, especially before the fall renewal events (except in August 2008; Fig. 5.8). Below, we discuss potential processes that could explain the observed anomalous $NO_3^-$ isotope signatures.

#### 5.5.3.1. Causes of the nitrate isotope anomalies

Below, we describe the N processes that could have generated the observed values of Δ(15,18) in surface (section 5.5.3.1.1) and bottom waters (section 5.5.3.1.2). We then use a simple box-model to evaluate the contribution from the most plausible processes (section 5.5.3.1.3).

##### 5.5.3.1.1. Surface waters

Several processes can be invoked to explain the observed negative $NO_3^-$ isotope anomalies observed during nitrate assimilation in surface waters (Fig. 5.8), including nitrification, low-$\delta^{15}N$ input from atmospheric precipitation and $N_2$ fixation. $N_2$ fixation adds a $\delta^{15}N$ of about -2‰ to 0‰, with only little fractionation (Carpenter *et al.,* 1997). Following complete OM ammonification and nitrification, this low $\delta^{15}N$ is transferred to the $NO_3^-$ pool, generating $NO_3^-$ isotope anomalies in oceanic surface waters (Sigman *et al.,* 2005; Knapp *et al.,* 2008; Bourbonnais *et al.,* 2009). However, *Trichodemsium* spp. and other unicellular cyanobacterial diazotrophs only proliferate in relatively warm (>20$^o$C) marine surface waters (e.g. Moisander *et al.,* 2010). Furthermore, while planktonic heterocystous planktonic diazotrophs are common in freshwater and low-

salinity (<12 ppt) estuaries and coastal seas (Sellner, 1997), they are not significant in saline estuaries, possibly because of their slow growth rates and intense grazing (Marino *et al.,* 2006). In this study, the maximum temperature in surface waters was always <15ºC and salinity typically more than 27 ppt. Additionally, Gargett *et al.* (2003) proposed that N limitation in surface waters usually lasts less than 2 weeks because of periodic horizontal advective nutrient re-supply, so that the environmental motivation for $N_2$ fixation is constantly erased. We thus conclude that $N_2$ fixation in the euphotic zone of Saanich Inlet was not likely to have caused negative $NO_3^-$ isotope anomalies.

Atmospheric N input from precipitation can significantly contribute to a low $\delta^{15}N$ in $NO_3^-$ in the surface ocean waters, e.g. the Sargasso Sea (Knapp *et al.,* 2010), and the Eastern Mediterranean Sea (Emeis *et al.,* 2010). Knapp *et al.* (2010) observed that the $\delta^{15}N$ of total nitrogen, i.e. reduced nitrogen ($NH_4^+$ + organic N) and $NO_3^-$, in Bermuda rain was significantly lower during the cool season (up to -5‰ lower than during the warm season), suggesting that more negative Δ(15,18) could be generated during winter. Generally high $\delta^{18}O$ values in atmospheric $NO_3^-$ (up to 77‰, Hasting *et al.,* 2003) could further amplify negative $NO_3^-$ isotope anomalies. In this study, increased rainfall during late fall and winter could explain why the highest anomalies were observed very close to the surface only (first 10 m) (Fig. 5.8). Fixed N input from precipitation have been found to be minor compared to other N sources in the surface waters (e.g. nutrient re-supply from below) (Prospero *et al.,* 1996; Knapp *et al.,* 2010).

The most likely explanation for the observed $NO_3^-$ isotope anomalies is nitrification in the euphotic zone, where $NO_3^-$ assimilation concurrently takes place. For a long time, it was assumed that nitrification was inhibited by light (Eppley and Peterson, 1979), but

recent studies have revealed the occurrence of nitrification within the euphotic zone (e.g. Yool *et al.,* 2007). Nitrification generally adds a lower $\delta^{15}N$ to the nitrate pool compared to the $\delta^{18}O$, because of the relatively large isotope effect associated with this process (+14 ‰ to +38‰; Mariotti *et al.,* 1981 and reference therein) compared to the smaller isotopic fractionation associated with O incorporation (mostly from water; see Casciotti *et al.,* 2010; Buchwald and Casciotti., 2010). In cases where $NO_2^-$, an obligate intermediate during nitrification, also accumulates, we expect the $\Delta(15,18)$ to be less negative because of the unusual inverse isotope fractionation reported during $NO_2^-$ oxidation, i.e. the product $NO_3^-$ is enriched in $^{15}N$ with a $^{15}\varepsilon$=-12.8‰ (Casciotti, 2009). Indeed, both $NH_4^+$ and $NO_2^-$ oxidation have been measured in and below the euphotic zone in Saanich Inlet, with rates up to 0.3 and 0.5 μmol N $L^{-1}$ $d^{-1}$, respectively, in October 2008 (Grundle and Juniper, 2011), the higher $NO_2^-$ oxidation rates being attributed to fortnightly spring-tide nutrient renewal. Additionally, as described in Wankel *et al.* (2007), if we assume a larger $^{15}N$ isotope effect for $NH_4^+$ oxidation compared to $NH_4^+$ assimilation, the N isotope branching between these two processes could further enhance the magnitude of the $NO_3^-$ isotope anomalies.

#### 5.5.3.1.2. Bottom waters:

As already mentioned in section 5.5.2.2, partial $NH_4^+$ or $NO_2^-$ oxidation by microaerophilic archaea and bacteria (see Lam *et al.,* 2007 and Füssel *et al.,* 2012) or anaerobic bacteria (coupled to Mn reduction) (Hulth *et al.,* 1999; Javanaud *et al.,* 2011), could be a source of low $\delta^{15}N$-$NO_3^-$, and thus cause negative $NO_3^-$ isotope anomalies

(Fig. 5.8). As mentioned above (section 5.5.3.1.1) and shown in our model below, partial $NO_2^-$ oxidation would overall decrease the magnitude of the $NO_3^-$ isotope anomalies. Nitrate reduction coupled to complete $NO_2^-$ re-oxidation near the hypoxic/suboxic interface has also been proposed to explain pronounced $NO_3^-$ isotope anomalies in the ocean (Sigman *et al.,* 2005; Casciotti and McIlvin, 2007; Bourbonnais *et al.,* 2012a). Briefly, during $NO_3^-$ reduction, $^{16}O$ is preferentially lost and following $NO_2^-$ re-oxidation, an O atom, coming mostly from water, with a higher $\delta^{18}O$ value than that of the $NO_3^-$ originally lost, is added to newly produced $NO_3^-$. In contrast, the $\delta^{15}N$ of $NO_3^-$ is not affected by a complete cycle of $NO_3^-$ reduction/ $NO_2^-$ re-oxidation.

#### 5.5.3.1.3. Evaluating the contribution from different N regeneration processes

To get a rough idea about the contributions of the different N processes (i.e. $NO_3^-$ input from precipitation and $NO_3^-$ regeneration from nitrification and the $NO_3^-$/ $NO_2^-$ redox cycle) described above, we adapted the simple qualitative box model described in Bourbonnais *et al.* (2012a) (and originally adapted from Sigman *et al.,* 2005 and Bourbonnais *et al.,* 2009). Briefly, we assumed isotope effects of 5‰ during $NO_3^-$ assimilation (Altabet, 2001), 26‰ during $NH_4^+$ oxidation (Mariotti *et al.,* 1981 and references therein), -12.8‰ during $NO_2^-$ oxidation (Casciotti, 2009) and 25‰ (Brandes *et al.,* 1998a and references therein) as well as 3‰ (Brandes and Devol 1997; Lehmann *et al.,* 2007; Alkhatib *et al.,* 2012) during water-column and sedimentary denitrification, respectively. We assumed an initial $NO_3^-$ isotopic composition of 7.5‰ for $\delta^{15}N$ and 2‰ for $\delta^{18}O$, i.e. the average values observed between the euphotic zone and the

hypoxic/suboxic transition during this study, resupplied by advective exchange driven by fortnightly spring tides in surface waters and vertical exchange in deeper waters. We assumed that $NO_3^-$ with a $\delta^{18}O$ of -3.8‰ (average value in Casciotti *et al.,* 2010; Bushwald and Casciotti., 2010) and 0‰ (as in Sigman *et al.,* 2005) is produced during $NH_4^+$ and $NO_2^-$ oxidation, respectively. Finally, we assumed that ¼ of the O atoms in $NO_2^-$ would equilibrate with water (with $\varepsilon_{eq}$-$NO_2^-$ = +14‰, Casciotti *et al.,* 2007) before being oxidized, so that no positive Δ(15,18) would be generated.

In surface waters, we calculated the anomalies generated for different ratios of $NH_4^+$ oxidation and $NO_2^-$ re-oxidation (scenario 1a) and N inputs from precipitation (scenario 2a) relative to $NO_3^-$ assimilation (Fig. 5.9e). For scenario 1a, we assumed that 50% of the $NH_4^+$ produced from OM remineralization (with an average $\delta^{15}N$-$NH_4^+$ of 3‰, as observed in surface waters) was consumed by $NH_4^+$ oxidation and that 75% of the produced $NO_2^-$ was nitrified, the remaining $NH_4^+$ and $NO_2^-$ pools either accumulating in surface waters (as observed during some months in our profiles, Fig. 5.3, c to f) or being completely assimilated by phytoplankton. We calculated the $\delta^{15}N$ of newly nitrified $NO_3^-$ ($\delta^{15}N_{product}$) from the following equation (Mariotti *et al.,* 1981):

$$\delta^{15}N_{product} = \delta^{15}N\text{-}NH_4^+{}_{initial} + \varepsilon_{nit} \{\ln(f)\} \times \{f/(1-f)\} \quad (5.6)$$

where $\delta^{15}N$-$NH_4^+$ is the initial composition of $NH_4^+$, $\varepsilon_{nit}$ is the isotope effect associated with $NH_4^+$ oxidation and f is the fraction of the remaining reactant. Given the current uncertainties regarding isotope effects associated with $NH_4^+$ assimilation by phytoplankton and nitrification, we neglected the N isotope branching between $NH_4^+$ consumption in our model. However, if we assume a higher isotope effect during nitrification compared to $NH_4^+$ consumption, as explained in Wankel *et al.* (2007), we

should expect even lower Δ(15,18) values. In scenario 2a, we assumed an average f-ratio (i.e. the fraction of total primary production fueled by $NO_3^-$) of 0.5, as calculated in Grundle and Juniper (2011) for the Saanich Inlet. We also assumed a $\delta^{15}N$ of -2‰ for total nitrogen (Knapp *et al.,* 2010) and a $\delta^{18}O$-$NO_3^-$ of 35‰ in atmospheric $NO_3^-$, implying that half of the total nitrogen is $NO_3^-$ (with a $\delta^{18}O$ of 70‰, resulting from the interactions of precursor NOx with ozone, which as a high $^{18}O/^{16}O$ ratio (Hastings *et al.,* 2003), the other half being reduced nitrogen (e.g. $NH_4^+$ and organic N) that is subsequently nitrified in oxic waters, adding a $\delta^{18}O$ of 0‰.

Based on our simulation, negative Δ(15,18) values of up to ~-2‰ (as observed in this study) were obtained when the fraction of nitrification (i.e. $NH_4^+$ and $NO_2^-$ oxidation) relative to net $NO_3^-$ assimilation (i.e. new production) was ~20%, which is close to the maximum value of 15% estimated in the study by Grundle and Juniper (2011) in Saanich Inlet (Fig. 5.9a, c, e). Relative to euphotic-zone nitrification, N input from precipitation generated more negative Δ(15,18) values, and a relatively small (<10%) atmospheric N input relative to net $NO_3^-$ assimilation was sufficient to produce the observed lowest Δ(15,18) of -2‰. Interestingly, the high $\delta^{18}O$-$NO_3^-$ value and the large negative anomaly in the top 10 m in February 2009 could only be reconstructed in our model by invoking atmospheric N (see Figs. 5d and 9c, e). Therefore, while, to date, only the occurrence of nitrification has been confirmed in and below the euphotic zone (Grundle and Juniper, 2011), our model suggests that N input from precipitation must play an important role in generating negative $NO_3^-$ isotope anomalies in Saanich Inlet surface waters, at least seasonally and especially during winter.

In bottom waters, we assumed that 50% of the total denitrification is occurring in the sediments (see section 5.5.4). For scenario 1b, we assumed an initial $\delta^{15}N\text{-}NH_4^+$ (from OM remineralization) of 6‰ based on the value for $\delta^{15}N$ of OM measured in Saanich Inlet sediments (70m and 100m water depth, unpublished data). This assumption is reasonable since the $\delta^{15}N$ of remineralized porewater $NH_4^+$ have been shown to be similar to the $\delta^{15}N$ of sediment OM, at least in the Santa Barbara Basin (Sweeney and Kaplan, 1980). We also assumed that 50% of the $NH_4^+$ was re-oxidized. The $NO_3^-$ isotopes and Δ(15,18) values generated for different ratios of partial $NH_4^+$ oxidation (scenario 1b) and complete or partial $NO_2^-$ -reoxidation (i.e. $NO_3^-$/ $NO_2^-$ redox cycle, scenarios 2b and 3b) relative to denitrification are shown in Fig. 5.9b, d, f.

As found in previous studies in marine environments (Sigman *et al.,* 2005; Bourbonnais *et al.,* 2012a), nitrification ($NH_4^+$ oxidation to $NO_3^-$) (scenario 1b) as well as a complete cycle of $NO_3^-$ reduction followed by $NO_2^-$ re-oxidation (scenario 2b) yielded the most negative Δ(15,18), producing values as low as ~-6‰. Anomalies generated under the assumption that 50% of the original $NO_3^-$ supplied from below was denitrified and only 50% of the $NO_2^-$ produced by denitrification was re-oxidized (scenario 3b) were significantly lower (i.e. the Δ(15,18) was up to ~3‰ less negative). Recently, Manning *et al.* (2010) estimated (based on $N_2$/Ar measurements of samples collected at the same time and site as those presented here) that up to 86 ±20 nmol N $kg^{-1}$ $d^{-1}$ is lost in anoxic bottom waters by suboxic $N_2$ production during the summer. In our model, the fractions of partial nitrification (scenario 2a) and complete $NO_2^-$ re-oxidation (scenario 2b) relative to denitrification necessary to generate the lowest Δ(15,18) of -5.5‰ observed in July 2008 were close to 0.4 and 1.2, respectively (Fig. 5.9f). Therefore, $NH_4^+$ oxidation rates

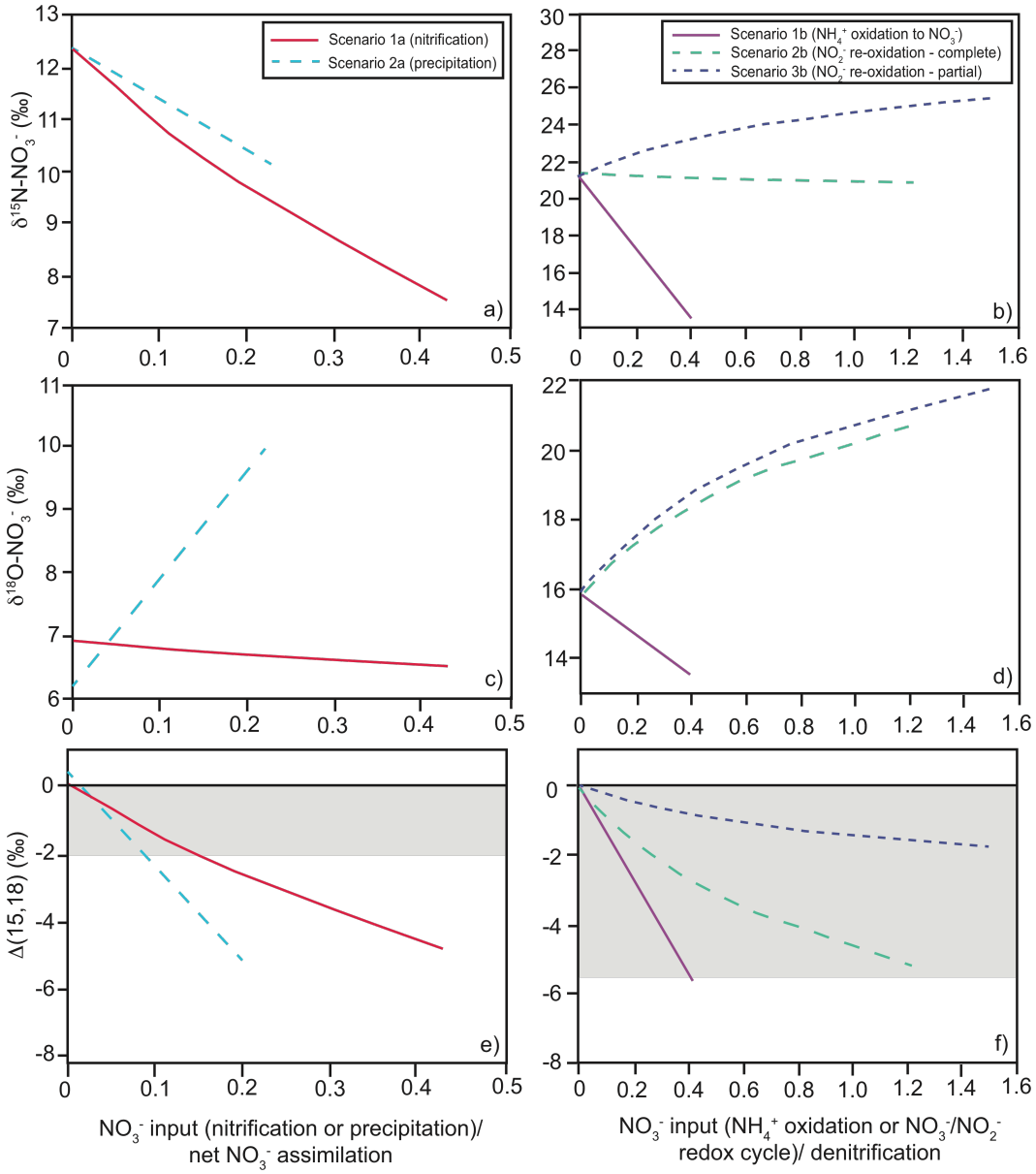


**Figure 5.9.** Results from simple box-model simulations evaluating the capacity of different $NO_3^-$ production processes to generate $\delta^{15}N$ and $\delta^{18}O$ of $NO_3^-$ and negative $\Delta(15,18)$ in Saanich Inlet surface (**a, c, e**) and bottom (**b, d, e**) waters (adapted from Bourbonnais *et al.,* 2009; 2012a). The ranges of $\Delta(15,18)$ (**e, f**) observed in Saanich Inlet during our study are indicated by the grey shaded area. In **b, d**, and **e**, denitrification includes anammox. The lines only indicate $\Delta(15,18)$ generated from plausible modeled $\delta^{15}N$ and $\delta^{18}O$ of $NO_3^-$ values, as observed in surface and bottom waters of the Inlet in this study. See text (section 5.5.3.1.3) for more detail.

(to $NO_3^-$) and $NO_2^-$ re-oxidation rates (complete $NO_3^-$/ $NO_2^-$ redox cycle) could be up to ~35 nmol N $kg^{-1}$ $d^{-1}$ and ~100 nmol N $kg^{-1}$ $d^{-1}$, respectively, under our model assumptions. Yet unfortunately our dual isotope model/measurement comparison still leaves ambiguities with respect to the actual $NO_3^-$ regeneration process. Resolving these uncertainties would require $NO_3^-$ isotope measurements to be coupled with direct rate measurements of $NO_3^-$ regeneration processes.

### 5.5.4. Constraints on water-column versus sedimentary denitrification in bottom waters

The global partition of oceanic water-column versus sedimentary denitrification is still poorly constrained, with estimates varying between ~50% (Altabet, 2007) to ~80% Gruber (2004). We constrained the partitioning of water-column and sedimentary denitrification in Saanich Inlet (as in Sigman *et al.,* 2003). We first calculated the net community N isotope effect for net $NO_3^-$ consumption with ongoing $NO_3^-$ loss after the bottom water renewal event during fall. We first considered a Rayleigh closed system model (Mariotti *et al.,* 1981), using samples from the deepest isopycnals, close to the sediments. The model assumes the gradual consumption of $NO_3^-$ in the deep water $NO_3^-$ reservoir, with no exchange with overlying waters after the renewal:

$$\delta^{15}N_{final} = \delta^{15}N_{initial}\,(f = 1) - \varepsilon \times \ln[f] \qquad (5.7)$$

where f is the fraction of $NO_3^-$ remaining, $\delta^{15}$N-initial is the isotopic composition of $NO_3^-$ when f=1 (i.e. set at the time of the renewal event, in September/October 2008), $\delta^{15}$N final is the final isotopic composition of $NO_3^-$ following consumption and $\varepsilon$ is the N isotope effect for denitrification. Second, we used an open, steady-state model, where

$NO_3^-$ is continuously consumed and re-supplied from an infinite reservoir of $NO_3^-$ (i.e. the $[NO_3^-]$ at any time point equal is equal to the initial $[NO_3^-]$) with an N isotopic composition equivalent to $\delta^{15}N_{initial}$ (Barford *et al.,* 1999):

$$\delta^{15}N_{final} = \delta^{15}N_{initial}\,(f = 1) + \varepsilon \times [1 - f] \qquad (5.8)$$

These models represent extreme scenarios, and other "less extreme" mixing regimes (e.g. Rayleigh consumption followed by incomplete mixing, partially resetting the initial conditions, and violating the closed-system aspect) are likely to occur, yielding N isotope effects that should lie between the closed- and open-system derived values for ε (see Sigman *et al.,* 2003). We calculated $\varepsilon_{app}$ values of 11.4‰ and 15.9‰ for a closed and an open system, respectively (for the isopycnals corresponding to 170-185 m depth). The $\varepsilon_{app}$ calculated for shallower isopycnals (140-170 m depth) were significantly higher, i.e. 14.4‰ to 23.6‰, and closer to the ε expected for water-column denitrification of 20-30‰, indicating less contribution from sedimentary denitrification at shallower depths (Fig. 5.10), which is expected based on the basin geometry and the low mixing rates in the inlet (Gargett *et al.,* 2003). To estimate the possible bias by $NO_3^-$ regeneration processes (see section 5.5.3.1), we assumed that the negative Δ(15,18) values were produced solely by processes lowering the $\delta^{15}N$ of $NO_3^-$ (e.g. $NH_4^+$ or $NO_2^-$ oxidation), since the $\varepsilon_{app}$ were calculated using $\delta^{15}N\text{-}NO_3^-$ values. By adding the Δ(15,18) to the $\delta^{15}N$ of $NO_3^-$ values, we calculated that the isotopes effects would always be more elevated and would change by ~+2‰ considering the relatively small $NO_3^-$ isotope anomalies observed during and following the fall 2008 renewal events. This error is low compared to combined analytical errors of ~1‰ for Δ(15,18) and likely an over-estimate. Indeed, as

mentioned in section 5.5.3.1.2, a complete cycle of $NO_3^-$ reduction/ $NO_2^-$ re-oxidation, if this process is significant, should not affect the $\delta^{15}N$ of $NO_3^-$.

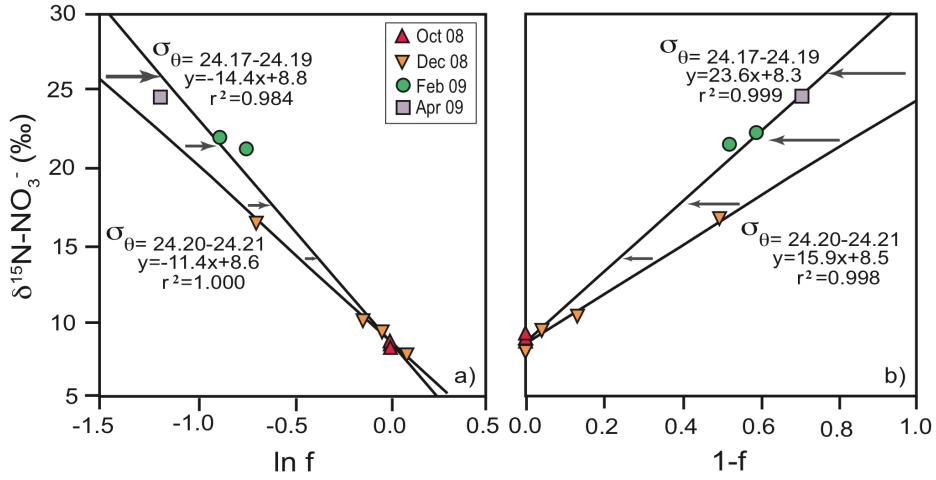


**Figure 5.10.** $\delta^{15}N$-$NO_3^-$ (relative to air) versus ln f (**a**, Rayleigh, closed system model) and versus 1-f (**b**, steady-state, open system model) along different isopycnals after a series of major renewal events in September-October 2008. f is the fraction of $NO_3^-$ remaining. Estimated N isotope effects are represented by the absolute values of the slopes. $\sigma_\theta$ values of 24.20-24.21 kg/m$^3$ and 24.17-24.19 kg/m$^3$ represent depths of 170-185 m and 140-170 m, respectively. Arrows indicate an increase in isotope effects at lower depths (associated with decreasing $\sigma_\theta$ values).

Community N isotope effect estimates based on samples above 125 m were strongly affected by dilution through lateral exchange with waters from outside the inlet between 50 to 125 m depths during winter months (data not shown). These intruding waters were not dense enough to displace bottom waters (Manning *et al.,* 2010). The almost complete $NO_3^-$ consumption near the hypoxic/suboxic transition makes these waters particularly susceptible to a suppressed denitrification N isotope effect due to low-$\delta^{15}N$ $NO_3^-$ resupply by the advection of $NO_3^-$ replete waters. During mixing of two water parcels, where one has undergone near-complete denitrification and, as a consequence, has a low [$NO_3^-$] and

high $\delta^{15}N\text{-}NO_3^-$, and the other one has a high-$[NO_3^-]$ and a low $\delta^{15}N\text{-}NO_3^-$, the resulting mixed water displays $\delta^{15}N$ that is constrained by the $NO_3^-$ replete water mass. Therefore, barely any net $^{15}N$ enrichment will be observed, even though $[NO_3\text{-}]$ will be depleted (e.g. Sigman *et al.,* 1999; Thunell *et al.,* 2004). Thunnel *et al.* (2004), for example, observed a relatively small degree of $^{15}N$ enrichment (corresponding to a $\varepsilon = 1.5‰$) for the degree of $NO_3^-$ consumption near the hypoxic/suboxic transition in the Cariaco Basin, Venezuela. The authors invoked the interaction of $NO_3^-$ consumption and resupply to explain the low apparent $NO_3^-$ N isotope effect. A similar concept (although less pronounced) likely applies to the steep Saanich Inlet redox transition zone: only a fraction of the intrinsic N isotope fractionation of denitrification is apparent in the water column $NO_3^-$ pool. Indeed, the calculated apparent N isotope effect for these depths ($\sigma_t$ = 24.14-24.16 kg/m$^3$, between 115 and 135 m depth) after the renewal events in September-October 2008 ranged between ~8‰ and 11‰ for closed and open systems (data not shown), respectively.

To quantify the partitioning of water-column versus sedimentary denitrification, we assumed average apparent N isotope effects during water-column and sedimentary denitrification of 20-30‰ (Brandes *et al.,* 1998a and references therein) and 0 to 5‰ (Brandes and Devol, 1997 and references therein), respectively. Analogous to the approach by Sigman *et al.* (2003), using the observed community N isotope effects for the isopycnals corresponding to 170-180 m depth ($\sigma_\theta$ = 24.20-24.21) and the above-mentioned endmember N isotope effects, we calculated that between 38±17% (open system model) and 59±13% (closed system model) is denitrified in the sediments of the Inlet, following major bottom-water renewal events.

The fraction of sedimentary denitrification in Saanich Inlet is lower than estimates for the Santa Barbara Basin (more than 75% sediment denitrification) reported by Sigman *et al.* (2003). The Saanich Inlet and the Santa Barbara Basin are in many aspects akin (redox, renewal events, semi-enclosed character). While our results imply variations in the partitioning between water-column versus sedimentary denitrification in these similar environments possibly due to sill depth or basin geometry differences, the differences observed may also be due to the slightly different methods used for isotope effect calculations. Indeed, our study had more temporal resolution as we calculated the isotope effect for the deepest isopycnals close to the sediments over time, whereas Sigman *et al.* (2003) approximated this isotope effect directly from isotope depth profiles collected during 3 sampling campaigns in 1995 and 1999. More importantly, as mentioned before, the renewal event in Saanich Inlet allowed us to follow denitrification from a known starting point, eliminating assumptions with respect to initial conditions as in Sigman *et al.* (2003).

## 5.6. Summary and concluding remarks

In this study, we used DIN isotope measurements to constrain N loss processes in Saanich Inlet. The N isotopic composition of $NH_4^+$ in subsurface waters displayed significant temporal variability, with no clear trends. The $\delta^{15}N$ of $NH_4^+$ in bottom waters increased 1) over time and 2) with decreasing depth toward the hypoxic/suboxic transition, indicating isotopic fractionation during consumption of $NH_4^+$ by nitrification under micro-aerobic or anaerobic conditions, or other processes, i.e. $NH_4^+$ uptake and

anammox (as discussed in section 5.5.2). The N isotope effect determined for community $NH_4^+$ consumption (ε = ~3‰) in August 2008 was relatively low, suggesting the co-occurrence of $NH_4^+$ consumption and production processes. Additionally, the calculated isotope effect may have been affected by bacterial $NH_4^+$ uptake.

N-to-O negative $NO_3^-$ isotope anomalies were observed in surface waters (~-2‰) and in anoxic bottom waters (up to ~-5.5‰) confirming the occurrence of N regeneration and/or external $NO_3^-$ input (in the case of the surface $NO_3^-$ pool). The processes that best explain these anomalies in surface waters are partial nitrification and an input of low $\delta^{15}N$ (and high $\delta^{18}O$ $NO_3^-$) from precipitation. In the bottom waters, Δ(15,18) anomalies were explained by partial nitrification and the $NO_3^-$/ $NO_2^-$ redox cycling in bottom waters.

Apparent N isotope effects associated with net denitrification for bottom-water isopycnals following renewal events in September-October 2008 were low (~11-14‰), compared to the isotope effect of ~25‰ expected for pure $NO_3^-$ consumption by water-column denitrification. We argue that the reduced isotope effect observed in the deepest portion of the inlet is caused by the contribution from sedimentary denitrification, occurring with a highly reduced isotope effect of <3‰. Using the intermediate community N isotope effect for net $NO_3^-$ reduction, we calculated that sedimentary denitrification could account for ~50% of the total denitrification in Saanich Inlet.

While this study provides a first look into inorganic nitrogen isotopes dynamic in Saanich Inlet under changing redox conditions, several aspects require further investigations. First, direct rates of both N removal (denitrification and anammox) and regeneration (aerobic, micro-aerobic or anaerobic $NH_4^+$ oxidation) processes as well as $NH_4^+$ uptake rates near the hypoxic/suboxic transition should be seasonally measured in

the Inlet to calibrate our isotope signatures for more quantitative purpose. Second, measurements of the isotope effect during sedimentary denitrification under different conditions (e.g. taking OM reactivity of the sediments into account), should be directly performed in Saanich Inlet in order to improve our estimates of the global partitioning of water-column and sedimentary denitrification. Finally, as global denitrification is expected to increase with expanding OMZs (e.g. Bianchi *et al.,* 2012), evaluation of the global ocean N budget will require closer investigations of spatial and temporal evolutions in the partitioning of these two processes. As renewal events occurring during late summer/early fall in Saanich Inlet provide the unique opportunity to directly observe the development of an expanding suboxic zone over time, future research in the Inlet could thus help us to better understand temporal changes in sedimentary versus water-column denitrification in other suboxic and anoxic marine environments.

# Chapter 6
# General summary and future outlook

In the first part of this dissertation, we reported, for the first time, measurements of nitrate $\delta^{15}N$ and $\delta^{18}O$ and ammonium $\delta^{15}N$, potential denitrification, anammox and DNRA rates and description of denitrifying bacteria biodiversity and abundance (from 16S rRNA and *nirS* genes clone libraries) in diffuse hydrothermal vent fluids of the Juan de Fuca ridge.

In chapter 2, we presented nitrate $\delta^{15}N$ and $\delta^{18}O$ and ammonium $\delta^{15}N$ data. Highest $\delta^{15}N$ for $NH_4^+$ were observed at Axial Volcano in high-T fluids (6.7‰), indicating deep-sea water nitrate (6.4‰) as the initial source of N for ammonium in the subsurface. The $\delta^{15}N$ of ammonium in high-T fluids was significantly lower at both the Endeavour (3.7‰) and Cobb Segments (4.1‰), indicating a less enriched (in $^{15}N$), potentially sedimentary source of N for ammonium at these sites. In low-temperature fluids, DIN concentration changes were mostly explained by advective mixing, but we observed DIN isotopic evidence for biological N transformations at some low-temperature vent sites. Lowered $NH_4^+$ community N isotope effects (<3‰) for net $NH_4^+$ consumption suggested an important contribution from ammonium regeneration. The low apparent nitrate N and O isotope effects (<9‰) suggest that fixed N uptake by bacteria or denitrification in subsurface microbial mats/biofilms, which impart a highly suppressed isotope effect because of substrate diffusion limitation or nitrification, are important nitrate consuming processes in low-temperature fluids. We observed variable nitrate isotope anomalies, i.e. deviations from the $^{15}N$:$^{18}O$ isotopic enrichment of 1:1 in the ocean, in diffuse HV fluids

indicating spatial and temporal variability of nitrate regeneration either by nitrite reoxidation, partial nitrification of hydrothermal ammonium and/or $N_2$ fixation and the remineralization/nitrification of the newly fixed N. Using a simple isotopic box model, we demonstrated that all three processes can produce negative Δ(15,18) at levels that were observed at the Endeavour Segment, but only a combination of processes (e.g., nitrite re-oxidation and partial $NH_4^+$ oxidation) can generate the most negative Δ(15,18) values (~8‰), as observed at Axial Volcano. Overall, our DIN isotope data provided qualitative evidence that net loss of N from hydrothermal fluids can be attributed to microbial processes in diffuse fluids, highlighting the role of subsurface microbial communities in modulating hydrothermal geochemical fluxes to the deep ocean.

In Chapter 3, we presented $^{15}N$ paired isotope rate measurements (denitrification, anammox and DNRA) at 13 different sites at Axial Volcano and Endeavour Segment and clearly showed that denitrification (up to ~1000 nmol N $l^{-1}$ $day^{-1}$, Hermosa, AV) was the dominant N-loss process in the subsurface biosphere of hydrothermal systems, with important spatial and temporal variability. In comparison, anammox rates were always below 5 nmol N $l^{-1}$ $day^{-1}$ and the abundance of anammox bacteria were undetectable by qPCR. Cloning and sequencing of the 16S rRNA genes revealed the dominance of ε- and γ- proteobacteria in hydrothermal vent fluids with the potential to oxidize sulfide or hydrogen, using nitrate as terminal electron acceptor. Our qPCR results indicated that a single γ-proteobacteria, related to the sulfur-oxidizing, nitrate-reducing SUP05 bacteria, contributed up to 38 % of the total bacterial population, suggesting an important role for chemolithoautotrophic denitrification in hydrothermal vent fluids. We found that DIN availability may ultimately regulate N loss (denitrification and anammox rates) in the

subsurface biosphere of hydrothermal vents. Combining potential rates from this study with published data on hydrothermal vent fluid residence times in the subsurface and annual seawater fluxes, we estimated that, up to ~10 Tg N $yr^{-1}$ could be removed by denitrification in the subsurface of the world's hydrothermal systems, representing a minor portion of the global marine N loss (up to 450 Tg N $yr^{-1}$, Codispoti, 2007).

In chapter 4, we presented nitrite reductase (*nirS*) and 16S rRNA (from pyrosequencing of the variable V1-V3 region) gene biodiversity and abundance data in diffuse vent fluids of the Juan de Fuca Ridge. While bacterial communities (from 16S rRNA gene clone libraries) were highly diverse, *nirS* biodiversity was low at the two sampled sites at Axial Volcano (Shepherd), and Endeavour Segment (Hulk1), with Shannon diversity indices of <1.4. The *nirS* gene community memberships were significantly different between the two sites. Operational Taxonomic Units (OTU) from the two environments significantly clustered into different groups in a phylogenetic tree and only one OTU (out of a total of 20), 99% similar at the amino acid level to the γ-proteobacteria *Pseudomonas sp.* isolate BA2.5 from estuarine sediments, was shared. We proposed that small-scale geographic isolation or the different physico-chemical properties of the diffuse vent fluids at the time of sampling ultimately modulate (*nirS*) denitrifying populations. *nirS* gene abundance varied from ~0 to 8% (relative to bacterial 16S rRNA gene abundance). The factors controlling *nirS* abundances are still unclear, as no significant relationship was found between *nirS* abundance and measured physico-chemical variables.

While the results presented in the first part of the dissertation have provided a first look at N transformations and elimination in hydrothermal vents of the Juan de Fuca Ridge, our understanding of environmental controls on N-transformations in hydrothermal fluids

is still very limited. More studies are required to document spatial and temporal variations in DIN isotopic composition, N-loss (and DNRA) rates and denitrifying functional genes (i.e. *napA*, *narG*, *nirS*, *nirK*, *norB*, *nosZ*) biodiversity and abundance, and to understand their environmental controls in different hydrothermal vent habitats around the world. More specifically, high-resolution time-series measurements should be performed to resolve the strong variability of these systems over short time scales, and better understand environmental controls on N transformations. An improved understanding of the physical characteristics of the subsurface biosphere of hydrothermal vent systems (e.g. residence time, volume of the subsurface biosphere) is also necessary to refine estimates of global N loss in these systems.

In chapter 5, we used DIN isotopes to constraint N loss processes in Saanich Inlet during approximately one year period. A series of bottom-water renewal events in the fall provided the unique opportunity to follow the progression of anoxia and denitrification in the bottom waters of the Inlet from a known starting point. We observed notable increases in $[PO_4^{3-}]$ and $DIN_{def}$ (that were ~2 times higher than biological $N_2$ loss from $N_2$/Ar data calculated by Manning *et al*. (2010)). These occurred below the hypoxic/suboxic interface and were likely caused by dissolution of phosphate bound iron and manganese oxyhydroxides and preferential phosphate remineralization under anoxic conditions. Increases in the $\delta^{15}N$ of ammonium over time and toward the hypoxic/suboxic interface indicated that microaerobic or anaerobic ammonium oxidation to nitrite/nitrate or $N_2$ (e.g. anammox) could be significant processes in the bottom waters of the Inlet. We observed modest N-to-O negative nitrate isotope anomalies (less than 2‰) in surface waters and larger anomalies in anoxic bottom waters (up to ~5.5‰),

confirming the occurrence of N regeneration processes (i.e. partial ammonium and/or nitrite oxidation and an input of low $\delta^{15}N$ (and high $\delta^{18}O$ nitrate) from precipitation in surface waters and partial nitrification (microaerobic or coupled to manganese reduction) and the nitrate/nitrite redox cycling in bottom waters). We derived apparent isotope effects associated with denitrification along the deepest isopycnals near the sediment following the fall renewal events using both closed Rayleigh and open-system models, of as low as ~11‰ (closed system) and ~16‰ (open system). We argue that these reduced isotope effects are caused by sedimentary denitrification, which has a highly reduced isotope effect of <3‰, compared to water-column denitrification (Brandes and Devol, 1997; Lehmann *et al.*, 2004; 2007; Alkhatib *et al*., 2012). We calculated that sedimentary denitrification could account from ~50% of the total denitrification in Saanich Inlet.

Future research in Saanich Inlet should further examine nitrate regeneration processes that might produces the observed negative nitrate isotope anomalies, e.g. the influence of N input from atmospheric depositions in surface waters, as well as microaerobic or anaerobic ammonium and nitrite oxidation in bottom waters. A more comprehensive characterization of the bacterial community related to denitrification (or anammox) is also needed. More globally, recent research suggested that current OMZs expansion in the ocean could increase global denitrification (e.g. Bianchi *et al*., 2012). Future studies in Saanich Inlet and other anoxic environments should contribute to better resolving spatial and temporal (inter-annual) variability in the partition between water-column and sedimentary denitrification and the impacts that these changes will have on the global marine N budget.

# Bibliography

Alain, K., Zbinden, M., N. Le Bris, F. Lesongeur, J. Quérellou, F. Gaill, and M. A. Cambon-Bonavita (2004), Early steps in microbial colonization processes at deep-sea hydrothermal vents*, Environmental Microbiology, 6*, 227-241.

Alkhatib, M., M. Lehmann, and P. del Giorgio (2012), The nitrogen isotope effect of benthic remineralization-nitrification-denitrification coupling in an estuarine environment*, Biogeosciences, 9*, 1633-1646.

Altabet, M. A. (2001), Nitrogen isotopic evidence for micronutrient control of fractional $NO_3^-$ utilization in the equatorial pacific*, Limnology and Oceanography, 46*, 368-380.

Altabet, M. (2007), Constrains on oceanic N balance/imbalance from sedimentary $^{15}N$ records*, Biogeosciences, 4*, 75-86.

Altabet, M. A., R. Francois, D. W. Murray, and W. L. Prell (1995), Climate-Related Variations in Denitrification in the Arabian Sea from Sediment $^{15}N/^{14}N$ Ratios, *Nature, 373*, 506-509.

Altabet, M. A., C. Pilskaln, R. Thunell, C. Pride, D. Sigman, F. Chavez, and R. Francois (1999), The nitrogen isotope biogeochemistry of sinking particles from the margin of the Eastern North Pacific*, Deep Sea Research I, 46*, 655-680.

Altabet, M., M. Higginson, and D. W. Murray (2002), The effect of millennial-scale changes in Arabian sea denitrification on atmospheric $CO_2$, *Nature, 415*, 159-162.

Altschul, S. F., W. Gish, W. Miller, E. W. Myers, and D. J. Lipman (1990), Basic local alignment search tool*, Journal of Molecular Biology, 215*, 403-410.

Amano, T., I. Yoshinaga, K. Okada, T. Yamagishi, S. Ueda, A. Obuchi, Y. Sako, and Y. Suwa (2007), Detection of anammox activity and diversity of anammox bacteria-related 16S rRNA genes in coastal marine sediment in Japan, *Microbes and Environments, 22*, 232-242.

Anderson, I. C. and J. S. Levine (1986), Relative rates of nitric oxide and nitrous oxide production by nitrifiers, denitrifiers, and nitrate respirers*, Applied and Environmental Microbiology, 51*, 938-945.

Anderson, J. J. and A. H. Devol (1973), Deep water renewal in Saanich Inlet, an intermittently anoxic basin*, Estuarine and Coastal Marine Science, 1*, 1-10.

Anderson, R. E., W. J. Brazelton, and J. A. Baross (2011), Using CRISPRs as a metagenomic tool to identify microbial hosts of a diffuse flow hydrothermal vent viral assemblage*, FEMS Microbiology Ecology, 77,* 120-133.

Anderson, R. E., M. T. Beltrán, S. J. Hallam, and J.A. Baross (2012), Microbial community structure across fluid gradients in the Juan de Fuca Ridge hydrothermal system, *FEMS Microbiology Ecology*, doi: 10.1111/j.1574-6941.2012.01478.x.

Andersson, K. K. and A. B. Hooper (1983), $O_2$ and $H_2O$ are each the source of one O in $NO_2^-$ produced from $NH_3$ by *Nitrosomonas*: $^{15}$N-NMR evidence*, FEBS Letters, 164*, 236-240.

Andersson, K. K., S. B. Philson, and A. B. Hooper (1982), $^{18}$O isotope shift in $^{15}$N NMR analysis of biological N-oxidations: $H_2O$-$NO_2^-$ exchange in the ammoniaoxidizing bacterium *Nitrosomonas*, *Proceedings of the National Academy of Sciences, 79,* 5871-5875.

Ashelford, K. E., N. A. Chuzhanova, J. C. Fry, A. J. Jones, and A. J. Weightman (2006), New screening software shows that most recent large 16S rRNA gene clone libraries contain chimeras*, Applied and Environmental Microbiology, 72*, 5734-5741.

Bano, N. and J. T. Hollibaugh (2002), Phylogenetic composition of bacterioplankton assemblages from the Arctic Ocean*, Applied and Environmental Microbiology, 68*, 505-518.

Barford, C. C., J. P. Montoya, M. A. Altabet, and R. Mitchell (1999), Steady-state nitrogen isotope effects of $N_2$ and $N_2O$ production in Paracoccus denitrificans*, Applied and Environmental Microbiology, 65*, 989-994.

Barwell-Clarke, J. and F. Whitney (1996), Institute of Ocean Sciences nutrient methods and analysis, *Canadian Technical Report of Hydrography and Ocean Sciences, 82*, vi + 43 pp.

Baumann, B., M. Snozzi, A. Zehnder, and J. R. Van Der Meer (1996), Dynamics of denitrification activity of *Paracoccus denitrificans* in continuous culture during aerobic-anaerobic changes*, Journal of Bacteriology, 178*, 4367-4374.

Bender, M. L. (1990), The $\delta^{18}O$ of dissolved $O_2$ in seawater: A unique tracer of circulation and respiration in the deep sea*, Journal of Geophysical Research, 95*, 22243-22252.

Berman-Frank, I., J. T. Cullen, Y. Shaked, R. M. Sherrell, and P. G. Falkowski (2001), Iron availability, cellular iron quotas, and N fixation in *Trichodesmium*, *Limnology and Oceanography*, *46*(6), 1249-1260.

Berman-Frank, I., Y. B. Chen, Y. Gerchman, G. Dismukes, and P. Falkowski (2005), Inhibition of nitrogenase by oxygen in marine cyanobacteria controls the global nitrogen and oxygen cycles*, Biogeosciences Discussions, 2*, 261-273.

Betlach, M. R. and J. M. Tiedje (1981), Kinetic explanation for accumulation of nitrite, nitric oxide, and nitrous oxide during bacterial denitrification*, Applied and Environmental Microbiology, 42*, 1074-1084.

Bianchi, M., F. Feliatra, P. Treguer, M.-A. Vincendeau, and J. Morvan (1997), Nitrification rates, ammonium and nitrate distribution in upper layers of the water column and in sediments of the Indian sector of the Southern Ocean, *Deep Sea Research II*, *44*(5), 1017-1032.

Bianchi, D., J. P. Dunne, J. L. Sarmiento, and E. D. Galbraith (2012), Data-based estimates of suboxia, denitrification and $N_2O$ production in the ocean, and their sensitivities to change*, Global Biogeochemical Cycles, 26*, GB2009, doi:10.1029/2011GB004209.

Böhlke, J. K., S. J. Mroczkowski, and T. B. Coplen (2003), Oxygen isotopes in nitrate: new reference materials for $^{18}O$: $^{17}O$: $^{16}O$ measurements and observations on nitrate-water equilibration*, Rapid Communications in Mass Spectrometry, 17*, 1835-1846.

Bourbonnais, A., M. F. Lehmann, J. J. Waniek, and D. E. Schulz-Bull (2009), Nitrate isotope anomalies reflect $N_2$ fixation in the Azores Front region (subtropical NE Atlantic)*, Journal of Geophysical Research, 114*, C03003, doi:10.1029/2007JC004617.

Bourbonnais, A., M. F. Lehmann, D. A. Butterfield, and S. K. Juniper (2012a), Subseafloor nitrogen transformations in diffuse hydrothermal vent fluids of the Juan de Fuca Ridge evidenced by the isotopic composition of nitrate and ammonium*, Geochemistry Geophysics Geosystems, 13*, Q02T01, doi:10.1029/2011GC003863.

Bourbonnais, A., S. K. Juniper, D. A. Butterfield, A. Devol, M. M. M. Kuypers, G. Lavik, S. J. Hallam, C. B. Wenk, B. X. Chang, S. A. Murdock, and M. F. Lehmann (2012b), Activity and abundance of denitrifying bacteria in the subsurface biosphere of diffuse hydrothermal vents of the Juan de Fuca Ridge*, Biogeosciences Discussions, 9*, 4177-4223

Bowles, M. and S. Joye (2011), High rates of denitrification and nitrate removal in cold seep sediments*, The ISME Journal, 5*, 565-567.

Boyd, P. W., A. J. Watson, C. S. Law, E. R. Abraham, T. Trull, R. Murdoch, D. C. E. Bakker, A. R. Bowie, K. Buesseler, and H. Chang (2000), A mesoscale phytoplankton bloom in the polar Southern Ocean stimulated by iron fertilization*, Nature, 407*, 695-702.

Bradley, P. M., C. Marjorie Aelion, and D. A. Vroblesky (1992), Influence of environmental factors on denitrification in sediment contaminated with JP-4 jet fuel*, Ground Water, 30*, 843-848.

Braker, G., A. Fesefeldt, and K. P. Witzel (1998), Development of PCR primer systems for amplification of nitrite reductase genes (*nirK* and *nirS*) to detect denitrifying bacteria in environmental samples*, Applied and Environmental Microbiology, 64*, 3769-3775.

Braker, G., J. Zhou, L. Wu, A. H. Devol, and J. M. Tiedje (2000), Nitrite reductase genes (*nirK* and *nirS*) as functional markers to investigate diversity of denitrifying bacteria in Pacific Northwest marine sediment communities*, Applied and Environmental*

*Microbiology, 66*, 2096.

Braker, G., H. L. Ayala-del-Rio, A. H. Devol, A. Fesefeldt, and J. M. Tiedje (2001), Community structure of denitrifiers, Bacteria, and Archaea along redox gradients in Pacific Northwest marine sediments by terminal restriction fragment length polymorphism analysis of amplified nitrite reductase (*nirS*) and 16S rRNA genes*, Applied and Environmental Microbiology, 67*, 1893.

Braker, G., J. Schwarz, and R. Conrad (2010), Influence of temperature on the composition and activity of denitrifying soil communities*, FEMS Microbiology Ecology, 73*, 134-148.

Braman, R. S. and S. A. Hendrix (1989), Nanogram nitrite and nitrate determination in environmental and biological materials by vanadium (III) reduction with chemiluminescence detection*, Analytical Chemistry, 61*, 2715-2718.

Brandes, J. A. and A. H. Devol (1997), Isotopic fractionation of oxygen and nitrogen in coastal marine sediments*, Geochimica et Cosmochimica Acta, 61*, 1793-1801.

Brandes, J. A. and A. H. Devol (2002), A global marine-fixed nitrogen isotopic budget: Implications for Holocene nitrogen cycling*, Global Biogeochemical Cycles, 16*, 1120-1134.

Brandes, J. A., A. H. Devol, T. Yoshinari, D. A. Jayakumar, and S. W. A. Naqvi (1998a), Isotopic composition of nitrate in the central Arabian Sea and eastern tropical North Pacific: A tracer for mixing and nitrogen cycles*, Limnology and Oceanography, 43*, 1680-1689.

Brandes, J. A., N. Z. Boctor, G. D. Cody, B. A. Cooper, R. M. Hazen, and H. S. Yoder (1998b), Abiotic nitrogen reduction on the early Earth*, Nature, 395*, 365-367.

Brandes, J. A., R. M. Hazen, and H. S. Yoder Jr (2008), Inorganic nitrogen reduction and stability under simulated hydrothermal conditions*, Astrobiology, 8*, 1113-1126.

Broecker, W. S., and G. M. Henderson (1998), The sequence of events surrounding Termination II and their implications for the cause of glacial-interglacial $CO_2$ changes, *Paleoceanography*, *13*(4), 352-364.

Bru, D., A. Sarr, and L. Philippot (2007), Relative abundances of proteobacterial membrane-bound and periplasmic nitrate reductases in selected environments, *Applied and Environmental Microbiology, 73*, 5971-5974.

Buchwald, C. and K. L. Casciotti (2010), Oxygen isotopic fractionation and exchange during bacterial nitrite oxidation*, Limnology and Oceanography, 55*, 1064-1074.

Busigny, V., C. Laverne, and M. Bonifacie (2005), Nitrogen content and isotopic composition of oceanic crust at a superfast spreading ridge: A profile in altered basalts from ODP Site 1256, Leg 206*, Geochem. Geophys. Geosyst., 6*, Q12O01.

Butterfield, D. A., I. R. Jonasson, G. J. Massoth, R. A. Feely, K. K. Roe, R. E. Embley, J. F. Holden, R. E. McDuff, M. D. Lilley, and J. R. Delaney (1997), Seafloor eruptions and evolution of hydrothermal fluid chemistry *, Philosophical Transactions: Mathematical, Physical and Engineering Sciences, 355*, 369-386.

Butterfield, D. A., K. K. Roe, M. D. Lilley, J. A. Huber, J. A. Baross, R. W. Embley, and G. J. Massoth (2004), Mixing, reaction and microbial activity in the sub-seafloor revealed by temporal and spatial variation in diffuse flow vents at Axial Volcano, in *The Subseafloor Biosphere at Mid-Ocean Ridges,* edited by W. S. D. Wilcock, E. F. DeLong, D. S. Kelley, J. A. Baross and S. C. Cary, Geophysical Monograph Series, Vol. 144, pp. 269-289, American Geophysical Union, Washington, DC.

Byrne, N., M. Strous, V. Crépeau, B. Kartal, J. L. Birrien, M. Schmid, F. Lesongeur, S. Schouten, A. Jaeschke, and M. Jetten (2009), Presence and activity of anaerobic ammonium-oxidizing bacteria at deep-sea hydrothermal vents*, The ISME journal, 3*, 117-123.

Cabello, P., M. D. Roldán, and C. Moreno-Vivián (2004), Nitrate reduction and the nitrogen cycle in archaea*, Microbiology, 150*, 3527-3546.

Capone, D. G., J. P. Zehr, H. W. Paerl, B. Bergman, and E. J. Carpenter (1997), *Trichodesmium*, a globally significant marine cyanobacterium, *Science*, *276*, 1221-1229.

Capone, D. G., J. A. Burns, J. P. Montoya, A. Subramaniam, C. Mahaffey, T. Gunderson, A. F. Michaels, and E. J. Carpenter (2005), N fixation by *Trichodesmium* spp.: An important source of new N to the tropical and sub-tropical North Atlantic Ocean, *Global Biogeochemical Cycles*, *19*, 2024, doi:10.1029/2004GB002331.

Carpenter, E. J., H. R. Harvey, B. Fry, and D. G. Capone (1997), Biogeochemical tracers of the marine cyanobacterium *Trichodesmium, Deep Sea Research I, 44*, 27-38.

Carpenter, E. J., J. P. Montoya, J. Burns, M. R. Mulholland, A. Subramaniam, and D. G. Capone (1999), Extensive bloom of a $N_2$-fixing diatom/cyanobacterial association in the tropical Atlantic Ocean*, Marine Ecology Progress Series, 185*, 273-283.

Carter, J. P., Y. H. Hsaio, S. Spiro, D. J. Richardson (1995), Soil and sediment bacteria capable of aerobic nitrate respiration, *Applied and Environmental Microbiology, 61*, 2852-2858.

Casciotti, K. L. (2002), Molecular and stable isotopic characterization of enzymes involved in nitrification and nitrifier-denitrification, Ph.D. dissertation, Princeton University, Princeton, N. J.

Casciotti, K. L. (2009), Inverse kinetic isotope fractionation during bacterial nitrite oxidation*, Geochimica et Cosmochimica Acta, 73*, 2061-2076.

Casciotti, K. L. and M. R. McIlvin (2007), Isotopic analyses of nitrate and nitrite from

reference mixtures and application to Eastern Tropical North Pacific waters, *Marine Chemistry, 107*, 184-201.

Casciotti, K. L., D. M. Sigman, M. G. Hastings, J. K. Böhlke, and A. Hilkert (2002), Measurement of the oxygen isotopic composition of nitrate in seawater and freshwater using the denitrifier method, *Analytical Chemistry, 74*, 4905-4912.

Casciotti, K. L., D. M. Sigman, and B. B. Ward (2003), Linking diversity and stable isotope fractionation in ammonia-oxidizing bacteria, *Geomicrobiology Journal, 20*, 335-353.

Casciotti, K. L., J. K. Böhlke, M. R. McIlvin, S. J. Mroczkowski, and J. E. Hannon (2007), Oxygen isotopes in nitrite: Analysis, calibration, and equilibration, *Analytical Chemistry, 79*, 2427-2436.

Casciotti, K. L., M. McIlvin, and C. Buchwald (2010), Oxygen isotopic exchange and fractionation during bacterial ammonia oxidation, *Limnology and Oceanography, 55*, 753-762.

Castro-González, M., G. Braker, L. Farías, and O. Ulloa (2005), Communities of *nirS*-type denitrifiers in the water column of the oxygen minimum zone in the eastern South Pacific, *Environmental Microbiology, 7*, 1298-1306.

Chadwick Jr, W. W., S. L. Nooner, D. A. Butterfield, and M. D. Lilley (2012), Seafloor deformation and forecasts of the April 2011 eruption at Axial Seamount, *Nature Geoscience, 5*, 474-477.

Chang, B. X., A. H. Devol, and S. R. Emerson (2010), Denitrification and the nitrogen gas excess in the eastern tropical South Pacific oxygen deficient zone, *Deep Sea Research I, 57*, 1092-1101.

Chao, A. (1984), Nonparametric estimation of the number of classes in a population, *Scandinavian Journal of Statistics, 11*, 265-270.

Chao, A., R. L. Chazdon, R. K. Colwell, and T. J. Shen (2005), A new statistical approach for assessing similarity of species composition with incidence and abundance data, *Ecology Letters, 8*, 148-159.

Checkley Jr, D. M. and C. A. Miller (1989), Nitrogen isotope fractionation by oceanic zooplankton, *Deep Sea Research Part A, 36*, 1449-1456.

Chon, K., J. S. Chang, E. Lee, J. W. Lee, J. Y. Ryu, and J. Cho (2009), Abundance of denitrifying genes coding for nitrate (*narG*), nitrite (*nirS*), and nitrous oxide (*nosZ*) reductases in estuarine versus waste production water effluent fed constructed wetlands, *Ecological Engineering, 1500*, 1-6.

Christensen, J. P., J. W. Murray, A. H. Devol, and L. A. Codispoti (1987), Denitrification in continental shelf sediments has major impact on the oceanic nitrogen budget, *Global*

*Biogeochemical Cycles, 1*, 97-116.

Cline, J. D. (1969), Spectrophotometric determination of hydrogen sulfide in natural waters, *Limnology and Oceanography*, *14*, 454-458.

Cline, J. D. and I. R. Kaplan (1975), Isotopic fractionation of dissolved nitrate during denitrification in the eastern tropical north pacific ocean*, Marine Chemistry, 3*, 271-299.

Coale, K. H., *et al.* (1996), A massive phytoplankton bloom induced by an ecosystem-scale iron fertilization experiment in the equatorial Pacific Ocean, *Nature, 383*, 495-501.

Codispoti, L. A. (2007), An oceanic fixed nitrogen sink exceeding 400 Tg N $a^{-1}$ vs the concept of homeostasis in the fixed-nitrogen inventory*, Biogeosciences, 4*, 233-253.

Codispoti, L. A., G. E. Friederich, T. T. Packard, H. E. Glover, P. J. Kelly, R. W. Spinrad, R. T. Barber, J. W. Elkins, B. B. Ward, F. Lipschultz, and N. Lostaunau (1986), High nitrite levels off Northern Peru: a signal of instability in the marine denitrification rate, *Science, 233*(4769), 1200-1202.

Codispoti, L., J. A. Brandes, J. Christensen, A. Devol, S. Naqvi, H. W. Paerl, and T. Yoshinari (2001), The oceanic fixed nitrogen and nitrous oxide budgets: Moving targets as we enter the anthropocene?*, Scientia Marina, 65*, 85-105.

Cohen, Y. (1978), Consumption of dissolved nitrous oxide in an anoxic basin, Saanich Inlet, British Columbia, *Nature, 272*, 235-237.

Coyne, M., A. Arunakumari, B. Averill, and J. Tiedje (1989), Immunological identification and distribution of dissimilatory heme cd1 and non-heme copper nitrite reductases in denitrifying bacteria. *Applied and Environmental Microbiology, 55*, 2924-2931.

Dalsgaard, T., D. E. Canfield, J. Petersen, B. Thamdrup, and J. Acuña-González (2003), $N_2$ production by the anammox reaction in the anoxic water column of Golfo Dulce, Costa Rica*, Nature, 422*, 606-608.

Delwiche, C. C. and P. L. Steyn (1970), Nitrogen isotope fractionation in soils and microbial reactions*, Environmental Science & Technology, 4*, 929-935.

Deutsch, C., N. Gruber, R. M. Key, J. L. Sarmiento, and A. Ganachaud (2001), Denitrification and $N_2$ fixation in the Pacific Ocean*, Global Biogeochemical Cycles, 15*, 483-506.

Devol, A. H. (1991), Direct measurement of nitrogen gas fluxes from continental shelf sediments, *Nature, 349*, 319-321.

Devol, A., A. Uhlenhopp, S. Naqvi, J. Brandes, D. Jayakumar, H. Naik, S. Gaurin, L. Codispoti, and T. Yoshinari (2006), Denitrification rates and excess nitrogen gas concentrations in the Arabian Sea oxygen deficient zone*, Deep Sea Research I, 53*, 1533-

1547.

DeVries, T., C. Deutsch, P. A. Rafter, and F. Primeau (2012), Marine denitrification rates determined from a global 3-dimensional inverse model, *Biogeosciences Discussions*, *9*, 14013-14052.

Dispirito, A. A. and A. B. Hooper (1986), Oxygen exchange between nitrate molecules during nitrite oxidation by *Nitrobacter,The Journal of Biological Chemistry, 261*, 10534-10537.

Dong, L. F., C. J. Smith, S. Papaspyrou, A. Stott, A. M. Osborn, and D. B. Nedwell (2009), Changes in benthic denitrification, nitrate ammonification, and anammox process rates and nitrate and nitrite reductase gene abundances along an estuarine nutrient gradient (the Colne Estuary, United Kingdom)*, Applied and Environmental Microbiology, 75*, 3171-3179.

Dore, J. E., and D. M. Karl (1996), Nitrification in the euphotic zone as a source of nitrite, nitrate, and nitrous oxide at Station ALOHA, *Limnology and Oceanography*, *41*(8), 1619-1628.

Dörr, M., J. Käßbohrer, R. Grunert, G. Kreisel, W. A. Brand, R. A. Werner, H. Geilmann, C. Apfel, C. Robl, and W. Weigand (2003), A possible prebiotic formation of ammonia from dinitrogen on iron sulfide surfaces*, Angewandte Chemie International Edition, 42*, 1540-1543.

Dortch, Q. (1990), The interaction between ammonium and nitrate uptake in phytoplankton*, Marine Ecology Progress Series, 61*, 183-201.

Dugdale, V. A., and J. J. Goering (1967), Uptake of new and regenerated forms of N in primary productivity, *Limnology and Oceanography, 12*, 196-206.

Dugdale, R. C., J. J. Goering, R. T. Barber, R. L. Smith, and T. T. Packard (1977), Denitrification and hydrogen sulfide in the Peru upwelling region during 1976, *Deep Sea Research*, *24*(6), 601-608.

Dugdale, R. C., F. P. Wilkerson, V. E. Hogue, and A. Marchi (2007), The role of ammonium and nitrate in spring bloom development in San Francisco Bay*, Estuarine and Coastal Shelf Science, 73*, 17-29.

Edgar, R. C., B. J. Haas, J. C. Clemente, C. Quince, and R. Knight (2011), UCHIME improves sensitivity and speed of chimera detection*, Bioinformatics, 27*, 2194-2200.

Edmond, J. M., C. Measures, R. E. McDuff, L. H. Chan, R. Collier, B. Grant, L. I. Gordon, and J. B. Corliss (1979), Ridge crest hydrothermal activity and the balances of the major and minor elements in the ocean: the Galapagos data*, Earth and Planetary Science Letters, 46*, 1-18.

Engstrom, P., T. Dalsgaard, S. Hulth, R. C. Aller (2005), Anaerobic ammonium oxidation by nitrite (anammox) implications for $N_2$ production in coastal marine sediments, *Geochimica et Cosmochimica Acta, 69*, 2057-2065.

Elderfield, H. and A. Schultz (1996), Mid-ocean ridge hydrothermal fluxes and the chemical composition of the ocean*, Annual Review of Earth Planetary Sciences, 24*, 191-224.

Ellis, M. J., J. G. Grossmann, R. R. Eady, and S. S. Hasnain (2007), Genomic analysis reveals widespread occurrence of new classes of copper nitrite reductases*, Journal of Biological Inorganic Chemistry, 12*, 1119-1127.

Embley, R. W., K. M. Murphy, and C. G. Fox (1990), High-resolution studies of the summit of Axial Volcano*, J. Geophys. Res, 95*, 12785-12812.

Embley, R., W. Chadwick Jr, D. Clague, and D. Stakes (1999), 1998 eruption of axial volcano: Multibeam anomalies and sea-floor observations*, Geophysical Research Letters, 26*, 3425-3428.

Emeis, K.C., P. Mara, T. Schlarbaum, J. Möbius, K. Dähnke, U. Struck, N. Mihalopoulos, M. Krom (2010), External N inputs and internal N cycling traced by isotope ratios of nitrate, dissolved reduced nitrogen, and particulate nitrogen in the eastern Mediterranean Sea, *Journal of Geophysical Research, 115 (G4)*, G04041, doi:10.1029/2009JG001214.

Emerson, S., C. Stump, D. Wilbur, and P. Quay (1999), Accurate measurement of $O_2$, $N_2$, and Ar gases in water and the solubility of $N_2$*, Marine Chemistry, 64*, 337-347.

Eppley, R. W. and B. J. Peterson (1979), Particulate organic matter flux and planktonic new production in the deep ocean*, Nature, 282*, 677-680.

Falk, S., M. Hannig, C. Gliesche, R. Wardenga, M. Köster, K. Jürgens, and G. Braker (2007), *nirS*-containing denitrifier communities in the water column and sediment of the Baltic Sea*, Biogeosciences, 4*, 255-268.

Falkowski, P. G., (1997), Evolution of the N cycle and its influence on the biological sequestration of $CO_2$ in the ocean, *Nature*, *387*, 272-275.

Forget, N., S. Murdock, and S. Juniper (2010), Bacterial diversity in Fe-rich hydrothermal sediments at two South Tonga Arc submarine volcanoes*, Geobiology, 8*, 417-432.

Foustoukos, D. I., N. J. Pester, K. Ding, and W. E. Seyfried Jr (2009), Dissolved carbon species in associated diffuse and focused flow hydrothermal vents at the Main Endeavour Field, Juan de Fuca Ridge: Phase equilibria and kinetic constraints*, Geochemistry Geophysics Geosystems, 10*, Q10003, doi:10.1029/2009GC002472.

Füssel, J., P. Lam, G. Lavik, M. M. Jensen, M. Holtappels, M. Günter, and M. M. M.

Kuypers (2012), Nitrite oxidation in the Namibian oxygen minimum zone*, The ISME Journal*, *6*, 1200-1209.

Ganeshram, R. S., T. F. Pedersen, S. E. Calvert, and J. W. Murray (1995), Large changes in oceanic nutrient inventories from glacial to interglacial periods, *Nature, 376*, 755-758.

Ganeshram, R. S., T. F. Pedersen, S. E. Calvert, G. W. McNeill, and M. R. Fontugne (2000), Glacial-interglacial variability in denitrification in the world's oceans: Causes and consequences, *Paleoceanography*, *15*(4), 361-376.

Gargett, A. E., D. Stucchi, and F. Whitney (2003), Physical processes associated with high primary production in Saanich Inlet, British Columbia*, Estuarine and Coastal Shelf Science, 56*, 1141-1156.

German, C. R., A. Bowen, M. Coleman, D. Honig, J. A. Huber, M. V. Jakuba, J. C. Kinsey, M. D. Kurz, S. Leroy, and J. M. McDermott (2010), Diverse styles of submarine venting on the ultraslow spreading Mid-Cayman Rise*, Proceedings of the National Academy of Sciences, 107*, 14020-14025.

Gevertz, D., A. J. Telang, G. Voordouw, and G. E. Jenneman (2000), Isolation and characterization of strains CVO and FWKOB, two novel nitrate-reducing, sulfide-oxidizing bacteria isolated from oil field brine*, Applied and Environmental Microbiology, 66*, 2491-2501.

Gonzalez, J. M., M. C. Portillo, P. Belda-Ferre, and A. Mira (2012), Amplification by PCR Artificially Reduces the Proportion of the Rare Biosphere in Microbial Communities*, PloS one, 7*, e29973, doi:10.1371/journal.pone.0029973.

Granger, J. and D. M. Sigman (2009), Removal of nitrite with sulfamic acid for nitrate N and O isotope analysis with the denitrifier method*, Rapid Commununications in Mass Spectrometry, 23*, 3753-3762.

Granger, J., D. M. Sigman, J. A. Needoba, and P. J. Harrison (2004), Coupled nitrogen and oxygen isotope fractionation of nitrate during assimilation by cultures of marine phytoplankton*, Limnology and Oceanography, 49*, 1763-1773.

Granger, J., D. M. Sigman, M. G. Prokopenko, M. F. Lehmann, and P. D. Tortell (2006), A method for nitrite removal in nitrate N and O isotope analyses*, Limnology and Oceanography: Methods, 4*, 205-212.

Granger, J., D. M. Sigman, M. F. Lehmann, and P. D. Tortell (2008), Nitrogen and oxygen isotope fractionation during dissimilatory nitrate reduction by denitrifying bacteria*, Limnology and Oceanography, 53*, 2533-2545.

Grote, J., T. Schott, C. G. Bruckner, F. O. Glöckner, G. Jost, H. Teeling, M. Labrenz, and K. Jürgens (2012), Genome and physiology of a model Epsilonproteobacterium responsible for sulfide detoxification in marine oxygen depletion zones*, Proceedings of the National Academy of Sciences, 109*, 506-510.

Gruber, N. (2004), The dynamics of the marine N cycle and its influence on atmospheric $CO_2$, in *The Ocean Carbon Cycle and Climate*, edited by M. Follows and T. Oguz, pp. 97-148, Kluwer Academic, Dordrecht, The Netherlands.

Gruber, N. (2008), The marine nitrogen cycle: Overview and challenges, in *Nitrogen in the Marine Environment*, 2nd edn., edited by D. Capone, D. A. Bronk, M. R. Mulholland, and E. J. Carpenter, pp. 1-50, Elsevier, Amsterdam, The Netherlands.

Gruber, N. and J. Sarmiento (1997), Global patterns of marine nitrogen fixation and denitrification*, Global Biogeochemical Cycles, 11*, 235-266.

Gruber, N., and J. L. Sarmiento (2002), Biogeochemical/physical interactions in elemental cycles, in *THE SEA: Biological-Physical Interactions in the Oceans*, edited by A. R. Robinson, J. J. McCarthy, and B. J. Rothschild, vol. 12, pp. 337.399, John Wiley and Sons. New York.

Grundle, D. S. and S. K. Juniper (2011), Nitrification from the lower euphotic zone to the sub-oxic waters of a highly productive British Columbia fjord*, Marine Chemistry, 126,* 173-181.

Guindon, S., J. F. Dufayard, V. Lefort, M. Anisimova, W. Hordijk, and O. Gascuel (2010), New algorithms and methods to estimate maximum-likelihood phylogenies: assessing the performance of PhyML 3.0*, Systems Biology, 59*, 307-321.

Hall, A. (1989), Ammonium in spilitized basalts of southwest England and its implications for the recycling of nitrogen*, Geochemical Journal, 23*, 19-23.

Hamady, M., C. Lozupone, and R. Knight (2009), Fast UniFrac: facilitating high-throughput phylogenetic analyses of microbial communities including analysis of pyrosequencing and PhyloChip data*, The ISME Journal, 4*, 17-27.

Hamersley, M. R., G. Lavik, D. Woebken, J. E. Rattray, P. Lam, E. C. Hopmans, J. S. S. Damste, S. Krüger, M. Graco, and D. Gutiérrez (2007), Anaerobic ammonium oxidation in the Peruvian oxygen minimum zone*, Limnology and Oceanography, 52*, 923-933.

Hamme, R., and S. Emerson (2004), The solubility of neon, nitrogen and argon in distilled water and seawater, *Deep-Sea Research I*, *51*, 1517-1528.

Handelsman, J. (2004), Metagenomics: Application of Genomics to Uncultured Microorganisms, *Microbiology and molecular biology reviews, 68*(4), 669-685.

Hastings, M. G., D. M. Sigman, and F. Lipschultz (2003), Isotopic evidence for source changes of nitrate in rain at Bermuda*, Journal of Geophysical Research, 108*, 4790. doi:10.1029/2003JD003789.

Henry, S., E. Baudoin, J. C. López-Gutiérrez, F. Martin-Laurent, A. Brauman, and L. Philippot (2004), Quantification of denitrifying bacteria in soils by *nirK* gene targeted real-time PCR*, Journal of Microbiological Methods, 59*, 327-335.

Hentschel, U. and H. Felbeck (1993), Nitrate respiration in the hydrothermal vent tubeworm *Riftia pachyptila, Nature, 366*, 338-340.

Herlinveaux, R. H., (1962), Oceanography of Saanich inlet in Vancouver Island, British Columbia, *Journal of Fisheries Research Board of Canada, 19*, 1-37.

Hessler, R. R., and V. A. Kaharl (1995), The deep-sea hydrothermal vent community: an overview, in *Seafloor hydrothermal Systems: Physical, Chemical, Biological, and Geological Interactions,* edited by S. E. Humphris, R. A. Zierenberg, L. S. Mullineaux, and R. E. Thomson, Geophysical Monograph 91, pp. 72-82, American Geophysical Union, Washington, DC.

Heylen, K., D. Gevers, B. Vanparys, L. Wittebolle, J. Geets, N. Boon, and P. De Vos (2006), The incidence of *nirS* and *nirK* and their genetic heterogeneity in cultivated denitrifiers*, Environmental Microbiology, 8*, 2012-2021.

Hoch, M. P., M. L. Fogel, and D. L. Kirchman (1992), Isotope fractionation associated with ammonium uptake by a marine bacterium*, Limnology and Oceanography, 37*, 1447-1459.

Hodges, T. W. and J. B. Olson (2009), Molecular comparison of bacterial communities within iron-containing flocculent mats associated with submarine volcanoes along the Kermadec Arc*, Applied and Environmental Microbiology, 75*, 1650-1657.

Holloway, J. M., D. K. Nordstrom, J. K. Böhlke, R. B. McCleskey, and J. W. Ball (2011), Ammonium in thermal waters of Yellowstone National Park: Processes affecting speciation and isotope fractionation*, Geochimica et Cosmochimica Acta, 75*, 4611-4636.

Holmes, R. M., A. Aminot, R. Kérouel, B. A. Hooker, and B. J. Peterson (1999), A simple and precise method for measuring ammonium in marine and freshwater ecosystems*, Canadian Journal of Fisheries and Aquatic Science, 56*, 1801-1808.

Houlton, B. Z., D. M. Sigman, E. A. G. Schuur, and L. O. Hedin (2007), A climate-driven switch in plant nitrogen acquisition within tropical forest communities*, Proceedings of the National Academy of Sciences, 104*, 8902-8906.

Howell, E. A., S. C. Doney, R. A. Fine, and D. B. Olson (1997), Geochemical estimates of denitrification in the Arabian Sea and the Bay of Bengal during the WOCE, *Geophysical Research Letters*, *24*, 2549-2552.

Huber, J. A., D. A. Butterfield, and J. A. Baross (2002), Temporal changes in archaeal diversity and chemistry in a mid-ocean ridge subseafloor habitat*, Applied and Environmental Microbiology, 68*, 1585-1594.

Huber, J. A., D. A. Butterfield, and J. A. Baross (2003), Bacterial diversity in a subseafloor habitat following a deep-sea volcanic eruption*, FEMS Microbiology Ecology, 43*, 393-409.

Huber, J. A., D. B. Mark Welch, H. G. Morrison, S. M. Huse, P. R. Neal, D. A. Butterfield, and M. L. Sogin (2007), Microbial population structures in the deep marine biosphere, *Science, 318*, 97-100.

Huber, J. A., H. V. Cantin, S. M. Huse, D. B. Mark Welch, M. L. Sogin, and D. A. Butterfield (2010), Isolated communities of Epsilonproteobacteria in hydrothermal vent fluids of the Mariana Arc seamounts, *FEMS Microbiology Ecology, 73*, 538-549.

Huber, T., G. Faulkner, and P. Hugenholtz (2004), Bellerophon: a program to detect chimeric sequences in multiple sequence alignments, *Bioinformatics, 20*, 2317-2319.

Hulth, S., R. C. Aller, and F. Gilbert (1999), Coupled anoxic nitrification/manganese reduction in marine sediments, *Geochimica et Cosmochimica Acta, 63*, 49-66.

Humbert, S., J. Zopfi, and S. E. Tarnawski (2012), Abundance of anammox bacteria in different wetland soils, *Environmental Microbiology Reports*, *4*, 484-490.

Huse, S. M., D. M. Welch, H. G. Morrison, and M. L. Sogin (2010), Ironing out the wrinkles in the rare biosphere through improved OTU clustering, *Environmental Microbiology, 12*, 1889-1898.

Inagaki, F., K. Takai, H. Kobayashi, K. H. Nealson, and K. Horikoshi (2003), *Sulfurimonas autotrophica* gen. nov., sp. nov., a novel sulfur-oxidizing ε-proteobacterium isolated from hydrothermal sediments in the Mid-Okinawa Trough, *International Journal of Systematic and Evolutionary Microbiology, 53*, 1801-1805.

Inagaki, F., K. Takai, K. H. Nealson, and K. Horikoshi (2004), *Sulfurovum lithotrophicum* gen. nov., sp. nov., a novel sulfur-oxidizing chemolithoautotroph within the ∑-Proteobacteria isolated from Okinawa Trough hydrothermal sediments, *International Journal of Systematic and Evolutionary Microbiology, 54*, 1477-1482.

Ingall, E. and R. Jahnke (1994), Evidence for enhanced phosphorus regeneration from marine sediments overlain by oxygen depleted waters, *Geochimica et Cosmochimica Acta, 58*, 2571-2575.

Jaeschke, A., E. Hopmans, S. Wakeham, S. Schouten, and J Damsté (2007), The presence of ladderanes lipids in the oxygen minimum zone of the Arabian Sea indicates N loss through anammox, *Limnology and Oceanography, 52*, 780-786.

Jannasch, H. W. and M. J. Mottl (1985), Geomicrobiology of deep-sea hydrothermal vents, *Science, 229*, 717-725.

Javanaud, C., V. Michotey, S. Guasco, N. Garcia, P. Anschutz, M. Canton, and P. Bonin (2011), Anaerobic ammonium oxidation mediated by Mn-oxides: from sediment to strain level, *Research in Microbiology, 162,* 848-857.

Javoy, M. and F. Pineau (1991), The volatiles record of a "popping" rock from the Mid-Atlantic Ridge at 14°N: chemical and isotopic composition of gas trapped in the vesicles,

*Earth and Planetary Science Letters, 107*, 598-611.

Jayakumar, D. A., C. A. Francis, S. W. A. Naqvi, and B. B. Ward (2004), Diversity of nitrite reductase genes (*nirS*) in the denitrifying water column of the coastal Arabian Sea, *Aquatic Microbial Ecology, 34*, 69-78.

Jayakumar, A., G. O'Mullan, S. W. A. Naqvi, and B. Ward (2009), Denitrifying bacterial community composition changes associated with stages of denitrification in oxygen minimum zones, *Microbial Ecology, 58*, 350-362.

Jensen, M. M., M. M. M. Kuypers, G. Lavik, and B. Thamdrup (2008), Rates and regulation of anaerobic ammonium oxidation and denitrification in the Black Sea, *Limnology and Oceanography, 53*, 23-36.

Jensen, M. M., P. Lam, N. P. Revsbech, B. Nagel, B. Gaye, M. S. M. Jetten, and M. M. M. Kuypers (2011), Intensive nitrogen loss over the Omani Shelf due to anammox coupled with dissimilatory nitrite reduction to ammonium, *The ISME Journal, 5*, 1660-1670.

Johnson, H. P., M. A. Tivey, T. A. Bjorklund, and M. S. Salmi (2010), Hydrothermal circulation within the Endeavour Segment, Juan de Fuca Ridge, *Geochemistry Geophysics Geosystems, 11,* Q05002, doi:10.1029/2009GC002957.

Jones, C. M. and S. Hallin (2010), Ecological and evolutionary factors underlying global and local assembly of denitrifier communities, *The ISME Journal, 4*, 633-641.

Juniper, S. and R. Brinkhurst (1986), Water-column dark $CO_2$ fixation and bacterial-mat growth in intermittently anoxic Saanich Inlet, British Columbia, *Marine Ecology Progress Series, 33*, 41-50.

Juniper, S. K., P. Martineu, J. Sarrazin, and Y. Gelinas (1995), Microbial-mineral floc associated with nascent hydrothermal activity on CoAxial Segment, Juan de Fuca Ridge, *Geophysical Research Letters, 22*, 179-182.

Kalvelage, T., M. M. Jensen, S. Contreras, N. P. Revsbech, P. Lam, M. Günter, J. LaRoche, G. Lavik, and M. M. M. Kuypers (2011), Oxygen sensitivity of anammox and coupled N-cycle processes in oxygen minimum zones, PLoS ONE 6(12): e29299, doi:10.1371/journal.pone.0029299.

Karl, D., (1995), Ecology of free-living, hydrothermal vent microbial communities, *in The microbiology of Deep-Sea Hydrothermal Vents*, edited by D. Karl, pp. 53-124, CRC Press, Boca Raton, FL.

Karl, D., A. Michaels, B. Bergman, D. Capone, E. Carpenter, R. Letelier, F. Lipschultz, H. Paerl, D. Sigman, and L. Stal (2002), Dinitrogen fixation in the world's oceans, *Biogeochemistry*, *57/58*, 47-98.

Kaye, J. Z., M. C. Márquez, A. Ventosa, and J. A. Baross (2004), *Halomonas neptunia* sp. nov., *Halomonas sulfidaeris* sp. nov., *Halomonas axialensis* sp. nov. and *Halomonas*

*hydrothermalis* sp. nov.: halophilic bacteria isolated from deep-sea hydrothermal-vent environments*, International Journal of Systematic and Evolutionary Microbiology, 54*, 499-511.

Kennicutt, I. I. and R. A. Burke (1992), Stable isotope partitioning in seep and vent organisms: chemical and ecological significance*, Chemical Geology, 101*, 293-310.

Knapp, A. N., D. M. Sigman, and F. Lipschultz (2005), N isotopic composition of dissolved organic nitrogen and nitrate at the Bermuda Atlantic Time-series Study site*, Global Biogeochemical Cycles, 19*. GB1018, doi:10.1029/2004GB002320.

Knapp, A. N., P. J. DiFiore, C. Deutsch, D. M. Sigman, and F. Lipschultz (2008), Nitrate isotopic composition between Bermuda and Puerto Rico: Implications for $N_2$ fixation in the Atlantic Ocean*, Global Biogeochemical Cycles, 22*, GB3014, doi:10.1029/2007GB003107.

Knapp, A. N., M. G. Hastings, D. M. Sigman, F. Lipschultz, and J. N. Galloway (2010), The flux and isotopic composition of reduced and total nitrogen in Bermuda rain*, Marine Chemistry, 120*, 83-89.

Kuenen, J. G. (2008), Anammox bacteria: from discovery to application, *Nature, 6*, 320-326.

Kumar, S., D. J. D. Nicholas, and E. H. Williams (1983), Definitive $^{15}N$ NMR evidence that water serves as a source of O during nitrite oxidation by *Nitrobacter agilis, FEBS Letters, 152*, 71-74.

Kuypers, M. M. M., A. O. Sliekers, G. Lavik, M. Schmid, B. B. Jørgensen, J. G. Kuenen, J. S. S. Damsté, M. Strous, and M. S. M. Jetten (2003), Anaerobic ammonium oxidation by anammox bacteria in the Black Sea*, Nature, 422*, 608-611.

Kuypers, M. M. M., G. Lavik, D. Woebken, M. Schmid, B. M. Fuchs, R. Amann, B. B. Jørgensen, and M. S. M. Jetten (2005), Massive nitrogen loss from the Benguela upwelling system through anaerobic ammonium oxidation*, Proceedings of the National Academy of Sciences U. S. A., 102*, 6478-6483.

Kuypers, M. M. M., G. Lavik, and B. Thamdrup (2006), Anaerobic ammonium oxidation in the marine environment*,* in *Past and present water column anoxia*, NATO Science Series IV: Earth and Environmental Series, vol. 64, edited by L. N. Neretin , pp. 311-336, Springer, Dordrecht, The Netherlands.

Krebs, C. J.: Ecological methodology, 2nd ed., (1999), Addison-Welsey Educational Publishers, Inc., Menlo Park, CA, 620 pp.

Lam, P., J. P. Cowen, and R. D. Jones (2004), Autotrophic ammonia oxidation in a deep-sea hydrothermal plume*, FEMS Microbiology Ecology, 47*, 191-206.

Lam, P., M. M. Jensen, G. Lavik, D. F. McGinnis, B. Müller, C. J. Schubert, R. Amann,

B. Thamdrup, and M. M. M. Kuypers (2007), Linking crenarchaeal and bacterial nitrification to anammox in the Black Sea*, Proceedings of the National Academy of Sciences, 104*, 7104-7109.

Lam, P., J. P. Cowen, B. N. Popp, and R. D. Jones (2008), Microbial ammonia oxidation and enhanced nitrogen cycling in the Endeavour hydrothermal plume*, Geochimica et Cosmochimica Acta, 72*, 2268-2286.

Lam, P., G. Lavik, M. M. Jensen, J. van de Vossenberg, M. Schmid, D. Woebken, D. Gutiérrez, R. Amann, M. S. M. Jetten, and M. M. M. Kuypers (2009), Revising the nitrogen cycle in the Peruvian oxygen minimum zone*, Proceedings of the National Academy of Sciences USA, 106*, 4752-4757.

Lavik, G., T. Stührmann, V. Brüchert, A. Van der Plas, V. Mohrholz, P. Lam, M. Mumann, B. M. Fuchs, R. Amann, U. Lass, and M. M. M. Kuypers (2009), Detoxification of sulphidic African shelf waters by blooming chemolithotrophs*, Nature, 457*, 581-584.

Lee, R. W. and J. J. Childress (1994), Assimilation of inorganic nitrogen by marine invertebrates and their chemoautotrophic and methanotrophic symbionts*, Applied and Environmental Microbiology, 60*, 1852-1858.

Lehmann, M. F., P. Reichert, S. M. Bernasconi, A. Barbieri, and J. A. McKenzie (2003), Modelling nitrogen and oxygen isotope fractionation during denitrification in a lacustrine redox-transition zone*, Geochimica et Cosmochimica Acta, 67*, 2529-2542.

Lehmann, M. F., D. M. Sigman, and W. M. Berelson (2004), Coupling the $^{15}N/^{14}N$ and $^{18}O/^{16}O$ of nitrate as a constraint on benthic nitrogen cycling*, Marine Chemistry, 88*, 1-20.

Lehmann, M. F., D. M. Sigman, D. C. McCorkle, B. G. Brunelle, S. S. Hoffmann, M. Kienast, G. Cane, and J. Clement (2005), Origin of the deep Bering Sea nitrate deficit: Constraints from the nitrogen and oxygen isotopic composition of water column nitrate and benthic nitrate fluxes*, Global Biogeochemical Cycles, 19*, GB4005, doi:10.1029/2005GB002508.

Lehmann, M. F., D. M. Sigman, D. C. McCorkle, J. Granger, S. Hoffmann, G. Cane, and B. G. Brunelle (2007), The distribution of nitrate $^{15}N/^{14}N$ in marine sediments and the impact of benthic nitrogen loss on the isotopic composition of oceanic nitrate*, Geochimica et Cosmochimica Acta, 71*, 5384-5404.

Lehmann, M. F., B. Barnett, Y. Gélinas, D. Gilbert, R. J. Maranger, A. Mucci, B. Sundby, and B. Thibodeau (2009), Aerobic respiration and hypoxia in the Lower St. Lawrence Estuary: Stable isotope ratios of dissolved oxygen constrain oxygen sink partitioning*, Limnology and Oceanography, 54*, 2157-2169.

Levesque, C., H. Limén, and S. K. Juniper (2005), Origin, composition and nutritional quality of particulate matter at deep-sea hydrothermal vents on Axial Volcano, NE

Pacific*, Marine Ecology Progress Series, 289*, 43-52.

Levine, N. M., M. L. Bender, and S. C. Doney (2009), The $\delta^{18}O$ of dissolved $O_2$ as a tracer of mixing and respiration in the mesopelagic ocean*, Global Biogeochemical Cycles, 23*, GB1006, doi:10.1029/2007GB003162.

Lilley, M. D., D. A. Butterfield, E. J. Olson, J. E. Lupton, S. A. Macko, and R. E. McDuff (1993), Anomalous $CH_4$ and $NH_4^+$ concentrations at an unsedimented mid-ocean-ridge hydrothermal system*, Nature, 364*, 45-47.

Liu, K.-K., and I. R. Kaplan (1989), The eastern tropical Pacific as a source of $^{15}N$-enriched nitrate in seawater off southern California, *Limnology and Oceanography*, *34*(5), 820-830.

Liu, K.-K., M.-J. Su, C.-R. Hsueh, and G.-C. Gong (1996), The N isotopic composition of nitrate in the Kuroshio Water northeast of Taiwan: evidence for N fixation as a source of isotopically light nitrate, *Marine Chemistry*, *54*, 273-292.

Liu, X., S. M. Tiquia, G. Holguin, L. Wu, S. C. Nold, A. H. Devol, K. Luo, A. V. Palumbo, J. M. Tiedje, and J. Zhou (2003), Molecular diversity of denitrifying genes in continental margin sediments within the oxygen-deficient zone off the Pacific coast of Mexico*, Applied and Environmental Microbiology, 69*, 3549-3560.

López-García, P., F. Gaill, and D. Moreira (2002), Wide bacterial diversity associated with tubes of the vent worm *Riftia pachyptila, Environmental Microbiology, 4*, 204-215.

López-García, P., S. Duperron, P. Philippot, J. Foriel, J. Susini, and D. Moreira (2003), Bacterial diversity in hydrothermal sediment and epsilon proteobacterial dominance in experimental microcolonizers at the Mid-Atlantic Ridge*, Environmental Microbiology, 5*, 961-976.

Lozupone, C. and R. Knight (2005), UniFrac: a new phylogenetic method for comparing microbial communities*, Applied and Environmental Microbiology, 71*, 8228-8235.

Manning, C. C., R. C. Hamme, and A. Bourbonnais (2010), Impact of deep-water renewal events on fixed nitrogen loss from seasonally-anoxic Saanich Inlet*, Marine Chemistry, 122*, 1-10.

Marino, R., F. Chan, R. W. Howarth, M. L. Pace, and G. E. Likens (2006), Ecological constraints on planktonic nitrogen fixation in saline estuaries. I. Nutrient and trophic controls, *Marine Ecology Progress Series*, *309*, 25-39.

Mariotti, A., J. C. Germon, P. Hubert, P. Kaiser, R. Letolle, A. Tardieux, and P. Tardieux (1981), Experimental determination of nitrogen kinetic isotope fractionation: some principles; illustration for the denitrification and nitrification processes*, Plant Soil, 62*, 413-430.

Martin, A. P. (2002), Phylogenetic approaches for describing and comparing the diversity

of microbial communities*, Applied and Environmental Microbiology, 68*, 3673-3682.

Martin, J. H., *et al.* (1994), Testing the iron hypothesis in ecosystems of the equatorial Pacific Ocean, *Nature, 371*, 123-129.

Marty, B. and F. Humbert (1997), Nitrogen and argon isotopes in oceanic basalts*, Earth and Planetary Science Letters, 152*, 101-112.

McCollom, T. M. and E. L. Shock (1997), Geochemical constraints on chemolithoautotrophic metabolism by microorganisms in seafloor hydrothermal systems*, Geochimica et Cosmochimica Acta, 61*, 4375-4391.

McElroy, M. B., (1983), Marine biological controls on atmospheric $CO_2$ climate, *Nature*, *302*, 328-329.

McHatton, S. C., J. P. Barry, H. W. Jannasch, and D. C. Nelson (1996), High nitrate concentrations in vacuolate, autotrophic marine *Beggiatoa* spp*, Applied and Environmental Microbiology, 62*, 954-958.

Mehta, M. P. and J. A. Baross (2006), Nitrogen Fixation at 92$^{o}$C by a Hydrothermal Vent Archaeon*, Science, 314*, 1783-1786.

Mehta, M. P., D. A. Butterfield, and J. A. Baross (2003), Phylogenetic diversity of nitrogenase (*nifH*) genes in deep-sea and hydrothermal vent environments of the Juan de Fuca Ridge*, Applied and Environmental Microbiology, 69*, 960-970.

Mehta, M. P., J. A. Huber, and J. A. Baross (2005), Incidence of novel and potentially archaeal nitrogenase genes in the deep Northeast Pacific Ocean*, Environmental Microbiology, 7*, 1525-1534.

Middelburg, J. J., K. Soetaert, P. M. J. Herman, and C. H. R. Heip (1996), Denitrification in marine sediments: A model study, *Global Biogeochemical Cycles*, *10*, 661-673.

Minagawa, M. and E. Wada (1984), Stepwise enrichment of $^{15}$N along food chains: Further evidence and the relation between $^{15}$N and animal age*, Geochimica et Cosmochimica Acta, 48*, 1135-1140.

Moisander, P. H., R. A. Beinart, I. Hewson, A. E. White, K. S. Johnson, C. A. Carlson, J. P. Montoya, and J. P. Zehr (2010), Unicellular cyanobacterial distributions broaden the oceanic $N_2$ fixation domain*, Science, 327*, 1512-1514.

Montoya, J. P., E. J. Carpenter, and D. G. Capone (2002), Nitrogen fixation and nitrogen isotope abundances in zooplankton of the oligotrophic North Atlantic*, Limnology and Oceanography, 47*, 1617-1628.

Moyer, C. L., F. C. Dobbs, and D. M. Karl (1995), Phylogenetic diversity of the bacterial community from a microbial mat at an active, hydrothermal vent system, Loihi Seamount, Hawaii*, Applied and Environmental Microbiology, 61*, 1555-1562.

Mulder, C., E. Bazeley-White, P. Dimitrakopoulos, A. Hector, M. Scherer-Lorenzen, and B. Schmid (2004), Species evenness and productivity in experimental plant communities, *Oikos, 107*, 50-63.

Nakagawa, S., K. Takai, F. Inagaki, H. Hirayama, T. Nunoura, K. Horikoshi, and Y. Sako (2005a), Distribution, phylogenetic diversity and physiological characteristics of epsilon-Proteobacteria in a deep-sea hydrothermal field, *Environmental Microbiology, 7*, 1619-1632.

Nakagawa, S., F. Inagaki, K. Takai, K. Horikoshi, and Y. Sako (2005b), *Nitratiruptor tergarcus gen*. nov., sp. nov. and *Nitratifractor salsuginis* gen. nov., sp. nov., nitrate-reducing chemolithoautotrophs of the ε-Proteobacteria isolated from a deep-sea hydrothermal system in the Mid-Okinawa Trough, *International Journal of Systematic and Evolutionary Microbiology, 55*, 925-933.

Nakagawa S., K. Takai, F. Inagaki, K. Horikoshi, and Y. Sako (2005c), *Thioreductor micantisoli* gen.nov., sp. nov., a novel mesophilic, sulfur-reducing chemolithoautotroph within the ε-Proteobacteria isolated from hydrothermal sediments in the Mid-Okinawa Trough, *International Journal of Systematic and Evolutionary Microbiology*, 55, 599-605.

Nakagawa, S., Y. Takaki, S. Shimamura, A. L. Reysenbach, K. Takai, and K. Horikoshi (2007), Deep-sea vent ε-proteobacterial genomes provide insights into emergence of pathogens, *Proceedings of the National Academy of Sciences, 104*, 12146-12150.

Nakatsuka, T., N. Handa, E. Wada, and C. S. Wong (1992), The dynamic changes of stable isotopic ratios of carbon and nitrogen in suspended and sedimented particulate organic matter during a phytoplankton bloom, *Journal of Marine Research, 50*, 267-296.

Naqvi, S. W. A., R. J. Noronha, K. Somasundar, and R. SenGupta (1990), Seasonal changes in the denitrification regime of the Arabian Sea, *Deep Sea Research Part A, 37,* 593-611.

Naqvi, S., H. Naik, A. Pratihary, W. D'Souza, P. Narvekar, D. Jayakumar, A. Devol, T. Yoshinari, and T. Saino (2006), Coastal versus open-ocean denitrification in the Arabian Sea, *Biogeosciences, 3*, 621-633.

Nicholls, J. C., I. M. Davies and M. Trimmer (2007), High-resolution profiles and N isotope tracing reveal a dominant source of nitrous oxide and multiple pathways of N gas formation in the central Arabian Sea, *Limnology and Oceanography, 52*, 156-168.

Nielsen, L. P. (1992), Denitrification in sediment determined from nitrogen isotope pairing, *FEMS Microbiology Letters, 86*, 357-362.

Niemi, A. (1979), Blue-green algal blooms and N:P ratios in the Baltic Sea, *Acta Botanica Fennica*, *110*, 57-61.

Nogales, B., K. N. Timmis, D. B. Nedwell, and A. M. Osborn (2002), Detection and diversity of expressed denitrification genes in estuarine sediments after reverse transcription-PCR amplification from mRNA*, Applied and Environmental Microbiology, 68*, 5017-5025.

Oakley, B. B., C. A. Francis, K. J. Roberts, C. A. Fuchsman, S. Srinivasan, and J. T. Staley (2007), Analysis of nitrite reductase (*nirK* and *nirS*) genes and cultivation reveal depauperate community of denitrifying bacteria in the Black Sea suboxic zone*, Environmental Microbiology, 9*, 118-130.

Opatkiewicz, A. D., D. A. Butterfield, and J. A. Baross (2009), Individual hydrothermal vents at Axial Seamount harbor distinct subseafloor microbial communities*, FEMS Microbiology Ecology, 70*, 413-424

Opdyke, M. R. and M. B. David (2007), Response of sediment denitrification rates to environmental variables in streams heavily impacted by agriculture*, Journal of Freshwater Ecology, 22*, 371-382.

Paull, C. K., A. J. T. Jull, L. J. Toolin, and T. Linick (1985), Stable isotope evidence for chemosynthesis in an abyssal seep community*, Nature, 317*, 709-711.

Penton, C. R., A. H. Devol, and J. M. Tiedje (2006), Molecular evidence for the broad distribution of anaerobic ammonium-oxidizing bacteria in freshwater and marine sediments*, Applied and Environmental Microbiology, 72*, 6829-6832.

Perez-Rodriguez, I., J. Ricci, J. W. Voordeckers, V. Starovoytov, and C. Vetriani (2010), *Nautilia nitratireducens* sp. nov., a thermophilic, anaerobic, chemosynthetic, nitrate-ammonifying bacterium isolated from a deep-sea hydrothermal vent*, International Journal of Systematic and Evolutionary Microbiology, 60*, 1182-1186.

Price, M. N., P. S. Dehal, and A. P. Arkin (2010), FastTree 2–approximately maximum-likelihood trees for large alignments*, PLoS One, 5*(3), e9490. doi:10.1371/journal.pone.0009490.

Priemé, A., G. Braker, and J. M. Tiedje (2002), Diversity of nitrite reductase (*nirK* and *nirS*) gene fragments in forested upland and wetland soils*, Applied and Environmental Microbiology, 68*, 1893-1900.

Proctor, L. M. (1997), Nitrogen-fixing, photosynthetic, anaerobic bacteria associated with pelagic copepods*, Aquatic Microbial Ecology, 12*, 105-113.

Prospero, J., K. Barrett, T. Church, F. Dentener, R. Duce, J. Galloway, H. Levy, J. Moody, and P. Quinn (1996), Atmospheric deposition of nutrients to the North Atlantic Basin*, Biogeochemistry, 35*, 27-73.

Rau, G. H. (1981), Low $^{15}N/^{14}N$ in hydrothermal vent animals: ecological implications*, Nature, 289*, 484-485.

Ravenschlag, K., K. Sahm, J. Pernthaler, and R. Amann (1999), High bacterial diversity in permanently cold marine sediments, *Applied and Environmental Microbiology, 65*, 3982-3989.

Reed, D. C., C. P. Slomp, and B. G. Gustafsson (2011), Sedimentary phosphorus dynamics and the evolution of bottom-water hypoxia: A coupled benthic-pelagic model of a coastal system, *Limnology and Oceanography, 56*, 1075-1092.

Risgaard-Petersen, N., R. L. Meyer, and N. P. Revsbech (2005), Denitrification and anaerobic ammonium oxidation in sediments: effects of microphytobenthos and $NO_3^-$, *Aquatic Microbial Ecology, 40*, 67-76.

Robinson, R. S., A. Mix, and P. Martinez (2007), Southern Ocean control on the extent of denitrification in the southeast Pacific over the last 70 ka, *Quaternary Science Reviews, 26*(1-2), 201-212.

Roussel-Delif, L., S. Tarnawski, J. Hamelin, L. Philippot, M. Aragno, and N. Fromin (2005), Frequency and diversity of nitrate reductase genes among nitrate-dissimilating *Pseudomonas* in the rhizosphere of perennial grasses grown in field conditions, *Microbial Ecology, 49*, 63-72.

Saleh-Lakha, S., K. E. Shannon, S. L. Henderson, C. Goyer, J. T. Trevors, B. J. Zebarth, and D. L. Burton (2009), Effect of pH and temperature on denitrification gene expression and activity in *Pseudomonas mandelii, Applied and Environmental Microbiology, 75*, 3903-3911.

Santoro, A. E., A. B. Boehm, and C. A. Francis (2006), Denitrifier community composition along a nitrate and salinity gradient in a coastal aquifer, *Applied and Environmental Microbiology, 72*, 2102-2109.

Sarrazin, J., P. Rodier, M. K. Tivey, H. Singh, A. Schultz, and P. M. Sarradin (2009), A dual sensor device to estimate fluid flow velocity at diffuse hydrothermal vents, *Deep Sea Research Part I, 56*, 2065-2074.

Scala. D. J., and L. J. Kerkhof (1998), Nitrous oxide reductase (*nosZ*) gene specific PCR primers for detection of denitrifiers and three *nosZ* genes from marine sediments. *FEMS Microbiology Letters, 162*, 61-68.

Schloss, P. D., S. L. Westcott, T. Ryabin, J. R. Hall, M. Hartmann, E. B. Hollister, R. A. Lesniewski, B. B. Oakley, D. H. Parks, and C. J. Robinson (2009), Introducing mothur: open-source, platform-independent, community-supported software for describing and comparing microbial communities, *Applied and Environmental Microbiology, 75*, 7537-7541.

Schoonen, M. A. A. and Y. Xu (2001), Nitrogen reduction under hydrothermal vent conditions: Implications for the prebiotic synthesis of CHON compounds, *Astrobiology, 1*, 133-142.

Schrenk, M. O., J. A. Huber, and K. J. Edwards (2010), Microbial provinces in the subseafloor*, Annual Review of Marine Science, 2*, 279-304.

Schultz, A. and H. Elderfield (1997), Controls on the physics and chemistry of seafloor hydrothermal circulation*, Philosophical Transactions of the Royal Society of London. Series A: Mathematical, Physical and Engineering Sciences, 355*, 387-425.

Sebilo, M., G. Billen, M. Grably, and A. Mariotti (2003), Isotopic composition of nitrate –nitrogen as a marker of riparian and benthic denitrification at the scale of the whole Seine River system, *Biogeochemistry*, *63*(1), 35-51.

Sellner, K. G. (1997), Physiology, ecology, and toxic properties of marine cyanobacteria blooms*, Limnology and Oceanography*, *42*, 1089-1104.

Seyfried Jr, W. (1987), Experimental and theoretical constraints on hydrothermal alteration processes at mid-ocean ridges*, Annual Review of Earth and Planetary Sciences, 15*, 317-335.

Shao, M. F., T. Zhang, and H. H. P. Fang (2010), Sulfur-driven autotrophic denitrification: diversity, biochemistry, and engineering applications*, Applied Microbiology and Biotechnology, 88*, 1027-1042.

Shiller, A. M., J. M. Gieskes, and N. Brian Price (1985), Particulate iron and manganese in the Santa Barbara Basin, California*, Geochimica et Cosmochimica Acta, 49*, 1239-1249.

Sievert, S. M., E. Wieringa, C. O. Wirsen, and C. D. Taylor (2007), Growth and mechanism of filamentous-sulfur formation by Candidatus *Arcobacter sulfidicus* in opposing oxygen-sulfide gradients*, Environmental Microbiology, 9*, 271-276.

Sievert, S. M., K. M. Scott, M. G. Klotz, P. S. G. Chain, L. J. Hauser, J. Hemp, M. Hügler, M. Land, A. Lapidus, and F. W. Larimer (2008), Genome of the epsilonproteobacterial chemolithoautotroph *Sulfurimonas denitrificans, Applied and Environmental Microbiology, 74*, 1145-1156.

Sigman, D. M. and K. L. Casciotti (2001), Nitrogen isotopes in the ocean, in *Encyclopedia of Ocean Sciences*, edited by J. H. Steele, S. A. Thorpe, and K. K. Turekian, pp. 1884-1894, Academic Press, New York.

Sigman, D. M., M. A. Altabet, R. Michener, D. C. McCorkle, B. Fry, and R. M. Holmes (1997), Natural abundance-level measurement of the nitrogen isotopic composition of oceanic nitrate: an adaptation of the ammonia diffusion method*, Marine Chemistry, 57*, 227-242.

Sigman, D., M. Altabet, D. McCorkle, R. Francois, and G. Fischer (1999), The $d^{15}N$ of nitrate in the Southern Ocean: Consumption of nitrate in surface waters*, Global Biogeochemical Cycles, 13*, 1149-1166.

Sigman, D. M., K. L. Casciotti, M. Andreani, C. Barford, M. Galanter, and J. K. Böhlke (2001), A bacterial method for the nitrogen isotopic analysis of nitrate in seawater and freshwater, *Analytical Chemistry, 73*, 4145-4153.

Sigman, D. M., R. Robinson, A. N. Knapp, A. van Geen, D. C. McCorkle, J. A. Brandes, and R. C. Thunell (2003), Distinguishing between water column and sedimentary denitrification in the Santa Barbara Basin using the stable isotopes of nitrate, *Geochemistry Geophysics Geosystems, 4*, 1040.

Sigman, D. M., J. Granger, P. J. DiFiore, M. M. Lehmann, R. Ho, G. Cane, and A. van Geen (2005), Coupled nitrogen and oxygen isotope measurements of nitrate along the eastern North Pacific margin, *Global Biogeochemical Cycles, 19*, GB4022, doi:10.1029/2005GB002458

Sigman, D. M., P. J. DiFiore, M. P. Hain, C. Deutsch, Y. Wang, D. M. Karl, A. N. Knapp, M. F. Lehmann, and S. Pantoja (2009), The dual isotopes of deep nitrate as a constraint on the cycle and budget of oceanic fixed nitrogen, *Deep Sea Research I, 56*, 1419-1439.

Smith, L. K., M. A. Voytek, J. K. Böhlke, and J. W. Harvey (2006), Denitrification in nitrate-rich streams: application of $N_2$: Ar and $^{15}N$-tracer methods in intact cores, *Ecological Applications, 16*, 2191-2207.

Smith, C. J., D. B. Nedwell, L. F. Dong, and A. M. Osborn (2007), Diversity and abundance of nitrate reductase genes (*narG* and *napA*), nitrite reductase genes (*nirS* and *nrfA*), and their transcripts in estuarine sediments, *Applied and Environmental Microbiology, 73*, 3612-3622.

Smith, W., A. R. Solow, and P. E. Preston (1996), An estimator of species overlap using a modified beta-binomial model, *Biometrics*, *52*, 1472-1477.

Solorzano, L. (1969), Determination of ammonia in natural waters by the phenolhypochlorite method, *Limnology and Oceanography*, *14*, 799-801.

Stevens, H. and O. Ulloa (2008), Bacterial diversity in the oxygen minimum zone of the eastern tropical South Pacific, *Environmental Microbiology, 10*, 1244-1259.

Stewart, F. J., O. Ulloa, and E. F. DeLong (2012), Microbial metatranscriptomics in a permanent marine oxygen minimum zone, *Environmental Microbiology, 14*(1):23-40.

Stramma, L., G. C. Johnson, J. Sprintall, and V. Mohrholz (2008), Expanding oxygen-minimum zones in the tropical oceans, *Science, 320*, 655-658.

Stres, B., I. Mahne, G. Avgustin, and J. M. Tiedje (2004), Nitrous oxide reductase (*nosZ*) gene fragments differ between native and cultivated Michigan soils, *Applied and Environmental Microbiology, 70*, 301-309.

Strous, M., E. Van Gerven, J. G. Kuenen and M, Jetten (1997), Effects of aerobic and microaerobic conditions on anaerobic ammonium-oxidizing (Anammox) sludge. *Applied and Environmental Microbiology, 63*, 2446-2448.

Strous, M., J. A. Fuerst, E. H. M. Kramer, S. Logemann, G. Muyzer, K. T. Van De Pas-Schoonen, R. Webb, J. G. Kuenen, and M. S. M. Jetten (1999), Missing lithotroph identified as new planctomycete*, Nature, 400*, 446-449.

Sunamura, M., Y. Higashi, C. Miyako, J. Ishibashi, and A. Maruyama (2004), Two bacteria phylotypes are predominant in the Suiyo seamount hydrothermal plume*, Applied and Environmental Microbiology, 70*, 1190-1198.

Sweeney, R.E., and I. R. Kaplan (1980), Natural abundances of $^{15}N$ as a source indicator for near-shore marine sedimentary and dissolved nitrogen, *Marine Chemistry*, *9*, 81-94.

Takai, K., K. H. Nealson, and K. Horikoshi (2004), *Hydrogenimonas thermophila* gen. nov., sp. nov., a novel thermophilic, hydrogen-oxidizing chemolithoautotroph within the ε-Proteobacteria, isolated from a black smoker in a Central Indian Ridge hydrothermal field*, International Journal of Systematic and Evolutionary Microbiology, 54*, 25-32.

Takai, K., M. Suzuki, S. Nakagawa, M. Miyazaki, Y. Suzuki, F. Inagaki, and K. Horikoshi (2006), *Sulfurimonas paralvinellae* sp. nov., a novel mesophilic, hydrogen-and sulfur-oxidizing chemolithoautotroph within the Epsilonproteobacteria isolated from a deep-sea hydrothermal vent polychaete nest, reclassification of *Thiomicrospira denitrificans* as *Sulfurimonas denitrificans* comb. nov. and emended description of the genus *Sulfurimonas, International Journal of Systematic and Evolutionary Microbiology, 56*, 1725-1733.

Tal, Y., J. E. Watts, and H. J. Schreier (2005), Anaerobic ammonia-oxidizing bacteria and related activity in Baltimore inner harbour sediment, *Applied and Environmental Microbiology, 71*, 1816-1821.

Tamegai, H., L. Li, N. Masui, and C. Kato (1997), A denitrifying bacterium from the deep sea at 11 000-m depth*, Extremophiles, 1*, 207-211.

Thamdrup, B. and T. Dalsgaard (2002), Production of $N_2$ through anaerobic ammonium oxidation coupled to nitrate reduction in marine sediments*, Applied and Environmental Microbiology, 68*, 1312-1318.

Thamdrup, B., T. Dalsgaard, M. M. Jensen, O. Ulloa, L. Farías, and R. Escribano (2006), Anaerobic ammonium oxidation in the oxygen-deficient waters off northern Chile, *Limnology and Oceanography*, *51*(5), 2145-2156.

Thompson, J. D., D. G. Higgins, and T. J. Gibson (1994), CLUSTAL W: improving the sensitivity of progressive multiple sequence alignment through sequence weighting, position-specific gap penalties and weight matrix choice*, Nucleic Acids Research, 22*, 4673-4680.

Thompson, J. R., L. A. Marcelino, and M. F. Polz (2002), Heteroduplexes in mixed-template amplifications: formation, consequence and elimination by 'reconditioning PCR', *Nucleic Acids Research, 30*, 2083-2088.

Throbäck, I. N., K. Enwall, A. Jarvis, and S. Hallin (2004), Reassessing PCR primers targeting *nirS*, *nirK*, and *nosZ* genes community surveys of denitrifying bacteria with DGGE, *FEMS Microbiology Ecology*, *49*(3), 401-417.

Thunell, R. C. and A. B. Kepple (2004), Glacial-holocene $\delta^{15}N$ record from the Gulf of Tehuantepec, Mexico: Implications for denitrification in the eastern Equatorial Pacific and changes in atmospheric $N_2O$, *Global Biogeochemical Cycles, 18*, GB1011, doi:10.1029/2002GB002028.

Thunell, R. C., D. M. Sigman, F. E. Muller-Karger, Y. Astor, and R. Varela (2004), Nitrogen isotope dynamics of the Cariaco Basin, Venezuela*, Global Biogeochemical Cycles, 18,* GB3001, doi:10.1029/2003GB002185.

Timothy, D. A., and M. Y. S. Soon (2001), Primary production and deep-water oxygen content of two British Columbian fjords, *Marine Chemistry*, *73*, 37-51.

Tortell, P. D. (2005), Dissolved gas measurements in oceanic waters made by membrane inlet mass spectrometry*, Limnology and Oceanography: Methods, 3*, 24-37.

Trimmer, M., J. Nicholls, and B. Deflandre (2003), Anaerobic ammonium oxidation measured in sediments along the Thames estuary, United Kingdom, *Applied and Environmental Microbiology, 69*, 6447-6454.

Trimmer, M., J. C. Nicholls, N. Morley, C. A. Davies, and J. Aldridge (2005), Biphasic behavior of anammox regulated by nitrite and nitrate in an estuarine sediment*, Applied and Environmental Microbiology, 71*, 1923

Tunnicliffe, V. (1991), The biology of hydrothermal vents: ecology and evolution*, Oceanography and Marine Biology, 29*, 319-407.

Tunnicliffe, V., S. K. Juniper, and M. E. De Burgh (1985), The hydrothermal vent community on Axial Seamount, Juan de Fuca Ridge*, Bulletin of the Biological Society of Washington, 6,* 453-464.

Tyrrell, T., and M. I. Lucas (2002), Geochemical evidence of denitrification in the Benguela upwelling system, *Continental Shelf Research*, *22*(17), 2497-2511.

Richards, F. A. (1965), Anoxic basins and fjords. In: Riley, J.P., Skirrow, G. (Eds.), Chemical Oceanography, volume 1, Academic Press, London, pp. 611–645.

Van Dover, C. L. (2002), Trophic relationships among invertebrates at the Kairei hydrothermal vent field (Central Indian Ridge)*, Marine Biology, 141*, 761-772.

Van Dover, C. L. and B. Fry (1994), Microorganisms as food resources at deep-sea

hydrothermal vents*, Limnology and Oceanography, 39*, 51-57.

Velinsky, D. J., M. L. Fogel, J. F. Todd, and B. M. Tebo (1991), Isotopic fractionation of dissolved ammonium at the oxygen-hydrogen sulfide interface in anoxic waters, *Geophysical Research Letters, 18,* (4), 649-652.

Vetriani, C., M. D. Speck, S. V. Ellor, R. A. Lutz, and V. Starovoytov (2004), *Thermovibrio ammonificans* sp. nov., a thermophilic, chemolithotrophic, nitrate-ammonifying bacterium from deep-sea hydrothermal vents*, International Journal of Systematic and Evolutionary Microbiology, 54*, 175-181.

Voordeckers, J. W., V. Starovoytov, and C. Vetriani (2005), *Caminibacter mediatlanticus* sp. nov., a thermophilic, chemolithoautotrophic, nitrate-ammonifying bacterium isolated from a deep-sea hydrothermal vent on the Mid-Atlantic Ridge*, International Journal of Systematic and Evolutionary Microbiology, 55*, 773-779.

Voss, M., J. W. Dippner, and J. P. Montoya (2001), Nitrogen isotope patterns in the oxygen-deficient waters of the Eastern Tropical North Pacific Ocean*, Deep Sea Research I, 48*, 1905-1921.

Wallenstein, M. D., D. D. Myrold, M. Firestone, and M. Voytek (2006), Environmental controls on denitrifying communities and denitrification rates: insights from molecular methods*, Ecological Applications, 16*, 2143-2152.

Walsh, D. A., E. Zaikova, C. G. Howes, Y. C. Song, J. J. Wright, S. G. Tringe, P. D. Tortell, and S. J. Hallam (2009), Metagenome of a Versatile Chemolithoautotroph from Expanding Oceanic Dead Zones*, Science, 326*, 578-582.

Wang, F., H. Zhou, J. Meng, X. Peng, L. Jiang, P. Sun, C. Zhang, J. D. Van Nostrand, Y. Deng, and Z. He (2009), GeoChip-based analysis of metabolic diversity of microbial communities at the Juan de Fuca Ridge hydrothermal vent*, Proceedings of the National Academy of Sciences, 106*, 4840-4845.

Wang, Q., G. M. Garrity, J. M. Tiedje, and J. R. Cole (2007), Naive Bayesian classifier for rapid assignment of rRNA sequences into the new bacterial taxonomy*, Applied and Environmental Microbiology, 73*, 5261-5267.

Wankel, S. D., C. Kendall, J. T. Pennington, F. P. Chavez, and A. Paytan (2007), Nitrification in the euphotic zone as evidenced by nitrate dual isotopic composition: Observations from Monterey Bay, California*, Global Biogeochemical Cycles, 21*, GB2009, doi:10.1029/2006GB002723.

Wankel, S. D., L. N. Germanovich, M. D. Lilley, G. Genc, C. J. DiPerna, A. S. Bradley, E. J. Olson, and P. R. Girguis (2011), Influence of subsurface biosphere on geochemical fluxes from diffuse hydrothermal fluids*, Nature Geoscience, 4*, 461-468.

Ward, B. B. (1982), Oceanic distribution of ammonium-oxidizing bacteria determined by immunofluorescent assay*, Journal of Marine Research, 40*, 1155-1172.

Ward, B. B. (2005a), Temporal variability in nitrification rates and related biogeochemical factors in Monterey Bay, California, USA, *Marine Ecology Progress Series*, *292*, 97-109.

Ward, B. B. (2005b), Molecular approaches to marine microbial ecology and the marine nitrogen cycle*, Annual Review of Earth and Planetary Sciences, 33*, 301-333.

Ward, B. B., K. A. Kilpatrick, E. H. Renger, and R. W. Eppley (1989), Biological N cycling in the nitracline, *Limnology and Oceanography*, *34*(3), 493-513.

Ward, B. B., A. H. Devol, J. J. Rich, B. X. Chang, S. E. Bulow, H. Naik, A. Pratihary, and A. Jayakumar (2009), Denitrification as the dominant nitrogen loss process in the Arabian Sea*, Nature, 461*, 78-81.

Waser, N. A. D., P. J. Harrison, B. Nielsen, S. E. Calvert, and D. H. Turpin (1998), Nitrogen isotope fractionation during the uptake and assimilation of nitrate, nitrite, ammonium, and urea by a marine diatom*, Limnology and Oceanography, 43*, 215-224.

Watson, A. J., D. C. E. Bakker, A. J. Ridgwell, P. W. Boyd, and C. S. Law (2000), Effect of iron supply on Southern Ocean $CO_2$ uptake and implications for glacial atmospheric $CO_2$, *Nature, 407*, 730-733.

Weiss, R. F. and B. A. Price (1980), Nitrous oxide solubility in water and seawater*, Marine Chemistry, 8*, 347-359.

Wenk, C. B., J. Blees, J. Zopfi, M. Veronesi, A. Bourbonnais, J. Schubert, H. Niemann, and M. F. Lehmann (2012), Anammox bacteria and sulfide-dependent denitrifiers co-exist in the water column of a meromictic south-alpine lake, *Limnology and Oceanography*, in press.

Xie, W., F. Wang, L. Guo, Z. Chen, S. M. Sievert, J. Meng, G. Huang, Y. Li, Q. Yan, and S. Wu (2010), Comparative metagenomics of microbial communities inhabiting deep-sea hydrothermal vent chimneys with contrasting chemistries*, The ISME Journal, 5*, 414-426.

Yayanos, A. A. (1995), Microbiology to 10,500 meters in the deep sea*, Annual Reviews in Microbiology, 49*, 777-805.

Yool, A., A. P. Martin, C. Fernández, and D. R. Clark (2007), The significance of nitrification for oceanic new production*, Nature, 447*, 999-1002.

Yoshida, N. (1988), $^{15}N$-depleted $N_2O$ as a product of nitrification*, Nature, 335*, 528-529.

Yue, J. C. and M. K. Clayton (2005), A similarity measure based on species proportions*, Communications in Statistics-Theory and Methods, 34*, 2123-2131.

Zaikova, E., D. A. Walsh, C. P. Stilwell, W. W. Mohn, P. D. Tortell, and S. J. Hallam (2010), Microbial community dynamics in a seasonally anoxic fjord: Saanich Inlet, British Columbia*, Environmental Microbiology, 12*, 172-191.

Zehr, J. P., B. D. Jenkins, S. M. Short, and G. F. Steward (2003), Nitrogenase gene diversity and microbial community structure: a cross-system comparison*, Environmental Microbiology, 5*, 539-554.

Zhong, J., C. Fan, G. Liu, L. Zhang, J. Shang, and X. Gu (2010), Seasonal variation of potential denitrification rates of surface sediment from Meiliang Bay, Taihu Lake, China*, Journal of Environmental Sciences, 22*, 961-967.

Zumft, W. G. (1997), Cell biology and molecular basis of denitrification*, Microbiology and Molecular Biology Reviews, 61*, 533-616.

# Appendix A
# Metadata tables

**Table A.1.** Geochemical parameters measured for all hydrothermal vent fluids samples from Axial Volcano (AV), Cobb Segment (CS) and Endeavour Segment (ES) on the Juan de Fuca Ridge (northeast Pacific Ocean) used in this dissertation (chapters 2-4). Generally 1-5 samples were collected at the same exact location during the same dive at each site, and average values were calculated. Samples are classified in alphabetical order by vent fields, by years, and then by vent names, with low (<50°C) to average (<100°C) temperature fluids reported first. The research cruises took place in September 2004, August-September 2006, August 2007, June (2008a), August-September (2008b), and June 2009. √ marks indicate data that are available upon request whereas "na" means data are not available.

| Field/ Vent/ year | Latitude (°N) | Longi-tude (°W) | depth (m) | Avera-ge tempe-rature ($^{o}$C) | pH | [$Mg_2^+$] | [$Si_4^+$] | [$H_2S$] | Nutrients ([$NO_3^-$] (a), [$NO_2^-$] (b), [$NH_4^+$] (c), [$PO_4^{3-}$] (d)) | [$N_2O$] | $\delta^{15}N$- and $\delta^{18}O$-$NO_3^-$ | $\delta^{15}N$-$NH_4^+$ | Denitrifica-tion (a), anammox (b) and DNRA (c) rates |
|---|---|---|---|---|---|---|---|---|---|---|---|---|---|
| AV/ Bag City/ 2004 | 45.9163 | 129.9893 | 1536 | 17.1 ± 0.5 | √ | √ | √ | √ | √ | na | na | na | na |
| AV/ Cloud/ 2004 | 45.9333 | 129.9817 | 1526 | 6.9 | √ | √ | √ | √ | √ | na | na | na | na |
| AV/ Gollum/ 2004 | 45.9336 | 45.9336 | 1546 | 29.4 ± 11.0 | √ | √ | √ | √ | √ | na | na | na | na |
| AV/ Marker 33/ 2004 | 45.9331 | 129.9823 | 1526 | 19.8 | √ | √ | √ | √ | √ | na | na | na | na |
| AV/ Marker 113/ 2004 | 45.9227 | 129.9883 | 1525 | 23.5 ± 0.3 | √ | √ | √ | √ | √ (c only) | na | na | na | na |

**Table A.1.** Continued.

| Field/ Vent/ year | Latitude (°N) | Longi-tude (°W) | depth (m) | Avera-ge tempe-rature ($^{o}$C) | pH | [$Mg_2^+$] | [$Si_4^+$] | [$H_2S$] | Nutrients ([$NO_3^-$] (a), [$NO_2^-$] (b), [$NH_4^+$] (c), [$PO_4^{3-}$] (d)) | [$N_2O$] | $\delta^{15}N$- and $\delta^{18}O$-$NO_3^-$ | $\delta^{15}N$-$NH_4^+$ | Denitrifica-tion (a), anammox (b) and DNRA (c) rates |
|---|---|---|---|---|---|---|---|---|---|---|---|---|---|
| AV/ Marker N3/ 2004 | 45.9438 | 129.9852 | 1528 | 23.0 | √ | √ | √ | √ | √ | na | na | na | na |
| AV/ Marsh-mallow/ 2004 | 45.9337 | 130.0135 | 1546 | 68.2 | √ | √ | √ | √ | √ | na | na | na | na |
| AV/ Village/ 2004 | 45.9261 | 129.9805 | 1522 | 40.6 ± 5.1 | √ | √ | √ | √ | √ | na | na | na | na |
| AV/ Hell-DiveR853/ 2004 | 45.9333 | 130.0141 | 1544 | 174.7 ± 15.1 | √ | √ | √ | √ | √ | na | na | na | na |
| AV/ Hell-DiveR857/ 2004 | 45.9333 | 130.0139 | 1543 | 175.9 | √ | √ | √ | √ | √ (c only) | na | na | na | na |
| AV/ Vixen-DiveR856/ 2004 | 45.9174 | 129.9931 | 1521 | 192.4 ± 0.6 | √ | √ | √ | √ | √ (c only) | na | na | na | na |
| AV/ Vixen-DiveR857/ 2004 | 45.9174 | 129.9931 | 1538 | 184.6 ± 2.9 | √ | √ | √ | √ | √ (c only) | na | na | na | na |

**Table A.1.** Continued.

| Field/ Vent/ year | Latitude (°N) | Longi-tude (°W) | depth (m) | Avera-ge tempe-rature (°C) | pH | $[Mg_2^+]$ | $[Si_4^+]$ | $[H_2S]$ | Nutrients ($[NO_3^-]$ (a), $[NO_2^-]$ (b), $[NH_4^+]$ (c), $[PO_4^{3-}]$ (d)) | $[N_2O]$ | $\delta^{15}N$- and $\delta^{18}O$-$NO_3^-$ | $\delta^{15}N$-$NH_4^+$ | Denitrifica-tion (a), anammox (b) and DNRA (c) rates |
|---|---|---|---|---|---|---|---|---|---|---|---|---|---|
| AV/ VM/ 2004 | 45.9337 | 130.0134 | 1546 | 170.4 | √ | √ | √ | √ | √ (c only) | na | na | na | na |
| AV/ Bag City/ 2006 | 45.9163 | 129.9892 | 1536 | 14.7 ± 0.0 | √ | √ | √ | √ | √ | na | √ | na | na |
| AV/ Forum/ 2006 | 45.9466 | 129.9834 | 1529 | 77.5 ± 4.3 | √ | √ | √ | √ | √ | na | √ | na | na |
| AV/ Gollum/ 2006 | 45.9336 | 130.0133 | 1546 | 27.7 ± 2.3 | √ | √ | √ | √ | √ | na | √ | na | na |
| AV/ Marker 33/ 2006 | 45.9332 | 129.9823 | 1524 | 18.2 ± 0.2 | √ | √ | √ | √ | √ | na | na | na | na |
| AV/ Marker 113/ 2006 | 45.9227 | 129.9884 | 1524 | 28.3 ± 0.1 | √ | √ | √ | √ | √ | na | na | √ | na |
| AV/ Marker N3(52)/ 2006 | 45.9436 | 129.9852 | 1530 | 24.0 ± 0.7 | √ | √ | √ | √ | √ | na | √ | na | na |
| AV/ Mush-room/ 2006 | 45.9336 | 130.0136 | 1547 | 57.1 ± 1.8 | √ | √ | √ | √ | √ | na | √ | na | na |

**Table A.1.** Continued.

| Field/ Vent/ year | Latitude (°N) | Longi-tude (°W) | depth (m) | Avera-ge tempe-rature ($^{o}$C) | pH | [$Mg_2^+$] | [$Si_4^+$] | [$H_2S$] | Nutrients ([$NO_3^-$] (a), [$NO_2^-$] (b), [$NH_4^+$] (c), [$PO_4^{3-}$] (d)) | [$N_2O$] | $\delta^{15}N$- and $\delta^{18}O$-$NO_3^-$ | $\delta^{15}N$-$NH_4^+$ | Denitrifica-tion (a), anammox (b) and DNRA (c) rates |
|---|---|---|---|---|---|---|---|---|---|---|---|---|---|
| AV/ Vixen/ 2006 | 45.9172 | 129.9930 | 1538 | 28.5 ± 0.1 | √ | √ | √ | √ | √ | na | √ | na | na |
| AV/ Casper/ 2006 | 45.9175 | 129.9930 | 1538 | 290.4 ± 0.6 | √ | √ | √ | √ | √ | na | na | na | na |
| AV/ El Guapo /2006 | 45.9266 | 129.9799 | 1509 | 312.3 ± 22.0 | √ | √ | √ | √ | √ | na | na | na | na |
| AV/ Hell /2006 | 45.9333 | 130.0139 | 1543 | 102.6 ± 13.2 | √ | √ | √ | √ | √ | na | √ | √ | na |
| AV/ Inferno /2006 | 45.9336 | 130.0136 | 1544 | 264.2 ± 20.6 | √ | √ | √ | √ | √ | na | na | √ | na |
| AV/ VM /2006 | 45.9337 | 130.0131 | 1546 | 246.5 ± 2.5 | √ | √ | √ | √ | √ | na | na | √ | na |
| AV/ Bag City /2007 | 45.9163 | 129.9893 | 1533 | 13.7 ± 0.9 | √ | √ | √ | √ | √ | na | √ | na | na |
| AV/ Cloud /2007 | 45.9333 | 129.9817 | 1521 | 6.5 ± 0.2 | √ | √ | √ | √ | √ | na | √ | na | na |
| AV/ Dave/ 2007 | 45.9334 | 130.0136 | 1543 | 11.6 | √ | √ | √ | √ | √ | na | √ | na | na |

**Table A.1.** Continued.

| Field/ Vent/ year | Latitude (°N) | Longi-tude (°W) | depth (m) | Avera-ge tempe-rature ($^{o}$C) | pH | [$Mg_2^+$] | [$Si_4^+$] | [$H_2S$] | Nutrients ([$NO_3^-$] (a), [$NO_2^-$] (b), [$NH_4^+$] (c), [$PO_4^{3-}$] (d)) | [$N_2O$] | $\delta^{15}N$- and $\delta^{18}O$-$NO_3^-$ | $\delta^{15}N$-$NH_4^+$ | Denitrifica-tion (a), anammox (b) and DNRA (c) rates |
|---|---|---|---|---|---|---|---|---|---|---|---|---|---|
| AV/ Escargot/ 2007 | 45.9263 | 129.9792 | 1516 | 94.8 ± 1.9 | √ | √ | √ | √ | √ | na | √ | √ | na |
| AV/ Forum/ 2007 | 45.9465 | 129.9839 | 1524 | 6.2 ± 0.3 | √ | √ | √ | √ | √ | na | √ | na | na |
| AV/ Gollum /2007 | 45.9335 | 130.0134 | 1544 | 22.0 ± 0.5 | √ | √ | √ | √ | √ | na | √ | √ | na |
| AV/ Hermosa/ 2007 | 45.9265 | 129.9794 | 1515 | 20.8 | √ | na | √ | √ | √ | na | √ | na | na |
| AV/ Inferno/ 2007 | 45.9337 | 130.0137 | 1542 | 17.3 | √ | √ | √ | √ | √ | na | √ | na | na |
| AV/ Marker 33 RAS-Dive J2-289/ 2007 | 45.9332 | 129.9824 | 1520 | 13.7 ± 4.8 | √ | √ | √ | √ | √ | na | √ | na | na |
| AV/ Marker 33 RAS-Dive J2-291/ 2007 | 45.9331 | 129.9824 | 1521 | 21.0 | na | √ | √ | √ | √ | na | √ | na | na |

**Table A.1.** Continued.

| Field/ Vent/ year | Latitude (°N) | Longi-tude (°W) | depth (m) | Avera-ge tempe-rature ($^{o}$C) | pH | [$Mg_2^+$] | [$Si_4^+$] | [$H_2S$] | Nutrients ([$NO_3^-$] (a), [$NO_2^-$] (b), [$NH_4^+$] (c), [$PO_4^{3-}$] (d)) | [$N_2O$] | $\delta^{15}N$- and $\delta^{18}O$-$NO_3^-$ | $\delta^{15}N$-$NH_4^+$ | Denitrifica-tion (a), anammox (b) and DNRA (c) rates |
|---|---|---|---|---|---|---|---|---|---|---|---|---|---|
| AV/ Marker 113/ 2007 | 45.9227 | 129.9883 | 1523 | 31.2 ± 0.4 | √ | √ | √ | √ | √ | na | √ | √ | na |
| AV/ Marker N3/ 2007 | 45.9439 | 129.9852 | 1527 | 24.6 ± 0.6 | √ | √ | √ | √ | √ | na | √ | √ | na |
| AV/ Ropos/ 2007 | 45.9333 | 130.0138 | 1542 | 31.8 | √ | √ | √ | √ | √ | na | √ | na | na |
| AV/ Shepherd/ 2007 | 45.9888 | 130.0275 | 1582 | 24.4 ± 3.8 | √ | √ | √ | √ | √ | na | √ | √ | na |
| AV/ T&S /2007 | 45.9892 | 130.0276 | 1580 | 73.0 | √ | √ | √ | √ | √ | na | √ | √ | na |
| AV/ T&S/ 2007 | 45.9891 | 130.0277 | 1580 | 39.7 ± 4.6 | √ | √ | √ | √ | √ | na | √ | √ | na |
| AV/ the Spot/ 2007 | 45.9173 | 129.9931 | 1535 | 30.0 ± 0.1 | √ | √ | √ | √ | √ | na | √ | √ | na |
| AV/ Village /2007 | 45.9262 | 129.9806 | 1520 | 22.7 ± 0.1 | √ | √ | √ | √ | √ | na | √ | na | na |

**Table A.1.** Continued.

| Field/ Vent/ year | Latitude (°N) | Longi-tude (°W) | depth (m) | Avera-ge tempe-rature (°C) | pH | [$Mg_2^+$] | [$Si_4^+$] | [$H_2S$] | Nutrients ([$NO_3^-$] (a), [$NO_2^-$] (b), [$NH_4^+$] (c), [$PO_4^{3-}$] (d)) | [$N_2O$] | $\delta^{15}N$- and $\delta^{18}O$-$NO_3^-$ | $\delta^{15}N$-$NH_4^+$ | Denitrifica-tion (a), anammox (b) and DNRA (c) rates |
|---|---|---|---|---|---|---|---|---|---|---|---|---|---|
| AV/ Zen Garden/ 2007 | 45.9372 | 129.9815 | 1518 | 23.8 ± 0.5 | √ | √ | √ | √ | √ | na | √ | √ | na |
| AV/ Zen Garden/ 2007 | 45.9372 | 129.9815 | 1518 | 7.3 | √ | √ | √ | √ | √ | na | √ | na | na |
| AV/ Zen Garden/ 2007 | 45.9374 | 129.9812 | 1519 | 5.4 | √ | √ | √ | √ | √ | na | √ | na | na |
| AV/ Casper/ 2007 | 45.9177 | 129.9930 | 1534 | 301.3 ± 0.1 | √ | √ | √ | √ | √ | na | na | √ | na |
| AV/ Castle/ 2007 | 45.9261 | 129.9801 | 1517 | 237.4 | √ | √ | √ | √ | √ | na | na | √ | na |
| AV/ El Guapo/ 2007 | 45.9265 | 129.9796 | 1506 | 319.3 ± 27.2 | √ | √ | √ | √ | √ | na | na | √ | na |
| AV/ Forum/ 2007 | 45.9463 | 129.9837 | 1519 | 256.1 ± 0.1 | √ | √ | √ | √ | √ | na | na | √ | na |
| AV/ Hell/ 2007 | 45.9334 | 130.0140 | 1541 | 252.8 ± 17.7 | √ | √ | √ | √ | √ | na | na | √ | na |

**Table A.1.** Continued.

| Field/ Vent/ year | Latitude (°N) | Longi-tude (°W) | depth (m) | Avera-ge tempe-rature ($^{o}$C) | pH | [$Mg_2^+$] | [$Si_4^+$] | [$H_2S$] | Nutrients ([$NO_3^-$] (a), [$NO_2^-$] (b), [$NH_4^+$] (c), [$PO_4^{3-}$] (d)) | [$N_2O$] | $\delta^{15}N$- and $\delta^{18}O$-$NO_3^-$ | $\delta^{15}N$-$NH_4^+$ | Denitrifica-tion (a), anammox (b) and DNRA (c) rates |
|---|---|---|---|---|---|---|---|---|---|---|---|---|---|
| AV/ Inferno/ 2007 | 45.9336 | 130.0137 | 1541 | 313.1 ± 0.4 | √ | √ | √ | √ | √ | na | na | √ | na |
| AV/ Mushroom /2007 | 45.9337 | 130.0136 | 1543 | 255.8 ± 0.4 | na | √ | √ | √ | √ | na | na | √ | na |
| AV/ Phoenix/ 2007 | 45.9333 | 130.0137 | 1542 | 284.1 ± 3.7 | √ | √ | √ | √ | √ | na | na | √ | na |
| AV/ T&S/ 2007 | 45.9891 | 130.0275 | 1577 | 305.1 ± 3.8 | √ | √ | √ | √ | √ | na | na | √ | na |
| AV/ Vixen/ 2007 | 45.9173 | 129.9930 | 1534 | 329.1 ± 1.6 | √ | √ | √ | √ | √ | na | na | √ | na |
| AV/ VM/ 2007 | 45.9336 | 130.0132 | 1544 | 251.1 | √ | √ | √ | √ | √ | na | na | √ | na |
| AV/ Bag City/ 2008b | 45.9158 | 129.9911 | 1532 | 11.2 ± 0 | √ | √ | √ | √ | √ | na | √ | na | √ (a only) |
| AV/ Cloud/ 2008b | 45.9332 | 129.9821 | 1522 | 6.8 ± 0 | √ | √ | √ | √ | √ | na | √ | na | √ (a only) |
| AV/ Escargot/ 2008b | 45.9263 | 129.9792 | 1520 | 86.7 ± 16.0 | √ | √ | √ | √ | √ | na | √ | √ | na |

**Table A.1.** Continued.

| Field/ Vent/ year | Latitude (°N) | Longi-tude (°W) | depth (m) | Avera-ge tempe-rature ($^{o}$C) | pH | [$Mg_2^+$] | [$Si_4^+$] | [$H_2S$] | Nutrients ([$NO_3^-$] (a), [$NO_2^-$] (b), [$NH_4^+$] (c), [$PO_4^{3-}$] (d)) | [$N_2O$] | $\delta^{15}N$- and $\delta^{18}O$-$NO_3^-$ | $\delta^{15}N$-$NH_4^+$ | Denitrifica-tion (a), anammox (b) and DNRA (c) rates |
|---|---|---|---|---|---|---|---|---|---|---|---|---|---|
| AV/ Gollum/ 2008b | 45.9335 | 130.0133 | 1547 | 20.4 ± 0.4 | √ | √ | √ | √ | √ | na | √ | na | na |
| AV/ Hermosa/ 2008b | 45.9264 | 129.9799 | 1519 | 28.1 ± 8.4 | √ | √ | √ | √ | √ | na | √ | √ | na |
| AV/ Marker 33/ 2008b | 45.9332 | 130.9823 | 1520 | 18.5 ± 2.1 | √ | √ | √ | √ | √ | na | √ | na | √ (a only) |
| AV/ Marker 113/ 2008b | 45.9229 | 129.9882 | 1521 | 23.5 ± 3.5 | √ | √ | √ | √ | √ | na | √ | √ | √ (a only) |
| AV/ Marsh-mallow/ 2008b | 45.9337 | 130.0135 | 1546 | 83.9 ± 2.5 | √ | √ | √ | √ | √ | na | √ | √ | na |
| AV/ Village (10 m W)/ 2008b | 45.9259 | 129.9805 | 1520 | 17.8 ± 0.4 | √ | √ | √ | √ | √ | na | √ | √ | na |
| AV/ Village (9 m)/ 2008b | na | na | 1517 | 31.3 ± 4.6 | √ | √ | √ | √ | √ | na | √ | na | na |

**Table A.1.** Continued.

| Field/ Vent/ year | Latitude (°N) | Longi-tude (°W) | depth (m) | Avera-ge tempe-rature ($^{o}$C) | pH | [$Mg_2^+$] | [$Si_4^+$] | [$H_2S$] | Nutrients ([$NO_3^-$] (a), [$NO_2^-$] (b), [$NH_4^+$] (c), [$PO_4^{3-}$] (d)) | [$N_2O$] | $\delta^{15}N$- and $\delta^{18}O$-$NO_3^-$ | $\delta^{15}N$-$NH_4^+$ | Denitrifica-tion (a), anammox (b) and DNRA (c) rates |
|---|---|---|---|---|---|---|---|---|---|---|---|---|---|
| AV/ Vixen/ 2008b | 45.9172 | 129.9931 | 1521 | 19.3 ± 2.0 | √ | √ | √ | √ | √ | na | √ | √ | na |
| AV/ Casper/ 2008b | 45.9173 | 129.9932 | 1538 | 302.9 ± 0.1 | √ | √ | √ | √ | √ (b,c,d only) | na | na | na | na |
| AV/ Diva/ 2008b | 45.9263 | 129.9791 | 1524 | 212.0 | √ | √ | √ | √ | √ (a, b, d only) | na | na | na | na |
| AV/ El Guapo/ 2008b | 45.9269 | 129.9793 | 1507 | 314.2 ± 3.9 | √ | √ | √ | √ | √ | na | na | √ | na |
| AV/ Hell/ 2008b | 45.9334 | 130.0140 | 1546 | 281.9 ± 5.5 | √ | √ | √ | √ | √ | na | na | √ | na |
| AV/ Inferno/ 2008b | 45.9336 | 130.0137 | 1547 | 318.4 ± 3.5 | √ | √ | √ | √ | √ | na | na | √ | na |
| AV/ Vixen/ 2008b | 45.9172 | 129.9931 | 1521 | 334.1 ± 0.1 | √ | √ | √ | √ | √ (b,c,d only) | na | na | na | na |
| AV/ VM/ 2008b | 45.9336 | 130.0132 | 1546 | 232.4 | √ | √ | √ | √ | √ | na | na | na | na |
| AV/ Cloud/ 2009 | 45.9332 | 129.9822 | 1522 | 4.6 ± 1.7 | √ | √ | √ | √ | √ (a, c only) | na | √ | na | na |

**Table A.1.** Continued.

| Field/ Vent/ year | Latitude (°N) | Longi-tude (°W) | depth (m) | Avera-ge tempe-rature ($^{o}$C) | pH | [$Mg_2^+$] | [$Si_4^+$] | [$H_2S$] | Nutrients ([$NO_3^-$] (a), [$NO_2^-$] (b), [$NH_4^+$] (c), [$PO_4^{3-}$] (d)) | [$N_2O$] | $\delta^{15}N$- and $\delta^{18}O$-$NO_3^-$ | $\delta^{15}N$-$NH_4^+$ | Denitrifica-tion (a), anammox (b) and DNRA (c) rates |
|---|---|---|---|---|---|---|---|---|---|---|---|---|---|
| AV/ Diva/ 2009 | 45.9263 | 129.9791 | 1520 | 16.9 ± 1.1 | √ | √ | √ | √ | √ (a, c only) | √ | √ | na | na |
| AV/ Gollum/ 2009 | 45.9335 | 130.0133 | 1542 | 14.2 ± 1.2 | √ | √ | √ | √ | √ (a, c only) | √ | √ | √ | √ (a, c only) |
| AV/ Hermosa/ 2009 | 45.9265 | 129.9794 | 1519 | 37.0 ± 4.1 | √ | √ | √ | √ | √ (a, c only) | √ | √ | √ | √ |
| AV/ Marker 33 (RAS)/ 2009 | 45.9332 | 129.9823 | 1520 | 34.4 ± 0.9 | √ | √ | √ | √ | √ (a, c only) | √ | √ | √ | √ |
| AV/ Marker 33 (Fat worms)/ 2009 | 45.9332 | 129.9823 | 1521 | 7.3 ± 3.4 | √ | √ | √ | √ | √ (c only) | na | na | na | na |
| AV/ Marker 33 (Skinny worms)/ 2009 | 45.9332 | 129.9823 | 1521 | 4.4 | √ | √ | √ | √ | √ (a, c only) | na | na | na | na |
| AV/ Marker 113/ 2009 | 45.9229 | 129.9885 | 1521 | 29.9 ± 5.0 | √ | √ | √ | √ | √ (a, c only) | √ | √ | √ | √ |

**Table A.1.** Continued.

| Field/ Vent/ year | Latitude (°N) | Longi-tude (°W) | depth (m) | Avera-ge tempe-rature ($^{o}$C) | pH | [$Mg_2^+$] | [$Si_4^+$] | [$H_2S$] | Nutrients ([$NO_3^-$] (a), [$NO_2^-$] (b), [$NH_4^+$] (c), [$PO_4^{3-}$] (d)) | [$N_2O$] | $\delta^{15}N$- and $\delta^{18}O$-$NO_3^-$ | $\delta^{15}N$-$NH_4^+$ | Denitrifica-tion (a), anammox (b) and DNRA (c) rates |
|---|---|---|---|---|---|---|---|---|---|---|---|---|---|
| AV/ Marker 113 (58 m S)/ 2009 | 45.9224 | 129.9884 | 1521 | 11.7 ± 0.1 | √ | √ | √ | √ | √ (a, c only) | na | √ | √ | na |
| AV/ Marker 113 (41 m S)/ 2009 | 45.9226 | 129.9884 | 1521 | 10.4 ± 0.2 | √ | √ | √ | √ | √ (a, c only) | na | √ | na | na |
| AV/ Mush-room (fat worms)/ 2009 | 45.9336 | 130.0136 | 1541 | 8.9 | √ | √ | √ | √ | √ (a, c only) | na | √ | na | na |
| AV/ Mush-room (skinny worms)/ 2009 | 45.9337 | 130.0137 | 1542 | 3.6 | √ | √ | √ | √ | √ (c only) | na | na | na | na |
| AV/ Diva/ 2009 | 45.9263 | 129.9791 | 1520 | 163.7 ± 4.2 | √ | √ | √ | √ | na | na | na | na | na |
| AV/ El Guapo/ 2009 | 45.9265 | 129.9796 | 1507 | 288.6 ± 0.4 | √ | √ | √ | √ | √ (a, c only) | na | na | √ | na |

**Table A.1.** Continued.

| Field/ Vent/ year | Latitude (°N) | Longi-tude (°W) | depth (m) | Avera-ge tempe-rature ($^{o}$C) | pH | [$Mg_2^+$] | [$Si_4^+$] | [$H_2S$] | Nutrients ([$NO_3^-$] (a), [$NO_2^-$] (b), [$NH_4^+$] (c), [$PO_4^{3-}$] (d)) | [$N_2O$] | $\delta^{15}N$- and $\delta^{18}O$-$NO_3^-$ | $\delta^{15}N$-$NH_4^+$ | Denitrifica-tion (a), anammox (b) and DNRA (c) rates |
|---|---|---|---|---|---|---|---|---|---|---|---|---|---|
| AV/ Inferno/ 2009 | 45.9335 | 130.0138 | 1539 | 295.6 ± 0.6 | √ | √ | √ | √ | na | na | na | na | na |
| CS/ Not Dead Yet (N, palm worms)/ 2007 | 46.6898 | 129.3772 | 2402 | 20.4 ± 1.0 | √ | √ | √ | √ | √ | na | √ | √ | na |
| CS/ Not Dead Yet (N, orange layer)/ 2007 | 46.6897 | 129.3772 | 2402 | 27.2 ± 3.3 | √ | √ | √ | √ | √ | na | √ | na | na |
| CS/ Hogwarts (Harry)/ 2007 | 46.6820 | 129.3840 | 2414 | 84.0 | √ | √ | √ | √ | √ | na | √ | √ | na |
| CS/ Hogwarts (Ron)/ 2007 | 46.6823 | 129.3839 | 2416 | 25.5 | √ | √ | √ | √ | √ | na | √ | √ | na |
| CS/ Not dead yet (N)/ 2007 | 46.6900 | 129.3774 | 2403 | 142.0 ± 10.6 | √ | √ | √ | √ | √ | na | √ | √ | na |

**Table A.1.** Continued.

| Field/ Vent/ year | Latitude (°N) | Longi-tude (°W) | depth (m) | Avera-ge tempe-rature (°C) | pH | $[Mg_2^+]$ | $[Si_4^+]$ | $[H_2S]$ | Nutrients ($[NO_3^-]$ (a), $[NO_2^-]$ (b), $[NH_4^+]$ (c), $[PO_4^{3-}]$ (d)) | $[N_2O]$ | $\delta^{15}N$- and $\delta^{18}O$-$NO_3^-$ | $\delta^{15}N$-$NH_4^+$ | Denitrifica-tion (a), anammox (b) and DNRA (c) rates |
|---|---|---|---|---|---|---|---|---|---|---|---|---|---|
| CS/ Not dead yet (NE)/ 2007 | 46.6897 | 129.3771 | 2399 | 167.4 ± 31.4 | √ | √ | √ | √ | √ | na | √ | √ | na |
| CS/ Hogwarts (Harry)/ 2007 | 46.6820 | 129.3839 | 2414 | 204.7 | √ | √ | √ | √ | √ | na | na | √ | na |
| CS/ Hogwarts (Harry)/ 2007 | 46.6820 | 129.3839 | 2414 | 204.7 | √ | √ | √ | √ | √ | na | na | √ | na |
| ES-MEF/ Dudley/ 2006 | 47.9495 | 129.0975 | 2207 | 14.3 | √ | √ | √ | √ | √ | na | √ | √ | na |
| ES-MEF/ Easter Island/ 2006 | 47.9485 | 129.0994 | 2204 | 21.8 | √ | √ | √ | √ | √ | na | √ | √ | na |
| ES-MEF/ Hulk (RAS)/ 2006 | 47.9503 | 129.0967 | 2210 | 28.9 | √ | √ | √ | na | √ | na | √ | √ | na |
| ES-MEF/ Hulk/ 2006 | 47.9503 | 129.0958 | 2210 | 21.9 | √ | √ | √ | √ | √ | na | √ | na | na |

**Table A.1.** Continued.

| Field/ Vent/ year | Latitude (°N) | Longi-tude (°W) | depth (m) | Avera-ge tempe-rature (°C) | pH | $[Mg_2^+]$ | $[Si_4^+]$ | $[H_2S]$ | Nutrients ($[NO_3^-]$ (a), $[NO_2^-]$ (b), $[NH_4^+]$ (c), $[PO_4^{3-}]$ (d)) | $[N_2O]$ | $\delta^{15}N$- and $\delta^{18}O$-$NO_3^-$ | $\delta^{15}N$-$NH_4^+$ | Denitrifica-tion (a), anammox (b) and DNRA (c) rates |
|---|---|---|---|---|---|---|---|---|---|---|---|---|---|
| ES-MEF/ S&M/ 2006 | 47.9485 | 129.0984 | 2201 | 20.1 | √ | √ | √ | na | √ | na | √ | √ | na |
| ES-MEF/ Dudley/ 2006 | 47.9494 | 129.0976 | 2198 | 300.0 | √ | √ | √ | √ | √ (only a, c) | na | na | √ | na |
| ES-MEF/ S&M/ 2006 | 47.9484 | 129.0982 | 2189 | 280.7 | √ | na | √ | √ | √ (only a, c) | na | na | √ | na |
| ES-MEF/ Dante/ 2007 | 47.9492 | 129.0977 | 2181 | 20.1 | √ | √ | √ | √ | √ | na | √ | √ | na |
| ES-MEF/ Easter Island (RAS)/ 2007 | 47.9481 | 129.0994 | 2198 | 21.0 ± 1.5 | √ | √ | √ | √ | √ | na | √ | √ | na |
| ES-MEF/ Hulk (RAS)/ 2007 | 47.9500 | 129.0970 | 2201 | 86.6 ± 3.1 | √ | √ | √ | √ | √ | na | √ | √ | na |
| ES-MEF/ Hulk (RAS)/ 2007 | 47.9500 | 129.0970 | 2202 | 11.0 | √ | √ | √ | √ | √ | na | √ | √ | na |
| ES-MEF/ S&M/ 2007 | 47.9480 | 129.0985 | 2181 | 31.5 ± 0.4 | √ | √ | √ | √ | √ | na | √ | √ | na |

**Table A.1.** Continued.

| Field/ Vent/ year | Latitude (°N) | Longi-tude (°W) | depth (m) | Avera-ge tempe-rature (°C) | pH | $[Mg_2^+]$ | $[Si_4^+]$ | $[H_2S]$ | Nutrients ($[NO_3^-]$ (a), $[NO_2^-]$ (b), $[NH_4^+]$ (c), $[PO_4^{3-}]$ (d)) | $[N_2O]$ | $\delta^{15}N$- and $\delta^{18}O$-$NO_3^-$ | $\delta^{15}N$-$NH_4^+$ | Denitrifica-tion (a), anammox (b) and DNRA (c) rates |
|---|---|---|---|---|---|---|---|---|---|---|---|---|---|
| ES-MEF/ Bastille/ 2007 | 47.9480 | 129.0993 | 2186 | 268.5 ± 0.4 | √ | √ | √ | √ | √ | na | na | √ | na |
| ES-MEF/ Dante/ 2007 | 47.9492 | 129.0978 | 2175 | 331.9 ± 0.1 | √ | √ | √ | √ | √ | na | na | √ | na |
| ES-MEF/ Hulk/ 2007 | 47.9502 | 129.0970 | 2187 | 324.1 ± 1.1 | √ | √ | √ | √ | √ | na | na | √ | na |
| ES-MEF/ S&M/ 2007 | 47.9480 | 129.0985 | 2187 | 324.1 ± 0.3 | √ | √ | √ | √ | √ | na | na | √ | na |
| ES-MEF/ Easter Island/ 2008a | 47.9480 | 129.0993 | 2199 | 20.0 | na | na | na | na | √ (a, c only) | na | na | na | √ (a, only) |
| ES-MEF/ Hulk (Osmo)/ 2008a | 47.9503 | 129.0970 | 2201 | 25.0 | na | na | na | na | √ (a, c only) | na | na | na | √ (a only) |
| ES/ Clam Bed/ 2008a | 47.9630 | 129.0915 | 2188 | 21.2 ± 4.0 | na | na | na | na | √ (a, c only) | na | na | na | √ (a only) |
| ES-MEF/ Bastille/ 2008b | 47.9479 | 129.0993 | 2186 | 74.4 | √ | √ | √ | √ | √ (a, b, d only) | na | √ | na | na |

**Table A.1.** Continued.

| Field/ Vent/ year | Latitude (°N) | Longi-tude (°W) | depth (m) | Avera-ge tempe-rature (°C) | pH | $[Mg_2^+]$ | $[Si_4^+]$ | $[H_2S]$ | Nutrients ($[NO_3^-]$ (a), $[NO_2^-]$ (b), $[NH_4^+]$ (c), $[PO_4^{3-}]$ (d)) | $[N_2O]$ | $\delta^{15}N$- and $\delta^{18}O$-$NO_3^-$ | $\delta^{15}N$-$NH_4^+$ | Denitrifica-tion (a), anammox (b) and DNRA (c) rates |
|---|---|---|---|---|---|---|---|---|---|---|---|---|---|
| ES/HR Boardwalk /2008b | 47.9684 | 129.0871 | 2136 | 20.5 ± 1.2 | √ | √ | √ | √ | √ | na | √ | √ | na |
| ES-MEF/ Cathedral /2008b | 47.9472 | 129.0997 | 2185 | 23.9 ± 0.2 | √ | √ | √ | √ | √ | na | √ | √ | na |
| ES-M/ Cauldron /2008b | 47.9258 | 129.1074 | 2249 | 36.3 ± 4.7 | √ | √ | √ | √ | √ | na | √ | √ | √ (a only) |
| ES-MEF/ Easter Island /2008b | 47.9480 | 129.0990 | 2197 | 16.6 ± 3.6 | √ | √ | √ | √ | √ | na | √ | √ | √ (a only) |
| ES-HR/ Godzilla /2008b | 47.9689 | 129.0869 | 2135 | 21.7 ± 8.6 | √ | √ | √ | √ | √ | na | √ | √ | √ (a only) |
| ES-MEF/ Grotto /2008b | 47.9491 | 129.0985 | 2188 | 17.1 ± 0.9 | √ | √ | √ | √ | √ | na | √ | √ | na |
| ES-MEF/ Hulk /2008b | 47.9500 | 129.0971 | 2197 | 16.4 ± 1.7 | √ | √ | √ | √ | √ | na | √ | √ | √ (a only) |
| ES-MEF/ Lobo /2008b | 47.9493 | 129.0983 | 2188 | 26.2 ± 3.9 | √ | √ | √ | √ | √ | na | √ | √ | na |
| ES-MEF/ MilliQ /2008b | 47.9474 | 129.0990 | 2179 | 70.6 ± 0.4 | √ | √ | √ | √ | √ | na | √ | √ | na |

**Table A.1.** Continued.

| Field/ Vent/ year | Latitude (°N) | Longi-tude (°W) | depth (m) | Avera-ge tempe-rature ($^{o}$C) | pH | [$Mg_2^+$] | [$Si_4^+$] | [$H_2S$] | Nutrients ([$NO_3^-$] (a), [$NO_2^-$] (b), [$NH_4^+$] (c), [$PO_4^{3-}$] (d)) | [$N_2O$] | $\delta^{15}N$- and $\delta^{18}O$-$NO_3^-$ | $\delta^{15}N$-$NH_4^+$ | Denitrifica-tion (a), anammox (b) and DNRA (c) rates |
|---|---|---|---|---|---|---|---|---|---|---|---|---|---|
| ES-MEF/ S&M /2008b | 47.9480 | 129.0985 | 2189 | 49.1 ± 26.4 | √ | √ | √ | √ | √ | na | √ | √ | na |
| ES-MEF/ Salut /2008b | 47.9464 | 129.0994 | 2187 | 55.4 ± 20.7 | √ | √ | √ | √ | √ | na | √ | √ | na |
| ES-MEF/ Bastille /2008b | 47.9479 | 129.0995 | 2193 | 302.7 ± 0 | √ | √ | √ | √ | √ | na | na | na | na |
| ES-HR/ Boardwalk /2008b | 47.9685 | 129.0872 | 2150 | 332.6 ± 5.9 | √ | √ | √ | √ | √ | na | na | √ | na |
| ES-MEF/ Cathedral /2008b | 47.9472 | 129.0997 | 2183 | 122.8 ± 21.3 | √ | √ | √ | √ | √ | na | √ | √ | na |
| ES-M/ Cauldron /2008b | 47.9258 | 129.1074 | 2249 | 291.1 ± 0 | √ | √ | √ | √ | √ | na | na | √ | na |
| ES-S/ Christmas Tree /2008b | 47.9967 | 129.0667 | 2153 | 275.0 | √ | √ | √ | √ | √ | na | na | na | na |
| ES-M/ Crab Basin /2008b | 47.9233 | 129.1093 | 2279 | 243.8 ± 3.1 | √ | √ | √ | √ | √ | na | na | √ | na |

**Table A.1.** Continued.

| Field/ Vent/ year | Latitude (°N) | Longi-tude (°W) | depth (m) | Avera-ge tempe-rature ($^{o}$C) | pH | [$Mg_2^+$] | [$Si_4^+$] | [$H_2S$] | Nutrients ([$NO_3^-$] (a), [$NO_2^-$] (b), [$NH_4^+$] (c), [$PO_4^{3-}$] (d)) | [$N_2O$] | $\delta^{15}N$- and $\delta^{18}O$-$NO_3^-$ | $\delta^{15}N$-$NH_4^+$ | Denitrifica-tion (a), anammox (b) and DNRA (c) rates |
|---|---|---|---|---|---|---|---|---|---|---|---|---|---|
| ES-MEF/ Crypto /2008b | 47.9498 | 129.0970 | 2201 | 328.0 ± 0 | √ | √ | √ | √ | √ | na | na | √ | na |
| ES-M/ Cuchalainn /2008b | 47.9220 | 129.1093 | 2291 | 292.9 ± 0.5 | √ | √ | √ | √ | √ | na | na | √ | na |
| ES-MEF/ Dante /2008b | 47.9492 | 129.0980 | 2186 | 296.9 ± 0.2 | √ | √ | √ | √ | √ | na | na | √ | na |
| ES-MEF/ Dante (Hobo) /2008b | 47.9493 | 129.0979 | 2175 | 322.9 ± 0 | √ | √ | √ | √ | √ | na | na | na | na |
| ES-MEF/ Dante (N) /2008b | 47.9494 | 129.0978 | 2174 | 337.2 ± 0 | √ | √ | √ | √ | √ | na | na | na | na |
| ES-S/ DK3-Flamingo /2008b | na | na | 2152 | 277.2 | √ | √ | √ | √ | √ | na | na | √ | na |
| ES-MEF/ Dudley /2008b | 47.9490 | 129.0975 | 2191 | 319.0 ± 0 | √ | √ | √ | √ | √ | na | na | √ | na |
| ES-HR/ Godzilla /2008b | 47.9688 | 129.0872 | 2137 | 345.2 ± 0.2 | √ | √ | √ | √ | √ | na | na | √ | na |

**Table A.1.** Continued.

| Field/ Vent/ year | Latitude (°N) | Longi-tude (°W) | depth (m) | Avera-ge tempe-rature ($^{o}$C) | pH | [$Mg_2^+$] | [$Si_4^+$] | [$H_2S$] | Nutrients ([$NO_3^-$] (a), [$NO_2^-$] (b), [$NH_4^+$] (c), [$PO_4^{3-}$] (d)) | [$N_2O$] | $\delta^{15}N$- and $\delta^{18}O$-$NO_3^-$ | $\delta^{15}N$-$NH_4^+$ | Denitrifica-tion (a), anammox (b) and DNRA (c) rates |
|---|---|---|---|---|---|---|---|---|---|---|---|---|---|
| ES-MEF/ Grotto /2008b | 47.9491 | 129.0985 | 2188 | 319.7 ± 0 | √ | √ | √ | √ | √ | na | na | √ | na |
| ES-M/ Harold /2008b | 47.9239 | 129.1088 | 2271 | 304.9 ± 19.0 | √ | √ | √ | √ | √ | na | na | √ | na |
| ES-MEF/ Hulk-dive 4447 /2008b | 47.9501 | 129.0971 | 2188 | 314.0 ± 8.5 | √ | √ | √ | √ | √ | na | na | na | na |
| ES-MEF/ Hulk-dive 4449 /2008b | 47.9500 | 129.0970 | 2191 | 311.0 ± 14.1 | √ | √ | √ | √ | √ | na | na | √ | na |
| ES-MEF/ Hulk-dive 4452 /2008b | 47.9501 | 129.0970 | 2190 | 324.0 ± 5.7 | √ | √ | √ | √ | √ | na | na | na | na |
| ES-MEF/ Lobo /2008b | 47.9494 | 129.0985 | 2188 | 320.4 ± 12.6 | √ | √ | √ | √ | √ | na | na | √ | na |
| ES-S/ Hobo /2008b | na | na | 2150 | 285.3 ± 0 | √ | √ | √ | √ | √ | na | na | √ | na |
| ES-HR/ Park Place /2008b | 47.9680 | 129.0874 | 2138 | 331.5 ± 1.2 | √ | √ | √ | √ | √ | na | na | na | na |

**Table A.1.** Continued.

| Field/ Vent/ year | Latitude (°N) | Longi-tude (°W) | depth (m) | Avera-ge tempe-rature (°C) | pH | $[Mg_2^+]$ | $[Si_4^+]$ | $[H_2S]$ | Nutrients ($[NO_3^-]$ (a), $[NO_2^-]$ (b), $[NH_4^+]$ (c), $[PO_4^{3-}]$ (d)) | $[N_2O]$ | $\delta^{15}N$- and $\delta^{18}O$-$NO_3^-$ | $\delta^{15}N$-$NH_4^+$ | Denitrifica-tion (a), anammox (b) and DNRA (c) rates |
|---|---|---|---|---|---|---|---|---|---|---|---|---|---|
| ES-MEF/ Puffer /2008b | 47.9477 | 129.0995 | 2193 | 252.4 | √ | √ | √ | √ | √ | na | na | √ | na |
| ES-MEF/ S&M- dive 4438 /2008b | 47.9479 | 129.0986 | 2181 | 322.0 ± 0 | √ | √ | √ | √ | √ | na | na | na | na |
| ES-MEF/ S&M- dive 4446 /2008b | 47.9479 | 129.0985 | 2181 | 210.2 ± 10.0 | √ | √ | √ | √ | √ | na | na | √ | na |
| ES-MEF/ Salut /2008b | 47.9465 | 129.0993 | 2187 | 267.1 ± 1.4 | √ | √ | √ | √ | √ | na | na | √ | na |
| ES-M/ Stone-henge /2008b | 47.9211 | 129.1096 | 2290 | 306.2 ± 0.4 | √ | √ | √ | √ | √ | na | na | √ | na |
| ES-MEF/ Sully /2008b | 47.9475 | 129.0992 | 2189 | 256.7 ± 0 | √ | √ | √ | √ | √ | na | na | na | na |
| ES-HR/ Baltic /2009 | 47.9678 | 129.0881 | 2147 | 22.1 ± 1.8 | √ | √ | √ | √ | √ (a, c only) | na | √ | √ | na |
| ES-MEF/ Bastille /2009 | 47.9480 | 129.0990 | 2193 | 8.8 ± 0.5 | √ | √ | √ | √ | √ (a, c only) | na | √ | √ | na |

**Table A.1.** Continued.

| Field/ Vent/ year | Latitude (°N) | Longi-tude (°W) | depth (m) | Avera-ge tempe-rature ($^{o}$C) | pH | [$Mg_2^+$] | [$Si_4^+$] | [$H_2S$] | Nutrients ([$NO_3^-$] (a), [$NO_2^-$] (b), [$NH_4^+$] (c), [$PO_4^{3-}$] (d)) | [$N_2O$] | $\delta^{15}N$- and $\delta^{18}O$-$NO_3^-$ | $\delta^{15}N$-$NH_4^+$ | Denitrifica-tion (a), anammox (b) and DNRA (c) rates |
|---|---|---|---|---|---|---|---|---|---|---|---|---|---|
| ES-HR/ Boardwalk /2009 | 47.9686 | 129.0877 | 2141 | 14.7 ± 1.4 | √ | √ | √ | √ | √ (a, c only) | na | √ | √ | na |
| ES-HR/ Fairy Castle /2009 | 47.9671 | 129.0881 | 2157 | 23.4 ± 1.8 | √ | √ | √ | √ | √ (a, c only) | √ | √ | √ | √ |
| ES-MEF/ Grotto /2009 | 47.9492 | 129.0983 | 2187 | 17.2 ± 0.6 | √ | √ | √ | √ | √ (a, c only) | na | √ | √ | na |
| ES-MEF/ Hulk (Barrel) /2009 | 47.9500 | 129.0969 | 2198 | 13-130 | √ | na | √ | √ | √ (a, c only) | na | na | √ | na |
| ES-MEF/ Hulk /2009 | 47.9500 | 129.0969 | 2198 | 29.5 ± 10.6 | √ | √ | √ | √ | √ (a, c only) | √ | √ | √ | √ (a, c only) |
| ES-MEF/ Hulk (floating worms) /2009 | 47.9500 | 129.0969 | 2189 | 26.1 ± 0.6 | √ | √ | √ | √ | √ (a, c only) | na | √ | √ | na |
| ES-MEF/ Lobo /2009 | 47.9494 | 129.0985 | 2188 | 7.8 | √ | √ | √ | √ | √ (a, c only) | na | √ | √ | na |
| ES-M/ Phang /2009 | 47.9237 | 129.1088 | 2277 | 24.1 ± 1.7 | √ | √ | √ | √ | √ (a, c only) | √ | √ | √ | √ |

**Table A.1.** Continued.

| Field/ Vent/ year | Latitude (°N) | Longi-tude (°W) | depth (m) | Avera-ge tempe-rature ($^{o}$C) | pH | [$Mg_2^+$] | [$Si_4^+$] | [$H_2S$] | Nutrients ([$NO_3^-$] (a), [$NO_2^-$] (b), [$NH_4^+$] (c), [$PO_4^{3-}$] (d)) | [$N_2O$] | $\delta^{15}N$- and $\delta^{18}O$-$NO_3^-$ | $\delta^{15}N$-$NH_4^+$ | Denitrifica-tion (a), anammox (b) and DNRA (c) rates |
|---|---|---|---|---|---|---|---|---|---|---|---|---|---|
| ES-HR/ Ventnor /2009 | 47.9237 | 129.0896 | 2163 | 20.9 ± 0.1 | √ | √ | √ | √ | √ (a, c only) | na | √ | √ | na |
| ES-HR/ Baltic-dive 4516 /2009 | 47.9678 | 129.0877 | 2147 | 333.0 | √ | √ | √ | √ | √ (a, c only) | na | na | na | na |
| ES-HR/ Baltic-dive 4526 /2009 | 47.9678 | 129.0881 | 2147 | 301.9 ± 2.6 | √ | √ | √ | √ | √ (a, c only) | na | na | √ | na |
| ES-MEF/ Bastille /2009 | 47.9480 | 129.0991 | 2194 | 316.8 ± 0.4 | √ | √ | √ | √ | √ (a, c only) | na | na | √ | na |
| ES-HR/ Broadwalk /2009 | 47.9686 | 129.0876 | 2140 | 339.4 ± 0.8 | √ | √ | √ | √ | √ (a, c only) | na | na | √ | na |
| ES-MEF/ Dante /2009 | 47.9491 | 129.0977 | 2179 | 336.0 | √ | √ | √ | √ | √ (a, c only) | na | na | na | na |
| ES-HR/ Fairy Castle /2009 | 47.9671 | 129.0881 | 2158 | 314.0 ± 2.5 | √ | √ | √ | √ | √ (a, c only) | na | na | √ | na |
| ES-HR/ Godzilla /2009 | 47.9687 | 129.0874 | 2137 | 349.0 | √ | √ | √ | √ | √ (a, c only) | na | na | √ | na |

**Table A.1.** Continued.

| Field/ Vent/ year | Latitude (°N) | Longi-tude (°W) | depth (m) | Avera-ge tempe-rature ($^{o}$C) | pH | [$Mg_2^+$] | [$Si_4^+$] | [$H_2S$] | Nutrients ([$NO_3^-$] (a), [$NO_2^-$] (b), [$NH_4^+$] (c), [$PO_4^{3-}$] (d)) | [$N_2O$] | $\delta^{15}N$- and $\delta^{18}O$-$NO_3^-$ | $\delta^{15}N$-$NH_4^+$ | Denitrifica-tion (a), anammox (b) and DNRA (c) rates |
|---|---|---|---|---|---|---|---|---|---|---|---|---|---|
| ES-MEF/ Grotto /2009 | 47.9492 | 129.0983 | 2187 | 319.0 ± 7.6 | √ | √ | √ | √ | √ (a, c only) | na | na | √ | na |
| ES-MEF/ Hulk /2009 | 47.9501 | 129.0969 | 2197 | 299.2 ± 0.6 | √ | √ | √ | √ | √ (a, c only) | na | na | √ | na |
| ES-MEF/ Lobo /2009 | 47.9494 | 129.0985 | 2187 | 164.9 | √ | √ | √ | √ | √ (a, c only) | na | na | √ | na |
| ES-HR/ Park Place /2009 | 47.9682 | 129.0878 | 2149 | 332.0 | √ | √ | √ | √ | √ (c only) | na | na | √ | na |
| ES-HR/ Ventnor-dive 4516 /2009 | 47.9676 | 129.0896 | 2164 | 332.0 | √ | √ | √ | √ | √ (a, c only) | na | na | na | na |
| ES-HR/ Ventnor-dive 4526 /2009 | 47.9677 | 129.0896 | 2163 | 331.3 ± 1.1 | √ | √ | √ | √ | √ (a, c only) | na | na | √ | na |

**Table A.2.** Microbiological data for all diffuse hydrothermal vent fluids collected at Axial Volcano, Cobb Segment and Endeavour Segment on the Juan de Fuca Ridge, northeast Pacific Ocean and used in this dissertation (chapters 2-4). Vent fluids were collected on Sterivex or Steripack filters for DNA extraction during 2007, 2008b and 2009 cruises (see Table 1). Cell counts were performed in Holden's and Baross laboratories (please direclty contact them for these data), in the associated vent fluids collected at the same time and location as the DNA samples (see Table A.1). Bacterial, Archaeal, SUP05 (i.e. a cluster of γ-proteobacteria capable of nitrate reduction coupled to sulfur oxidation) and *nirS* abundances were measured by qPCR. √ indicates that data are available upon request whereas na means non available. All sequences and pyrotags for diversity analyses have been submitted to Genbank and the National Center for Biotechnology Information Read Archive (SRA) (see chapters 3 and 4).

| Field/ Vent/ year | Latitude (°N) | Longitude (°W) | depth (m) | Average tempe-rature ($^{o}$C) | Volume filtered (L) | Cell count (cells/mL) | Bacteria (copies/mL) | Archaea (copies/mL) | SUP5 (copies/mL) | *nirS* (copies/mL) |
|---|---|---|---|---|---|---|---|---|---|---|
| AV/ Bag City /2007 | 45.9163 | 129.9893 | 1533.3 | 13.2 | 3.15 | √ | √ | √ | √ | √ |
| AV/ Cloud /2007 | 45.9333 | 129.9817 | 1521.1 | 6.8 | 3.01 | √ | √ | √ | √ | √ |
| AV/ Forum /2007 | 45.9465 | 129.9839 | 1523.9 | 5.7 | 2.05 | √ | √ | √ | √ | √ |
| AV/ Gollum /2007 | 45.9335 | 130.0134 | 1543.8 | 21.7 | 2.55 | √ | √ | √ | √ | √ |
| AV/ Marker 113 /2007 | 45.9227 | 129.9883 | 1522.8 | 31.3 | 2.62 | √ | √ | √ | √ | √ |
| AV/ Shepherd /2007 | 45.9888 | 130.0275 | 1581.8 | 25 | 3.05 | √ | √ | √ | √ | √ |

**Table A.2.** Continued.

| Field/ Vent/ year | Latitude (°N) | Longitude (°W) | depth (m) | Average tempe-rature ($^{o}$C) | Volume filtered (L) | Cell count (cells/mL) | Bacteria (copies/mL) | Archaea (copies/mL) | SUP5 (copies/mL) | *nirS* (copies/mL) |
|---|---|---|---|---|---|---|---|---|---|---|
| AV/ The Spot /2007 | 45.9173 | 129.9931 | 1534.8 | 29.95 | 3.56 | √ | √ | √ | √ | √ |
| AV/ T&S /2007 | 45.9892 | 130.0276 | 1580.3 | 75.9 | 2.81 | √ | √ | √ | √ | √ |
| AV/ Zen Garden /2007 | 45.9372 | 129.9815 | 1518.3 | 23.7 | 3.40 | √ | √ | √ | √ | √ |
| AV/ Zen Garden /2007 | 45.9372 | 129.9815 | 1518.3 | 7.2 | 2.90 | √ | √ | √ | √ | √ |
| AV Bag City /2008b | 45.9158 | 129.9911 | 1532.0 | 11.2 | 1.61 | √ | √ | √ | √ | √ |
| AV/ Cloud /2008b | 45.9332 | 129.9821 | 1522.0 | 6.8 | 1.21 | √ | √ | √ | √ | √ |
| AV/ Marker 33 /2008b | 45.9332 | 130.9823 | 1520.0 | 19.7 | 4.05 | √ | √ | √ | √ | √ |
| AV/ Marker 113 /2008b | 45.9229 | 129.9882 | 1521.0 | 23 | 4.00 | √ | √ | √ | √ | √ |

**Table A.2.** Continued.

| Field/ Vent/ year | Latitude (°N) | Longitude (°W) | depth (m) | Average tempe-rature (°C) | Volume filtered (L) | Cell count (cells/mL) | Bacteria (copies/mL) | Archaea (copies/mL) | SUP5 (copies/mL) | *nirS* (copies/mL) |
|---|---|---|---|---|---|---|---|---|---|---|
| AV/ Diva /2009 | 45.9263 | 129.9791 | 1520.0 | 17.7 | 2.51 | √ | √ | √ | √ | √ |
| AV/ Gollum /2009 | 45.9335 | 130.0133 | 1542.0 | 12.7 | 3.03 | √ | √ | √ | √ | √ |
| AV/ Hermosa /2009 | 45.9265 | 129.9794 | 1519.0 | 40.4 | 2.64 | √ | √ | √ | √ | √ |
| AV/ Marker 33 /2009 | 45.9332 | 129.9823 | 1520.0 | 34.5 | 3.00 | √ | √ | √ | √ | √ |
| AV/ Marker 113 /2009 | 45.9229 | 129.9885 | 1521.0 | 30.1 | 3.38 | √ | √ | √ | √ | √ |
| CS/ Not dead Yet /2007 | 46.6897 | 129.3772 | 2402.4 | 24.3 | 2.55 | √ | √ | √ | √ | √ |
| ES-M/ Cauldron /2008b | 47.9258 | 129.1074 | 2249.0 | 38.8 | 1.50 | √ | √ | √ | √ | √ |
| ES-HR/ Godzilla /2008b | 47.9689 | 129.0869 | 2135.0 | 29 | 3.96 | √ | √ | √ | √ | √ |

**Table A.2.** Continued.

| Field/ Vent/ year | Latitude (°N) | Longitude (°W) | depth (m) | Average tempe-rature (°C) | Volume filtered (L) | Cell count (cells/mL) | Bacteria (copies/mL) | Archaea (copies/mL) | SUP5 (copies/mL) | *nirS* (copies/mL) |
|---|---|---|---|---|---|---|---|---|---|---|
| ES-MEF/ Hulk /2008b | 47.9500 | 129.0971 | 2197.0 | 24.8 | 4.03 | √ | √ | √ | √ | √ |
| ES-HR/ Fairy Castle /2009 | 47.9671 | 129.0881 | 2157.0 | 28.9 | 2.53 | √ | √ | √ | √ | √ |
| ES-MEF/ Hulk (Barrel) /2009 | 47.9500 | 129.0969 | 2198.0 | 13-130 | 45.00 | √ | √ | √ | √ | √ |
| ES-MEF/ Hulk /2009 | 47.9500 | 129.0969 | 2198.0 | 22.8 | 3.00 | √ | √ | √ | √ | √ |
| ES-M/ Phang /2009 | 47.9237 | 129.1088 | 2277.0 | 24 | 2.71 | √ | √ | √ | √ | √ |
| ES/ Background /2009 | 48.0000 | 129.1000 | >2000 | 1.83 | 2.71 | √ | √ | √ | √ | √ |

**Table A.3.** Geochemical parameters for depth profiles collected at the main sampling station in Saanich Inlet and background station in Haro Strait used in this dissertation (chapter 5). √ indicates that data are available upon request whereas na means non available.

| Station | Latitude (°N) | Longi-tude (°W) | Sampling time | Water sampling depth | CTD sensors (pressure, temperature, fluorescence, salinity, $[O_2]$) | $[O_2]$ (Winkler titration) | Nutrients $[NO_3^-]$ (a), $[NO_2^-]$ (b), $[NH_4^+]$ (c), $[PO_4^{3-}]$ (d) $[Si^{4+}]$ (e) | $\delta^{15}N$ and $\delta^{18}O$ of $NO_3^-$ | $\delta^{15}N$ of $NH_4^+$ | $N_2$ excess (from $N_2$/Ar) and $\delta^{15}N$-$N_2$ |
|---|---|---|---|---|---|---|---|---|---|---|
| Main | 48.65 | 123.50 | 06/11/2007 | 4.2 | √ | na | √ | √ | na | na |
| Main | 48.65 | 123.50 | 06/11/2007 | 14.6 | √ | na | √ | √ | na | na |
| Main | 48.65 | 123.50 | 06/11/2007 | 25.2 | √ | na | √ | √ | na | na |
| Main | 48.65 | 123.50 | 06/11/2007 | 34.9 | √ | na | √ | √ | na | na |
| Main | 48.65 | 123.50 | 06/11/2007 | 49.7 | √ | na | √ | √ | na | na |
| Main | 48.65 | 123.50 | 06/11/2007 | 68.9 | √ | na | √ | √ | na | na |
| Main | 48.65 | 123.50 | 06/11/2007 | 89.2 | √ | na | √ | √ | na | na |
| Main | 48.65 | 123.50 | 06/11/2007 | 108.9 | √ | na | √ | √ | na | na |
| Main | 48.65 | 123.50 | 06/11/2007 | 129.9 | √ | na | √ | √ | na | na |
| Main | 48.65 | 123.50 | 06/11/2007 | 148.2 | √ | na | √ | √ | na | na |
| Main | 48.65 | 123.50 | 06/11/2007 | 167.8 | √ | na | √ | √ | na | na |
| Main | 48.65 | 123.50 | 06/11/2007 | 179.0 | √ | na | √ | √ | na | na |

**Table A.3.** Continued.

| Station | Latitude (°N) | Longi-tude (°W) | Sampling time | Water sampling depth | CTD sensors (pressure, temperature, fluorescence, salinity, $[O_2]$) | $[O_2]$ (Winkler titration) | Nutrients $[NO_3^-]$ (a), $[NO_2^-]$ (b), $[NH_4^+]$ (c), $[PO_4^{3-}]$ (d) | $\delta^{15}N$ and $\delta^{18}O$ of $NO_3^-$ | $\delta^{15}N$ of $NH_4^+$ | $N_2$ excess (from $N_2$/Ar) and $\delta^{15}N$-$N_2$ |
|---|---|---|---|---|---|---|---|---|---|---|
| Main | 48.65 | 123.51 | 16/04/2008 | 5.2 | √ | √ | √ | na | na | √ |
| Main | 48.65 | 123.51 | 16/04/2008 | 20.0 | √ | √ | √ | √ | na | na |
| Main | 48.65 | 123.51 | 16/04/2008 | 35.0 | √ | √ | √ | √ | na | √ |
| Main | 48.65 | 123.51 | 16/04/2008 | 50.0 | √ | √ | √ | √ | na | √ |
| Main | 48.65 | 123.51 | 16/04/2008 | 69.9 | √ | √ | √ | √ | √ | na |
| Main | 48.65 | 123.51 | 16/04/2008 | 84.3 | √ | √ | √ | √ | na | √ |
| Main | 48.65 | 123.51 | 16/04/2008 | 99.4 | √ | √ | √ | √ | na | √ |
| Main | 48.65 | 123.51 | 16/04/2008 | 114.3 | √ | √ | √ | √ | na | na |
| Main | 48.65 | 123.51 | 16/04/2008 | 133.9 | √ | √ | √ | √ | na | √ |
| Main | 48.65 | 123.51 | 16/04/2008 | 153.9 | √ | √ | √ | √ | na | √ |
| Main | 48.65 | 123.51 | 16/04/2008 | 173.4 | √ | √ | √ | na | na | na |
| Main | 48.65 | 123.51 | 16/04/2008 | 178.8 | √ | √ | √ | na | √ | √ |

**Table A.3.** Continued.

| Station | Latitude (°N) | Longi-tude (°W) | Sampling time | Water sampling depth | CTD sensors (pressure, temperature, fluorescence, salinity, $[O_2]$) | $[O_2]$ (Winkler titration) | Nutrients $[NO_3^-]$ (a), $[NO_2^-]$ (b), $[NH_4^+]$ (c), $[PO_4^{3-}]$ (d) | $\delta^{15}N$ and $\delta^{18}O$ of $NO_3^-$ | $\delta^{15}N$ of $NH_4^+$ | $N_2$ excess (from $N_2$/Ar) and $\delta^{15}N$-$N_2$ |
|---|---|---|---|---|---|---|---|---|---|---|
| Main | 48.65 | 123.51 | 15/05/2008 | 1.9 | √ | √ | √ | na | na | √ |
| Main | 48.65 | 123.51 | 15/05/2008 | 9.8 | √ | √ | √ | √ | na | na |
| Main | 48.65 | 123.51 | 15/05/2008 | 29.6 | √ | √ | √ | √ | √ | √ |
| Main | 48.65 | 123.51 | 15/05/2008 | 49.9 | √ | √ | √ | √ | √ | na |
| Main | 48.65 | 123.51 | 15/05/2008 | 69.5 | √ | √ | √ | √ | na | √ |
| Main | 48.65 | 123.51 | 15/05/2008 | 89.5 | √ | √ | √ | √ | na | na |
| Main | 48.65 | 123.51 | 15/05/2008 | 109.5 | √ | √ | √ | √ | na | √ |
| Main | 48.65 | 123.51 | 15/05/2008 | 129.0 | √ | na | √ | √ | na | na |
| Main | 48.65 | 123.51 | 15/05/2008 | 139.1 | √ | √ | √ | √ | na | √ |
| Main | 48.65 | 123.51 | 15/05/2008 | 149.0 | √ | √ | √ | √ | na | √ |
| Main | 48.65 | 123.51 | 15/05/2008 | 158.9 | √ | √ | √ | √ | na | √ |
| Main | 48.65 | 123.51 | 15/05/2008 | 168.7 | √ | √ | √ | na | na | √ |
| Main | 48.65 | 123.51 | 15/05/2008 | 183.8 | √ | √ | √ | na | √ | √ |

**Table A.3.** Continued.

| Station | Latitude (°N) | Longi-tude (°W) | Sampling time | Water sampling depth | CTD sensors (pressure, temperature, fluorescence, salinity, $[O_2]$) | $[O_2]$ (Winkler titration) | Nutrients $[NO_3^-]$ (a), $[NO_2^-]$ (b), $[NH_4^+]$ (c), $[PO_4^{3-}]$ (d) | $\delta^{15}N$ and $\delta^{18}O$ of $NO_3^-$ | $\delta^{15}N$ of $NH_4^+$ | $N_2$ excess (from $N_2$/Ar) and $\delta^{15}N$-$N_2$ |
|---|---|---|---|---|---|---|---|---|---|---|
| Main | 48.65 | 123.51 | 10/06/2008 | 2.1 | √ | √ | √ | na | na | √ |
| Main | 48.65 | 123.51 | 10/06/2008 | 10.0 | √ | √ | √ | √ | na | na |
| Main | 48.65 | 123.51 | 10/06/2008 | 29.8 | √ | √ | √ | √ | √ | na |
| Main | 48.65 | 123.51 | 10/06/2008 | 49.7 | √ | √ | √ | √ | √ | √ |
| Main | 48.65 | 123.51 | 10/06/2008 | 69.4 | √ | √ | √ | √ | na | na |
| Main | 48.65 | 123.51 | 10/06/2008 | 89.2 | √ | √ | √ | √ | na | √ |
| Main | 48.65 | 123.51 | 10/06/2008 | 109.0 | √ | √ | √ | √ | na | na |
| Main | 48.65 | 123.51 | 10/06/2008 | 129.1 | √ | √ | √ | √ | na | √ |
| Main | 48.65 | 123.51 | 10/06/2008 | 143.9 | √ | √ | √ | √ | na | √ |
| Main | 48.65 | 123.51 | 10/06/2008 | 153.9 | √ | √ | √ | √ | na | √ |
| Main | 48.65 | 123.51 | 10/06/2008 | 163.8 | √ | √ | √ | na | na | √ |
| Main | 48.65 | 123.51 | 10/06/2008 | 173.7 | √ | √ | √ | na | √ | √ |
| Main | 48.65 | 123.51 | 10/06/2008 | 183.9 | √ | √ | √ | na | √ | √ |

**Table A.3.** Continued.

| Station | Latitude (°N) | Longi-tude (°W) | Sampling time | Water sampling depth | CTD sensors (pressure, temperature, fluorescence, salinity, $[O_2]$) | $[O_2]$ (Winkler titration) | Nutrients $[NO_3^-]$ (a), $[NO_2^-]$ (b), $[NH_4^+]$ (c), $[PO_4^{3-}]$ (d) | $\delta^{15}N$ and $\delta^{18}O$ of $NO_3^-$ | $\delta^{15}N$ of $NH_4^+$ | $N_2$ excess (from $N_2$/Ar) and $\delta^{15}N$-$N_2$ |
|---|---|---|---|---|---|---|---|---|---|---|
| Main | 48.65 | 123.51 | 10/07/2008 | 2.1 | √ | √ | √ | na | na | √ |
| Main | 48.65 | 123.51 | 10/07/2008 | 9.5 | √ | √ | √ | √ | na | na |
| Main | 48.65 | 123.51 | 10/07/2008 | 32.4 | √ | √ | √ | √ | na | na |
| Main | 48.65 | 123.51 | 10/07/2008 | 49.7 | √ | √ | √ | √ | na | √ |
| Main | 48.65 | 123.51 | 10/07/2008 | 69.8 | √ | √ | √ | √ | na | na |
| Main | 48.65 | 123.51 | 10/07/2008 | 89.6 | √ | √ | √ | √ | na | √ |
| Main | 48.65 | 123.51 | 10/07/2008 | 109.4 | √ | √ | √ | √ | na | na |
| Main | 48.65 | 123.51 | 10/07/2008 | 128.7 | √ | √ | √ | √ | na | √ |
| Main | 48.65 | 123.51 | 10/07/2008 | 139.0 | √ | √ | √ | √ | na | √ |
| Main | 48.65 | 123.51 | 10/07/2008 | 149.5 | √ | √ | √ | √ | na | √ |
| Main | 48.65 | 123.51 | 10/07/2008 | 158.7 | √ | √ | √ | √ | na | √ |
| Main | 48.65 | 123.51 | 10/07/2008 | 169.2 | √ | √ | √ | na | √ | √ |
| Main | 48.65 | 123.51 | 10/07/2008 | 178.6 | √ | √ | √ | na | √ | √ |

**Table A.3.** Continued.

| Station | Latitude (°N) | Longi-tude (°W) | Sampling time | Water sampling depth | CTD sensors (pressure, temperature, fluorescence, salinity, $[O_2]$) | $[O_2]$ (Winkler titration) | Nutrients $[NO_3^-]$ (a), $[NO_2^-]$ (b), $[NH_4^+]$ (c), $[PO_4^{3-}]$ (d) | $\delta^{15}N$ and $\delta^{18}O$ of $NO_3^-$ | $\delta^{15}N$ of $NH_4^+$ | $N_2$ excess (from $N_2$/Ar) and $\delta^{15}N$-$N_2$ |
|---|---|---|---|---|---|---|---|---|---|---|
| Main | 48.65 | 123.51 | 06/08/2008 | 2.0 | √ | √ | √ | √ | na | √ |
| Main | 48.65 | 123.51 | 06/08/2008 | 9.9 | √ | √ | √ | √ | na | na |
| Main | 48.65 | 123.51 | 06/08/2008 | 32.7 | √ | √ | √ | √ | na | na |
| Main | 48.65 | 123.51 | 06/08/2008 | 49.4 | √ | √ | √ | √ | na | √ |
| Main | 48.65 | 123.51 | 06/08/2008 | 69.5 | √ | √ | √ | √ | na | na |
| Main | 48.65 | 123.51 | 06/08/2008 | 88.9 | √ | √ | √ | √ | na | √ |
| Main | 48.65 | 123.51 | 06/08/2008 | 109.0 | √ | √ | √ | √ | na | na |
| Main | 48.65 | 123.51 | 06/08/2008 | 128.8 | √ | √ | √ | √ | na | √ |
| Main | 48.65 | 123.51 | 06/08/2008 | 143.7 | √ | √ | √ | √ | na | √ |
| Main | 48.65 | 123.51 | 06/08/2008 | 153.5 | √ | √ | √ | √ | na | √ |
| Main | 48.65 | 123.51 | 06/08/2008 | 163.5 | √ | √ | √ | na | √ | √ |
| Main | 48.65 | 123.51 | 06/08/2008 | 173.6 | √ | √ | √ | na | √ | √ |
| Main | 48.65 | 123.51 | 06/08/2008 | 184.0 | √ | √ | √ | na | √ | √ |

**Table A.3.** Continued.

| Station | Latitude (°N) | Longi-tude (°W) | Sampling time | Water sampling depth | CTD sensors (pressure, temperature, fluorescence, salinity, $[O_2]$) | $[O_2]$ (Winkler titration) | Nutrients $[NO_3^-]$ (a), $[NO_2^-]$ (b), $[NH_4^+]$ (c), $[PO_4^{3-}]$ (d) | $\delta^{15}N$ and $\delta^{18}O$ of $NO_3^-$ | $\delta^{15}N$ of $NH_4^+$ | $N_2$ excess (from $N_2$/Ar) and $\delta^{15}N$-$N_2$ |
|---|---|---|---|---|---|---|---|---|---|---|
| Main | 48.65 | 123.51 | 22/10/2008 | 0.99 | √ | √ | √ | √ | na | √ |
| Main | 48.65 | 123.51 | 22/10/2008 | 7.93 | √ | √ | √ | √ | na | na |
| Main | 48.65 | 123.51 | 22/10/2008 | 28.75 | √ | √ | √ | √ | na | √ |
| Main | 48.65 | 123.51 | 22/10/2008 | 49.94 | √ | √ | √ | √ | na | na |
| Main | 48.65 | 123.51 | 22/10/2008 | 68.90 | √ | √ | √ | √ | na | √ |
| Main | 48.65 | 123.51 | 22/10/2008 | 89.90 | √ | √ | √ | √ | na | na |
| Main | 48.65 | 123.51 | 22/10/2008 | 105.08 | √ | √ | √ | √ | na | √ |
| Main | 48.65 | 123.51 | 22/10/2008 | 114.00 | √ | √ | √ | √ | na | na |
| Main | 48.65 | 123.51 | 22/10/2008 | 123.76 | √ | √ | √ | √ | na | √ |
| Main | 48.65 | 123.51 | 22/10/2008 | 138.77 | √ | √ | √ | √ | na | √ |
| Main | 48.65 | 123.51 | 22/10/2008 | 153.63 | √ | √ | √ | na | na | √ |
| Main | 48.65 | 123.51 | 22/10/2008 | 168.49 | √ | √ | √ | na | na | √ |
| Main | 48.65 | 123.51 | 22/10/2008 | 183.42 | √ | √ | √ | na | na | √ |

**Table A.3.** Continued.

| Station | Latitude (°N) | Longi-tude (°W) | Sampling time | Water sampling depth | CTD sensors (pressure, temperature, fluorescence, salinity, $[O_2]$) | $[O_2]$ (Winkler titration) | Nutrients $[NO_3^-]$ (a), $[NO_2^-]$ (b), $[NH_4^+]$ (c), $[PO_4^{3-}]$ (d) | $\delta^{15}N$ and $\delta^{18}O$ of $NO_3^-$ | $\delta^{15}N$ of $NH_4^+$ | $N_2$ excess (from $N_2$/Ar) and $\delta^{15}N$-$N_2$ |
|---|---|---|---|---|---|---|---|---|---|---|
| Main | 48.65 | 123.51 | 09/12/2008 | 2.1 | √ | √ | √ | √ | na | √ |
| Main | 48.65 | 123.51 | 09/12/2008 | 9.8 | √ | √ | √ | √ | na | na |
| Main | 48.65 | 123.51 | 09/12/2008 | 30.1 | √ | √ | √ | √ | na | √ |
| Main | 48.65 | 123.51 | 09/12/2008 | 50.0 | √ | √ | √ | √ | na | na |
| Main | 48.65 | 123.51 | 09/12/2008 | 69.3 | √ | √ | √ | √ | na | √ |
| Main | 48.65 | 123.51 | 09/12/2008 | 89.9 | √ | √ | √ | √ | na | na |
| Main | 48.65 | 123.51 | 09/12/2008 | 105.0 | √ | √ | √ | √ | na | √ |
| Main | 48.65 | 123.51 | 09/12/2008 | 114.9 | √ | √ | √ | √ | na | na |
| Main | 48.65 | 123.51 | 09/12/2008 | 125.3 | √ | √ | √ | √ | na | √ |
| Main | 48.65 | 123.51 | 09/12/2008 | 139.3 | √ | √ | √ | √ | na | √ |
| Main | 48.65 | 123.51 | 09/12/2008 | 155.3 | √ | √ | √ | √ | na | √ |
| Main | 48.65 | 123.51 | 09/12/2008 | 169.6 | √ | √ | √ | √ | na | √ |
| Main | 48.65 | 123.51 | 09/12/2008 | 184.9 | √ | √ | √ | √ | √ | √ |

**Table A.3.** Continued.

| Station | Latitude (°N) | Longi-tude (°W) | Sampling time | Water sampling depth | CTD sensors (pressure, temperature, fluorescence, salinity, $[O_2]$) | $[O_2]$ (Winkler titration) | Nutrients $[NO_3^-]$ (a), $[NO_2^-]$ (b), $[NH_4^+]$ (c), $[PO_4^{3-}]$ (d) | $\delta^{15}N$ and $\delta^{18}O$ of $NO_3^-$ | $\delta^{15}N$ of $NH_4^+$ | $N_2$ excess (from $N_2$/Ar) and $\delta^{15}N$-$N_2$ |
|---|---|---|---|---|---|---|---|---|---|---|
| Main | 48.65 | 123.51 | 05/02/2009 | 2.3 | √ | √ | √ | √ | na | na |
| Main | 48.65 | 123.51 | 05/02/2009 | 9.9 | √ | √ | √ | √ | na | √ |
| Main | 48.65 | 123.51 | 05/02/2009 | 30.2 | √ | √ | √ | √ | na | na |
| Main | 48.65 | 123.51 | 05/02/2009 | 50.2 | √ | √ | √ | √ | na | √ |
| Main | 48.65 | 123.51 | 05/02/2009 | 70.2 | √ | √ | √ | √ | na | na |
| Main | 48.65 | 123.51 | 05/02/2009 | 89.9 | √ | √ | √ | √ | na | √ |
| Main | 48.65 | 123.51 | 05/02/2009 | 100.1 | √ | √ | √ | √ | na | na |
| Main | 48.65 | 123.51 | 05/02/2009 | 110.1 | √ | √ | √ | √ | na | √ |
| Main | 48.65 | 123.51 | 05/02/2009 | 124.9 | √ | √ | √ | √ | na | na |
| Main | 48.65 | 123.51 | 05/02/2009 | 134.8 | √ | √ | √ | √ | na | √ |
| Main | 48.65 | 123.51 | 05/02/2009 | 159.2 | √ | na | √ | √ | na | √ |
| Main | 48.65 | 123.51 | 05/02/2009 | 169.8 | √ | √ | √ | √ | na | na |
| Main | 48.65 | 123.51 | 05/02/2009 | 184.0 | √ | √ | √ | na | na | √ |

**Table A.3.** Continued.

| Station | Latitude (°N) | Longi-tude (°W) | Sampling time | Water sampling depth | CTD sensors (pressure, temperature, fluorescence, salinity, $[O_2]$) | $[O_2]$ (Winkler titration) | Nutrients $[NO_3^-]$ (a), $[NO_2^-]$ (b), $[NH_4^+]$ (c), $[PO_4^{3-}]$ (d) | $\delta^{15}N$ and $\delta^{18}O$ of $NO_3^-$ | $\delta^{15}N$ of $NH_4^+$ | $N_2$ excess (from $N_2$/Ar) and $\delta^{15}N$-$N_2$ |
|---|---|---|---|---|---|---|---|---|---|---|
| Main | 48.65 | 123.51 | 06/04/2009 | 2.09 | √ | na | √ | na | na | √ |
| Main | 48.65 | 123.51 | 06/04/2009 | 10.18 | √ | √ | √ | √ | √ | √ |
| Main | 48.65 | 123.51 | 06/04/2009 | 29.94 | √ | √ | √ | √ | √ | √ |
| Main | 48.65 | 123.51 | 06/04/2009 | 50.14 | √ | √ | √ | √ | na | √ |
| Main | 48.65 | 123.51 | 06/04/2009 | 70.42 | √ | √ | √ | √ | na | na |
| Main | 48.65 | 123.51 | 06/04/2009 | 90.32 | √ | √ | √ | √ | na | √ |
| Main | 48.65 | 123.51 | 06/04/2009 | 99.93 | √ | √ | √ | √ | na | na |
| Main | 48.65 | 123.51 | 06/04/2009 | 110.19 | √ | √ | √ | √ | na | √ |
| Main | 48.65 | 123.51 | 06/04/2009 | 129.88 | √ | √ | √ | √ | na | na |
| Main | 48.65 | 123.51 | 06/04/2009 | 150.86 | √ | √ | √ | √ | na | √ |
| Main | 48.65 | 123.51 | 06/04/2009 | 165.01 | √ | √ | √ | na | na | √ |
| Main | 48.65 | 123.51 | 06/04/2009 | 174.91 | √ | √ | √ | na | na | √ |
| Main | 48.65 | 123.51 | 06/04/2009 | 184.15 | √ | √ | √ | na | √ | √ |

**Table A.3.** Continued.

| Station | Latitude (°N) | Longi-tude (°W) | Sampling time | Water sampling depth | CTD sensors (pressure, temperature, fluorescence, salinity, $[O_2]$) | $[O_2]$ (Winkler titration) | Nutrients $[NO_3^-]$ (a), $[NO_2^-]$ (b), $[NH_4^+]$ (c), $[PO_4^{3-}]$ (d) | $\delta^{15}N$ and $\delta^{18}O$ of $NO_3^-$ | $\delta^{15}N$ of $NH_4^+$ | $N_2$ excess (from $N_2$/Ar) and $\delta^{15}N$-$N_2$ |
|---|---|---|---|---|---|---|---|---|---|---|
| Bkgd | 48.67 | 123.26 | 06/04/2009 | 2.19 | √ | na | √ (except c) | √ | na | √ |
| Bkgd | 48.67 | 123.26 | 06/04/2009 | 10.31 | √ | na | √ (except c) | √ | na | √ |
| Bkgd | 48.67 | 123.26 | 06/04/2009 | 30.13 | √ | na | √ (except c) | √ | na | √ |
| Bkgd | 48.67 | 123.26 | 06/04/2009 | 51.03 | √ | na | √ (except c) | √ | na | na |
| Bkgd | 48.67 | 123.26 | 06/04/2009 | 70.47 | √ | na | √ (except c) | √ | na | √ |
| Bkgd | 48.67 | 123.26 | 06/04/2009 | 89.74 | √ | na | √ (except c) | √ | na | na |
| Bkgd | 48.67 | 123.26 | 06/04/2009 | 109.91 | √ | na | √ (except c) | √ | na | √ |
| Bkgd | 48.67 | 123.26 | 06/04/2009 | 145.43 | √ | na | √ (except c) | √ | na | na |
| Bkgd | 48.67 | 123.26 | 06/04/2009 | 190.93 | √ | na | √ (except c) | √ | na | √ |
| Bkgd | 48.67 | 123.26 | 06/04/2009 | 221.21 | √ | na | √ (except c) | √ | na | √ |
| Bkgd | 48.67 | 123.26 | 06/04/2009 | 250.98 | √ | na | √ (except c) | √ | na | √ |
| Bkgd | 48.67 | 123.26 | 06/04/2009 | 283.02 | √ | na | √ (except c) | √ | na | √ |
| Bkgd | 48.67 | 123.26 | 06/04/2009 | 314.55 | √ | na | √ (except c) | √ | na | √ |

# Appendix B
# Nitrate isotope box-model calculations

## B.1. Nitrate isotope box-model equations used in chapter 2

Below are the equations used for all nitrate isotope box-model scenarios presented in chapter 2. See chapter 2 (section 2.4.4.3, Table 2.2 and Figure 2.10) for major assumptions and model results.

Term definitions:

a = partial $NH_4^+$ oxidation to $NO_3^-$ or $N_2$ fixation flux

b = seawater mixing flux

c = nitrate removal (by nitrate assimilation ($c_{upt}$) and/or denitrification ($c_{denitrif}$) fluxes

d = organic matter remineralization and nitrification flux (recycled production)

e = nitrate reduction to nitrite ($e_{red\ NO2-}$) and nitrite re-oxidation ($e_{NO2-\ re\text{-}oxid}$) fluxes

$\delta^{15}N_{Box}$ = steady-state $\delta^{15}N\text{-}NO_3^-$ (under model assumptions)

$\delta^{18}O_{Box}$ = steady-state $\delta^{18}O\text{-}NO_3^-$ (under model assumptions)

$\delta^{15}N_{NH4+\ oxid}$ = $\delta^{15}N\text{-}NH_4^+$ added from partial ammonium oxidation to nitrate (assuming an isotope effect of 26‰ for ammonium oxidation).

$\delta^{15}N\text{-}N_{fix}$ = $\delta^{15}N\text{-}NH_4^+$ added from $N_2$ fixation (~-1‰)

$\delta^{18}O\text{-}N_{fix}$ = $\delta^{18}O$ returned following organic matter remineralization and nitrification (-3.8‰)

$\delta^{18}O_{NH4+\ oxid}$ = $\delta^{18}O$ added (mostly from seawater, -3.8‰) during partial ammonium oxidation to nitrate

$\delta^{15}N_{sw\ mix}$ = $\delta^{15}N$-$NO_3^-$ added from mixing with seawater (~6 ‰)

$\delta^{18}O_{sw\ mix}$= $\delta^{18}O$-$NO_3^-$ added from mixing with seawater (~2 ‰)

* Note that for all scenarios, the different initial deep-sea water nitrate N and O isotopic compositions at ES and AV were taken into account in the calculations.

$\delta^{15}N_{upt}$ = $\delta^{15}N_{Box}$ - $\varepsilon_{upt}$ (‰) = nitrate N isotope fractionation from nitrate assimilation

$\delta^{15}N_{denitrif}$ = $\delta^{15}N_{Box}$ - $\varepsilon_{denitrif}$ (‰) = nitrate N isotope fractionation from denitrification

$\delta^{18}O_{upt}$ = $\delta^{18}O_{Box}$ - $\varepsilon_{upt}$ (‰) = nitrate O isotope fractionation from nitrate assimilation

$\delta^{18}O_{denitrif}$ = $\delta^{18}O_{Box}$ - $\varepsilon_{denitrif}$ (‰) = nitrate O isotope fractionation from denitrification

where

$\varepsilon_{upt}$ (‰) = nitrate assimilation isotope effect (5 ‰) and $\varepsilon_{denitrif}$ (‰) = denitrification isotope effect (25‰ and 1.5‰ for water-column and sedimentary denitrification, respectively)

$\delta^{15}N_{nitrif}$ = $\delta^{15}N$ returned following organic matter remineralization and nitrification.

$\delta^{18}O_{nitrif}$ = $\delta^{18}O$ returned following organic matter remineralization and nitrification (-3.8‰)

$\delta^{18}O_{NO2-\ re\text{-}oxid}$ = $\delta^{18}O$-$NO_3^-$ returned following nitrate reduction to nitrite and nitrite re-oxidation (~0‰)

### B.1.1. Chapter 2, scenarios 1, 2, and 3

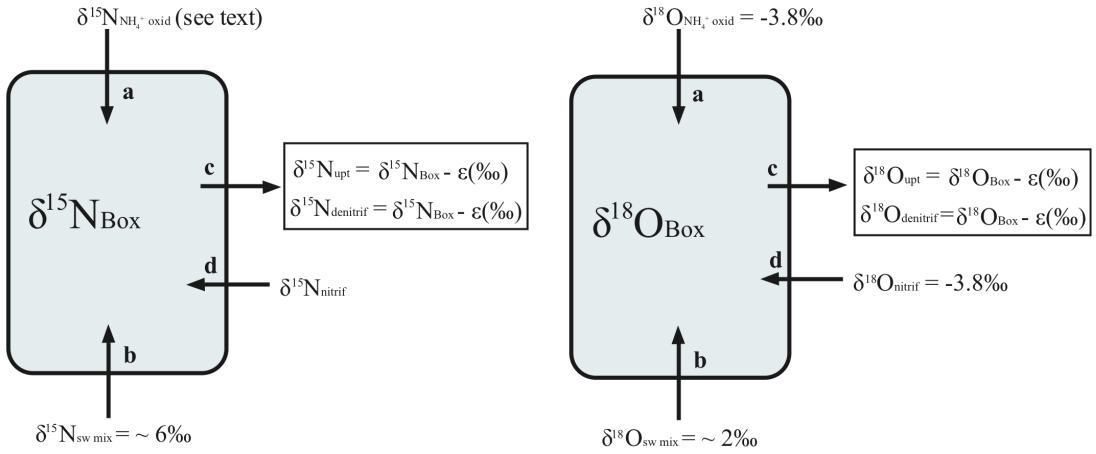


**Figure B.1.** Nitrate isotope box-model for scenarios 1, 2 and 3 (see chapter 2, section 2.4.4.3).

The equation for $\delta^{15}N_{Box}$ is derived from:

$$\delta^{15}N_{Box} = [\delta^{15}N_{NH4+\ oxid} \times a] + [\delta^{15}N_{sw\ mix} \times b] - [(c_{upt} - d) \times (\delta^{15}N_{Box} - {}^{15}\varepsilon_{upt})] - [c_{denitrif} \times (\delta^{15}N_{Box} - {}^{15}\varepsilon_{denitrif})]$$

$$\delta^{15}N_{Box} = [\delta^{15}N_{NH4+\ oxid} \times a] + [\delta^{15}N_{sw\ mix} \times b] - [(c_{upt} - d) \times \delta^{15}N_{Box}] + [(c_{upt} - d) \times {}^{15}\varepsilon_{upt}] - [c_{denitrif} \times \delta^{15}N_{Box}] + [c_{denitrif} \times {}^{15}\varepsilon_{denitrif}]$$

$$\delta^{15}N_{Box} + [(c_{upt} - d) \times \delta^{15}N_{Box}] + [c_{denitrif} \times \delta^{15}N_{Box}] = [\delta^{15}N_{NH4+\ oxid} \times a] + [\delta^{15}N_{sw\ mix} \times b] + [(c_{upt} - d) \times {}^{15}\varepsilon_{upt}] + [c_{denitrif} \times {}^{15}\varepsilon_{denitrif}]$$

$$\delta^{15}N_{Box} + [(c_{upt} - d) \times \delta^{15}N_{Box}] + [c_{denitrif} \times \delta^{15}N_{Box}] = [\delta^{15}N_{NH4+\ oxid} \times a] + [\delta^{15}N_{sw\ mix} \times b] + [(c_{upt} - d) \times {}^{15}\varepsilon_{upt}] + [c_{denitrif} \times {}^{15}\varepsilon_{denitrif}]$$

$$\delta^{15}N_{Box} + [1 + (c_{upt} - d) + c_{denitrif}] = [\delta^{15}N_{NH4+\ oxid} \times a] + [\delta^{15}N_{sw\ mix} \times b] + [(c_{upt} - d) \times {}^{15}\varepsilon_{upt}] + [c_{denitrif} \times {}^{15}\varepsilon_{denitrif}]$$

The final equation for $\delta^{15}N_{Box}$ is:

$$\delta^{15}N_{Box} = [(\delta^{15}N_{NH4+\ oxid} \times a] + [\delta^{15}N_{sw\ mix} \times b] + [(c_{upt} - d) \times {}^{15}\varepsilon_{upt}] + [c_{denitrif} \times {}^{15}\varepsilon_{denitrif})] / [1 + (c_{upt} - d) + c_{denitrif}]$$

The equation for $\delta^{18}O_{box}$ is derived from:

$$\delta^{18}O_{Box} = [\delta^{18}O_{NH4+\ oxid} \times a] + [\delta^{18}O_{sw\ mix} \times b] - [c_{upt} \times (\delta^{18}O_{Box} - {}^{18}\varepsilon_{upt})] - [c_{denitrif} \times (\delta^{18}O_{Box} - {}^{18}\varepsilon_{denitrif})] + [d \times \delta^{18}O_{nitrif}]$$

$$\delta^{18}O_{Box} = [\delta^{18}O_{NH4+\ oxid} \times a] + [\delta^{18}O_{sw\ mix} \times b] - [c_{upt} \times \delta^{18}O_{Box}] + [c_{upt} \times {}^{18}\varepsilon_{upt}] - [c_{denitrif} \times \delta^{18}O_{Box}] + [c_{denitrif} \times {}^{18}\varepsilon_{denitrif}] + [d \times \delta^{18}O_{nitrif}]$$

$$\delta^{18}O_{Box} + [c_{upt} \times \delta^{18}O_{Box}] + [c_{denitrif} \times \delta^{18}O_{Box}] = [\delta^{18}O_{NH4+\ oxid} \times a] + [\delta^{18}O_{sw\ mix} \times b] + [c_{upt} \times {}^{18}\varepsilon_{upt}] + [c_{denitrif} \times {}^{18}\varepsilon_{denitrif}] + [d \times \delta^{18}O_{nitrif}]$$

$$\delta^{18}O_{Box} \times [1 + c_{upt} + c_{denitrif}] = [\delta^{18}O_{NH4+\ oxid} \times a] + [\delta^{18}O_{sw\ mix} \times b] + [c_{upt} \times {}^{18}\varepsilon_{upt}] + [c_{denitrif} \times {}^{18}\varepsilon_{denitrif}] + [d \times \delta^{18}O_{nitrif}]$$

The final equation for $\delta^{18}O_{Box}$ is:

$$\delta^{18}O_{Box} = [\delta^{18}O_{NH4+\ oxid} \times a] + [\delta^{18}O_{sw\ mix} \times b] + [c_{upt} \times {}^{18}\varepsilon_{upt}] + [c_{denitrif} \times {}^{18}\varepsilon_{denitrif}] + [d \times \delta^{18}O_{nitrif}] / [1 + c_{upt} + c_{denitrif}]$$

The $\Delta(15,18)$ is calculated according to equation 2.3.

### B.1.2. Chapter 2, scenarios 4 and 5

The equations used for scenarios 4 and 5 are the same than for scenarios 1, 2, 3 (see B.1.1), except that the low $\delta^{15}N\text{-}NO_3^-$ is coming from $N_2$ fixation instead of partial nitrification of ammonium to nitrate.

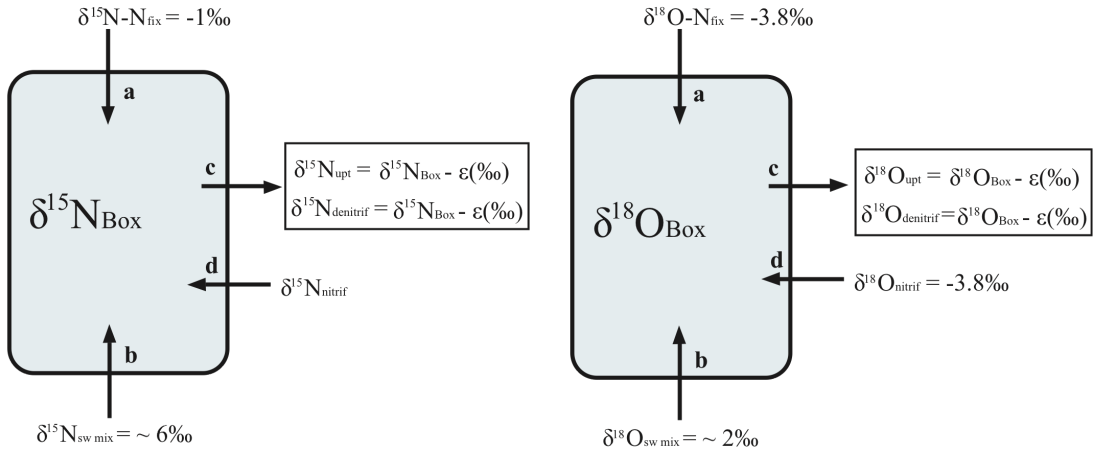


**Figure B.2.** Nitrate isotope box-model for scenarios 4 and 5 (see chapter 2, section 2.4.4.3).

The final equation for $\delta^{15}N_{Box}$ is:

$$\delta^{15}N_{Box} = [(\delta^{15}N\text{-}N_{fix} \times a] + [\delta^{15}N_{sw\ mix} \times b] + [(c_{upt} - d) \times {}^{15}\varepsilon_{upt}] + [c_{denitrif} \times {}^{15}\varepsilon_{denitrif})] / [1 + (c_{upt} - d) + c_{denitrif}]$$

The final equation for $\delta^{18}O_{Box}$ is:

$$\delta^{18}O_{Box} = [\delta^{18}O\text{-}N_{fix} \times a] + [\delta^{18}O_{sw\ mix} \times b] + [c_{upt} \times {}^{18}\varepsilon_{upt}] + [c_{denitrif} \times {}^{18}\varepsilon_{denitrif}] + [d \times \delta^{18}O_{nitrif}] / [1 + c_{upt} + c_{denitrif}]$$

The $\Delta(15,18)$ is calculated according to equation 2.3.

### B. 1. 3. Chapter 2, scenarios 6 and 7

The equations used for scenario 7 are presented below. The same equations were used for scenario 6, minus the first term of each equations for $\delta^{15}N_{Box}$ and $\delta^{18}O_{Box}$ (i.e. $[\delta^{15}N_{NH4+\ oxid} \times a]$ and $[\delta^{18}O_{NH4+\ oxid} \times a]$).

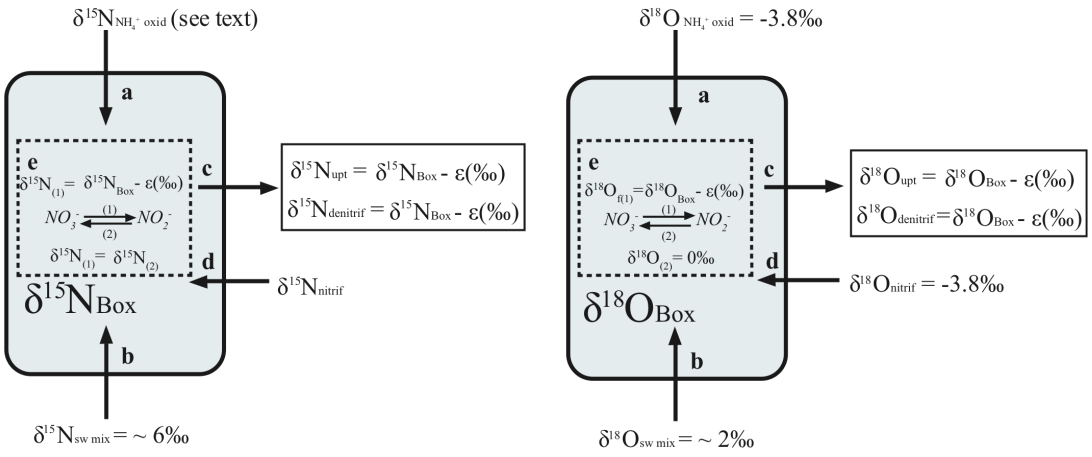


**Figure B.3.** Nitrate isotope box-model for scenarios 6 and 7 (see chapter 2, section 2.4.4.3).

The equation for $\delta^{15}N_{Box}$ is derived from:

$$\delta^{15}N_{Box} = [\delta^{15}N_{NH4+\ oxid} \times a] + [\delta^{15}N_{sw\ mix} \times b] - [(c_{upt} - d) \times (\delta^{15}N_{Box} - {}^{15}\varepsilon_{upt})] - [c_{denitrif} \times (\delta^{15}N_{Box} - {}^{15}\varepsilon_{denitrif})] - [(e_{red\ NO2-} - e_{NO2-\ re\text{-}oxid}) \times (\delta^{15}N_{Box} - {}^{15}\varepsilon_{denitrif})]$$

$$\delta^{15}N_{Box} = [\delta^{15}N_{NH4+\ oxid} \times a] + [\delta^{15}N_{sw\ mix} \times b] - [(c_{upt} - d) \times \delta^{15}N_{Box}] + [(c_{upt} - d) \times {}^{15}\varepsilon_{upt})] - [c_{denitrif} \times \delta^{15}N_{Box}] + [c_{denitrif} \times {}^{15}\varepsilon_{denitrif})] - [(e_{red\ NO2-} - e_{NO2-\ re\text{-}oxid}) \times \delta^{15}N_{Box}] + [(c_{red\ NO2-} - e_{NO2-\ re\text{-}oxid}) \times {}^{15}\varepsilon_{denitrif})]$$

$$\delta^{15}N_{Box} + [(c_{upt} - d) \times \delta^{15}N_{Box}] + [c_{denitrif} \times \delta^{15}N_{Box}] + [(e_{red\ NO2-} - e_{NO2-\ re\text{-}oxid}) \times \delta^{15}N_{Box}] = [\delta^{15}N_{NH4+\ oxid} \times a] + [\delta^{15}N_{sw\ mix} \times b] + [(c_{upt} - d) \times {}^{15}\varepsilon_{upt})] + [c_{denitrif} \times {}^{15}\varepsilon_{denitrif})] + [(e_{red\ NO2-} - e_{NO2-\ re\text{-}oxid}) \times {}^{15}\varepsilon_{denitrif})]$$

$\delta^{15}N_{Box} \times [1+ (c_{upt} - d) + c_{denitrif} + (e_{red\ NO2-} - e_{NO2-\ re\text{-}oxid})] = [\delta^{15}N_{NH4+\ oxid} \times a] + [\delta^{15}N_{sw\ mix} \times b] + [(c_{upt} - d) \times {}^{15}\varepsilon_{upt})] + [c_{denitrif} \times {}^{15}\varepsilon_{denitrif})] + [(e_{red\ NO2-} - e_{NO2-\ re\text{-}oxid}) \times {}^{15}\varepsilon_{denitrif})]$

The final equation for $\delta^{15}N_{Box}$ is:

$\delta^{15}N_{Box} = [\delta^{15}N_{NH4+\ oxid} \times a] + [\delta^{15}N_{sw\ mix} \times b] + [(c_{upt} - d) \times {}^{15}\varepsilon_{upt})] + [c_{denitrif} \times {}^{15}\varepsilon_{denitrif})] + [(e_{red\ NO2-} - e_{NO2-\ re\text{-}oxid}) \times {}^{15}\varepsilon_{denitrif})] / [1+ (c_{upt} - d) + c_{denitrif} + (e_{red\ NO2-} - e_{NO2-\ re\text{-}oxid})]$

The equation for $\delta^{18}O_{Box}$ is derived from:

$\delta^{18}O_{Box} = [\delta^{18}O_{NH4+\ oxid} \times a] + [\delta^{18}O_{sw\ mix} \times b] - [c_{upt} \times (\delta^{18}O_{Box} - {}^{18}\varepsilon_{upt})] - [c_{denitrif} \times (\delta^{18}O_{Box} - {}^{18}\varepsilon_{denitrif})] - [e_{red\ NO2-} \times (\delta^{18}O_{Box} - {}^{18}\varepsilon_{denitrif})] + [d \times \delta^{18}O_{nitrif}] + [e_{NO2-\ re\text{-}oxid} \times \delta^{18}O_{NO2-\_re\text{-}oxid}]$

$\delta^{18}O_{Box} = [\delta^{18}O_{NH4+\ oxid} \times a] + [\delta^{18}O_{sw\ mix} \times b] - [c_{upt} \times \delta^{18}O_{Box}] + [c_{upt} \times {}^{18}\varepsilon_{upt}] - [c_{denitrif} \times \delta^{18}O_{Box}] + [c_{denitrif} \times {}^{18}\varepsilon_{denitrif}] - [e_{red\_NO2-} \times \delta^{18}O_{Box}] + [e_{red\ NO2-} \times {}^{18}\varepsilon_{denitrif})] + [d \times \delta^{18}O_{nitrif}] + [e_{NO2-\ re\text{-}oxid} \times \delta^{18}O_{NO2-\_re\text{-}oxid}]$

$\delta^{18}O_{Box} + [c_{upt} \times \delta^{18}O_{Box}] + [c_{denitrif} \times \delta^{18}O_{Box}] + [e_{red\ NO2-} \times \delta^{18}O_{Box}] = [\delta^{18}O_{NH4+\ oxid} \times a] + [\delta^{18}O_{sw\ mix} \times b] + [c_{upt} \times {}^{18}\varepsilon_{upt}] + [c_{denitrif} \times {}^{18}\varepsilon_{denitrif}] + [e_{red\ NO2-} \times {}^{18}\varepsilon_{denitrif})] + [d \times \delta^{18}O_{nitrif}] + [e_{NO2-\ re\text{-}oxid} \times \delta^{18}O_{NO2-\_re\text{-}oxid}]$

$\delta^{18}O_{Box} \times [1 + c_{upt} + c_{denitrif} + e_{red\ NO2-}] = [\delta^{18}O_{NH4+\ oxid} \times a] + [\delta^{18}O_{sw\ mix} \times b] + [c_{upt} \times {}^{18}\varepsilon_{upt}] + [c_{denitrif} \times {}^{18}\varepsilon_{denitrif}] + [e_{red\ NO2-} \times {}^{18}\varepsilon_{denitrif})] + [d \times \delta^{18}O_{nitrif}] + [e_{NO2-\ re\text{-}oxid} \times \delta^{18}O_{NO2-\_re\text{-}oxid}]$

The final equation for $\delta^{18}O_{Box}$ is:

$$\delta^{18}O_{Box} = [\delta^{18}O_{NH4+\ oxid} \times a] + [\delta^{18}O_{sw\ mix} \times b] + [c_{upt} \times {}^{18}\varepsilon_{upt}] + [c_{denitrif} \times {}^{18}\varepsilon_{denitrif}] + [e_{red\ NO2-} \times {}^{18}\varepsilon_{denitrif})] + [d \times \delta^{18}O_{nitrif}] + [e_{NO2-\ re\text{-}oxid} \times \delta^{18}O_{NO2-\ re\text{-}oxid}] / [1 + c_{upt} + c_{denitrif} + e_{red\ NO2-}]$$

The Δ(15,18) is calculated according to equation 2.3.

## B.2. Nitrate isotope box-model equations used in chapter 5

Below are the equations used for all nitrate isotope box-model scenarios presented in chapter 5. All terms, except the one defined below, are the same as in section B.1. of this appendix. See chapter 5 (section 5.5.3.1.3 and Figure 5.9) for major assumptions and model results.

Additional term definitions:

a = partial $NH_4^+$ oxidation to $NO_3^-$ or N from precipitation flux

$\delta^{15}N_{rain} = \delta^{15}N\text{-}NO_3^-$ from precipitation (~-2 ‰)

$\delta^{18}O_{rain} = \delta^{18}O\text{-}NO_3^-$ from precipitation (~35 ‰)

$\delta^{15}N_{dw\ mix} = \delta^{15}N\text{-}NO_3^-$ added from vertical mixing with deep-water (~7.5 ‰)

$\delta^{18}O_{dw\ mix} = \delta^{18}O\text{-}NO_3^-$ added from vertical mixing with deep-water (~2 ‰)

$\delta^{15}N_{uw\ mix} = \delta^{15}N\text{-}NO_3^-$ added from vertical mixing with upper-water (~7.5 ‰)

$\delta^{18}O_{uw\ mix} = \delta^{18}O\text{-}NO_3^-$ added from vertical mixing with upper-water (~2 ‰)

$\delta^{15}N_{NO2-\ re\text{-}oxid} = \delta^{15}N\text{-}NO_3^-$ returned following nitrate reduction to nitrite and nitrite re-oxidation

### B.2.1. Chapter 5, scenario 1a

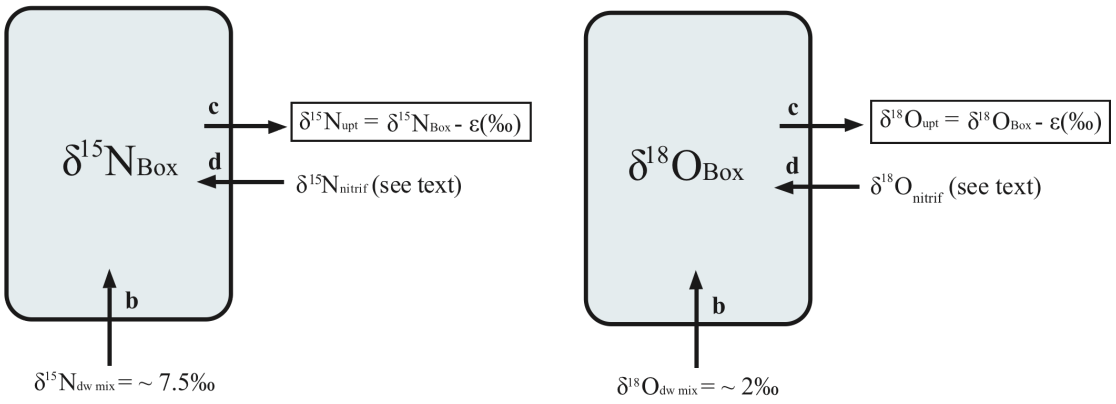


**Figure B.4.** Nitrate isotope box-model for scenario 1a (see chapter 5, section 5.5.3.1.3).

The equation for $\delta^{15}N_{Box}$ is derived from:

$$\delta^{15}N_{Box} = [\delta^{15}N_{sw\ mix} \times b] - [c_{upt} \times (\delta^{15}N_{Box} - {}^{15}\varepsilon_{upt})] + [d \times \delta^{15}N_{nitrif}]$$

Note: Here, the $\delta^{15}N_{nitrif}$ term represents the input of low $\delta^{15}N\text{-}NO_3^-$ from organic matter ammonification, partial ammonium oxidation to nitrite, and partial nitrite oxidation to nitrate (see text, section 5.5.3.1.3).

$$\delta^{15}N_{Box} = [\delta^{15}N_{dw\ mix} \times b] - [c_{upt} \times \delta^{15}N_{Box}] + [c_{upt} \times {}^{15}\varepsilon_{upt})] + [d \times \delta^{15}N_{nitrif}]$$

$$\delta^{15}N_{Box} + [c_{upt} \times \delta^{15}N_{Box}] = [\delta^{15}N_{dw\ mix} \times b] + [c_{upt} \times {}^{15}\varepsilon_{upt})] + [d \times \delta^{15}N_{nitrif}]$$

$$\delta^{15}N_{Box} \times [1 + c_{upt}] = [\delta^{15}N_{dw\ mix} \times b] + [c_{upt} \times {}^{15}\varepsilon_{upt})] + [d \times \delta^{15}N_{nitrif}]$$

The final equation for $\delta^{15}N_{Box}$ is:

$$\delta^{15}N_{Box} = [\delta^{15}N_{dw\ mix} \times b] + [c_{upt} \times {}^{15}\varepsilon_{upt})] + [d \times \delta^{15}N_{nitrif}] / [1 + c_{upt}]$$

The equation for $\delta^{18}O_{Box}$ is derived from:

$$\delta^{18}O_{Box} = [\delta^{18}O_{dw\ mix} \times b] - [c_{upt} \times (\delta^{18}O_{Box} - {}^{18}\varepsilon_{upt})] + [d \times \delta^{18}O_{nitrif}]$$

$$\delta^{18}O_{Box} = [\delta^{18}O_{dw\ mix} \times b] - [c_{upt} \times \delta^{18}O_{Box}] + [c_{upt} \times {}^{18}\varepsilon_{upt})] + [d \times \delta^{18}O_{nitrif}]$$

$$\delta^{18}O_{Box} + [c_{upt} \times \delta^{18}O_{Box}] = [\delta^{18}O_{dw\ mix} \times b] + [c_{upt} \times {}^{18}\varepsilon_{upt})] + [d \times \delta^{18}O_{nitrif}]$$

$$\delta^{18}O_{Box} \times [1 + c_{upt}] = [\delta^{18}O_{dw\ mix} \times b] + [c_{upt} \times {}^{18}\varepsilon_{upt})] + [d \times \delta^{18}O_{nitrif}]$$

The final equation for $\delta^{18}O_{Box}$ is:

$$\delta^{18}O_{Box} = [\delta^{18}O_{dw\ mix} \times b] + [c_{upt} \times {}^{18}\varepsilon_{upt})] + [d \times \delta^{18}O_{nitrif}] / [1 + c_{upt}]$$

The Δ(15,18) is calculated according to equation 5.3.

### B. 2. 2. Chapter 5, scenario 1b

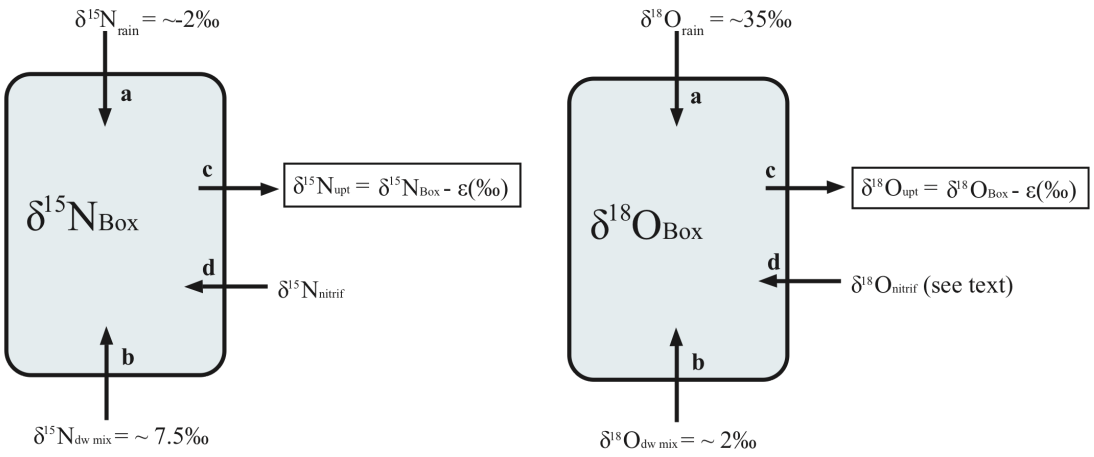


**Figure B.5.** Nitrate isotope box-model for scenario 1b (see chapter 5, section 5.5.3.1.3).

The equation for $\delta^{15}N_{Box}$ is derived from:

$$\delta^{15}N_{Box} = [\delta^{15}N_{rain} \times a] + [\delta^{15}N_{dw\ mix} \times b] - [(c_{upt} - d) \times (\delta^{15}N_{Box} - {}^{15}\varepsilon_{upt})]$$

$\delta^{15}N_{Box} = [\delta^{15}N_{rain} \times a] + [\delta^{15}N_{dw\ mix} \times b] - [(c_{upt} - d) \times \delta^{15}N_{Box}] + [(c_{upt} - d) \times {}^{15}\varepsilon_{upt}]$

$\delta^{15}N_{Box} + [(c_{upt} - d) \times \delta^{15}N_{Box}] = [\delta^{15}N_{rain} \times a] + [\delta^{15}N_{dw\ mix} \times b] + [(c_{upt} - d) \times {}^{15}\varepsilon_{upt}]$

$\delta^{15}N_{Box} + [(c_{upt} - d) \times \delta^{15}N_{Box}] = [\delta^{15}N_{rain} \times a] + [\delta^{15}N_{dw\ mix} \times b] + [(c_{upt} - d) \times {}^{15}\varepsilon_{upt}]$

$\delta^{15}N_{Box} \times [1 + (c_{upt} - d)] = [\delta^{15}N_{rain} \times a] + [\delta^{15}N_{dw\ mix} \times b] + [(c_{upt} - d) \times {}^{15}\varepsilon_{upt}]$ The final equation for $\delta^{15}N_{Box}$ is:

$\delta^{15}N_{Box} = [(\delta^{15}N_{rain} \times a] + [\delta^{15}N_{dw\ mix} \times b] + [(c_{upt} - d) \times {}^{15}\varepsilon_{upt}] / [1 + (c_{upt} - d)]$

The equation for $\delta^{18}O_{box}$ is derived from:

$\delta^{18}O_{Box} = [\delta^{18}O_{rain} \times a] + [\delta^{18}O_{sw\ mix} \times b] - [c_{upt} \times (\delta^{18}O_{Box} - {}^{18}\varepsilon_{upt})] + [d \times \delta^{18}O_{nitrif}]$

$\delta^{18}O_{Box} = [\delta^{18}O_{rain} \times a] + [\delta^{18}O_{sw\ mix} \times b] - [c_{upt} \times \delta^{18}O_{Box}] + [c_{upt} \times {}^{18}\varepsilon_{upt})] + [d \times \delta^{18}O_{nitrif}]$

$\delta^{18}O_{Box} + [c_{upt} \times \delta^{18}O_{Box}] = [\delta^{18}O_{rain} \times a] + [\delta^{18}O_{sw\ mix} \times b] + [c_{upt} \times {}^{18}\varepsilon_{upt})] + [d \times \delta^{18}O_{nitrif}]$

$\delta^{18}O_{Box} \times [1+ c_{upt}] = [\delta^{18}O_{rain} \times a] + [\delta^{18}O_{sw\ mix} \times b] + [c_{upt} \times {}^{18}\varepsilon_{upt})] + [d \times \delta^{18}O_{nitrif}]$

The final equation for $\delta^{18}O_{Box}$ is:

$\delta^{18}O_{Box} = [\delta^{18}O_{rain} \times a] + [\delta^{18}O_{sw\ mix} \times b] + [c_{upt} \times {}^{18}\varepsilon_{upt})] + [d \times \delta^{18}O_{nitrif}] / [1+ c_{upt}]$

The $\Delta(15,18)$ is calculated according to equation 5.3.

### B. 2. 3. Chapter 5, scenario 2a

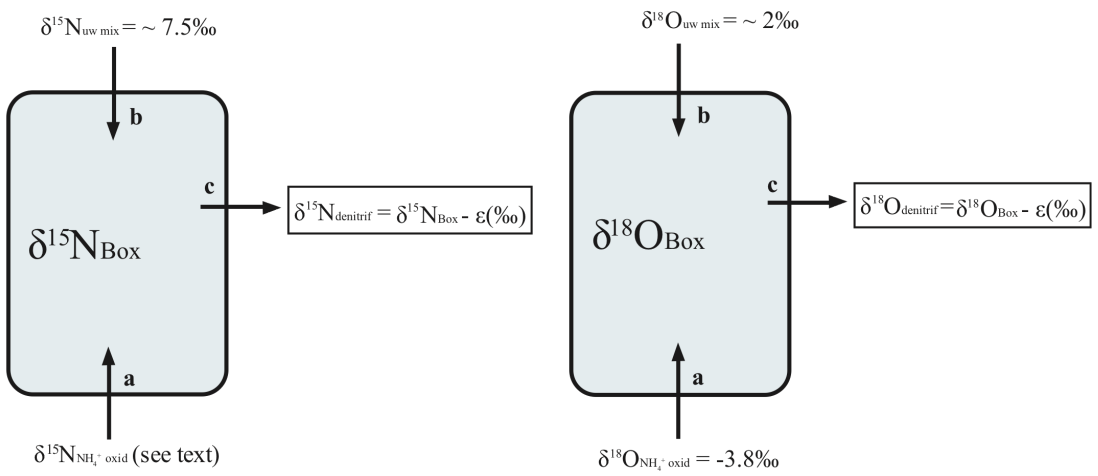


**Figure B.6.** Nitrate isotope box-model for scenario 2a (see chapter 5, section 5.5.3.1.3).

The equation for $\delta^{15}N_{Box}$ is derived from:

$$\delta^{15}N_{Box} = [\delta^{15}N_{NH4+\ oxid} \times a] + [\delta^{15}N_{uw\ mix} \times b] - [c_{denitrif} \times (\delta^{15}N_{Box} - {}^{15}\varepsilon_{denitrif})]$$

$$\delta^{15}N_{Box} = [\delta^{15}N_{NH4+\ oxid} \times a] + [\delta^{15}N_{uw\ mix} \times b] - [c_{denitrif} \times \delta^{15}N_{Box}] + [c_{denitrif} \times {}^{15}\varepsilon_{denitrif})]$$

$$\delta^{15}N_{Box} + [c_{denitrif} \times \delta^{15}N_{Box}] = [\delta^{15}N_{NH4+\ oxid} \times a] + [\delta^{15}N_{uw\ mix} \times b] + [c_{denitrif} \times {}^{15}\varepsilon_{denitrif})]$$

$$\delta^{15}N_{Box} \times [1 + c_{denitrif}] = [\delta^{15}N_{NH4+\ oxid} \times a] + [\delta^{15}N_{uw\ mix} \times b] + [c_{denitrif} \times {}^{15}\varepsilon_{denitrif})]$$

The final equation for $\delta^{15}N_{Box}$ is:

$$\delta^{15}N_{Box} = [\delta^{15}N_{NH4+\ oxid} \times a] + [\delta^{15}N_{uw\ mix} \times b] + [c_{denitrif} \times {}^{15}\varepsilon_{denitrif})] / [1 + c_{denitrif}]$$

The equation for $\delta^{18}O_{Box}$ is derived from:

$$\delta^{18}O_{Box} = [\delta^{18}O_{NH4+\ oxid} \times a] + [\delta^{18}O_{uw\ mix} \times b] - [c_{denitrif} \times (\delta^{18}O_{Box} - {}^{18}\varepsilon_{denitrif})]$$

$$\delta^{18}O_{Box} = [\delta^{18}O_{NH4+\ oxid} \times a] + [\delta^{18}O_{uw\ mix} \times b] - [c_{denitrif} \times \delta^{18}O_{Box}] + [c_{denitrif} \times {}^{18}\varepsilon_{denitrif})]$$

$$\delta^{18}O_{Box} + [c_{denitrif} \times \delta^{18}O_{Box}] = [\delta^{18}O_{NH4+\ oxid} \times a] + [\delta^{18}O_{uw\ mix} \times b] + [c_{denitrif} \times {}^{18}\varepsilon_{denitrif})]$$

$$\delta^{18}O_{Box} \times [1 + c_{denitrif}] = [\delta^{18}O_{NH4+\ oxid} \times a] + [\delta^{18}O_{uw\ mix} \times b] + [c_{denitrif} \times {}^{18}\varepsilon_{denitrif})]$$

The final equation for $\delta^{18}O_{Box}$ is:

$$\delta^{18}O_{Box} = [\delta^{18}O_{NH4+\ oxid} \times a] + [\delta^{18}O_{uw\ mix} \times b] + [c_{denitrif} \times {}^{18}\varepsilon_{denitrif})] / [1 + c_{denitrif}]$$

The Δ(15,18) is calculated according to equation 5.3.

### B. 2. 4. Chapter 5, scenarios 2b and c

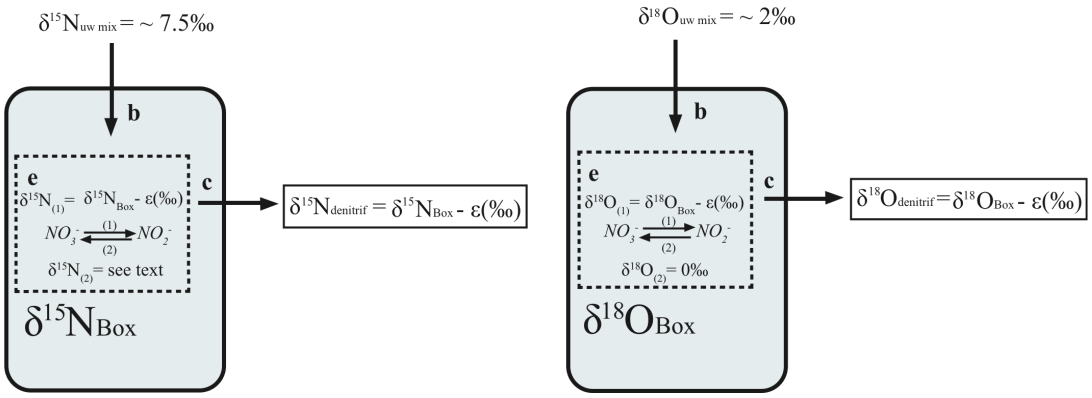


**Figure B.7.** Nitrate isotope box-model for scenario 2b and c (see chapter 5, section 5.5.3.1.3).

The equations for scenario 2b are the same as for scenario 7 in section B.1.3, minus the terms for partial nitrification of ammonium to nitrate ($[\delta^{15}N_{NH4+\ oxid} \times a]$ and $[\delta^{18}O_{NH4+\ oxid} \times a]$) as well as nitrate assimilation and recycled production ($[(c_{upt} - d) \times (\delta^{15}N_{Box} - {}^{15}\varepsilon_{upt})]$, $[c_{upt} \times (\delta^{18}O_{Box} - {}^{18}\varepsilon_{upt})]$ and $[d \times \delta^{18}O_{nitrif}]$).

For scenario 2b, the final equation for $\delta^{15}N_{Box}$ is:

$$\delta^{15}N_{Box} = [\delta^{15}N_{uw\ mix} \times b] + [c_{denitrif} \times {}^{15}\varepsilon_{denitrif})] + [(e_{red\ NO2-} - e_{NO2-\ re\text{-}oxid}) \times {}^{15}\varepsilon_{denitrif})] / [1 + c_{denitrif} + (e_{red\ NO2-} - e_{NO2-\ re\text{-}oxid})]$$

For scenario 2b, the final equation for $\delta^{18}O_{Box}$ is:

$$\delta^{18}O_{Box} = [\delta^{18}O_{uw\ mix} \times b] + [c_{denitrif} \times {}^{18}\varepsilon_{denitrif}] + [c_{red\_NO2-} \times {}^{18}\varepsilon_{denitrif})] + [e \times \delta^{18}O_{NO2-\_re-oxid}] / [1 + c_{denitrif} + c_{red\_NO2-}]$$

The $\Delta(15,18)$ is calculated according to equation 5.3.

For scenario 2c, the following equations are used:

The equation for $\delta^{15}N_{Box}$ is derived from:

$$\delta^{15}N_{Box} = [\delta^{15}N_{uw\ mix} \times b] - [c_{denitrif} \times (\delta^{15}N_{Box} - {}^{15}\varepsilon_{denitrif})] - [e_{red\ NO2-} \times (\delta^{15}N_{Box} - {}^{15}\varepsilon_{denitrif})] + [\delta^{15}N_{NO2-\ re-oxid} \times e_{NO2-\ re-oxid}]$$

$$\delta^{15}N_{Box} = [\delta^{15}N_{uw\ mix} \times b] - [c_{denitrif} \times \delta^{15}N_{Box}] + [c_{denitrif} \times {}^{15}\varepsilon_{denitrif})] - [e_{red\ NO2-} \times \delta^{15}N_{Box}] + [e_{red\ NO2-} \times {}^{15}\varepsilon_{denitrif})] + [\delta^{15}N_{NO2-\ re-oxid} \times e_{NO2-\ re-oxid}]$$

$$\delta^{15}N_{Box} + [c_{denitrif} \times \delta^{15}N_{Box}] + [e_{red\ NO2-} \times \delta^{15}N_{Box}] = [\delta^{15}N_{uw\ mix} \times b] + [c_{denitrif} \times {}^{15}\varepsilon_{denitrif})] + [e_{red\ NO2-} \times {}^{15}\varepsilon_{denitrif})] + [\delta^{15}N_{NO2-\ re-oxid} \times e_{NO2-\ re-oxid}]$$

$$\delta^{15}N_{Box} \times [1 + c_{denitrif} + c_{red\_NO2-}] = [\delta^{15}N_{uw\ mix} \times b] + [c_{denitrif} \times {}^{15}\varepsilon_{denitrif})] + [e_{red\ NO2-} \times {}^{15}\varepsilon_{denitrif})] + [\delta^{15}N_{NO2-\ re-oxid} \times e_{NO2-\ re-oxid}]$$

The final equation for $\delta^{15}N_{Box}$ is:

$$\delta^{15}N_{Box} = [\delta^{15}N_{uw\ mix} \times b] + [c_{denitrif} \times {}^{15}\varepsilon_{denitrif})] + [e_{red\ NO2-} \times {}^{15}\varepsilon_{denitrif})] + [\delta^{15}N_{NO2-\ re-oxid} \times e_{NO2-\ re-oxid}] / [1 + c_{denitrif} + e_{red\ NO2-}]$$

The equation for $\delta^{18}O_{Box}$ is derived from:

$$\delta^{18}O_{Box} = [\delta^{18}O_{NH4+\ oxid} \times a] + [\delta^{18}O_{uw\ mix} \times b] - [c_{denitrif} \times (\delta^{18}O_{Box} - {}^{18}\varepsilon_{denitrif})] - [e_{red\ NO2-} \times (\delta^{18}O_{Box} - {}^{18}\varepsilon_{denitrif})] + [e_{NO2-\ re\text{-}oxid} \times \delta^{18}O_{NO2-\_re\text{-}oxid}]$$

$$\delta^{18}O_{Box} = [\delta^{18}O_{NH4+\ oxid} \times a] + [\delta^{18}O_{uw\ mix} \times b] - [c_{denitrif} \times \delta^{18}O_{Box}] + [c_{denitrif} \times {}^{18}\varepsilon_{denitrif})] - [e_{red\ NO2-} \times \delta^{18}O_{Box}] + [e_{red\ NO2-} \times {}^{18}\varepsilon_{denitrif})] + [e_{NO2-\ re\text{-}oxid} \times \delta^{18}O_{NO2-\_re\text{-}oxid}]$$

$$\delta^{18}O_{Box} + [c_{denitrif} \times \delta^{18}O_{Box}] + [e_{red\ NO2-} \times \delta^{18}O_{Box}] = [\delta^{18}O_{NH4+\ oxid} \times a] + [\delta^{18}O_{uw\ mix} \times b] - [c_{denitrif} \times \delta^{18}O_{Box}] + [c_{denitrif} \times {}^{18}\varepsilon_{denitrif})] + [e_{red\ NO2-} \times {}^{18}\varepsilon_{denitrif})] + [e_{NO2-\ re\text{-}oxid} \times \delta^{18}O_{NO2-\_re\text{-}oxid}]$$

$$\delta^{18}O_{Box}\ [1 + c_{denitrif} + e_{red\ NO2-}] = [\delta^{18}O_{NH4+\ oxid} \times a] + [\delta^{18}O_{uw\ mix} \times b] - [c_{denitrif} \times \delta^{18}O_{Box}] + [c_{denitrif} \times {}^{18}\varepsilon_{denitrif})] + [e_{red\ NO2-} \times {}^{18}\varepsilon_{denitrif})] + [e_{NO2-\ re\text{-}oxid} \times \delta^{18}O_{NO2-\_re\text{-}oxid}]$$

The final equation for $\delta^{18}O_{Box}$ is:

$$\delta^{18}O_{Box} = [\delta^{18}O_{NH4+\ oxid} \times a] + [\delta^{18}O_{uw\ mix} \times b] - [c_{denitrif} \times \delta^{18}O_{Box}] + [c_{denitrif} \times {}^{18}\varepsilon_{denitrif})] + [e_{red\ NO2-} \times {}^{18}\varepsilon_{denitrif})] + [e_{NO2-\ re\text{-}oxid} \times \delta^{18}O_{NO2-\_re\text{-}oxid}] / [1 + c_{denitrif} + e_{red\ NO2-}]$$

The $\Delta(15,18)$ is calculated according to equation 5.3.

# Appendix C
# Supplementary materials

## C.1. Supplementary materials (chapter 3)

**Table C.1.** Copy numbers of bacterial 16S rRNA genes (for both total and SUP05 bacteria) in diffuse hydrothermal vent fluids of the Juan de Fuca Ridge. Standard deviations for three replicate qPCR assays are indicated. BDL = Below Detection Limit.

| Field | Vent | Year | Total bacteria (copy number/mL seawater) | SUP05 bacteria (copy number/mL seawater) |
|---|---|---|---|---|
| AV | Bag City | 2007 | $(14.0 \pm 0.4) \times 10^4$ | $(1.1 \pm 0.2) \times 10^3$ |
| AV | Cloud Pit | 2007 | $(16.0 \pm 0.6) \times 10^3$ | $(4.1 \pm 0.4) \times 10^3$ |
| AV | Gollum | 2007 | $(2.2 \pm 0.2) \times 10^4$ | BDL |
| AV | Marker 113 | 2007 | $(9.8 \pm 0.7) \times 10^5$ | $(1.1 \pm 0.2) \times 10^3$ |
| AV | Bag City | 2008b | $(1.4 \pm 0.1) \times 10^5$ | $(7.7 \pm 0.6) \times 10^3$ |
| AV | Cloud Pit | 2008b | $(3.8 \pm 0.1) \times 10^4$ | $(1.2 \pm 0.5) \times 10^3$ |
| AV | Marker 33 | 2008b | $(0.8 \pm 0.2) \times 10^4$ | $(0.7 \pm 0.1) \times 10^3$ |
| AV | Marker 113 | 2008b | $(0.6 \pm 0.2) \times 10^5$ | BDL |
| AV | Gollum | 2009 | $(5.2 \pm 0) \times 10^3$ | BDL |
| AV | Hermosa | 2009 | $(0.7 \pm 0.7) \times 10^4$ | BDL |
| AV | Marker 33 | 2009 | $(3.2 \pm 0.3) \times 10^4$ | $(1.3 \pm 0.4) \times 10^3$ |
| AV | Marker 113 | 2009 | $(0.9 \pm 0.2) \times 10^5$ | BDL |
| AV | Bkgd | 2009 | na | na |
| ES | Clam bed | 2008a | na | na |
| ES-MEF | Easter Island | 2008a | na | na |
| ES-MEF | Hulk | 2008a | na | na |
| ES-M | Cauldron | 2008b | $(6.0 \pm 0.7) \times 10^4$ | BDL |
| ES-MEF | Easter Island | 2008b | na | na |
| ES-HR | Godzilla | 2008b | $(4.6 \pm 0.1) \times 10^4$ | $(70.0 \pm 0.3) \times 10^1$ |
| ES-MEF | Hulk | 2008b | $(4.4 \pm 0.3) \times 10^3$ | $(1.7 \pm 0.2) \times 10^3$ |
| ES-HR | Fairy Castle | 2009 | $(0.4 \pm 0.1) \times 10^5$ | $(1.7 \pm 0.1) \times 10^3$ |
| ES-MEF | Hulk | 2009 | $(1.0 \pm 0.4) \times 10^5$ | BDL |
| ES-M | Phang | 2009 | $(1.1 \pm 0.2) \times 10^5$ | BDL |
| ES | Bkgd | 2009 | $(4.9 \pm 0.6) \times 10^5$ | $(0.8 \pm 0.1) \times 10^3$ |


**Figure C.1.** Partial 16S rRNA gene ε-proteobacteria phylogenetic tree constructed using the maximum likelihood method implemented in PHYML. Clone prefixes were assigned as follow: the first letters indicate the vent fields: AV= Axial Volcano (in blue) and ES= Endeavour Segment (in red), followed by the year (07= 2007 and 08=2008) and the last letters the diffuse vent sampled: CP= Cloud Pit, BC= Bag City, H= Hulk, and G= Godzilla. The last numbers indicate clones #. The number of clones that are ≥97% identical to a given hydrothermal vent clone is indicated in parentheses. GenBank accession numbers are provided (in brackets) for all other clones not sequenced in this study. The percentage of 100 bootstrap resamplings above 50% is indicated. The scale bar indicates the number of amino acid substitutions per site.

## C.2. Supplementary materials (chapter 4)

**Table C.2.** Copy numbers of % SUP05 bacteria relative to total bacterial abundance in hydrothermal vent fluids of the JFR. The background seawater sample was collected near Endeavour Segment. Standard deviation for triplicate qPCR essays is indicated. SUP05 data from Bag City, Cloud Pit, Gollum and Marker 113 collected in 2007 and all data from 2009 (except Diva and Hulk1) are from Bourbonnais *et al.* (2012b). See Bourbonnais *et al.* (2012b) for analysis protocol. Sample names as in Table 4.1.

| Field/ sample year | Vent | SUP05 bacteria (%) |
|---|---|---|
| AV07 | Bag City | 0.8±0.1 |
| AV07 | Cloud Pit | 26±3 |
| AV07 | Forum | 0.4±0.3 |
| AV07 | Gollum | BDL |
| AV07 | Marker 113 | 0.12±0.02 |
| AV07 | Shepherd | 1.6±0.3 |
| AV07 | The Spot | 0.26±0.02 |
| AV07 | T&S | 0.8±0.3 |
| AV07 | Zen Garden1 | BDL |
| AV07 | Zen Garden2 | 1.8±0.3 |
| AV09 | Diva | BDL |
| AV09 | Gollum | BDL |
| AV09 | Hermosa | BDL |
| AV09 | Marker 33 | 4.0±1.2 |
| AV09 | Marker 113 | BDL |
| CS07 | Not dead yet | BDL |
| ES09 | Fairy Castle | 4±1 |
| ES09 | Hulk1 | BDL |
| ES09 | Hulk2 | BDL |
| ES09 | Phang | BDL |
| ES | Background seawater | 0.16±0.03 |

**Table C.3.** P-values from P-test (Martin *et al*., 2002) and UniFrac distance metric (Lozupone *et al*., 2005) implemented in Fast-UniFrac to compare 16S rRNA gene (V1-V3 regions) bacterial communities in hydrothermal vent fluids of the JFR. The p-values have been corrected using the Bonferroni correction. Significance is indicated by an asterix next to the p-value. Sample names as in Table 4.2.

| | AV07BC | AV07F | AV07S | AV07TS | ES09H |
|---|---|---|---|---|---|
| **P-test** | | | | | |
| AV07BC | | | | | |
| AV07F | <=1.0e-03* | | | | |
| AV07S | <=1.0e-03* | <=1.0e-03* | | | |
| AV07TS | <=1.0e-03* | <=1.0e-03* | <=1.0e-03* | | |
| ES09H | <=1.0e-03* | <=1.0e-03* | <=1.0e-03* | <=1.0e-03* | |
| ES09P | <=1.0e-03* | <=1.0e-03* | <=1.0e-03* | <=1.0e-03* | <=1.0e-03* |
| **UniFrac/ un-weighted** | | | | | |
| AV07BC | | | | | |
| AV07F | <=1.0e-03* | | | | |
| AV07S | <=1.0e-03* | <=1.0e-03* | | | |
| AV07TS | <=1.0e-03* | 1 | <=1.0e-03* | | |
| ES09H | <=1.0e-03* | <=1.0e-03* | <=1.0e-03* | <=1.0e-03* | |
| ES09P | <=1.0e-03* | <=1.0e-03* | <=1.0e-03* | <=1.0e-03* | <=1.0e-03* |
| **UniFrac/ weighted** | | | | | |
| AV07BC | | | | | |
| AV07F | 0.33 | | | | |
| AV07S | <=1.0e-03* | <=1.0e-03* | | | |
| AV07TS | <=1.0e-03* | 1 | <=1.0e-03* | | |
| ES09H | <=1.0e-03* | 1 | <=1.0e-03* | 1 | |
| ES09P | <=1.0e-03* | 0.18 | <=1.0e-03* | 0.045* | 0.03* |

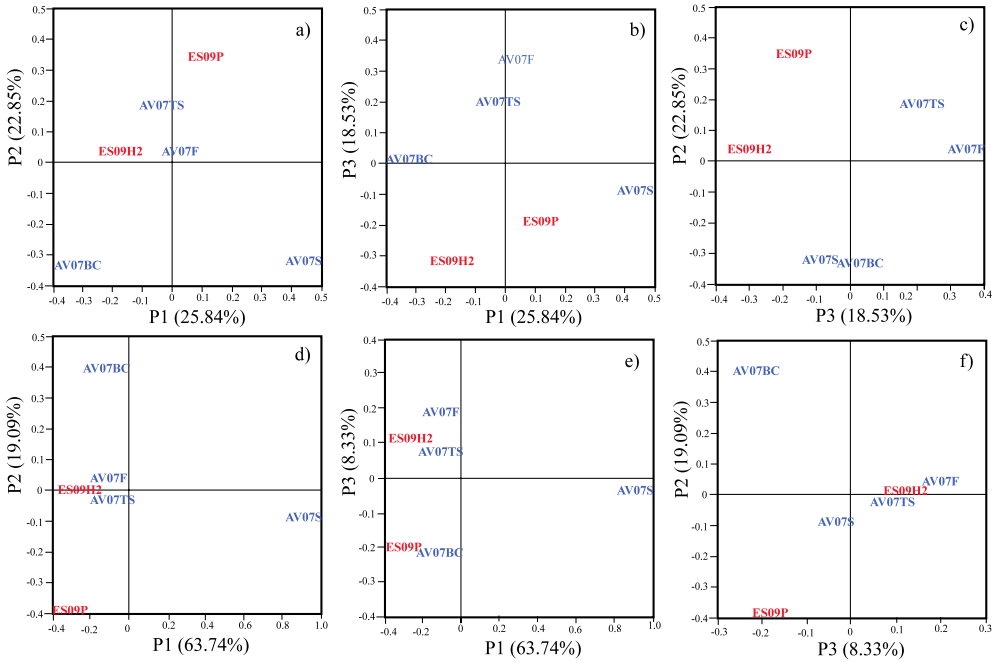


**Figure C.2.** Comparison of 16S rRNA gene bacterial communities obtained from pyrosequencing of the variable V1-V3 regions in hydrothermal vent fluids at Axial Volcano (blue) and Endeavour Segment (red) on the JFR. The scatter-plots were generated using the un-weighted (**a, b, c**) and weighted (**d, e, f**) UniFrac matrix of pairwise distances between communities and Principal Coordinate Analysis (PCoA). The three main components (explaining 67.2% and 91.2% of the variance for the un-weighted and weighted abundance analysis, respectively) are presented. Sample names were assigned as in Table 4.2. The percent of variation explained for each component is indicated in brackets.

# APPENDIX D
# CURRICULUM VITAE - ANNIE BOURBONNAIS

School of Earth and Ocean Sciences, Bob Wright Centre,
University of Victoria,
3800 Finnerty Road (Ring Road),
Victoria, BC, Canada, V8P 5C2,
e-mail: annieb@uvic.ca

Spoken and written languages: English and French

---

## RESEARCH INTERESTS

Marine biogeochemistry, Marine nitrogen cycle, Nitrogen and carbon isotopes, Molecular microbial ecology, Chemosynthetic deep-sea ecosystems

## EDUCATION

| | |
|---|---|
| Sep 2007- Nov 2012 | Ph.D. Earth and Ocean Sciences, University of Victoria (UVic), Victoria, BC, Canada (supervisor: Dr. S. Kim Juniper). |
| Sep 2005- Oct 2007 | M.Sc. Earth Sciences (Mention Excellent), University of Québec in Montréal (UQAM), GEOTOP UQAM-McGill Research Center, Montréal, QC, Canada (supervisor: Dr. Moritz F. Lehmann). |
| Sep 2001- Jun 2005 | B.Sc. Environmental Sciences with Honours in Environmental geochemistry (*Summa Cum Laude*), University of Ottawa, Ottawa, ON, Canada. |

## MAJOR HONORS AND AWARDS

| | |
|---|---|
| Aug 2011- Aug 2012 | PEO Scholar Award (15000$) |
| Sep 2009- Aug 2011 | Rix Family Leading Edge Student Award (5000$/year) |
| Sep 2008- Aug 2010 | University of Victoria President's Scholarship (4000$/year) |
| Sep 2008- Aug 2010 | Doctoral Canada Postgraduate Scholarships (PGS D), Natural Sciences and Engineering Research Council of Canada (NSERC) (25000$/year) |
| Sep 2008- Aug 2010 | Doctoral Research Scholarship, Fonds Québeçois de Recherche sur la Nature et les Technologies (FQRNT) (20000$/year, declined) |
| Sep 2007- Aug 2008 | University of Victoria Fellowship (10000$/year) |
| Sep 2007- Aug 2008 | University of Victoria Pacific Century Scholarship (7800$/year) |
| Sep 2005- Aug 2007 | Master Canada Graduate Scholarships (CGS M), NSERC (17500$/year) |

| | |
|---|---|
| Sep 2005- Aug 2007 | Master Graduate Scholarship, FQRNT (15000$/year, declined) |
| May 2005- Aug 2005 | Undergraduate Student Research Awards (USRA), NSERC (4500$) |
| Jun 2005 | Plaque of the Department of Environmental Sciences, for the highest standing in the Honours Baccalaureate in Science in Environmental Sciences |
| May 2004- Aug 2004 | Undergraduate Student Research Awards (USRA), NSERC (4500$) |
| Sep 2000- Apr 2005 | Admission scholarship, University of Ottawa (2500$/year) |
| Sep 2000- Apr 2005 | Dean's honour list of the faculty of Sciences, University of Ottawa |

**WORK AND TEACHING EXPERIENCE**

| | |
|---|---|
| Jan – Apr 2012 | Laboratory instructor, General Biology II (190B), UVic, Victoria, BC |
| Sep – Dec 2011 | Laboratory instructor, Animal Behavior (345), UVic, Victoria, BC |
| Jan – Apr 2011 | Laboratory instructor, General Biology II (190B), UVic, Victoria, BC |
| Sep – Dec 2010 | Laboratory instructor, Oceans and Atmosphere (EOS/GEOG 110), UVic, Victoria, BC |
| Jan – Apr 2007 | Teaching assistant, Oceanography (SCT 4320), UQAM, Montréal, QC |
| May 2005- Aug 2007 | Research assistant (Marine biogeochemistry), UQAM, Montréal, QC |
| May 2004- Apr 2005 | Research assistant (Groundwater geochemistry), University of Ottawa, ON |

**JOURNAL REVIEWS**

Global Biogeochemical Cycles
Chinese Journal of Oceanology and Limnology

**PARTICIPATION IN SCIENTIFIC EXPEDITIONS**

| | |
|---|---|
| 13-28 Jun 2009 | R/V Atlantis, Northeast Pacific, Chief Scientist: James Holden (University of Massachusetts (UMass), USA). |
| Apr 2008- Apr 2009 | R/V Strickland, Saanich Inlet, British Columbia, 9 one-day cruises, Chief Scientist: **Annie Bourbonnais** (UVic). |
| 18 Aug – 7 Sep 2008 | R/V Atlantis, Northeast Pacific, Chief Scientist: James Holden (UMass, USA). |
| 18-24 Jun 2008 | R/V John P. Tully, Northeast Pacific, Chief Scientist: Kim Juniper (UVic). |

| | |
|---|---|
| 3-20 Aug 2007 | R/V Atlantis, Northeast Pacific, Chief Scientists: David Butterfield and Bill Chadwick (University of Washington, USA). |
| 2-11 May 2005 | R/V Poseidon, Azores Front, Subtropical Northeast Atlantic, Chief Scientist: Tom J. Müller (IFM-GEOMAR, University of Kiel, Germany) |

**PEER-REVIEWED PUBLICATIONS**

**Bourbonnais, A.**, S. K. Juniper, D. A. Butterfield, R. E. Anderson, M. F. Lehmann (2012), Diversity and abundance of Bacteria and *nirS*-encoding denitrifiers associated with the Juan de Fuca Ridge hydrothermal system, *Geobiology*, Submitted (9/10/2012, #GBI-O82-2012), 46 pages.

Wenk, C. B., J. Blees, J. Zopfi, M. Veronesi, **A. Bourbonnais**, C. J. Schubert, H. Niemann, M. F. Lehmann (2013), Anammox bacteria and sulfide-dependent denitrifiers co-exist in the water column of a meromictic south-alpine lake, *Limnology and Oceanography*, 58, 1-12.

**Bourbonnais, A**., S. K. Juniper, D. A. Butterfield, A. H. Devol, M. M. M. Kuypers, G. Lavik, S. J. Hallam, C. B. Wenk, B. X. Chang, S. A. Murdock, and M. F. Lehmann (2012), Activity and abundance of denitrifying bacteria in the subsurface biosphere of diffuse hydrothermal vents of the Juan de Fuca Ridge, *Biogeosciences,* 9, 4661–4678.

**Bourbonnais, A**., M. F. Lehmann, D. A. Butterfield, and S. K. Juniper (2012), Subseafloor nitrogen transformations in diffuse hydrothermal vent fluids of the Juan de Fuca Ridge evidenced by the isotopic composition of nitrate and ammonium, *Geochemistry Geophysics Geosystems*, *13*, Q02T01, doi:10.1029/2011GC003863.

Somes, C, A. Schmittner, E. D. Galbraith, M. F. Lehmann, M. A. Altabet, J. P. Montoya, R. M. Letelier, A. C. Mix, **A. Bourbonnais**, and M. Eby (2010), Simulating the global distribution of nitrogen isotopes in the Ocean, *Global Biogeochemical Cycles*, vol. 24, GB4019, doi: 10.1029/2009GB003767.

Manning, C. C, R. C. Hamme, and **A. Bourbonnais** (2010), Impact of deep-water renewal events on fixed nitrogen loss from seasonally-anoxic Saanich Inlet, *Marine Chemistry*, 122(1-4), 1-10, doi:10.1016/j.marchem.2010.08.002.

**Bourbonnais, A**., M. F. Lehmann, J. J. Waniek and D. E. Schultz-Bull (2009), Nitrate isotope anomalies as indicator of $N_2$ fixation in the Azores Front region (subtropical N-E Atlantic), *Journal of geophysical Research*, 114, C03003, doi:1029/2007JC004617.

Clark, I.D., R. Timlin, **A. Bourbonnais,** K. Jones, K. Wickens (2008), Origin and fate of industrial ammonia in municipal groundwaters – tracing anaerobic oxidation (anammox) and apportionment with $^{15}N_{NH4}$, *Ground Water Monitoring and Remediation*, 28: 73-82.

Mohammadzadeh, H., I. D. Clark, R. Aravena, **A. Bourbonnais**, I. Liu and P. Middlestead (2006), Isotopic analysis of Ammonium ($d^{15}N$), Nitrate ($d^{18}O$ & $d^{15}N$) and Dissolved Carbon ($d^{13}C$) in Landfill Leachate, *Proceedings of the Environmental Science and Technology 2006 II*, August 19-22, Houston, USA.

**OTHER PUBLICATION**

Bourbonnais, Annie. (2007). *Anomalies isotopiques du nitrate comme indication de la fixation de l'azote dans la région du front des Açores (Atlantique Nord-est subtropical)* (Master's thesis). University of Québec in Montreal, Montréal, QC.

**SELECTED PRESENTATIONS AND PUBLISHED ABSTRACTS**

**Bourbonnais**, **A**., S. K. Juniper, D. A. Butterfield, S. J. Hallam, R. E. Anderson, J. A. Huber and M. F. Lehmann (2012), Diversity and abundance of nitrite reductase (*nirS*) genes in the subsurface biosphere of hydrothermal vents of the Juan de Fuca Ridge, The deep-sea & sub-seafloor frontiers conference, March 11-14, Sitges (Barcelona), Spain (poster).

**Bourbonnais, A.,** M. F. Lehmann, R. C. Hamme, C. C. Manning, and S. K. Juniper (2011), Nitrate isotope fractionation during denitrification in Saanich Inlet: water column versus sediment effects. 45th CMOS congress, June 5-9, Victoria (BC), Canada (oral presentation).

**Bourbonnais, A.,** M. F. Lehmann, D. A. Butterfield, S. J. Hallam, A. H. Devol, M. M. M. Kuypers, G. Lavik, R. Roy, B. X. Chang, and S. K. Juniper (2011), Activity, biodiversity and abundance of denitrifying bacteria in hydrothermal vents of the Juan de Fuca Ridge, North- East Pacific Ocean. EGU meeting, April 3-8, Vienna, Austria (oral presentation).

**Awarded the "InterRidge hottest Student Talk" during the session: Biochemical function and diversity of chemosynthetic deep-sea ecosystems.**

**Bourbonnais,** A., M. F. Lehmann, D. A. Butterfield[c], M. M. M. Kuypers, G. Lavik and K. S. Juniper (2010), Denitrication as the dominant N-elimination process in hydrothermal vents of the Juan de Fuca Ridge, North-East Pacific Ocean, SEOS Graduate Students Workshop, April 23rd 2010, University of Victoria, Victoria, British Columbia (oral presentation).

**Bourbonnais, A**., M. F. Lehmann, D. A. Butterfield, A. Devol, B. X. Chang and K. S. Juniper (2009), Denitrification in diffuse hydrothermal vent fluids of Axial Volcano and the Endeavour Segment on the Juan de Fuca Ridge, AGU fall meeting, December 14-18, USA (poster).

**Bourbonnais, A**., M. F. Lehmann, and D. A. Butterfield (2009), The isotopic composition of dissolved inorganic nitrogen in hydrothermal vent fluids, SEOS Graduate Students Workshop, April 20th 2009, University of Victoria, Victoria, British Columbia (poster).

**Bourbonnais, A**., M. F. Lehmann, and D.A. Butterfield (2007), Dual nitrogen and oxygen isotope composition of nitrate in hydrothermal vents systems, Fourth Interdisciplinary McGill Graduate Student Research Symposium, March 29-30, Montréal, Canada (poster).

Lehmann, M. F., **A. Bourbonnais** and D.A. Butterfield (2006), The isotopic composition of dissolved inorganic nitrogen in hydrothermal vent fluids. AGU fall meeting, December 10-15, San Francisco, USA (poster, presenting author).

**Bourbonnais**, **A.**, M. F. Lehmann and J. J. Waniek (2006), The isotopic composition of nitrate, dissolved organic nitrogen and export particulate matter in the Azores Front

region : Implications for $N_2$ fixation in the subtropical North-East Atlantic. AGU fall meeting, December 10-15, San Francisco, USA (oral presentation).

**Bourbonnais**, **A.** and M. F. Lehmann (2006), Dual nitrate isotope measurements in the Azores Front region: indication for $N_2$ fixation in the subtropical North-East Atlantic Ocean. GAC-MAC, May 14-17, Montréal, Canada (oral presentation).

**Bourbonnais**, **A.** and M. F. Lehmann (2006), Le $^{15}N/^{18}O$ du nitrate dans la région du Front des Açores : indication pour la fixation de l'azote dans l'Atlantique nord subtropical. 74$^{th}$ meeting of the Association Francophone pour le Savoir (ACFAS), May 15-19, Montréal, Canada. (oral presentation).

**PROFESSIONAL AFFILIATIONS**

European Geophysical Union (EGU) (since 2011)
The Explorers Club – Exploration and Field Sciences (since 2009)
American Geophysical Union (AGU) (since 2006)
Canadian Water Network (since 2006)
Golden Key Award Society (since 2003)